Investigation of transcriptional and translational regulation of the *Neurospora crassa* alternative oxidase

by

Natasa Bosnjak

A thesis submitted in partial fulfillment of the requirements for the degree of

Master of Science

in

Molecular Biology and Genetics

Department of Biological Sciences

University of Alberta

ABSTRACT

Mitochondria are organelles found in most eukaryotes and supply the cell with the majority of its energy needs in the form of ATP. Most of the proteins needed for mitochondrial function are nuclear encoded. Therefore, mitochondria communicate their functional status to the nucleus, resulting in the modulation of nuclear gene expression. In the event of a disruption of the standard mitochondrial electron transport chain, the nuclear-encoded *aod-1* gene is induced in *Neurospora crassa*. *Aod-1* encodes an alternative oxidase (AOX) that provides a branch point off the standard chain. When present, AOX transfers electrons from coenzyme Q directly to oxygen.

The induction of AOX is dependent on two transcription factors in *N. crassa*: AOD2 and AOD5. Previous ChIP-seq analysis identified several other genes bound by these transcription factors. The most robust binding peak was found to be in the promoter of NCU06940, a gene encoding a hypothetical protein. Using qPCR analysis on strains lacking AOD2 or AOD5, I demonstrated that the expression of NCU06940 was dependent on these proteins. I hypothesized that NCU06940 had a role in stress because transcripts were upregulated in the presence of an AOX inducer. I examined the growth of a strain in which the NCU06940 gene had been deleted. I found that the growth of the strain on various carbon sources, at different temperatures, and in the presence of inhibitors of mitochondrial function was indistinguishable from wild-type. Thus, the function of the gene remains unknown.

In *N. crassa,* the AOX is encoded by the *aod-1* gene. In normal (non-inducing) conditions, *aod-1* is transcribed at very low levels and no protein can be detected. A strain of *N. crassa* that carries mutations in the tyrosinase gene (T) was previously found to produce relatively high amounts of *aod-1* transcript in non-inducing conditions with no detectable AOD1

protein. Growth of the strain in inducing conditions results in an increase in transcription and production of the protein. I was able to rule out the tyrosinase gene as a regulator of *aod-1* transcription using qPCR analysis for *aod-1* transcript levels by examining the progeny of a cross between a wild-type strain and the tyrosinase mutant strain. Furthermore, I analyzed whole genome sequencing data on the parents and selected progeny strains and identified the *flbA* gene and the *kin-9* genes mutated in only the high *aod-1* transcript expressing progeny and parental strains. Further analysis strongly suggested that the mutated *flbA* gene was responsible for the elevated transcripts.

I also attempted to determine why non-induced cells with high levels of *aod-1* transcript do not contain AOD1 protein in their mitochondria. I showed that the protein does not accumulate in the cytosol due to lack of import into mitochondria. I also showed that it is likely not synthesized and rapidly degraded. Thus, the *aod-1* mRNA may be subjected to translational control in non-inducing conditions.

ACKNOWLEDGMENTS

First and foremost, I would like to thank my supervisor, Dr. Frank Nargang, for his unfailing support over the years, for his patience with me as I was learning, and for his guidance. It was an honor and a privilege to be his last graduate student. I believe I have gained someone to admire and look up to for the remainder of my life, as a mentor, and as a role model. Thank you.

I would like to thank former members of the Nargang Lab, in particular Zhigang Qi and Nishka Kishore. I would like to express gratitude to my examination committee, including Dr. Martin Srayko, Dr. John Locke, and Dr. Enrico Scarpella for their assessments. Additionally, I would like to thank members of the Dr. Kirst King-Jones lab for use and assistance with the qPCR equipment. As well, a special thank you to Troy Locke and Cheryl Nargang in MBSU for all of their help.

Lastly, I would like to thank my family, and my brother, Stefan, in particular, for all of the much-needed positive encouragement. I would also like to thank my friends for all of their support outside of the lab. Specifically, I would like to thank Jenna Hutchen who was with me from start to finish, and Kieran Steer, for always giving me something to look forward to. Finally, I would like to thank my dog, Charlie, who made thesis writing much more bearable. I could not have done this without you. Thank you.

TABLE OF CONTENTS

LIST OF FIGURES

LIST OF TABLES

LIST OF ABBREVIATIONS

A	adenine
A. fumigatus	*Aspergillus fumigatus*
A. nidulans	*Aspergillus nidulans*
A. niger	*Aspergillus niger*
AA	antimycin A
AAC	ADP/ATP carrier
ADP	adenosine diphosphate
AIM	alternative oxidase induction motif
ALS	amyotrophic lateral sclerosis
AOX	alternative oxidase
ATP	adenosine triphosphate
BLAST	Basic Local Alignment Search Tool
BN-PAGE	Blue native polyacrylamide gel electrophoresis
C	cytosine
C. elegans	*Caenorhabditis elegans*
cDNA	complementary deoxyribonucleic acid
ChIP	chromatin immunoprecipitation
CHiP-seq	chromatin immunoprecipitation and sequencing
CM	chloramphenicol
CN	cyanide
Complex I	NADH:ubiquinone oxidoreductase
Complex II	succinate:ubiquinone oxidoreductase
Complex III	ubiquinol:cytochrome *c* oxidoreductase
Complex IV	cytochrome *c* oxidase
Complex V	ATP synthase
conidia	conidiaspores
Cys	cysteine
dH2O	distill water
DNA	deoxyribonucleic acid
dNTP	deoxynucleotide triphosphate
E. coli	*Escherichia coli*
EDTA	ethylenediaminetetraacetic acid
EMSA	electrophoretic mobility shift assay
ER	endoplasmic reticulum
ERMES	ER-mitochondrial encounter structure

FAD	flavin adenine dinucleotide
FBP	fructose 1,6-bisphosphatase
Fe-S	iron-sulfur
FGSC	Fungal Genetic Stock Center
g	gravity force
G	guanine
gm	gram
GPCR	G-protein coupled receptor
GTP	Guanosine triphosphate
H2O2	hydrogen peroxide
Hog1	high osmolarity glycerol response-1
hr	hour
IBM	inner boundary membrane
IGV	Integrative Genomics Viewer
IMS	intermembrane space
IMS	mitochondrial intermembrane space
ISG	Interferon stimulated genes
ITS	IMS-targeting signals
kDa	kilodalton
kV	kilo volt
L	liter
M	molar
M. oryzae	*Magnaporthe oryzae*
MAM	mitochondrial associated membrane
Max	maximum
MFA	monofluoroacetate
mg	milli gram
MIA	mitochondrial IMS import and assembly machinery
MICOS	mitochondrial contact site and cristae organizing system
MIM	mitochondrial inner membrane
min	minute
MISS	mitochondria IMS sorting signals
mL	milli liter
mM	milli molar
MnSOD	mitochondrial superoxide dismutase
MOM	mitochondrial outer membrane

MPP	mitochondrial processing peptidase
MRR	mitochondrial retrograde regulation
mtDNA	mitochondrial DNA
mTOR	mammalian TOR
N. crassa	*Neurospora crassa*
NAD	nicotinamide adenine dinucleotide
ng	nano gram
NLR	NOD-like receptor
NO	nitric oxide
O2-	superoxide anion
ºC	degree celcius
OH·	hydroxyl radical
P. anserina	*Podospora anserina*
PAGE	polyacrylamide gel electrophoresis
pan	pantothenic acid
PAS	Per-Arnt-Sim
PCR	polymerase chain reaction
PEPCK	phosphoenolpyruvate carboxykinase
PiC	phosphate carrier
PMSF	phenylmethanesulfonylfluoride
qPCR	quantitative polymerase chain reaction
RNA	ribonucleic acid
ROS	reactive oxygen species
rpm	revolutions per minute
RT	reverse transcription
RT-PCR	reverse transcriptase polymerase chain reaction
RTG	retrograde pathway
S. cerevisiae	*Saccharomyces cerevisiae*
S. pombe	*Schizosaccharomyces pombe*
SAM	sorting and assembly machinery
SAPK	stress activated protein kinase
SDS	sodium dodecyl sulfate
sec	second
sETC	standard electron transport chain
T	thymine
TAO	*Trypanosoma brucei* AOX

TCA	the citric acid
TCA	tricarboxylic acid
TFAM	Mitochondrial transcription factor A
TIM	translocase of the inner membrane
Tm	melting temperature
TOM	translocase of the outer membrane
TOR	target of rapamycin
UPR^{mt}	mitochondrial unfolded protein response
UTR	untranslated region
V	volt
VCF	variant call format
VDAC	voltage-dependent anion channel
Y. lipolytica	*Yarrowia lipolytica*
µg	microgram
µL	microliter
µM	micromolar

1.0 Introduction

1.1 Mitochondrial structure, morphology, dynamics

Mitochondria are organelles found in most eukaryotes. They play a central role in a variety of cellular and metabolic pathways such as the intrinsic pathway of cellular apoptosis (Bhola and Letai, 2016). In addition, they are involved in cellular calcium homeostasis (Contreras et al., 2010), which is important in the regulation of many crucial cellular processes (Granatiero et al., 2017; Smaili et al., 2009; Valero et al., 2008). Mitochondria are also the site of iron-sulfur cluster synthesis (Braymer and Lill, 2017), which serve as co-factors for enzymes involved in important cellular reactions such as gene expression and respiration (reviewed in Johnson et al., 2005). Mitochondria also contain the enzymes that catalyze four steps in the biosynthesis of heme in most eukaryotes (Ajioka et al., 2006). These organelles also house the enzymes of the citric acid cycle. Intermediates from the cycle serve as precursors in the biosynthesis of several important molecules required by the cell (Martínez-Reyes et al., 2016). The citric acid cycle also generates reduced electron carriers which are consumed during mitochondrial ATP production by the process of oxidative phosphorylation (discussed further in Section 1.4).

Mitochondria are composed of four sub-compartments which include the mitochondrial outer membrane (MOM), mitochondrial inner membrane (MIM), the intermembrane space (IMS), and the matrix, which contains the mitochondrial DNA (mtDNA) (Fig. 1.1). The MOM contains pore-forming β-barrel membrane proteins called porins (Mannella et. al. 1983; Mannella 1986; Wimley et. al. 2003). Thus, the MOM is porous and allows ions and other small molecules up to about 5 kDA to freely traverse the membrane. The IMS is a hydrophilic lumen layer located between the MOM and MIM.

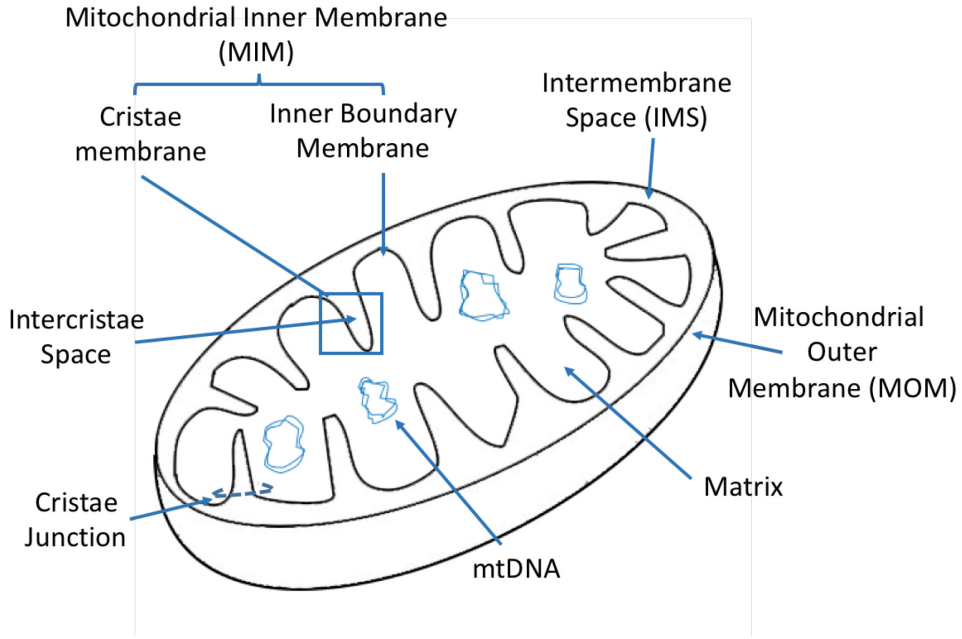

Figure 1.1. The structure of the mitochondrion. The mitochondrial outer membrane (MOM) is the outer most structure that encloses the mitochondrion. The intermembrane space (IMS) is the space between the MOM and mitochondrial inner membrane (MIM). The MIM contains the proteins of the respiratory chain and the ATP synthase. Infoldings of the MIM give rise to cristae. The MIM is further subdivided into the cristae membrane, and the inner boundary membrane (IBM). Cristae junctions connect the cristae to the IBM. The matrix is enclosed by the MIM, and contains the mitochondrial DNA (mtDNA).

The MIM does not contain pores so that charged molecules require carrier proteins, or translocases to traverse the membrane. For example, pyruvate binds the mitochondrial pyruvate carrier, or MPC, which utilizes the proton gradient generated by electron transport to facilitate movement of the molecule into the matrix (Bender and Martinou, 2016). Protein molecules synthesized in the cytosol that are destined for mitochondria are translocated to the appropriate subcompartment by a series of complex translocases in the MOM and MIM (discussed in section 1.6). Another MIM protein is the ADP/ATP carrier, which simultaneously moves ADP into the matrix and ATP into the IMS (Bender and Martinou, 2016).

The MIM is morphologically distinct from the MOM in that it can be subdivided into two different regions (Fig. 1.1): cristae, which are formed by invaginations of the MIM, and the inner boundary membrane (IBM) which runs adjacent to the MOM (Zick et. al. 2009). Originally, a "baffle" model was proposed that interpreted the cristae as simple invaginations of the MIM which increased surface area (Palade 1952; 1953). However, later microscopy studies using serial mitochondrial sections (Daems and Wisse, 1966; Mannella et al., 2001; Frey and Mannella, 2000) and immunogold electron microscopy (Vogel et al., 2006) revealed the distinct natures of the cristae and IBM.

Cristae morphology varies by cell and tissue type. In tissues with high energy demand, like muscle, cristae are present in a "stacked" conformation and take up the majority of the space in the mitochondrial matrix. In lower energy demand tissues like liver and kidney, the cristae are less stacked, leaving more space in the matrix for biosynthetic reactions (Mannella et. al., 2001). The abundance and shape of cristae varies between organisms and tissue types, but cristae junctions are relatively uniform round or oval tubules. The cristae membrane contains most of the complexes of the standard electron transport chain (sETC) and the ATP synthase, while the

cristae lumen contains the majority of the soluble electron carrier, cytochrome *c* (Cogliati et al., 2016). Cristae are formed at cristae junctions (see below) and kept separate from the IBM. Immuno-staining has revealed that respiratory chain complexes are enriched in the cristae compared to the IBM. However, the reverse is true for the protein translocases found in the MIM, which are enriched in the IBM (Vogel et al., 2006). Therefore, it is presumed that at least one of the functions of the cristae junction is to form a diffusion barrier to prevent lateral diffusion of proteins and maintain their segregation in the different regions of the MIM.

Cristae are formed by the action of the mitochondrial contact site and cristae organizing system (MICOS) (Pfanner et al., 2014). As recently reviewed (Horvath et al., 2015; Wollweber et al., 2017), the MICOS acts by stabilizing the region where cristae invaginate from the IBM giving rise to structures called the cristae junctions (Fig. 1.1). In addition, the MICOS interacts with several proteins and complexes of the MOM, including the TOM complex, the sorting and assembly machinery (SAM) complex, and porin. As a result of the these interactions, MICOS is involved in the formation of contact sites between the MOM and MIM. These sites facilitate maximum levels of import of several mitochondrial proteins. Another type of MOM-MIM contact site is formed between the TOM complex and the TIM23 complex (see section 1.6), as proteins in the process of being imported span both complexes (Gold et al., 2014; Horvath et al., 2015).

The innermost compartment of the mitochondria is the mitochondrial matrix. It houses the mtDNA that is transcribed in the matrix. The protein coding genes of the mtDNA are translated on mitochondrial ribosomes, which are distinct from cytosolic ribosomes. The matrix is also the site of the biosynthetic reactions of the citric acid cycle, as well as β-oxidation of fatty acids and oxidation of pyruvate (Gray et al., 2017).

Mitochondrial morphology varies among cell and tissue types. For example, mitochondria found in fibroblast cells are most often observed as long filaments (Amchenkova et al., 1988; Ding et. al., 2012), whereas mitochondria in hepatocytes tend to be more spherical (Das et. al. 2012). The number and size of mitochondria observed in different cell types is determined by the process of mitochondrial fission and fusion. Mitochondrial fission involves the division of one mitochondrion into two or more organelles. Since mitochondria cannot be formed *de novo*, fission is essential for populating the daughters of dividing cells with mitochondria. Mitochondrial fusion results in the creation of a single mitochondrion from smaller, independent mitochondria. The processes of mitochondrial fission and fusion can respond to physiological and developmental changes. Thus, interplay and regulation of the processes allows the proper shape, size and number of mitochondria to be optimally maintained in a given cell or organism (Labbé et al., 2014; Mishra and Chan, 2016; Wai and Langer, 2016). Both fission and fusion are mediated by dynamin-related GTPases (Labbé et al., 2014).

1.2 Mitochondrial origins

The most commonly accepted theory of mitochondrial origin is the endosymbiont theory which states that mitochondria arose from bacteria inside another cell. The original version of this theory for the origin of mitochondria and plastids was published in 1905 (Mereschkowski, 1905). The theory came into prominence in the 1970s, when Lynn Margulis published the *Origin of Eukaryotic Cells* (Margulis, 1970). DNA sequencing of mtDNAs in the 1970s and 1980s, confirmed the bacterial origins of mitochondrial and plastid genomes (Gray, 2012). It is now widely accepted that mitochondria arose via a single endosymbiotic event in which a bacterium was taken into a host cell (Archibald, 2015). The α-proteobacteria are the extant group that is

most clearly related to mitochondria (Gray, 2012). Interestingly, this group includes the *Rickettsiales* and other species that exist as obligate intracellular parasites within a host cell (Gray, 1998; Williams et al., 2007; Roger et al., 2017). One popular model for the origin of mitochondria by endosymbiosis is the hydrogen hypothesis. It was proposed by Martin and Mueller in 1998, and states that a hydrogen-dependent host cell, of archaebacterial origin, acquired an anaerobic, hydrogen-waste producing bacterium (Martin and Müller, 1998). Structure and metabolic adaptation, gene transfer, and cooperative energy contribution eventually led to the evolution of mitochondria and the establishment of the eukaryotic cell (Martin and Koonin, 2006; Roger et al, 2017).

There are examples of extant unicellular eukaryotes without any mitochondrial related organelles. However, they exist as amitocondriates due to a secondary loss of the organelle (Karnkowska et al., 2016). Thus, there are no known primary eukaryotes lacking a mitochondrial related organelle. This suggests that the host organism that engulfed the bacterium, which eventually evolved into mitochondria, was not a eukaryote at the time of engulfment (Martin et al., 2015). A current favored hypothesis suggests that the original host was an archaea (Cox et al., 2008; Guy and Ettema, 2011; Williams et al., 2012).

Recently, an archaeal clade called Lokiarchaeota was discovered by metagenomics analysis from an Arctic ocean hydrothermal vent site called Loki's castle, found between Greenland and Norway (Spang et al., 2015). Lokiarchaeota was shown to be the most closely related prokaryote to eukaryotes and was found to contain genes encoding proteins with homology to various eukaryotic signature proteins (Spang et al., 2015). Very recently, a number of other groups related to Lokiarcheaota that include Thorarchaoeta, Odinarcheota, and Heimdallarcheaota have been characterized from sites around the world. It has been proposed

that these related groups be given phylum status and that they all be placed in a superphylum called Asgard (Eme et al., 2018; Zaremba-Niedzwiedzka et al., 2017). The Heimdollarchaeota appear to be the most closely related to eukaryotes.

With respect to the Asgard group representing the original host cell that took up the endosymbiont according to the aforementioned hydrogen hypothesis, it is important to know aspects of the energetic metabolism of the Asgard archaea. While it is possible that they could utilize hydrogen, the metabolic features of the group remain unclear (Martin et al., 2015).

1.3 mtDNA

The size and arrangement of mitochondrial chromosomes show considerable variation in different organisms. Protists display the most variation in mitochondrial genome organization across different species with linear, circular, or multiple linear chromosomes that are transcribed separately (Gray et. al. 2004a). Monomeric circular molecules are present in some animals (Borst and Kroon, 1969) and kinetoplastids (Simpson, 1986). In mammals, the mtDNA is a small, double-stranded, circular molecule (Taanman, 1999). Linear monomeric mtDNA is present in a small number of taxa including ciliates (Burger et al. 2000; Pritchard et al. 1990; Suyama et al. 1985), green algae (Fan and Lee, 2002), oomycetes (Martin, 1995), Jakobids (Gray et al. 1998), and fungi (Forget et al., 2002; Fukuhara et al., 1993; Kováč et al., 1984; Nosek et al., 1995).

Unlike the nuclear genome which is typically made up of several chromosomes carrying different information, mtDNA in most organisms consists of one type of molecule that exists in multiple copies that can range from 10 to 1000 per cell depending on the organisms and tissue. There is considerable variation in the size of mtDNA that exists on a species-to-species basis. For example, Ctenophora (cone jellies) have a mitogenome around 11 kb which is among the

smallest for animal mitogenomes (Pett et al., 2011; Kohn et al., 2012). The mtDNA in *Plasmodium falciparum* (the malaria parasite) is the smallest known at only 6 kb, and contains only 3 protein coding genes (Wilson and Williamson, 1997). In contrast, the mtDNA of Jakobid protists can encode up to 67 proteins (Burger et al., 2013). The mitogenome of *Neurospora crassa,* a filamentous fungus that is the subject of this thesis, consists of a 68, 840 bp circle encoding 28 proteins, 28 tRNAs, and 2 rRNA molecules (Kennell et al., 2004). Generally, metazoan mtDNA encodes 13 intron-less, protein-coding genes. Compared to animals, plant mitogenomes have large intragenic regions that can house repeated DNA sequences and a variable number of introns (Fauron et al., 2004). For example, the plant mitogenome can range from 200 to 2500 kb, and introns and repeated DNA sequences are typically 90% of the sequence (Galtier, 2011). For the most part, mtDNA is inherited maternally but exceptions do exist. For example, in *S. cerevisiae,* mtDNA is inherited biparentally (Yaffe, 1999). An unusual example of mtDNA inheritance occurs in unionid mussels where inheritance is doubly uniparental. Females pass on their mtDNA to both sons and daughters, but males pass on mtDNA to only sons (Hoeh et al., 2002).

1.4 ATP production

Mitochondria have been dubbed the "powerhouse" of the cell because they produce ATP via oxidative phosophorylation (Lenaz and Genova, 2009). Oxidative phosphorylation occurs with the transfer of electrons from reduced electron carriers produced by glycolysis and the TCA cycle through the enzyme complexes and carrier molecules of the standard electron transport chain (sETC). All of these sETC components are found in the MIM and contain multiple subunits with the exception of cytochrome c, which is a peripheral membrane protein associated

with the outer surface of the MIM (Fig. 1.2). The electrons are ultimately passed to molecular oxygen resulting in the formation of H_2O. In the sETC, Complex I (NADH dehydrogenase) accepts electrons from NADH and passes them to coenzyme Q. Electrons are also passed from $FADH_2$ to the coenzyme Q pool by Complex II (succinate dehydrogenase). Electrons are then removed from coenzyme Q by Complex III (ubiquinol-cytochrome c oxidoreductase) and passed to cytochrome *c*. Complex IV (cytochrome c oxidase) then transfers electrons from cytochrome *c* to oxygen. The energy released from electron transfer through complexes I, III, and IV is used to pump protons from the matrix to the IMS, creating an electrochemical proton gradient across the MIM. The proton gradient is then utilized by the ATP synthase (Complex V) to make ATP from ADP and P_i (Fig. 1.2).

Mitochondria from many plants and fungi contain simpler alternative NADH:ubiquinone oxidoreductases (Bonner and Voss, 1961; Weiss et al., 1970; Weidner et al., 1993; Matus-Ortega et al., 2015). Alternative NADH:ubiquinone oxidoreductase was first discovered in plant mitochondria that were capable of oxidizing externally added NAD(P)H in a reaction that was completely insensitive to amytal and rotenone (Complex I inhibitors) (Bonner and Voss, 1961). While the alternative NADH:ubiquinone oxidoreductase catalyzed the same reaction as Complex I, it did not contribute to the electrochemical proton gradient across the MIM. In some species, like *Saccharomyces cerevisiae*, Complex I is totally absent and alternative NADH:ubiquinone oxidoreductases are the only enzyme capable of oxidizing NADH to feed into the respiratory chain (Büschges et al., 1994). Some other organisms, for example, *Neurospora crassa,* contain

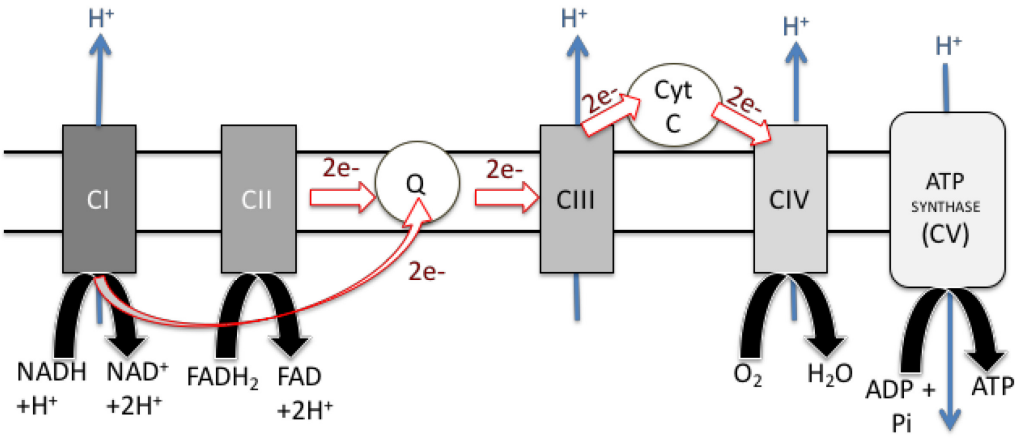

Figure 1.2. The standard electron transport chain (sETC). Electrons (e-) are harnessed from NADH or $FADH_2$ and passed through the complexes and molecules of the sETC in the MIM. Complexes I, III, and IV (CI, CIII, and CIV, respectively) are sites of proton pumping. O_2 is the final electron acceptor and is converted to H_2O by CIV. Energy stored in the proton gradient is harnessed by the ATP synthase (Also known as Complex V) to synthesize ATP. (Q: the Q pool, or coenzyme Q).

both functional Complex I as well as alternative NADH:ubiquinone oxidoreductases (Carneiro et al., 2004).

In 2000, evidence of multi-complex "supercomplex" units in yeast and mammalian mitochondria were revealed by the technique of Blue Native Polyacrylamide Gel Electrophoresis (BN-PAGE) experiments. BN-PAGE of *S. cerevisiae* mitochondria revealed a supercomplex consisting of a dimer containing a monomer of Complex III and a monomer of Complex IV, as well as larger supercomplexes consisting of a dimer of Complex III with a monomer Complex IV (Schägger and Pfeiffer, 2000). In bovine heart mitochondria, supercomplexes formed between complexes I and III were most evident, which formed subsequent supercomplexes with varying copy numbers of Complex IV. Supercomplexes in *Neurospora crassa* consist of Complex I dimers, as well as I-III-IV and III-IV supercomplexes (Marques et al., 2007). While the role of supercomplexes was initially not well understood, it has been now shown that cells lacking a protein required for effective supercomplex formation have increased ROS, suggesting that supercomplexes may help prevent electron leakage (Chen et al., 2012; Vukotic et al., 2012). In addition, it has been shown that supercomplex assembly is dynamic which may allow the cell a means of regulation to adjust electron flow to maximize the use of available substrates (Lapuente-Brun et al., 2013).

1.5 The role of mitochondria in aging and disease

The role of mitochondria in aging and disease has been well studied. Many past studies have supported the free radical theory, which suggested that the accumulation of reactive oxygen species (ROS) damages cell constituents (Harman, 1956, 1969). Since mitochondria are the major source of ROS in the cell, the theory was modified to the mitochondrial theory of aging

(Harman, 1972). ROS products would be expected to be most prominent where electron leaks between the complexes of the respiratory chain would lead to the accumulation of superoxide radicals, with complexes I and III being the sites of majority of electron leaks (Nakamura et al., 2009; Noctor et al., 2007). mtDNA is estimated to have a mutation rate greater than that of nuclear DNA because of its histone-lacking structure and its proximity to the respiratory chain (Singh et al., 2015). The mitochondrial theory of aging (Harman, 1972) postulates that mutations in mtDNA lead to dysfunction of the respiratory chain. This is because the mtDNA encodes subunits of the sETC. Poorly functioning sETC complexes would further result in increased electron leakage, an increase in ROS, and further damage of the mtDNA resulting in an exponentially increasing vicious cycle (Alexeyev et al., 2004).

However, many studies have shown that ROS levels are not increased when mtDNA mutations occur. For example, many studies using mice (referred to as "mutator mice") expressing an mtDNA polymerase that has been modified to be devoid of proof-reading activity have shown that these mice accumulate mutations in their mtDNA, age and die much more rapidly than normal mice (Kujoth et al., 2005; Trifunovic et al., 2004). However, no increase ROS in the mutator mice could be detected. In addition, other mouse studies have shown that overexpression of enzymes that degrade ROS, such as superoxide dismutase, or catalase, do not increase lifespan (Chen et al., 2004; Huang et al., 2000).

While much evidence still supports a role for mtDNA mutations and mitochondrial function in the aging process (Kauppila et al., 2017; Payne and Chinnery, 2015), it now appears that most mtDNA mutations arise not from ROS damage, but from replication errors made by the mtDNA polymerase (Kennedy et al., 2013; Zheng et al., 2006), or as deletions that probably arise during mtDNA replication (Ahmed et al., 2015; Dong et al., 2014).

Besides normal aging, there are a number of human diseases that are caused by decreased mitochondrial function. These are most often found to be due to mutations of mtDNA, which can either be de novo or inherited (Copeland, 2008; Niyazov et al., 2016). Most diseases are caused by respiratory chain defects that are due to mutations of genes in mtDNA or nuclear DNA that encodes respiratory chain subunits. They are typically fatal and usually show early onset, though occasionally they may not present until adulthood. Most mitochondrial mutations function recessively, and require a mutation load of 60-90% before a biochemical or physiological effect is observed (DiMauro, 2013). Nuclear DNA mutations can also cause mitochondrial disease as they can affect mtDNA structure or content, such as assembly and maintenance of respiratory chain complexes. Many human diseases associated with aging, such as Parkinsons, Alzheimer's, and ALS (Amyotrophic Lateral Sclerosis) have been associated with defects in mitochondrial maintenance or function (Hawking, 2016; Hu and Wang, 2016; Smith et al., 2017)

1.6 Protein import into the mitochondria

A few mitochondrial proteins are produced within mitochondria. These include some subunits of the electron transport chain complexes as well as the ATP synthase. However, most protein coding genes from the original endosymbiont have been transferred to the nucleus or lost outright (Ku et al., 2015). Thus, the vast majority of mitochondrial proteins are nuclear encoded, translated on cytosolic ribosomes, and then imported into mitochondria. The process of import has been well studied. The majority of this work has been done in *S. cerevisiae* although mechanisms of mitochondrial protein import have been shown to be highly conserved in higher eukaryotes (MacKenzie and Mark Payne, 2007; Murcha et al., 2014; Wrobel et al., 2016).

It was long thought that most proteins are imported into mitochondria in a post-translational fashion, while co-translational import occurred for only a few precursors (Endo and Yamano, 2010; Neupert, 2015). However, a significant number of reports have suggested that mRNAs for many nuclear encoded mitochondrial proteins accumulate on the surface of the organelle. Translation of the mRNAs at the outer surface of the MOM most likely results in co-translational import (reviewed in Fox, 2012; Lesnik et al., 2015; Schulz et al., 2015). To prevent mitochondrial precursor proteins that are released into the cytosol from misfolding and aggregrating, hydrophobic segments are shielded by chaperones (Young et al., 2003; Bhangoo et al., 2007; Zara et al., 2009).

Proteins destined to enter mitochondria are generally referred to as precursor proteins until they reside within the organelle at their final destination. With the exception of proteins anchored in the MOM by α-helical transmembrane domains, all precursor proteins enter mitochondria through the TOM (translocase of the outer membrane) complex entry gate. Proteins destined for mitochondria contain mitochondrial targeting signals within their amino acid sequence (Chacinska et al., 2009). These signals are recognized by the initial docking site proteins Tom20 and Tom70 which form part of the TOM holo-complex (Abe et al., 2000; Brix et al., 1997; Saitoh et al., 2007; Dudek et al., 2013). From there, the TOM complex mediates the transport of precursors with diverse import signals across the MOM. Different routes of transport exist that are specific to the precursor and its targeting signal, and the TOM complex interacts with downstream import complexes to ensure that the different precursors reach their correct final destination.

Virtually all proteins destined for the matrix and many destined for the MIM have N-terminal presequences that are proteolytically removed by the mitochondrial processing peptidase (MPP)

in the matrix (Taylor et al., 2001; Mossmann et al., 2012). The transport of presequence containing proteins across the MOM is coupled to the translocation across or into the MIM. Precursors enter the mitochondria by first passing through the TOM complex of the MOM and associate with the IMS domain of the Tom22 receptor (Moczko et al., 1997; Komiya et al., 1998). The N-terminal portion is then transferred to the protein-conducting pore of the TIM23 complex, although the C-terminal region may still be inside the TOM complex and extending into the cytosol. The TIM23 complex is the major protein translocase of the MIM. The TIM23 complex uses ATP and membrane potential to facilitate translocation of MIM targeted proteins containing positively charged, N-terminal signals into the MIM or across the MIM and into the matrix (Mokranjac and Neupert, 2010). Thus the precursor protein can effectively traverse both membranes and connect the TOM complex and TIM23 complex, forming contact sites between the OM and the MIM, called the TOM-Tim23 supercomplex (Schleyer and Neupert, 1985; Schwaiger et al., 1987; Rassow et al., 1989; Pon et al., 1989; Schülke et al., 1997). At the MIM, depending on the import signal, preproteins either translocate into the mitochondrial matrix or are inserted into the MIM lipid bilayer. Inducing translocation arrest and release of preproteins into the MIM requires a hydrophobic sorting signal downstream of the N-terminal presequence (Glick et al., 1992; Bömer et al., 1997; Van der Laan et al., 2007; Bohnert et al. 2010).

MOM proteins belonging to the structural class of β-barrel proteins, such as porin and Tom40, exist as a series of β-strands when finally assembled in the MOM. They are recognized by the TOM complex and guided through the Tom40 pore (Hill et. al. 1998). After entering the IMS, β-barrel precursor proteins are met by the so-called small TIM (translocase of the inner membrane) proteins which act as chaperones (Höhr et al., 2015; Stojanovski et al., 2012; Wiedemann et al., 2004). They are delivered from the small Tim chaperones to the Sorting and

Assembly Machinery (SAM) complex in the outer membrane (Wiedemann et al., 2003; Dolezal et al., 2006; Paschen et al., 2003; Gentle et al., 2004). The major component of the complex is a β-barrel protein itself, named Sam50. The last β-strand of the β-barrel precursor proteins contains the so-called β-signal (Kutik et al., 2008). Once the precursor is in the IMS, the β-signal strand enters the lumen of the Sam50 in the MOM and binds to the first β-strand of Sam50 by displacing Sam50's sixteenth and most C-terminal β-strand. This induces an opening in the Sam50 β-barrel called the lateral gate. Additional β-strands of the precursor then enter the lateral gate and the full length precursor is ultimately released from the lateral gate into the MOM (Höhr et al., 2018).

Signal-anchored proteins of the MOM include Tom20 and Tom70. These proteins are classified by their α-helical membrane-spanning domains located near their N-terminus (Vögtle et al., 2009). The biogenesis of these proteins depends on the MOM protein Mim1 which supports insertion into the lipid bilayer (Popov-čeleketić et al., 2008; Hulett et al., 2008). Because no factors of the IMS are involved in the biogenesis of α-helical proteins, the insertion of α-helical proteins presumably occurs from the cytosolic side of the MOM. Tail anchored MOM proteins contain transmembrane-spanning domains near their C-terminus. They require no protein-dependent insertion machinery, but rather, are dependent on the lipid composition of the MOM (Setoguchi et al., 2006; Kemper et al., 2008).

Many proteins targeted for the IMS contain sets of cysteine residues that are implicated in the formation of disulfide bridges, and are generally found in Cx_3C or Cx_9C motifs. These motifs are typically flanked by mitochondrial IMS sorting signals (MISS) also known as IMS-targeting signals (ITS). These signals target proteins to the IMS via the MIA (mitochondrial IMS assembly) pathway (Milenkovic et al., 2009; Sideris et al., 2009). The MIA machinery consists

of two major players: Mia40, the receptor, and the sulfhydryl oxidase *Erv1* (Chacinksa et al., 2004; Allen et al., 2005; Grumbt et al., 2007; Milenkovic et al. 2007; Backes and Herrmann, 2017). Incoming precursor proteins are trapped in the IMS by Mia40, which forms transient intermolecular disulfide bonds with the incoming proteins as they emerge from the TOM complex (von der Malsburg et al., 2011; Chacinska et al., 2004; Müller et al., 2008). Next, Mia40 catalyzes formation of intramolecular disulfide bridges within the precursor proteins, leading to substrate release into the IMS (Chacinska et al., 2004; Grumbt et al., 2007; Milenkovic et al., 2007; Müller et al., 2008). This step results in the reduction of Mia40, which is reoxidized by the Erv1 protein that passes the electrons to either molecular oxygen or cytochrome *c* (Dabir et al., 2007; Mesecke et al., 2005; Bihlmaier et al., 2007; Banci et al., 2011; Stojanovski et. al. 2008).

Metabolic carrier proteins, such as the ADP/ATP carrier (AAC) or phosphate carrier (PiC), are MIM proteins that have several membrane spanning domains and have internal import signals for entry into mitochondria and insertion into the MIM. Because of their hydrophobic nature, chaperones from the Hsp70 and Hsp90 families are required to bind the precursors of the proteins in the cytosol (Young et al., 2003; Zara et al., 2009). Chaperone binding prevents aggregation and provides assistance to target proteins to the mitochondria. Precursor-chaperone complexes are brought to the surface of the mitochondria by binding to the cytosolic domain of the Tom70 receptor, and are then passed to the TOM complex import channel. Precursor proteins bind to TIM chaperone complexes containing the small Tim9 and Tim10 proteins or Tim8 and Tim13 in the IMS to prevent aggregation in the aqueous IMS environment (Sirrenberg et. al. 1998; Endres et al., 1999; Luciano et al., 2001; Truscott et al., 2002). The carrier proteins are then inserted into the MIM by the TIM22 complex (Wiedemann and Pfanner, 2017).

It should be noted that the mitochondrial import machinery is subject to regulation related to levels of various metabolites and signaling molecules (reviewed in Harbauer et al., 2014; Opalińska and Meisinger, 2015). For example, in *S. cerevisiae*, when glucose levels are high, the assembly of the TOM complex is inhibited by phosphorylation of Tom40 and Tom22 (Gerbeth et al., 2013; Rao et al., 2012).

1.7 Mitochondria as signaling organelles

Mitochondria were long viewed simply as sites of ATP production and certain biosynthetic reactions. However, the discovery of cytochrome *c* as a component involved in cellular apoptosis (Liu et al., 1996) opened up the study of mitochondria as regulators of signal transduction. We now know that mitochondria have the capacity to signal various events in the cell through the release of proteins (such as cytochrome c), ROS, and metabolites. For a long time, it was widely believed that ROS were produced only under stress or disease conditions. However, later studies determined that ROS also act as signaling molecules that allow communication between the mitochondria and the rest of the cell under normal physiological conditions (reviewed in Angelova and Abramov, 2016). A decrease in ROS diminishes the activation of pathways necessary for cell proliferation, differentiation and metabolic adaptation (Sena and Chandel, 2012). For example, hydrogen peroxide has the ability to reversibly modify proteins, resulting in the modulation of signaling pathways. One target of hydrogen peroxide is certain phosphatases. For example, phosphatases that possess reactive cysteines in their catalytic domain are susceptible to reversible oxygenation. Oxygenation inhibits the dephosphorylation activity of these phosphatases (Ray et al., 2012). PTPs (protein tyrosine phosphatases) are regulated in this manner. PTPs are defined by the possession of a HCX_5R motif, in which the

Cys residue is necessary for the catalytic reaction of the phosphatase. Oxidation of the Cys residue inhibits the ability of PTP to remove phosphates from tyrosine residues (Meng et al., 2002).

Furthermore, mtDNA itself may have a role as a signaling molecule. Evidence has surfaced that implicates the release of mtDNA in regulating antiviral immune response, though the mechanism whereby mtDNA is released into the cytosol is unknown (Kanneganti et al., 2015). Once in the cytosol, mtDNA engages the NLRP3 inflammasome (West et al., 2015). The NLRP3 inflammasome is part of the NLR (NOD-like receptor) subset of inflammasomes which are characterized by a nuclear binding domain and a C-terminal leucine rich repeat which serves as a ligand recognition domain. Inflammasomes are large complexes formed in the cytosol and are responsible for the inflammatory response by activating caspases-1 and -5 (reviewed in Abderrazak et al., 2015). In addition, mtDNA instability, such as that caused by heterozygosity (TFAM heterozygous knock out) of mitochondrial transcription factor A (TFAM), leads to upregulation of ISGs (Interferon stimulated genes) which provide a defense against invading pathogens (Schneider et al., 2014).

Mitochondrial membranes also reversibly associate with other organelle membranes, most notably the ER, to facilitate signaling in mammals (Diogo et al., 2017). These associated regions are called mitochondrial associated membranes, or MAMs. The ER in MAMs becomes reversibly tethered to the mitochondria, and is enriched in lipid biosynthetic enzymes. MAMs supply some lipids to mitochondria and play a role in calcium homeostasis, mitochondrial function, autophagy glucose homeostasis in humans, and apoptosis (reviewed in Vance, 2014). MAM dysfunction is implicated in neurodegenerative diseases, such as Alzheimer disease (Schon and Area-Gomez, 2013). In fungi, mitochondrial-ER associations are termed ERMES

(ER-mitochondria encounter structure) (Kornmann et al., 2009). These have been implicated in maintenance of mitochondrial morphology, mitophagy, mtDNA maintenance and inheritance, mitochondrial protein import, and cellular growth (Kornmann and Walter, 2010).

1.8 Mitochondrial retrograde regulation

To achieve proper mitochondrial biogenesis, communication between the mitochondria and the nucleus is vital to coordinate the expression of genes found on both mtDNA and nuclear DNA. In addition, changes in mitochondrial function or status must be communicated to the nucleus to modulate the expression of nuclear-encoded mitochondrial proteins according to specific requirements. Communication between the mitochondria and the nucleus can be broken down into two different signaling systems: anterograde signaling (communication of the nucleus to the mitochondria), and retrograde signaling (communication of the mitochondria to the nucleus).

The first retrograde pathway (RTG) was discovered in yeast in 1987 (Parikh et al., 1987) and has since been extensively characterized. The *Cit2* gene is a nuclear gene encoding the glyoxylate cycle isoform of citrate synthase in yeast (Kim et al., 1986). Its expression is upregulated by as much as 60-fold in the event of mitochondrial dysfunction, allowing for an adjustment in carbon and nitrogen metabolism. Rtg1p and Rtg3p are transcription factors that bind as a heterodimer at a region called the R-box in the promoter of *Cit2* and regulate its expression in a positive fashion (Jia et al., 1997). Rtg2p, another positive regulatory factor, functions upstream of Rtg1P and Rtg3p, and acts as both a sensor for mitochondrial dysfunction as well as a transducer of mitochondrial signaling (Sekito et al., 2000). These positive regulators of *Cit2* control the expression of both basal and induced expression of Cit2. In their inactive

forms, Rtg1p and Rtg3p are sequestered in the cytosol, and Rtg3p is phosphorylated at multiple sites. Activation of the retrograde pathway in the event of mitochondrial dysfunction results in a partial dephosphorylation of Rtg3p, and entry of the Rtg1p/Rtg3p heterodimer into the nucleus to activate expression of *Cit2*, as reviewed in Butow and Avadhani (2004).

Further studies revealed the importance of Rtg2p in dictating the intracellular localization of the Rtg1/3p complex. Cells lacking Rtg2p contain hyperphoshorylated Rtg3p, and the complex remains in the cytosol. Although Rtg2p is required for the dephosphorylation of Rtg3p, it does not perform this function itself (Sekito et al., 2000, 2002). Genetic screens conducted to bypass the requirement of Rtg2p identified a negative regulator of *Cit2* expression. Mks1p, first identified as a negative regulator of the Ras2-cAMP pathway (Matsuura and Anraku, 1993), is a phosphoprotein that interacts with Rtg2p when the retrograde pathway is on. When the pathway is off, it ceases interactions with Rtg2p, becomes phosphorylated, and forms a complex with Bmh1p and Bmh2p (14-3-3 proteins). This complex appears to prevent the dephosphorylation, and therefore nuclear translocation, of Rtg3p by an unknown mechanism. Thus, the major role of Rtg2p in activation of the RTG complex may be to keep Mks1p in an active form (Liu et al., 2003).

There is a connection between TOR (target of rapamycin) signaling and the retrograde response. The TOR signaling pathway acts as a nutrient sensor and is involved in cellular growth as well as aging (Loewith and Hall, 2011). Mutant alleles of Lst8, a component of the TOR complex, and negative regulator of the retrograde response, were identified in a genetic screen that attempted to bypass the requirement of Rtg2 to achieve *Cit2* expression (Liu et al., 2001). *Cit2* expression in a Lst8 mutant background was found to be constitutively high, categorizing Lst8 as a negative regulator of Rtg1/3p dependent gene expression (Chen and Kaiser, 2003). In

addition, Rtg1/3p dependent gene expression was induced in cells where TOR signaling was inhibited by rapamycin, an antifungal agent (Komeili et al., 2000). Activation of Rtg1/3p gene expression by rapamycin is dependent on Rtg2p. Studies conducted on animals cells revealed that compromised mitochondrial activity inhibited the kinase activity of mammalian TOR (mTOR) (Kim et al., 2002).

RTG-dependent signaling also plays a role in resistance to osmotic stress. The SAPK (stress activated protein kinase) encoded by the *Hog1* gene (high osmolarity glycerol response) is activated under stresses including hyperosmolarity and controls the activity of several transcription factors involved in expression of stress response genes. Under osmotic stress conditions, Hog1 is required for the accumulation of the Rtg1/Rtg3 heterodimer in the nucleus. Using mutants expressing a Hog1 protein lacking Hog1 activity, it was shown that this does not depend on the catalytic activity of Hog1. Rather, it requires interaction of the heterodimer with the Hog1 protein. However, Hog1 activity is required for association of the heterodimer with chromatin and the transcriptional activity of Rtg3. Hog1 SAPK binds to Rtg1/3p and facilitates translocation to the nucleus (Ruiz-Roig et al., 2012).

In addition to the RTG system, there are other pathways that are involved in mitochondrial communication to the nucleus in yeast, although they are not as extensively studied. For example, in 2006, a different kind of retrograde signaling was reported in yeast mutants null for the i-AAA (intermembrane space ATPases associated with diverse cellular activities) protease, an inner membrane ATP-dependent protease involved in degradation of mitochondrial proteins (Arnold et al., 2006). The i-AAA protease is encoded by the *YME1* gene. Microarray analysis of a *YME1* gene deletion strain showed the induction of many nuclear genes, particularly those involved in mitochondrial gene expression and respiratory chain biogenesis

when yeast cells were grown on the non-fermentable carbon source lactate, but not when cells were grown on fermentable carbon sources. Strains lacking *Yme1* were also found to be deficient in the membrane potential across the MIM, the activity of the electron transport chain, and the ATP synthase. Chemical inhibition of these three activities showed that only reduced ATP synthase activity gave rise to the altered expression of nuclear genes seen in *Yme1* deficient cells. Therefore, the authors suggested that changes in ATP synthase function may provide the signal for the Yme1 response (Arnold et al., 2006).

No orthologues of the yeast RTG system proteins have been identified in animals, but other pathways by which dysfunctional or stressed mitochondria signal the nucleus are known. One of the most interesting systems is the mitochondrial unfolded protein response (UPR^{mt}) (reviewed in Fiorese and Haynes, 2017; Haynes et al., 2013; He et al., 2016; Qureshi et al., 2017). This system was first described in cultured mammalian cells where it was shown that either depletion of mtDNA (Martinus et al., 1996) or accumulation of a misfolded protein in the matrix (Zhao et al., 2002) led to increased expression of nuclear genes encoding mitochondrial proteases and chaperones.

A similar system was found in *C. elegans* and several factors involved in the response were identified using genetic screens (Haynes et al., 2010; Nargund et al., 2012, 2015). As described in recent reviews (Quereshi et al., 2017; Fiorese and Haynes, 2017), these findings have resulted in the development of a complex model for initiating the UPR^{mt} in *C. elegans*. The matrix-localized ClpP protease degrades mitochondrial proteins that are incorrectly folded (Haynes et. al. 2007). The resulting small peptides are exported out of the matrix via the HAF-1 mitochondrial peptide exporter (Haynes et al. 2010). The role and mechanism of action of the peptides released from the mitochondria are currently not well understood. However, it has been

shown (Haynes et. al 2010) that loss of either ClpP or HAF-1 decreased the nuclear localization of the bZIP transcription factors ATFS-1, which is a key factor in regulation of the UPR^{MT}. ATFS-1 is known to activate the transcription of several nuclear encoded mitochondrial proteins including chaperones and proteases (Nargund et al., 2012). The regulation of ATFS-1 activity appears to be controlled by its localization within the cell. This, in turn, depends on the functional status of the mitochondria. The ATFS-1 protein contains signals for both nuclear and mitochondrial localization. In normal growth conditions, the protein is imported to the mitochondria and degraded by that organelle's Lon protease. However, when mitochondrial function is perturbed by various conditions, including misfolding of mitochondrial proteins, there is a decrease in overall mitochondrial protein import efficiency (Nargund et al. 2012; Wright et al., 2001; Wrobel et al., 2015). Such conditions result in the accumulation of ATFS-1 in the cytosol, with eventual translocation to the nucleus, allowing it to function as a transcription factor and express its target genes.

1.9.0 Alternative Oxidase

The alternative oxidase (AOX) is found in all green plants that have been examined, many fungi (notably excluding *Saccharomyces cerevisiae*), some animals, some bacteria and some protists (McDonald and Vanlerberghe 2006; McDonald, 2008; McDonald et al. 2009; Neimanis et al., 2013). In eukaryotes, AOX is encoded by a nuclear gene. In many organisms, AOX is not expressed under normal conditions but is expressed and localized to mitochondria when the function of the sETC is disrupted by chemical inhibitors or mutations (Rogov et al., 2014; Vanlerberghe, 2013a). For example, antimycin A (AA) inhibits electron flow at Complex III, while cyanide (CN) inhibits complex IV. Treatment with either results in the induction of AOX. Another drug used to induce AOX is chloramphenicol (CM). CM works indirectly by inhibiting

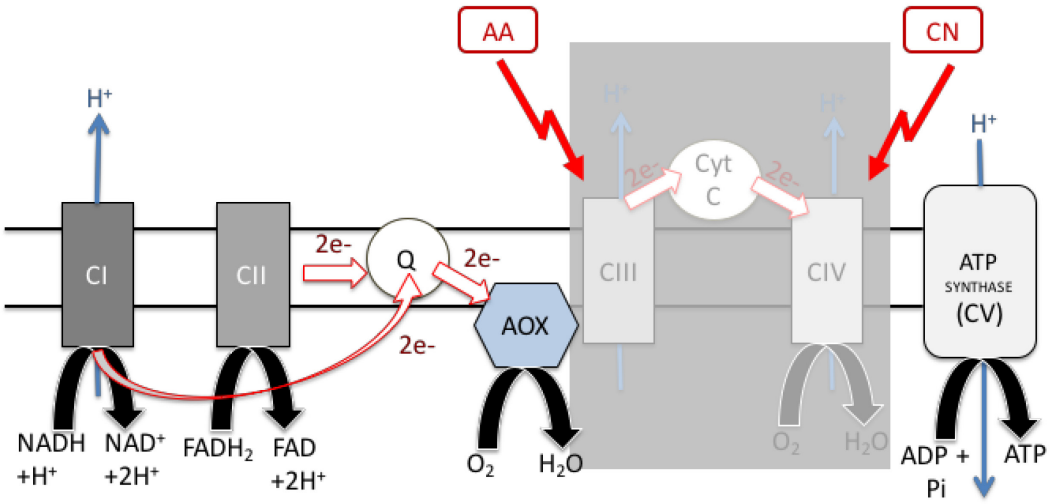

Figure 1.3. The sETC plus AOX. In conditions where the function of Complex III or IV is compromised by a mutation or chemical inhibition (eg: Antimycin A (AA) which affects Complex III or cyanide (CN) which affects Complex IV), electrons are donated directly from coenzyme Q (Q) to AOX which passes them to O_2, the final electron acceptor, converting O_2 to H_2O. In such conditions, Complex I is the only site of proton pumping resulting in a lower rate of ATP synthesis by Complex V.

mitochondrial (but not cytosolic) protein synthesis, thus impairing oxidative phosphorylation by reducing the levels of complexes that contain mitochondrial-encoded subunits (complexes I, III, IV and V) (Fig. 1.3). AOX is inhibited by salicyl hydroxyamic acid (SHAM) and n-propyl gallate. SHAM and n-propyl gallate inhibit AOX by blocking the flow of electrons through AOX.

Because AOX is nuclear-encoded and expressed upon mitochondrial stress, it is also a good model for studying mitochondrial retrograde regulation. The AOX protein is synthesized on cytosolic ribosomes and imported into the mitochondria where it resides on the matrix side of the MIM. In mitochondria, AOX acts as a branching point off the sETC. Electrons from coenzyme Q are transferred by AOX directly to the final electron acceptor oxygen, forming water (Fig. 1.3). The AOX does not pump protons. Therefore, since this alternative pathway bypasses complexes III and IV, complex I is left as the only site of proton pumping. As a result, ATP production still occurs but at a lower rate (Chaudhuri et al., 2006; Schertl and Braun, 2014).

1.9.1 **Taxonomic Distribution of AOX**

The AOX was long thought to exist only in plants and fungi. However, bioinformatics studies in the early 2000 identified AOX in all kingdoms with the exception of Archaebacteria (McDonald et al., 2003; McDonald and Vanlerberghe, 2004; McDonald and Vanlerberghe, 2006). In the animal kingdom, AOX was initially found in four species belonging to the phyla Mollusca, Nematoda, and Chordata (McDonald and Vanlerberghe, 2004). This was later expanded to include 28 animals representing 9 phyla (Porifera, Placozoa, Cnidaria, Mollusca, Annelida, Nematoda, Echinodermata, Hemichordata and Chordata) (McDonald et al., 2009). The presence of AOX in only certain animal lineages is hypothesized to be due to loss of the gene from most animal groups (McDonald et al., 2009). A homologue of eukaryotic AOX has been

found in the alpha-proteobacterium *Novosphingobium aromaticivorans* (Balkwill et al., 1997; Stenmark and Nordlund, 2003). In addition, AOX has been identified in some human parasites including *Trypanosoma brucei,* a parasitic kinetoplastid (flagellated protest) (Chaudhuri et al., 1995)*, Trypanosoma vivax,* also a parasitic kinetoplastid (Suzuki et. al. 2004) and *Cryptosporidium parvum,* another parasitic protist (Roberts et. al. 2004).

AOX has been extensively studied in plants, most notably the Viridiplantae lineage which contains green algae and land plants. Bioinformatic studies originally identified two AOX subfamilies, AOX1 and AOX2 in angiosperms (Considine et al., 2002). The AOX1 subfamily occurs in both eudicots and monocots, while the AOX2 group is exclusive to eudicots (Considine et al., 2002). In general, the AOX1 group is responsive to induction by various stresses while the AOX2 subfamily is either constitutive or developmentally expressed in specific tissues and is not stress responsive (Considine et al., 2002). However, there are occasional exceptions to this rule as some AOX2 genes have been shown to be induced by stress (Cavalcanti et al., 2013; Clifton et al., 2005; Costa et al., 2010). A third AOX subfamily (AOX3) was suggested (Costa et al., 2004), but subsequent analysis placed AOX3 within the AOX2 group (Borecký et al., 2006). The latter study also subdivided the two families into four major clades: Aox1 a, b, c, e; Aox1d; Aod2 a, b, c; and Aox2d. Although study of AOX families has been done most intensely in angiosperms, several other plant families, such as mosses, liverworts, and conifers are now known to contain AOX genes (Neimanis et al., 2013).

AOX is also found in most yeast species, with the notable exceptions of *S. cerevisiae* and *Schizosaccharomyces pombe*. AOX has been found in *Candida albicans* (Costa-de-Oliveira et. al. 2012)*,* and *Cryptococcus neoformans,* (Akhter et. al. 2003) which can cause infections in humans with compromised immune systems. AOX has also been identified in many, if not most,

fungal species including *Aspergillus niger* (Honda et. al. 2012), *Aspergillus fumigatus* (Magnani et. al. 2007), *Podospora anserina* (El-Khoury and Sainsard-Chanet, 2010; Scheckhuber et. al. 2011), and *Neurospora crassa* (Lambowitz et. al. 1989). As in plants, many fungi have been found to have more than one AOX gene. For example, in *N. crassa*, AOX is encoded by the nuclear gene *aod-1* which shares sequence similarity with another gene, *aod-3*. However, no expression of *aod-3* could be detected under any conditions tested (Tanton et. al. 2003). Multigene families of AOX appear to be conserved in only plants and fungi.

1.9.2 Structure of Alternative Oxidase

AOX is a member of the R2-type diiron carboxylate family of proteins (Berthold et. al., 2000). After some debate in the literature, a model for its structure was proposed based on alignments and mutagenesis studies. The protein was suggested to be an interfacial membrane protein, interacting with one leaflet of the MIM on the matrix side. The two iron atoms were suggested to be bound by four glutamate and two histidine residues in a bundle consisting of 4 α-helices (Andersson and Norlund, 1999, Berthold et. al. 2000).

In 2013, the crystal structure of the *Trypanosoma brucei* AOX (TAO) was elucidated, and confirmed many aspects of the earlier model (Shiba et. al. 2013; Moore et al., 2013). The TAO was shown to be a member of the diiron carboxylate family. It was found to exist as a homodimer. Each monomer within the dimer contains a long N-terminal arm, six long α-helices (α1-α6) and four short helices (S1-S4). The long helices form an anti-parallel four-helix bundle to accommodate the diiron center active site with each monomer shaped as a cylinder (excluding the N-terminal arm) (Fig. 1.4). The dimer interface contains six residues that are conserved in all known AOX sequences as well as eight other residues that are very highly conserved. This

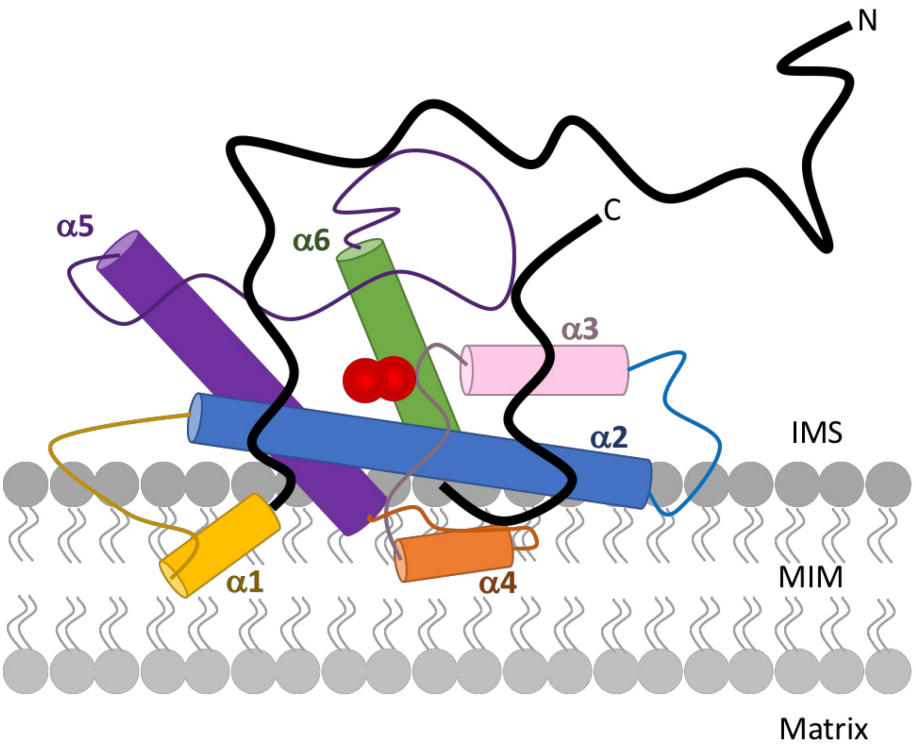

Figure 1.4. Structural model of the *Trypanosoma brucei* AOX (TAO). The TAO contains six long α-helices (α1 - α6) and four short helices (not shown). Additionally, although the TAO is dimeric, only one monomer is shown for simplicity. The N and C terminal regions are shown in dark black and indicated by N for N-terminal and C for C-terminal. The N-terminal extends to the other monomer (not shown). The diiron shown in red associates with the α2, α3, α5 and α6 helices. AOX is presumed to be anchored in the inner leaflet of the MIM by the α1 and α4 helices. The lipid bilayer is represented in grey. The figure was adapted from the TAO crystal structure by Shiba et. al. (2013).

suggests that the dimeric structure may be common to all AOXs. Furthermore, consistent with the earlier model, the dimer is bound interfacially in the MIM by a hydrophobic region made of the α1 and α4 helices as well as parts of α2 and α5 (Fig. 1.4). The diiron site, as predicted by spectroscopic studies, is an oxidized Fe(III)-Fe(III) with a single hydroxo-bridge. The diiron center together with four glutamate and two histidine residues form the active site within a hydrophobic pocket. These six residues are fully conserved in all AOXs. An unexpected finding was that unlike other proteins with oxidizable diiron active sites, the two His residues in the TAO active site were found to form hydrogen bonds with other residues in the site but not to bind directly to the iron atoms. Consideration of previous mutagenesis studies identifying residues that affected the activity of the enzyme, along with modeling of the crystal structure, suggested two hydrophobic channels through which the enzyme substrate, ubiquinol (reduced coenzyme Q)5, could access the active site from the MIM. It was speculated that a third channel might allow the entrance of oxygen and the exit of water (Shiba et. al. 2013; Moore et. al. 2013).

1.9.3 Functions of AOX

AOX is predominately described as a terminal oxidase that acts as an alternative to the cytochrome *c* oxidase of the sETC and is induced in the event of sETC perturbations. However, AOX may have a much wider range of functions depending on the organism and tissue. For example, thermogenic plants use AOX for heat generation. The heating of reproductive organs above ambient temperatures can be used to volatilize chemicals to attract pollinators or to aid floral development (Watling et. al., 2008).

AOX has an important influence on ROS generation by mitochondria, which depends on the reduction state of sETC components. There is now *in planta* evidence that AOX prevents the

over-reduction of these components that lead to electron leaks. In tobacco, leaves with suppressed AOX showed an increase in localized mitochondrial O_2^- (Cvetovska and Vanlerberghe, 2012). Additionally, AOX can reduce the accumulation of nitric oxide, which is also produced in mitochondria via single electron leaks from the sETC (Planchet et. al . 2005). Studies in Arabidopsis as well as tobacco have shown that a lack of AOX results in upregulation of ROS-scavenging enzymes (Amirsadeghi et. al. 2006; Giraud et. al. 2008). Work in plants has also defined a relationship between various stresses and mitochondrial metabolism to the expression of AOX. These have recently been summarized by Del-Saz et. al. (2018). For example, a link exists between AOX activity and ascorbate synthesis. Studies in AOX-overexpressing *Arabidopsis* showed an increased accumulation of ascorbic acid compared to wild-type plants (Bartoli et al., 2006). However, this observation appears to be confined to Arabidopsis AOX (Wang et al., 2011).

There is a convincing role for AOX in temperature stress, as studies in numerous species have revealed an upregulation of AOX transcripts and/or protein in the presence of low temperature growth conditions. For example, studies of cold-sensitive maize subjected to short-term cooling treatment (5°C for 5 days) revealed an increase in AOX activity, as well as a redirection of the majority of respiration to the AOX (Ribas-Carbo et. al. 2000). A similar observation was made in *Arabidopsis* (Armstrong et al., 2008). Another study in Arabidopsis showed an impairment in leaf development as well as a reduction in rosette size in AOX knockdown plants when the plants were grown at 12°C compared to plants grown at 23°C (Fiorani et al., 2005). One possible explanation for elevated AOX levels in low temperature conditions comes from a study where transgenic AOX-suppressed tobacco plants had an upregulation of transcripts encoding ROS-scavenging enzymes compared to wild-type plants

when transferred to growth in colder temperatures. As a result, these plants had a decrease in oxidative damage (Wang et al. 2011). As such, AOX may be playing a role in modulating ROS stress-signaling pathway activity. As well as temperature stress, AOX may also play a role in drought stress. Drought conditions were shown to increase AOX activity in soybean leaves, where AOX consumed 30% more O_2 in drought conditions compared to normal conditions (Ribas-Carbo et. al. 2005).

Nutrient limitation has also been shown to increase AOX activity. Phosphate deficiency results in a strong reduction of P_i, which is required for oxidative phosphorylation. A study conducted in P_i-deficient bean roots observed as increase in the activity of AOX compared to bean roots grown on complete nutrient medium. Therefore, AOX was postulated to have a role in maintaining carbon metabolism and electron flow during phosphate deficiency (Rychter and Mikulska, 1990). In support of this idea, another study in tobacco cells lacking AOX showed that phosphate deficiency resulted in a decreased rate of respiration, an increase in cellular ROS levels and an accumulation of carbohydrates (Parsons et al., 1999; Sieger et al., 2005). Salt stress also negatively impacts mitochondrial function, increasing mitochondrial ROS and impeding the function of the sETC (Mittova et. al .2003; Mittova et. al. 2004; Chen et. al. 2009). Interestingly, salt stress has also been shown to increase AOX transcript and protein levels in a number of plant species, including *Arabidopsis* (Kreps et. al. 2002) and tobacco (Andronis et. al. 2010).

Metal toxicity has been shown to impact the function of sETC proteins. In acidic soils, aluminum limits the growth of plants, and was found to inhibit respiratory oxygen consumption in several plant species (Yamamoto et. al. 2002). Furthermore, studies in Arabidopsis have shown that aluminum causes sETC dysfunction and promotes leakage of electrons (Li and Xing, 2011). This was correlated to an increase in the capacity of AOX respiration, possibly as a

cellular response to the sETC disruption. Studies done in the *Euglena* protist have shown that cadmium, which also interferes with sETC function, induces AOX (Castro-Guerrero, et. al. 2008).

Work with plants and bacterial pathogens has revealed that AOX may be a potential regulator of a mitochondrial O_2^- based signaling pathway that determines plant response to bacterial infection. One study examined a strain of *Pseudomonas syringae* infecting tobacco plants. *Phaseolicola,* a pathogenic variety of *P. syringae* that causes necrosis in bean plants, induced AOX and mitochondrial superoxide dismutase (MnSOD) (Cvetkovska and Vanlerberghe, 2012).

AOX function studies in animals are limited because the enzyme has only recently been identified in a limited number of animals. Transgenic studies have attempted to assess the effect of AOX in human tissue culture cells, and other organism that do not natively express AOX. For example, when the AOX gene from the tunicate *Ciona intestinalis* was expressed in cultured human cells, the cells became resistant to inhibitors of complex III and IV (see Fig. 1.3) (Hakkaart et. al. 2006). AOX may eventually serve a use as a by-pass therapy for human patients with complexes III and/or complex IV deficiencies. *C. intestinalis* AOX, for example, was expressed in mice with no negative effects. Following chemical inhibition of the respiratory chain in the transgenic mice, the presence of AOX led to decreased production of ROS, enabled cyanide-resistant respiration, and enabled viability in the presence of concentrations of hydrogen cyanide that are normally lethal (El-Khoury et al., 2013; Szibor et al., 2017). However, in at least some studies, the expression of AOX in non-native animal systems has been shown to have detrimental effects. For example, when *C. intestinalis* AOX was expressed in *D. melanogaster* males, they displayed a significant decrease in the number of mature sperm cells produced (Saari

et. al. 2017).

In fungi, there is a role for AOX in mitochondrial energy production, as AOX inhibition in isolated and/or whole cell mycelia caused rapid collapse of mitochondrial membrane potential in several fungal species, such as *Fusarium oxysporum* and *Gaeumannomyces graminis* (Joseph-Horne et. al. 1998; Joseph-Horne et. al. 2001). Furthermore, inhibition of AOX in *G. graminis* decreased the rate of ATP synthesis regardless of whether or not electron flow could occur through complex III (Joseph-Horne et. al. 1998). Certain fungal pathogens have been shown to depend on AOX for maximal ability to infect their host. This has been shown for *Cryptococcus neoformans* (Cox et al., 2003), *Aspergillus fumigatus* (Magnani et al., 2008), and *Paracoccidioides brasiliensis* (Ruiz et al., 2011), and *Moniliophthora perniciosa (Thomazella et al., 2012).*

1.9.4 Regulation of AOX transcription

The majority of work done on regulation of AOX has been in plants such as *Arabidopsis* and in fungi. Many previous studies (some highlighted in section 1.9.3) have shown that AOX genes are either constitutively expressed at specific stages, organs or tissues during development or are induced by a number of different stress factors and other outside stimuli (Vanlerberghe, 2013b). As outlined in section 1.9.1, the groups of plant AOX are generally considered as inducible (AOX1 group) or constitutive or developmentally regulated (AOX2).

There are at least two pathways that induce plant AOX: ROS-independent or ROS-dependent. ROS-independent induction has been well studied in tobacco, where, for example, the addition of citrate is capable of inducing both AOX transcript and protein without increasing ROS (Vanlerberghe et. al. 1998; Gray et. al. 2004b). The ROS-dependent pathways of induction

provide a response to various stresses since many induce ROS production. Although AOX is a multigene family, many organisms have one AOX gene of the family that is most responsive to stress and other stimuli. For example, in an *Arabidopsis* study, plants were exposed to five different abiotic stresses: heat, drought, salt, cold, or intense light. A microarray analysis confirmed all stresses, with the exception of intense light, induced *AOX1a* expression (Mittler et. al. 2004). The regulation of *AOX1a* in *Arabidopsis* was studied using deletion and mutageneic analysis of the gene promoter. This study resulted in the identification of a region important for strong induction of the gene by chemicals like monofluoroacetate (MFA) and AA which inhibit the TCA cycle and complex III, respectively. A 93bp region in the promoter of the *AOX1a* gene was identified as important for maximum expression in the presence of either AA or MFA. Based on these studies, researchers concluded that a complex set of interactions are required at the promoter to induce strong AOX expression (Dojcinovic et. al. 2005). Another study examined variation of AOX expression in stress-sensitive and stress-tolerant genotypes of *Vigna unguiculata* (cowpea) (Costa et al., 2007). The study examined transcript and protein expression of VuAox1, VuAox2a, and VuAox2b in the roots of the two strains after exposure to salt and osmotic stress. VuAox1 and VuAox2a remained unchanged in both cultivars. VuAox2b was expressed at low levels under salt stress conditions but was induced under osmotic stress in the tolerant cultivar. On the other hand, in the sensitive cultivar, VuAox2b was overexpressed under salt stress conditions, but not under osmotic stress.

In fungi, AOX induction usually occurs in response to inhibition of the sETC. Therefore, studies have focused on AOX expression in response to perturbation of the sETC by chemicals such as AA and CN: inhibitors of complex III and IV, respectively. For example, in *Magnaporthe grisea,* nuclear run-on assays showed that AOX transcription is constitutive under

normal conditions. However, the transcript produced was found to be actively degraded (Yukioka et al., 1998a). When the fungus was exposed to an inhibitor of sETC Complex III (called SSF-126), transcription was induced and the alternative pathway became functional (Mizutani et al., 1995; Yukioka et al., 1998a). Potential regulatory elements in the promoter region of *M. grisea* have been identified (Yukioka et al., 1998b) but have not been directly tested for a role in expression. *Candida albicans* contains two AOX genes called AOX1a and AOX1b. AOX1a was shown to be constitutively transcribed at low levels. Growth in the presence of sETC inhibitors or ROS, such as hydrogen peroxide, was required to express AOX1b. It was also found that a histidine kinase was required for maximal AOX activity (Huh and Kang, 2001). In *N. crassa*, various genes required for *aod-1* expression have been discussed. The best studied are the zinc cluster transcription actors *aod-2* and *aod-5.* Orthologues of these factors have also been described in *P. anserina* and *A. nidulans.* These studies are described in section 1.10.

Certain animals found to contain AOX have been investigated with respect to AOX expression. AOX transcripts were found in the gill, heart, adductor muscle, haemolymph and mantle tissues of *Crassostrea gigas* (Pacific oyster) (MacDonald et. al. 2009). EST data has indicated that AOX transcripts can be detected in *C. gigas* that is exposed to bacterial or sewage challenge (Medeiros et al., 2008; Roberts et al., 2009). Furthermore, AOX transcripts have been found in some tissues of some species of gastropod, particularly in the central nervous system (MacDonald et. al. 2009). Other animals where AOX transcripts have been found include some annelids and two members of Ecdysozoa (protostome animals) (MacDonald et. al. 2009). Studies of AOX in animals have not yet focused on regulation of these transcripts (MacDonald et. al. 2009).

AOX is found in some bacteria, such as *Vibrio fischeri,* a symbiotic bioluminescent

bacterium found in the Hawaiian bobtail squid. RT-PCR studies and reporter assays determined that *aox* expression in *V. fischeri* is induced by nitric oxide (NO). This induction is prevented by the NsrR protein, a known NO-responsive regulatory protein, in the absence of NO. A binding site for the protein was identified upstream of the coding sequence of AOX via bioinformatics. Deletion of NsrR further showed that the protein negatively regulates *aox* expression (Dunn et. al. 2010).

The mechanism of transcriptional control of AOX is not fully understood in any organism, however positive regulators and negative regulators of transcription have been identified in various organisms, and continue to be discovered. There are kinases, such as CDKE1, that were identified by genetic screen in *Arabidopsis* known to influence AOX transcript expression. CDKE1 is associated with cell division and development. In *Arabidopsis*, mutations in CDKE1 result in a flowering defect phenotype (Wang and Chen, 2004). Further studies showed that CDKE1 mutations had reduced *AOX1a* transcripts by 30-50%. A decrease in AOX protein was also observed in CDKE1 mutants (Ng et. al. 2013a).

A transcription factor called AB14 has been shown to be a negative regulator in *Arabidopsis*. AB14 repressed AOX1a by binding to a 5 bp region located upstream of the transcriptional start site of AOX1a. Absence of AB14 resulted in a highly active promoter. Furthermore, this study showed that AOX1a is constitutively repressed by transcription factors in the absence of a signal to induce AOX1a. (Giraud et. al. 2009). In *Arabidopsis*, ANAC013 and ANAC017 (De Clercq et. al. 2013) have been shown to induce *AOX1a*. ANAC013 and ANAC017 are NAC transcription factors. NAC transcription factors are named after three transcription factors that share the same DNA-binding domain: NAM (no apical meristem), ATAF1-2 (*Arabidopsis thaliana* activating factor) and CUC2 (cup-shaped cotyledon)

(Nuruzzaman et al., 2015). They are required for plant growth and development, as well as response to environmental stresses. CHiP experiments followed by qPCR showed greater than 10-fold enrichment for ANAC013 binding for the AOX1a promoter in *Arabidopsis* compared to negative control genes only when seedlings were grown in the presence of AA. Furthermore, overexpression of ANAC013 led to significant increase in AOX1a protein levels. In ANAC017 mutant lines, *Aox1a* transcripts in the presence of AA decreased by approximately 50% and protein amounts decreased by four-fold (Ng et. al. 2013b).

Different WRKY transcription factors (named so after conserved amino acid sequences) also induce Aox1a in *Arabidopsis.* WRKY transcription factors respond to many factors, including both abiotic and biotic stresses, senescence, seed dormancy and germination, and some developmental processes. W-box (TTGAC) sites, where WRKY transcription factors bind, were found in the *Aox1a* promoter (Dojcinović et al., 2005). Various studies on these WRKY proteins have revealed roles in AOX regulation in *A. thaliana.* A study using a yeast one hybrid system identified 12 WRKY proteins capable of binding the W-boxes in the *Aox1a* promoter (Van Aken et al., 2013). Binding at one of the two W boxes was confirmed for WRKY57, -63, and -75 using EMSA analysis. The WRKY40 protein was shown to be a negative regulator of *Aox1a* since, in the presence of AA, transcript levels were doubled in a WRKY40 mutant. WRKY63 was found to be a positive regulator under high light stress (Van Aken et al., 2013).

Some hormones (Rhoads and McIntosh, 1992; Ederli et. al. 2006) are known to induce *AOX1a*, as well. In tobacco plants, treatment of leaf discs with ethylene, jasmonic acid, and sodium nitroprusside resulted in elevated *Aox1a* transcripts (Ederli et al., 2006).

1.9.5 Post-translational regulation of AOX

Post-translational regulation of AOX has been well studied in plants and mechanisms have been identified. Most plant AOX isoforms have two conserved cysteines, Cys_1 and Cys_2, that allow for modifications that influence the activity of the enzyme. As discussed in section 1.9.2, the crystal structure of AOX revealed that it exists as a homo-dimer. The dimers can exist in a noncovalent association, where Cys_1 is reduced on both subunits. Alternatively, the dimers can be covalently linked, where the Cys_1 sulfyhydryl groups are oxidized and form an intermolecular disulfide bridge been the two monomeric subunits. The latter results in a less active version of the protein (Umbach and Siedow, 1993; Berthold et. al. 2000; Rhoads et. al. 1998).

A second type of regulation at the post-translational level is observed when the Cys_1 residues are reduced. The enzyme becomes activated in the presence of alpha-keto acids, such as pyruvate. Activation by pyruvate is eliminated if Cys_1 is substituted with other amino acids, but a similar effect was not seen for Cys_2 (Rhoads et. al. 1998; Vanlerberghe et. al. 1998). Plant AOX can also be activated by glyoxylate, another α-keto acid. Mutated strains of the glyoxylate stimulation showed that it occurs when either Cys_1 or Cys_2 was individually present in the enzyme (Umbach et al., 2002; Umbach et al., 2006). The mechanisms of activation are not well understood. There also appears to be differences in the activation between thermogenic and non-thermogenic plants, based on other conserved sequences in the two groups, as reviewed by Moore et al. (2013).

The vast majority of plant species investigated have the Cys_1 and Cys_2 residues. However, a few plant species, such as *Nelumbo nucifera* (sacred lotus) do not possess a Cys_1 and therefore cannot form disulfide linked dimer. A unique third cysteine residue (Cys_3) is found in

the protein, but its function is currently unknown (Grant et al., 2009).

1.10 *Neurospora crassa* AOX

Cyanide-resistant respiration was first observed in the *Neurospora crassa* mtDNA "[*poky*]" mutants (Tissieres et al., 1953), which are characterized by extremely low levels of cytochrome aa_3 and *b* (related to complex IV and III, respectively) and high levels of cytochrome *c* (Lambowitz and Slayman, 1971). [*poky*] mutants were of considerable interest because *N. crassa* is an obligate aerobe, and despite their extreme deficiency of the two complexes, [*poky*] cells were still viable and respiring (Mitchell and Mitchell, 1952; A. Haskins et al., 1953). A later study concluded that wild-type had a very low level of AOX but [*poky*] mutants had a high level of a cyanide-insensitive AOX. Furthermore, the activity of the AOX in wild-type cells could be increased by as much as 20-fold by growth in the presence of AA, CN, or CM (Lambowitz and Slayman, 1971).

Further investigation of *N. crassa* AOX and its expression was done using a genetic screen (Bertrand et. al., 1983). Strains were exposed to N'-nitro-N-nitrosoguanidine and then grown in the presence of AA. The logic of the selection was that AA should inhibit the sETC. Normal strains would still be capable of growth via the alternative pathway using AOX. However, if a strain was mutated to prevent the AOX function, it would not grow in the presence of AA. Strains unable to grow in the presence of AA were chosen as potential AOX mutant gene candidates. Twenty-seven strains were isolated and their mutations were found to fall into two complementation groups named *aod-1* and *aod-2*. Radiolabelling of proteins synthesized under both AOX inducing and non-inducing conditions showed a polypeptide that was not present in non-inducing conditions in any strain, but was seen in induced wild-type cultures and in 19 of 20

aod-1 mutants examined. The protein was thought to be associated with AOX activity and the mutants were expressing an inactive form of the protein. The protein was later confirmed to be AOX using a monoclonal AOX antibody derived against the *S. guttatum* AOX (Lambowitz et. al. 1989). The strains in the *aod-2* complementation group did not contain this protein following growth in either non-inducing or inducing conditions. Therefore, *aod-2* was thought to play a role in regulation of AOX synthesis (Bertrand et. al. 1983).

Cloning and sequencing analysis of the *N. crassa aod-1* gene by Li et. al (1996) showed that the gene encodes a protein of 362 amino acids and contains two introns. The 41.4 kDa size of the protein is reduced to 34.7 kDa after cleavage of the mitochondrial targeting sequence. Typically, the protein is only expressed when the sETC is disrupted by chemicals such as those listed in 1.9.0. The sequence in the upstream region of the gene suggested possible regulatory sequences, such as a cAMP responsive element (CRE) found 746 bp upstream from a putative transcription start site also identified in the study. As well, a TATA box, and a CAAT box were identified in the sequence. However, promoter deletion studies later revealed that the CRE was not essential for AOX induction (Tanton et. al. 2003). A second AOX encoding gene was identified in *N. crassa* using BLAST analysis of the *Neurospora* genome (Tanton et. al 2003). However, Northern blot studies were unable to show expression of *aod-3* under any growth conditions, despite its sequence similarity to *aod-1*.

To identify other genes that may be involved in the regulation of AOX, a tyrosinase reporter gene was fused to 3.3 kb of DNA from upstream of the *aod-1* coding sequence. The construct was transformed into a *N. crassa* tyrosinase null strain. Conidia from the transformed strain were exposed to EMS, and potential regulatory mutants were identified based on their ability to express the *tyrosinase* gene, which turned colonies brown in the presence of tyrosine.

Colonies that remained white were identified as potential regulatory mutants. Complementation studies revealed four novel genes: *aod-4, aod-5, aod-6,* and *aod-7* (Descheneau et. al. 2005).

Gene rescue experiments, sequencing, and bioinformatics (Chae et. al. 2007b) identified *aod-2* and *aod-5* as zinc cluster transcription factors. Both transcription factors were found to contain a nuclear localization signal, and a per-arnt-sim (PAS) domain located near the C-terminus. The PAS domain is commonly found in proteins that are involved in signal transduction (Möglich et al., 2009). Earlier promoter deletion studies had identified a 255 bp region upstream of the *aod-1* transcription start site to be necessary for the proper expression of AOX (Tanton et. al. 2003). This work and further mutation studies led to the identification of the alternative oxidase induction motif (AIM). The motif consists of a set of CGG repeats separated by 7 nucleotides (Chae et. al. 2007a). It was predicted that the AIM binds an activator of transcription, as loss of the site reduces expression of AOX. Furthermore, EMSA experiments showed that the AOD2/AOD5 transcription factors bind to the AIM synergistically (Chae et al., 2007b). The two proteins could also be isolated as a heterodimer from cell extracts (Chae and Nargang, 2009). The existence of the heterodimer was later confirmed by co-immunoprecipitation experiments (Qi et al., 2016). Orthologues of AOD2 and AOD5 exist in other fungi. For example, *Aspergillus nidulans* transcriptional activators AcuM and AcuK, and *Podospora anserina* transcription factors Rse2 and Rse3 are orthologues of AOD2 and AOD5, respectively, and are required for induction of AOX in those organisms (Suzuki et. al. 2012; Bovier et. al. 2014).

1.11 AOD2/AOD5 ChIP-Seq

Chromatin immunoprecipitation and sequencing (ChIP-seq) experiments were conducted

by our lab in 2016 to determine if other promoters in the *N. crassa* genome are bound by the AOD2/AOD5 transcription factors (Qi et. al. 2016). Many other binding sites were identified suggesting that other genes are regulated by these transcription factors. This was confirmed by qPCR analysis of transcripts for several of the identified genes in wild-type and *aod-2* and *aod-5* mutants. Many of the genes play a role in metabolic pathways and energy production. The data also revealed that the transcription factors are constitutively bound to the promoter of *aod-1* and other genes. Therefore, activation of the transcription factors appears to be dependent on one of more unknown signal(s) present in certain conditions that activate the proteins in the nucleus.

The most robust peaks of binding for AOD2 and AOD5 were located between two divergently genes: NCU06939 (an endosome-associated ubiquitin isopeptidase) and NCU06940 (a hypothetical protein). The peaks were observed in strains grown either in the absence or presence of CM (Fig. 3.1). Given the large amount of AOD2/AOD5 binding at this site, I hypothesized that one or both of these genes is regulated by these transcription factors. Conceivably, the gene(s) might complement AOX function or provide a response to another stress. The first part of this thesis identifies NCU06940 as requiring AOD2/AOD5 for its expression and explores its possible function.

1.12 Alternative oxidase expression in *Neurospora crassa* strain T1P11

Past work using Northern Blot analysis in our lab revealed that *aod-1* mRNA is rarely detectable in wild-type cultures grown in non-inducing conditions, but is readily detectable in cultures grown in the presence of chloramphenicol, AA, and in cytochrome-deficient mutants (Li at. al. 1996; Tanton et. al., 2003). Later, nuclear run-on experiments showed that AOX is constitutively transcribed in very low amounts under non-inducing conditions and that the low

level of transcript is not translated into protein. RT-PCR experiments confirmed this observation (Chae et. al. 2007b). However, exceptions do exist. Randomly, relatively high levels of *aod-1* transcript have been observed occasionally in uninduced wild-type cultures (Tanton et. al. 2003). Furthermore, a *tyrosinase* mutant *N. crassa* strain, T1P11, consistently had readily detectable levels of *aod-1* mRNA in uninduced conditions as determined by Northern blot analysis. However, a Western blot revealed that these detectable transcripts were not being translated into protein (Descheneau et al., 2005). To determine if the *tyrosinase* mutation was responsible for the upregulation, a cross between T1P11 and a wild-type (NCN233) was performed, and progeny were analyzed for *aod-1* mRNA levels. The tyrosinase mutation and the high levels of *aod-1* transcripts were found to segregate independently (Descheneau et. al. 2005). Therefore, some other unknown factor(s) has a role in the regulation of *aod-1* gene expression. The remainder of this thesis focuses on the transcriptional and post-transcriptional factors that influence the expression of *aod-1* transcript and protein, particularly in the T1P11 strain.

1.13 FlbA

As will be seen in the Results section, my work led me to the discovery of the FlbA protein as a possible player in *aod-1* regulation. The protein is known as a regulator of G-proteins (RGS) in other systems. Therefore, I will briefly review G-proteins and previous work on FlbA. The gene name was coined in the original paper describing flbA in *Aspergillus nidulans* (Lee and Adams, 1994). Mutants had a fluffy phenotype and low expression of a gene required for conidiophore development, called brIA. Thus, fluffy low brIA expression (flbA).

Heterotrimeric G-proteins are membrane-bound proteins that are conserved from yeast to humans. In fungi, G-proteins play important roles in many processes, including cell division,

mating, cell fusion, morphogenesis, chemotaxis, as well as production of secondary metabolites (reviewed in Morris and Malbon, 1999; Neves et al., 2002; McCudden et al., 2005). G-proteins consist of α, β, and γ subunits which play a role in transduction of extracellular signals resulting in a response at the cellular level. When a ligand binds a G-protein coupled receptor (GPCR), activation is mediated by GTP/GDP exchange on the Gα subunit. When activated, the GTP-bound Gα subunit dissociates from the Gβγ dimer. The Gα and Gβγ dissociated proteins can then amplify and propagate signals by modulating a number of effectors. For example, fungi have three main pathways of transmitting G-protein signaling: 1) adenylyl cyclase-cAMP-dependent protein kinase (PKA) 2) mitogen-activated protein kinase (MAPK) pathways; and 3) IP3-[Ca++]-DAG (diacyl-glycerol)-dependent protein kinase C (PKC) (Morris and Malbon, 1999; Feldbrügge et al., 2004; McCudden et al., 2005).

The typical GPCR protein consists of 7 transmembrane spanning (or hepta-helical) domains. The *N. crassa* genome has 10 GPCRs that fall into five classes: pheromone receptors, cAMP receptor-like proteins, carbon sensors, putative nitrogen sensors, and microbial opsins (reviewed in Xue et al., 2008). In *A. nidulans*, the Gα subunit is known as FadA (fluffy autolytic dominant) and was discovered by investigating an uncontrolled vegetative growth phenotype followed by autolysis (Yu et. al. 1996). *Neurospora crassa* has 3 Gα subunits: GNA-1, GNA-2, and GNA-3. Δ*gna-1* strains are growth defective and have reduced mycelial mass compared to wild-type strains (Ivey et al., 1996)). Both Δ*gna-1* and Δ*gna-2* have decrease cAMP levels and adenylyl cyclase activity (Ivey et. al. 1999).

RGS proteins regulate G-protein signaling by controlling the specificity and intensity of the signaling pathways. This is typically done by regulating the rate of GTP hydrolysis by the Gα subunit. The first RGS protein was discovered in *S. cerevisiae*, and was called SST2. It was

shown to be involved in regulating the signaling pathway in response to mating pheromone (Dohlman et. al. 1996). In *Aspergillus fumigatus*, 6 putative RGS proteins have been identified, including flbA, RgsA, RgsB, RgsC, RgsD, and GrpK (Yu et al., 1996; Lafon et al., 2006; Han et al., 2004). FlbA was one of the first studied, and was found to play a role in vegetative growth signaling mediated by G-proteins. The *flbA* loss of function mutation results in the loss of GTPase activity of the GPCR, and results in uncontrolled proliferation of vegetative cells, lack of development, and autolysis (Yu et al.,1996). This is similar to constitutively active FadA phenotypes in *Aspergillus nidulans*, as FlbA negatively regulates FadA. In *Aspergillus fumigatus*, FlbA downregulates hyphal proliferation by inactivating GpaA, the *A. nidulans* homologue of FadA (Yu et al., 2006; Mah and Yu, 2006).

Deletion studies of *flbA* have been well investigated in *Aspergillus*. *ΔflbA* studies in *Aspergillus niger* have shown that the secretome of the fungus is impacted. Furthermore, strains with the *ΔflbA* mutation display a "fluffy" phenotype, where mycelium forms masses of undifferentiated aerial hyphae and conidiate poorly (Krijgsheld et al., 2013). Deletion of cAMP-dependent protein kinase A catalytic subunit gene *pkaA* does not cause conidiation defects suggesting that conidiation defects of the FlbA mutants are cAMP independent (Krijgsheld et al., 2013). *ΔflbA* strains also exhibit thin cell walls and cell lysis (Krijgsheld et al., 2013). Interestingly, conidia production in *N. crassa* was reported to be normal for *flbA* (NCU08319) knock out mutants. However, the protoperithecia, which is the structure that develops into the sexual fruiting body, were noted as having abnormal morphology. The mature perithecia, asci, and ascospores are not formed. This phenotypic data is available for *N. crassa* on FungiDB (http://fungidb.org/).

1.14 Objectives of this study

ChIP-seq performed by Zhigang Qi in our lab (Qi et. al. 2016) identified a number of promoters bound by the AOD2/AOD5 transcription factors. The most robust binding peak was determined to be in the upstream region of two divergently transcribed genes: NCU06939 (an endosome-associated ubiquitin isopeptidase) and NCU06940 (a hypothetical protein). The start of my first project involved determining if either or both of these genes were controlled by AOD2 and AOD5. It was conceivable that one of these genes may complement AOX function or possibly provide another stress response. Preliminary qPCR analysis of the NCU06940 knock-out strain revealed a chloramphenicol response. Various tests were undertaken on the knock-out strain to determine if the hypothetical protein had a role in stress.

My second project focused on a tyrosinase mutant (*T*ˉ) strain of *N. crassa,* T1P11. This strain was observed to consistently contain readily detectable levels of *aod-1* transcripts in the absence of any AOX inducer, unlike standard wild-type strains. However, no AOD1 protein was detected in the mitochondria (Note that AOD1 is the specific product of the *aod-1* gene in *N. crassa* that corresponds to the general AOX). Because T1P11 does contain transcript and protein when grown in inducing conditions, this raises two questions with respect to AOX in this strain. First, why are transcripts produced at a relatively high level in non-induced cells? Obvious possibilities included mutations in either the *aod-1* promoter or the AOD2 or AOD5 transcription factors. However, no such mutations were found. Therefore, I hypothesized that an unknown mutation in in another gene may be regulating *aod-1* transcript abundance. I began to analyze progeny obtained from a wild-type (NCN233) and T1P11 cross. My investigation included qPCR analysis as well as whole genome sequencing of progeny and parental strains. The second question was, if *aod-1* mRNA is present, why is there no AOD1 protein observed? My

hypothesis was that a control mechanism prevents translation of the *aod-1* mRNA in uninduced cells. I examined various mechanisms that might account for the lack of AOD1 protein in strains that contain high levels of *aod-1* transcript.

2.0 Materials and Methods

2.1 Handling and growth of *N. crassa* Strains

Table 2.1 lists the strains used in this study. Unless otherwise stated, all handling and growth of *N. crassa* strains was conducted as previously described by Davis and De Serres, (1970). Conidia for growing liquid cultures were produced by inoculating conidia in the center of 250 mL or 125 mL Erlenmeyer flasks containing 50 or 25 mL, respectively, of Vogel's salts, with sucrose as the carbon source (unless otherwise stated), trace elements, biotin (VSuTB), and solidified with 1.5% agar. Any additional supplements were added as required. The most commonly used supplement was pantothenic acid. Flasks were incubated for two to three days at 30°C (unless otherwise stated) and were then removed from the incubator to allow conidiation to occur in a well-lit room for four to five days. Conidia were used at no more than 10 days after formation. Stocks were maintained on agar slants containing VSuTB (and pantothenic acid, if required) and kept frozen at -80°C

Liquid cultures were grown by collecting conidia from solid agar VSuTB flasks using sterile dH_2O. Conidia were counted using a hemocytometer, and added to VSuTB liquid medium at a concentration of 10^6 conidia/mL, followed by shaking at 30°C for 12 to 18 hr, or as indicated. When required, CM (at a final concentration of 2 mg/mL) or AA (at a final concentration of 0.5 μg/mL) were added to media.

2.2 Measurements of Growth Rate

Conidia were harvested, counted, and suspended at a final concentration of 10^5 conidia/mL. If pelleting was necessary to increase the concentration of conidia, the suspension was spun in an IEC model CL clinical centrifuge (Damon IEC, Needham Heights) at top speed

for two min. 10 µl of the 10^5 conidia/mL suspension was inoculated on the center of a petri dish containing standard agar solidified VSuTB (and any required supplements) with various carbon sources: sucrose at 1.5%, acetate at 50 mM, glycerol at 2% or glucose at 2%. If required, CM or AA were added at the concentration given in section 2.1. Measurements of hyphal growth across the plate were taken roughly every 7 to 14 hr following growth at different temperatures as stated.

2.3 Quantitative Real Time Polymerase Chain Reaction (qPCR)

To isolate RNA, conidia were grown in liquid cultures as stated above for 12-14 hours in –CM conditions or 16-18 hours in +CM conditions. Mycelium pads were obtained via vacuum filtration. A portion of the pad weighing approximately 100 mg fresh weight was flash frozen in liquid nitrogen. All equipment (glassware, Buchner funnels, forceps, mortars, pestles, and aluminum foil) were baked at 240°C for at least 24 hrs to eliminate RNAse contamination. RNA was isolated using the Qiagen RNeasy Plant Kit following the manufacturer's instructions for fungi (Qiagen Inc, Hilden, Germany). RNA concentrations were measured using a Nanodrop ND 1000 spectrophotometer (Thermo Scientific, Rockford) and RNA integrity was analyzed using the Bioanalyzer 2100 Nano chip (Agilent Technologies, Santa Clara). cDNA was synthesized using 1 µg of RNA per reaction with Superscript III (Invitrogen, Carlsbad) and was diluted 20-fold with DNAse-free dH_2O for use in qPCR. qPCR was performed using the StepOnePlus RT-PCR system (Applied Biosystems, Foster City) provided by the Kirst King-Jones lab. The reactions contained 2.5 µL of 20-fold diluted cDNA, 2.5 µL diluted primer and 5 µL KAPA SYBR® Fast qPCR master mix (KAPA Biosystems, USA) for a total volume of 10 µL per well on a 96-well plate. β-tubulin was used as an endogenous control for ΔΔCt analysis. Unless stated otherwise, all qPCR data is based on four biological replicates and three technical replicates.

2.4 Mitochondrial and cytosolic fractions isolation

250 mL liquid VSuTB (with additional supplements as necessary) cultures were grown for 16 hr without CM and 18 hr in the presence of CM (unless stated otherwise). Cultures were vacuum filtered to obtain mycelium pads. Pads were kept on ice until they could be processed. Mycelia were broken by grinding with sand and mitochondria were isolated using the buffers and differential centrifugation procedure described in Nargang and Rapaport (2007). Cytosolic fractions were isolated by taking 5 mL of supernatant after pelleting the mitochondria (Nargang and Rapaport, 2007). This 5 mL of supernatant was then centrifuged again at 15 000 rpm for 30 min in a Sorvall RC-5C Plus centrifuge using the SA-600 rotor (Sorvall, Mandel Scientific, Guelph). Approximately 3 mL was taken for the final cytosolic sample. All samples were stored at -80°C. Protein concentrations were measured using the BioRad Protein Assay (Bio-Rad Laboratories Inc, Hercules).

2.5 SDS-PAGE and Western Blots

Western blots were conducted on mitochondrial and cytosolic protein fractions. Acrylamide gels for sodium dodecyl sulfate polyacrylamide gel electrophoresis (SDS-PAGE) were prepared as described by Sambrook and Russell (2001). The final acrylamide concentration was 12.5% with an acrylamide:bis-acrylamide ratio of 24:1. 30 μg of mitochondrial or cytosolic protein was loaded in one lane of a gel. The fractions to be analyzed were prepared by dissolving the samples in 5x cracking buffer (0.06 M Tris-HCl pH 6.7, 2.5% SDS, 0.01% β-mercaptoethanol, 5% sucrose), and the volume of each sample was brought up to 30 μL with sterile dH_2O. Samples were heated for 5 min at 95°C and centrifuged at maximum speed (13 000 g) in a Sorvall Biofuge® pico centrifuge (Sorvall, Mandel Scientific, Guelph) for 5 min prior to loading. The gels were electrophoresed at

220 V for 3 to 5 hr, and then transferred onto a Bio Rad Immun-Blot PVDF membrane (Bio Rad, Berkeley) using the procedure of Towbin et al. (1979). The membrane was blocked for one hr at room temperature in blocking solution (5% fat-free skim milk powder in TBST (0.2 M Tris-HCl pH 7.5, 0.15M NaCl, 0.5% Tween20)) with gentle shaking. The blocking solution was removed and the membrane was incubated with gentle shaking for one hr with primary antibody at an appropriate dilution in blocking solution. The membrane was then washed three times, with gentle shaking for 5 min with TBST, followed by a one hour incubation with gentle shaking at room temperature with secondary antibody (1:3000 dilution of goat anti-rabbit antibody HRP-conjugate solution) in 50 mL blocking solution. The membrane was then washed three times for 10 min with TBST, and once with TBS (TBST without Tween20). Detection of bound antibodies was facilitated using the LumiGLO chemiluminescent detection assay (KPL, Maryland) with Kodak XAR film (Eastman Kodak, New York).

2.6 Growth of *E. coli* cells, transformation of competent *E. coli* cells and plasmid DNA isolations

XL10-Gold Ultracompetent *E. coli* cells (Agilent Technologies, Santa Clara) were used for transformation procedures as specified by the manufacturer. Transformants of interest were selected for by plating onto lysogeny broth (LB: 1% tryptone, 0.5% yeast extract, 0.5% sodium chloride) with ampicillin (LB + amp) plates. The final ampicillin concentration was 150 μg/mL. Colonies that formed following over-night incubation at 37°C were then inoculated into 5 mL LB + Amp broth, and grown in a 37°C shaker for approximately 24 hr. Plasmid DNA was isolated using the GeneJet Plasmid Miniprep Kit (Thermo Scientific, Rockford) following the instructions provided by the manufacturer.

2.7 PCR, agarose gel electrophoresis and isolation of DNA from gels

All PCR products were amplified using Phusion High Fidelity PCR (New England Biolabs, Ipswich). Primers were customized and ordered from IDT (Integrated DNA Technologies, Coralville) and received through the Molecular Biology Service Unit (MBSU) facility at the University of Alberta. Following the PCR reaction, DNA was size-separated via gel electrophoresis on 1% agarose gels. Bands of interest were excised with a scalpel on a UV transilluminator, and DNA was extracted using a QiaQuick Gel extraction kit (Qiagen, Hilden), following the manufacturer's instructions.

2.8 Genomic DNA isolation

N. crassa genomic DNA was isolated using a procedure modified from Wendland et. al. (1996). Liquid cultures were grown in VSuTB at 30°C for approximately 24 to 48 hr. Mycelium pads were obtained by vacuum filtration, and were kept on ice for the entire process. Approximately 2 g of mycelium were used per preparation. Mycelium was ground using a mortar and pestle with 1.5 g sand and 5 mL New Isolation Buffer (100mM Tris-HCl pH 8.0, 10mM EDTA, 1% SDS). The mixture was transferred to a tube for the Sorvall SA-600 rotor (Sorvall, Mandel Scientific, Guelph) for later use in centrifugation. The mixture was then brought to 10 mL with New Isolation buffer, and covered with parafilm. The tubes were shaken vigorously, inverted slowly for approximately 1 min, then incubated in a 70°C water bath for 1 hr. Tubes were then placed on ice for 10 min, after which 0.64 mL 8M potassium acetate pH 6.0 was added to each tube. The samples were left on ice for 1 hr. Tubes were placed in a Sorvall RC-5C Plus centrifuge using the SA-600 rotor (Sorvall, Mandel Scientific, Guelph) centrifuge to spin at 14 000g for 15 min. The supernatant was transferred to a clean SA-600 tube. An equal

volume of isopropanol was added to the sample and mixed gently. The DNA precipitate was spooled around a sterile glass Pasteur pipette and transferred to 70% ethanol, rinsed with 70% ethanol and allowed to air dry. The pellet was then suspended in 400 µL 1 mM EDTA pH 8.0, and transferred to an Eppendorf tube. 200 µL HiSalt Buffer (100 mM NaCl, 25 mM Tris-base pH 7.4, 2 mM Na_2EDTA) and 15 µL of previously boiled RNAse A solution (10 mg/mL) was added. The pellet was incubated at 37°C for 30 min. Phenol/chloroform (1:1) extraction was then conducted by adding an equal volume of phenol/chloroform. The tubes were shaken vigorously for one min and centrifuged for 1 min at maximum speed in a Sorvall Biofuge® pico centrifuge (Sorvall, Mandel Scientific, Guelph). The top layer was transferred to a new Eppendorf tube and the phenol/chloroform extraction procedure was repeated once more. To precipitate final genomic DNA, one tenth volume of 3M sodium acetate, as well as three volumes of 95% ethanol were added to the Eppendorf tube and mixed. The tube was centrifuged at maximum speed for 5 min. The pellet was washed once more with 70% ethanol, spun at maximum speed for 1 min, and the remaining ethanol was removed. The pellet was left to air dry for one hr at room temperature in a fume hood and was then resuspended in sterile dH_2O.

2.9 Sequencing of DNA fragments

DNA sequencing reactions were set up according to the specifications of the MBSU at the University of Alberta. DNA sequencing was conducted by the MBSU using a 3730 Analyzer (Applied Biosystems, Foster City). FinchTV (Geospiza Inc.) and NCBI BLAST (https://blast.ncbi.nlm.nih.gov/Blast.cgi) were used for sequence alignment and analysis.

2.10 Whole Genome DNA Sequencing

Genomic DNAs from four strains expressing high uninduced levels of *aod-1* transcript (strains T1P11, 19, 23 and 26) and four expressing low levels of uninduced *aod-1* transcript (strains NCN233, 3, 4 and 6) were sent to our collaborators Michael Freitag and Kirstina Smith at Oregon State University for whole genome sequencing. The sequences were obtained using the Illumina HiSeq 2000 platform (Illumina, San Diego) with a read length of 101 nucleotides.

2.11 Analysis of Whole Genome Sequencing

The genomic sequence data was mounted in G-browse (http://ascobase.cgrb.oregonstate.edu/cgi-bin/gb2/gbrowse/ncrassa_public/) (Stein et al., 2002; Donlin, 2007) to allow viewing of each strain's sequence relative to the reference sequence (*N. crassa* OR74A assembly 10) and to each other. The data for all strains was also supplied as a vcf (variant call format) file. This file could be opened in the IGV (Integrative Genomics Viewer) platform (Thorvaldsdóttir et al., 2013; Robinson et al., 2011) which also allows viewing of each strain's sequence relative to each other and the reference sequence (OR74A assembly 10) (Fig. 2.1). The VCF file could also be opened in Excel using the delimited column data format with "tab" and "space" as the delimiters. This resulted in an Excel table where the changes present in each strain, relative to the reference sequence (OR74A assembly 10) were in separate columns. Other columns listed the supercontig, and numbered the position of each change (according to the reference sequence) and the actual sequence change. The sites of mutations occurring in any strain were listed in individual cells for all strains. A binary system was used where a "0" indicated a match to the reference sequence in a given strain while a "1" indicated a change relative to the reference sequence for that strain.

In the Excel sheet, conditional formatting criteria was applied to allow for filtering of the data. Conditional formatting involved the creation of a "New Rule" in the "Classic" style from

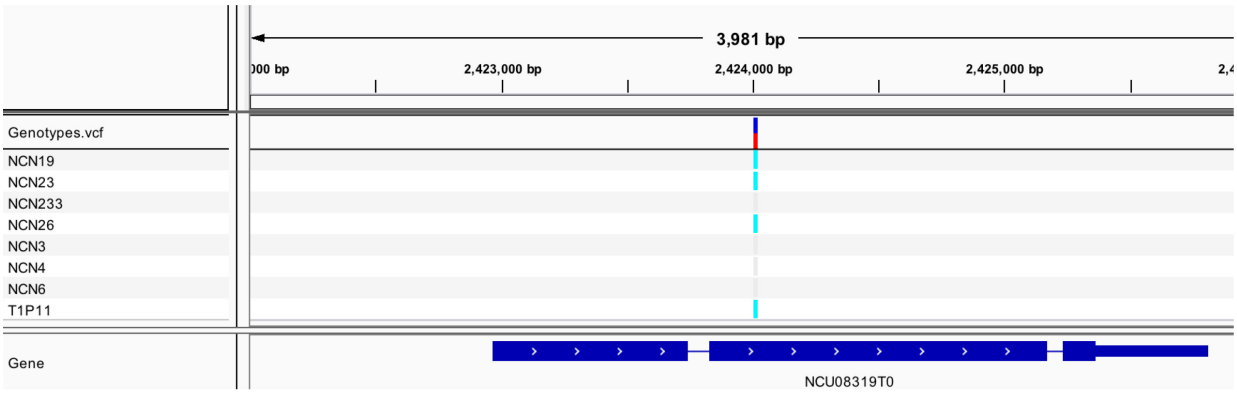
3,981 bp
000 bp
2,423,000 bp
2,424,000 bp
2,425,000 bp
Genotypes.vcf
NCN19
NCN23
NCN233
NCN26
NCN3
NCN4
NCN6
T1P11
Gene
NCU08319T0

Figure 2.1. Screen shot of NCU08319 (the *N. crassa flbA* gene). Integrative Genomics Viewer (IGV). IGV is a Java program developed by Robinson et. al. (2011) and Thorvaldsdóttir et. al. (2012). The *N. crassa* strain OR74A assembly 10 genome sequence (named as NC10 in IGV) was preloaded into IGV as the reference. "Genotypes.vcf" was the file obtained from Oregon State University that contained the sequence of the eight strains examined. This file was loaded into the IGV Java program. The different strains sequences are indicated in the left side bar under Genotypes.vcf (Note that the progeny strain numbers also contain an "NCN" prefix). The vertical blue and red bars in the Genotypes.vcf row indicate that there are strains that match the reference sequence at this position (blue), as well as strains that do not (red). Below the Genotype.vcf row, variants are noted in teal, with sequences that match the reference *N. crassa* OR74A in gray. The position of the variant in the genome in this example is noted above at approximately 2, 424, 000 bp. Not shown is a drop down menu present above the "3, 981 bp" indicator that allows the user to choose which supercontig (supercontig 10.1 to 10.7, corresponding to the seven *N. crassa* chromosomes) to examine. The window in the figure above allows the viewer to visualize 3, 981 bp, but can be expanded or zoomed in further. The gene in this region is indicted at the bottom in dark blue, with thick rectangles indicating coding regions, thinner rectangle indicating UTRs, and lines indicating introns. The gene NCU number is indicated at the bottom (NCU08319T0). The "T0" present after the gene name indicates that it is the most abundant transcript for the gene.

the drop-down menu. Cells were formatted wherein only cells that began with "1" were designated a color ie) pink. Cells that began with "0", indicating positions that match the reference sequence were kept white. This allowed me to choose between seeing positions that match the reference sequence (white) or positions that are different from the reference sequence (pink). Filtering was first applied to low-expressing *aod-1* transcript strains NCN233, 3, 4, and 6. Excel cells were filtered for white, indicating no change from the reference sequence at a certain position. High-expressing *aod-1* transcript strains (T1P11, 19, 23, 26) were analyzed on an individual basis. For each high-expressing *aod-1* transcript strain, a filter was applied to select only variants. Variants fit the criteria of beginning with "1" and were designated a color. The positions were copied, and then pasted into another spreadsheet with a VBA (Visual Basics for Application) FindData code (explained below). Before moving onto a different high-expressing *aod-1* transcript strain, the variant color filter for the previous high-expressing strain was cleared. This was done so as to not select for variants that are present in both high expressing strains, allowing a full list of variants to be generated independently of other variants in other high-expressing strains. A filter for low-expressing strains remained at "white" for the entire filtering analysis in Excel to ensure that no changes present in high-expressing strains would also be present in low-expressing strains.

To analyze the positions of variants in each strain, I wrote a VBA FindData code in a different Excel spreadsheet that would take the position of the change in question and search through the list of known coding regions in the Neurospora genome (Fig 2.2A). The data describing the coding regions in the VBA FindData excel sheet was deduced using the wild-type lab strain *Neurospora crassa* OR74A assembly 10 genome and was provided to us by our collaborators at the Freitag Lab. The filtering process described above resulted in a list of

A.

```
Sub FindData()
Dim a As Long
Dim x As Long
Dim min As Long
Dim max As Long
Dim pos As Long


a = Sheets("Sheet1").Cells(Rows.Count, "B").End(xlUp).Row
pos = Sheets("Sheet1").Cells(Rows.Count, "F").End(xlUp).Row

For i = 2 To pos
x = Cells(i, "F")
j = 0
  For j = 2 To a
    min = Cells(j, "A").Value
    max = Cells(j, "B").Value
   If x >= min And x <= max Then
    Cells(i, "J") = Cells(j, "C")
   End If

  Next j

Next i

End Sub
```

B.

	A	B	C	D	E	F	G	H	I	J	K	L
1	Start	End	Name		#CHROM	POS	REF	ALT	T1P11	Results		
2	1865896	1867317	NCU03846		supercont10.6	97586	C	T	1:6,10:16:99:180,0		Run	
3	1874956	1875019	NCU03847		supercont10.6	309894	C	T	1:17,21:38:99:174,0	NCU09968	Clear Results	
4	1875098	1875355	NCU03847		supercont10.6	314684	C	T	1:21,20:41:44:44,0	NCU09969		
5	1875526	1875873	NCU03847		supercont10.6	314692	C	T	1:15,22:37:99:220,0	NCU09969		
6	1875937	1876049	NCU03847		supercont10.6	341462	G	T	1:0,3:3:97:97,0			
7	1881755	1882111	NCU03848		supercont10.6	363086	A	AT	1:0,5:5:99:168,0			

Figure 2.2. Finding mutations in sequenced genomes relative to the reference sequence. **A)** The FindData code was written in Excel VBA to determine mutated positions in T1P11 coding regions of genes relative to the reference sequence. The FindData code was inserted into Excel by selecting Visual Basic Editor under the Tools drop down menu, followed by the Macros sidebar menu. **B)** Example of how the code finds variants in coding regions. The position of mutations (column F) searched through columns A (start position of a coding region, column A in panel B) and B (stop position of a coding region, column B in panel B) of super contig 10.6 (Chromosome 6). If the position (POS in panel B) of a mutation falls in any value between column A and B, then column J (Results in panel B) would return the contents of the corresponding row that column "C" belongs to (NCU number of the gene). If no match is found, the Results cell is left blank. No limit was applied to how many cells could be analyzed, making the program versatile for any number of values inputted. The program is linked to run to the button "Run", while the Clear Results button would clear the contents of column "J". Columns A and B were populated in the Excel sheet by data retrieved from the Freitag Lab for the *N. crassa* reference sequence from strain OR74A assembly 10. The code is also versatile and could be applied to any strain, contingent on the position of the mutation being numbered relative to a known reference strain.

positions with changes in only high-expressing strains throughout the genome, including non-coding regions, coding regions and UTRs. If the position was in the coding region of a gene, the program would list the NCU number of the gene (Fig 2.2B). One chromosome was examined at a time to meet Excel's RAM restrictions. A list of NCU numbers with changes in coding regions was generated for each strain expressing high levels of *aod-1* transcript (T1P11, 19, 23, and 26). The list of NCU numbers was then run in Venny (http://bioinfogp.cnb.csic.es/tools/venny/) to generate a Venn diagram, and therefore find genes that were mutated in all four strains.

Table 2.1 List of strains used in this thesis

Strain	Origin	Genotype
NCN251	FGSC #2489, Nargang Lab	Mating type A
NCN233	Nargang lab	*pan-, A*
T1P11	Steve Free Lab	*T-, al-2, a*
97B1	KO mutant library (FGSC #19465)	Δaod-2::hygR a
1C3	KO mutant library (FGSC #11227)	Δaod-5::hygR
ΔNCU06940 D1	KO mutant library (FGSC #15136)	A
ΔNCU06940 D2	KO mutant library (FGSC #15137)	a
3	NCN233 x T1P11, Adrian Lahola-Chomiak, Nargang Lab	*T+, al+, pan-*
4	NCN233 x T1P11, Adrian Lahola-Chomiak, Nargang Lab	*T+, al+, pan-*
6	NCN233 x T1P11, Adrian Lahola-Chomiak, Nargang Lab	*T-, al-, pan-*
9	NCN233 x T1P11, Adrian Lahola-Chomiak, Nargang Lab	*T-, al-, pan+*
11	NCN233 x T1P11, Adrian Lahola-Chomiak, Nargang Lab	*T-, al-, pan+*
16	NCN233 x T1P11, Adrian Lahola-Chomiak, Nargang Lab	*T-, al-, pan+*
17	NCN233 x T1P11, Adrian Lahola-Chomiak, Nargang Lab	*T+, al+, pan+*
19	NCN233 x T1P11, Adrian Lahola-Chomiak, Nargang Lab	*T+, al+, pan+*
23	NCN233 x T1P11, Adrian Lahola-Chomiak, Nargang Lab	*T-, al-, pan+*
26	NCN233 x T1P11, Adrian Lahola-Chomiak, Nargang Lab	*T-, al-, pan-*
33	NCN233 x T1P11, Adrian Lahola-Chomiak, Nargang Lab	*T-, al+, pan-*
34	NCN233 x T1P11, Adrian Lahola-Chomiak, Nargang Lab	*T+, al+, pan-*
36	NCN233 x T1P11, Adrian Lahola-Chomiak, Nargang Lab	*T+, al+, pan+*

3′UTR strains 6, 8, 11, 12, 21, 38	T1P11 transformed into PCSN44 with 3′UTR modified HA-tagged *aod-1,* this study	HygBR, ampR
5′UTR modified strains 1, 2	T1P11 transformed into PCSN44 with 5′UTR modified HA-tagged *aod-1,* this study	HygBR, ampR
HA-tagged AOD1 isolates 19, 24, 30, 40, 50	T1P11 transformed into PCSN44 with HA-tagged *aod-1,* this study	HygBR, ampR
ΔflbA	KO mutant library (FGSC #12373), position 13D1 of knockout library	a
ΔflbA	KO mutant library (FGSC #12372), position 13D2 of knockout library	A

Table 2.2. List of oligonucleotides used in this thesis.

Primer Name	Comment	Sequence (5′ to 3′)
NCU06940 qPCR primer F	qPCR Forward primer for NCU06940 gene	GGGTCAGGAGACTTGACGAC
NCU06940 qPCR primer R	qPCR Reverse primer for NCU06940 gene	GCTCTCGGCAAAGAGCTG
NCU06939 qPCR Primer F	qPCR Forward primer for NCU06939 gene	ACACCGTGGTTGAACAGCTT
NCU06939 qPCR Primer R	qPCR Reverse primer for NCU06939 gene	ACTTCGCATAGGCCTCCTCT
aod-1 qPCR Primer F	qPCR forward primer for *aod-1* gene (Z. Qi)	GGGGCGTTAATCATACATTGA
aod-1 qPCR Primer R	qPCR reverse primer for *aod-1* gene (Z. Qi)	AGTCGCTCACAAACGGATTC
B-tubulin qPCR Primer F	qPCR Forward primer for *B-tubulin* gene (Z. Qi)	GCCTCCGGTGTGTACAATG
B-tubulin qPCR Primer R	qPCR reverse primer for *B-tubulin* gene (Z. Qi)	CGGAAGCCTCGTTGAAGTAG
aod-1 seq 1	*aod-1* sequencing primer	ACAAAAACCATCAGTTCGCC
aod-1 seq 2	*aod-1* sequencing primer	GCAGAGCTTTAGCATCCAC
aod-1 seq 3	*aod-1* sequencing primer	GCGACTGGTGTTCCGTTTC
aod-1 seq 4	*aod-1* sequencing primer	CTCAAGCGAGTTCCATTACA
aod-1 seq 5	*aod-1* sequencing primer	TGTTCTATGGAGCCCTACG
aod-1 seq 6	*aod-1* sequencing primer	GGGGCGTTAATCATACATTG
aod-2 seq 1	*aod-2* sequencing primer	GCCGACAAATCGTGGACAAG
aod-2 seq 2	*aod-2* sequencing primer	CCAAGCCATCACTCAAAGGT
aod-2 seq 3	*aod-2* sequencing primer	AGAGAGCCATTTTCCCGAGA

aod-2 seq 4	*aod-2* sequencing primer	ACGGGAACAGAAGCCACGG
aod-2 seq 5	*aod-2* sequencing primer	CATGGGCTACCGTAACTGCC
aod-2 seq 6	*aod-2* sequencing primer	AGAGCGTGCTTGGGACTTCG
aod-2 seq 7	*aod-2* sequencing primer	CGACATGCACAACTTCCATCC
aod-2 seq 8	*aod-2* sequencing primer	GATAGGGAAGCCCGCGAGTA
aod-2 seq 9	*aod-2* sequencing primer	GATTTCGACCCAAGTTCCGC
aod-2 seq 10	*aod-2* sequencing primer	AGAGTCGAACGTGAGATACTGGG
aod-5 seq 1	*aod-5* sequencing primer	TCTATGTCGCCGTCGTCCTA
aod-5 seq 2	*aod-5* sequencing primer	ACCCCACGATGATGCTAATG
aod-5 seq 3	*aod-5* sequencing primer	GTTTGATAAGCGACTTCCTG
aod-5 seq 4	*aod-5* sequencing primer	TGGCACTAACTCGGATACTC
aod-5 seq 5	*aod-5* sequencing primer	ACTGGAAAGAGATGGTAAGC
aod-5 seq 6	*aod-5* sequencing primer	GTCCCTACCTGCTTCAGAGC
aod-5 seq 7	*aod-5* sequencing primer	GCAGGGCATTGGGCTGATTGA
aod-5 seq 8	*aod-5* sequencing primer	GGTCTTTCCAATGTTGTGAG

aod-5 seq 9	*aod-5* sequencing primer	TGCAGCAACACAATTAGGAT
aod-5 seq 10	*aod-5* sequencing primer	CTCGGTTTTGCTTCTTGCC
aod-5 seq 11	*aod-5* sequencing primer	CGCAATAGTTTGTTACCAGG
aod-5 seq 12	*aod-5* sequencing primer	CAGCAAGTCCAGTGAGAATACGA
aod-1 PCR F1	*aod-1* PCR primer F	GGAAAAGGGCTTTGTGACCAATTGG
aod-1 PCR R1	*aod-1* PCR primer R	GAACTGCTGCACAGAGAGAAGAAC
aod-2 PCR F1	aod-2 PCR forward primer fragment 1	ACTTGGTTGCGGTCAACAGACTTCC
aod-2 PCR R1	*aod-2* PCR reverse primer fragment 1	GCAGAGATGGCCGATGTTTCGCTTG
aod-2 PCR F2	*aod-2* PCR forward primer fragment 2	AAAGGCTGGCTCGGAATCAA
aod-2 PCR R2	*aod-2* PCR reverse primer fragment 2	GTTGCTCGGAAGTGAGACCA
aod-5 PCR F1A	*aod-5* PCR forward primer fragment 1A	ACTGGACATCCACATGCAAA
aod-5 PCR R1A	*aod-5* PCR reverse primer fragment 1A	TGACGGTCCGAGAGAGAACT
aod-5 PCR F1B	aod-5 PCR forward primer fragment 1B	TCAATCAGCCCAATGCCCTGC
aod-5 PCR R1B	*aod-5* PCR reverse primer fragment 1B	ATTCCCTTGGAGGTTGAGGAGC
aod-5 PCR F2	*aod-5* PCR forward primer fragment 2	CTCACGGTCGACCACAAAGTGGACAC
aod-5 PCR R2	*aod-5* PCR reverse primer fragment 2	GCTGGAGGGAAGCTATTCATAGGGC
aod-5 PCR F3	*aod-5* PCR forward primer fragment 3	CATGCCAACGGTGCATCAAACGTG

aod-5 PCR R3	*aod-5* PCR reverse primer fragment 3	TGGTTTCGCGATGAACCCAGCGAAG
SEQ FL46-49 3	Sequencing confirmation that native/modified *aod-1* gene construct cloned into PCSN44 plasmid	TATATCCGGCAGACACCACC
SEQ FL48 5	Sequencing confirmation that native/modified *aod-1* gene construct cloned into PCSN44 plasmid	ATACCCTGCTCGGTGGAATGC
SEQ FL46-49 4	Sequencing confirmation that native/modified *aod-1* gene construct cloned into PCSN44 plasmid	CGGCTGGATCGAGACTTTAC
SEQ FL46,49 5	Sequencing confirmation that native/modified *aod-1* gene construct cloned into PCSN44 plasmid	CTTGACAGATGGTTGTGGTTTG
SEQ FL46-49 1	Sequencing confirmation that native/modified *aod-1* gene construct cloned into PCSN44 plasmid	TAAAGGGAGGAAGGGCGAAC
SEQ Fl46-49 2	Sequencing confirmation that native/modified *aod-1* gene construct cloned into PCSN44 plasmid	CCTGGTTGAAGATCTGGAGC
46-48-49 Sequencing	Sequencing confirmation that native/modified *aod-1* gene construct cloned into PCSN44 plasmid	ATGAAGCCATTCGCAACTTATGGCC
R46-49	Reverse primer for *aod-1* HA-tagged 5′UTR modification and native, HA-tagged *aod-1*, contains *NotI* site	CTGAAGCGGCCGCGTCACAGAGAGAAGAACCCAGTATC
F46-48-49	Forward primer for native *aod-1* HA-tagged, and 5′ and 3′UTR modified HA-tagged *aod-1*, contains *HindIII* site	CGGCAAAGCTTCATGAAGCCATTCGCAACTTATGG
R 48	Reverse primer for *aod-1* HA-tagged 3′UTR modification, contains *NotI* site	CTGAAGCGGCCGCGTCTGACAGGTATATCTAGCAG
F Tyr PCR Primer	Forward PCR primer for the *tyrosinase* gene	GCTACTGCACGCACTCGTCCATCCTC

R Tyr PCR Primer	Reverse PCR primer for the *tyrosinase* gene	GAGCAGCAGCAGCCGAG ACGGTGCTC
F Tyr SEQ Primer	Sequencing primer for the *tyrosinase* gene	CTGTACGAGCAGGCCCT CTACG

Table 2.3. List of plasmids used in this study

Plasmid Name	Comment	Origin
PCSN44	*Aspergillus* trpC promoter with hygromycin B and ampicillin resistance, contains NotI and HindIII restriction sites	FGSC; Gritz and Davies, 1983
pUC57 + FL6546	Kanamycin resistant plasmid with 3xHA-tagged *aod-1* gene with 5′UTR replaced with 5′UTR of *porin* and cloned into the EcoRV/SalI site	Synthesized by BioBasic Inc.
pUC57 + FL6548	Kanamycin resistant plasmid with 3xHA-tagged *aod-1* gene with 3′UTR replaced with 3′UTR of *β-tubulin* and cloned into the SmaI site	Synthesized by BioBasic Inc.
pUC57 + FL6549	Kanamycin resistant plasmid with native 3xHA-tagged aod-1 gene cloned into the StuI/EcoRV site	Synthesized by BioBasic Inc.
PCSN44 + Fl6546	PCSN44 with 5′UTR from *porin* and 3xHA-tagged *aod-1* gene cloned into *HindIII* and *NotI* site	This study
PCSN44 + FL6548	PCSN44 with 3′UTR from *β-tubulin* 3xHA-tagged *aod-1* gene cloned into *HindIII* and *NotI* site	This study
PCSN44 + FL6549	PCSN44 with native 3xHA-tagged *aod-1* gene cloned into *HindIII* and *NotI* site	This study

3.0 Results

3.1 Examination of gene for hypothetical protein NCU06940

3.1.1 ChIP-Seq Library for promoters bound by AOD2/AOD5

As discussed in section 1.10, our lab had previously shown a binding site for the AOD2/AOD5 dimer upstream of the *aod-1* gene. This was accomplished using EMSA (Chae et al., 2007a) and analysis of the upstream region using mutations (Chae et al., 2007b; Tanton et al., 2003a). To search for other promoters that are bound by the AOD2/AOD5 transcription factors, CHiP-seq experiments were conducted in our lab (Qi et. al. 2017). These experiments were done using two tagged strains. The first was an *aod-2* mutant strain transformed with a randomly integrated functional *aod-2* gene encoding an AOD2 protein with a C-terminal 3X HA tag (AOD2-HA). The second was an *aod-5* mutant strain transformed with a randomly integrated functional *aod-5* gene encoding an AOD5 protein carrying a C-terminal 3X Myc tag (AOD5-Myc). Experimental data were collected by performing ChIP with antibodies to either HA or Myc for the appropriate strains. To eliminate false data from non-specific immunoprecipitation, control data were collected using the same antibodies with wild-type strains lacking any tag. Good binding was seen at the *aod-1* promoter and a series of other promoters controlling genes involved in various aspects of metabolism and energy production (Qi et al., 2017). The most robust peaks of binding for AOD2 and AOD5 were located between two divergently transcribed genes: NCU06939 (an endosome-associated ubiquitin isopeptidase) and NCU06940 (a hypothetical protein). The peaks were observed in strains grown either in the absence or presence of CM and exceeded the binding observed for NCU07953 in all conditions (Fig. 3.1). Given the large amount of AOD2/AOD5 binding at this site, I hypothesized that one of these genes is regulated by these transcription factors and that the gene might complement AOX function or

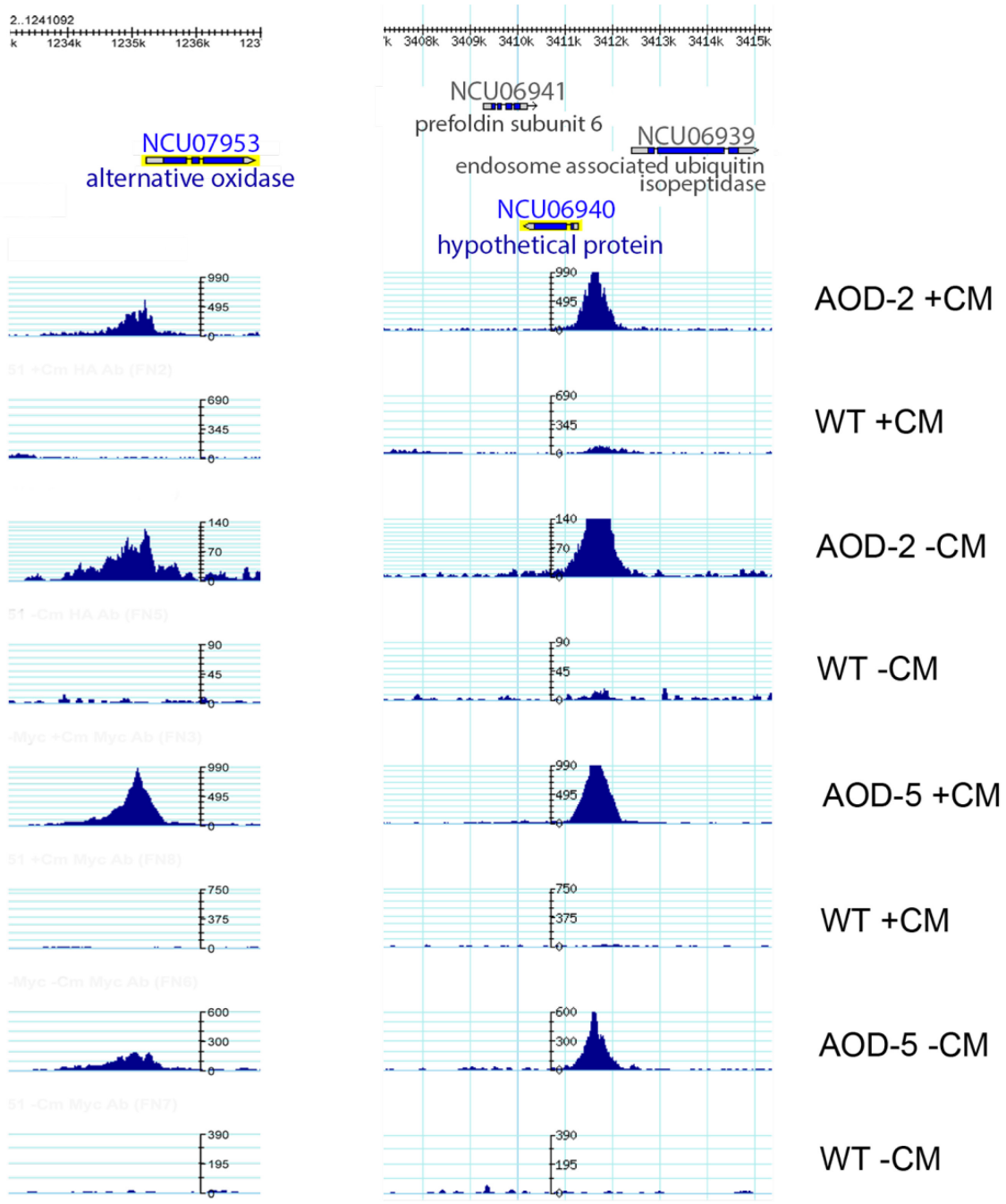
2..1241092
k 1234k 1235k 1236k 123
NCU07953
alternative oxidase
'k 3408k 3409k 3410k 3411k 3412k 3413k 3414k 3415k
NCU06941
prefoldin subunit 6
NCU06939
endosome associated ubiquitin isopeptidase
NCU06940
hypothetical protein
990
495
0
690
345
140
70
90
45
750
375
600
300
390
195
AOD-2 +CM
WT +CM
AOD-2 -CM
WT -CM
AOD-5 +CM
WT +CM
AOD-5 -CM
WT -CM

Figure 3.1. Chromatin immunoprecipitation and sequencing data (ChIP-Seq) from AOD2-HA tagged and AOD5-Myc tagged strains grown in the presence and absence of CM. The results for the promoter regions of the genes for alternative oxidase (NCU07953) and the hypothetical protein (NCU06940) are shown on the left and right, respectively. ChIP-Seq was performed by Zhigang Qi, sequence generated by Delta genomics, and data aligned to the *N. crassa genome* by M. Freitag and K. Smith at Oregon State University. The strains and experimental conditions used for each set of peaks are shown on the right (AOD-2, 3X HA tagged *aod-2* strain; WT, wild-type strain with no tagged proteins; AOD-5, 3X Myc tagged *aod-5* strain). Genes of interest are highlighted in yellow. Number of reads in a certain position is represented by the blue peaks. The y-axis is the same for both gene regions. The results for NCU06940 are off the scale, emphasizing the greater binding seen at this locus relative to the *aod-1* promoter.

possibly provide a response to respiratory or other stresses. Because the peaks occurred in the upstream region of the divergently transcribed NCU06939 and NCU06940 genes, they were both potential candidates for being regulated by these transcription factors.

3.1.2 qPCR to determine promoter bound by AOD2/AOD5

I analyzed expression of the NCU06939 and NCU06940 mRNAs in a wild-type strain (NCN251), and the knock-out mutants of *aod-2* (Δ*aod-2*) and *aod-5* (Δ*aod-5*) in an attempt to determine if either gene requires AOD2 and/or AOD5 for expression. qPCR primers were designed for both genes. Amplification of NCU06940 and NCU06939 was conducted in the following strains and growth conditions: Δ*aod-2* + CM, Δ*aod-2* – CM, Δ*aod-5* + CM, Δ*aod-5* – CM, wild-type (NCN251) + CM, and wild-type (NCN251) – CM. The knockout of either *aod-2* or *aod-5* did not have any striking effect on transcript levels of NCU06939 in either the presence or absence of CM (Fig. 3.2A). Growth of the wild-type cells (NCN251) in the presence of CM increased transcripts for this gene by about 50% and growth of the *Δaod-2* strain in CM slightly increased the amount of transcript over the +CM wild-type control. However, none of these differences were statistically significant ($p>0.05$) and we considered effects in the range of two-fold or less to be of questionable biological significance (Fig. 3.2A). On the other hand, there was a significant down-regulation of NCU06940 transcripts in both the *aod-2* and *aod-5* knock out strains, both in the presence and absence of CM. As well, there appeared to be a CM effect in the wild-type strain resulting in an approximately three-fold increase in transcripts (Fig. 3.2B). These results indicate that the peak identified by ChIP-seq data most likely affects the expression of NCU06940, a hypothetical protein.

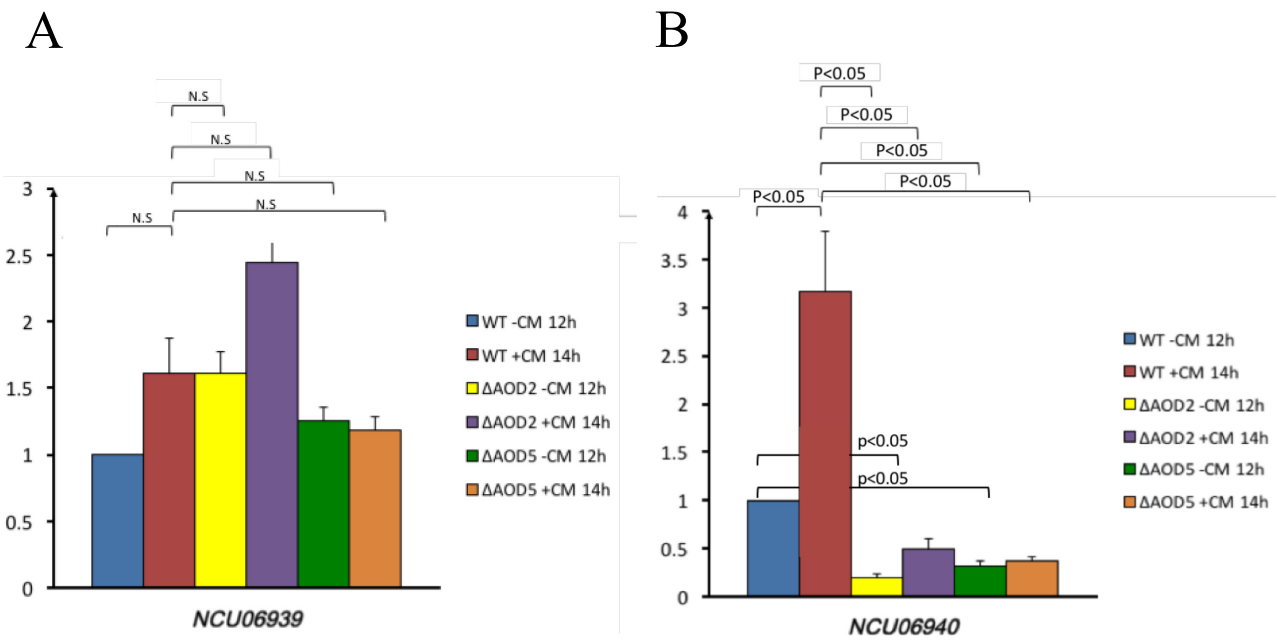

Figure 3.2. Transcript levels of NCU06939 and NCU06940. Cultures of wild-type strain NCN251 (WT) and the knock-out mutants for *aod-2* (Δ*aod-2*) and *aod-5* (Δ*aod-5*) were all grown in the presence (+CM) and absence (-CM) of CM. RNA was isolated, converted to cDNA and analyzed by qPCR. Cultures were grown for either 12 hr (-CM conditions) or 14 hr (+CM conditions). Each bar represents the average of results from four biological replicates and three technical replicates of each biological replicate. Error bars represent the standard error of the mean. **A,** NCU06939. **B,** NCU06940. The Student's T-test was used to determine significance. N.S indicates no significance at $p<0.05$.

3.1.3 NCU06940 bioinformatics analysis

NCU06940 is a non-essential gene, since a knock-out strain available from the *N. crassa* knockout project (Colot et al., 2006) is viable. The *N. crassa* gene is 1.3 kb long and contains one intron. Based on BLAST searches, NCU06940 contains no known functional domains. Similarly, I found no evidence for a mitochondrial targeting sequence, a nuclear localization signal, or transmembrane spanning domains. Based on these results, I would predict the protein to be localized to the cytosol. Surprisingly, BLAST analysis showed that homologues of NCU06940 are confined to only a few species in the fungal class Sordariomycetes (Fig. 3.3). Since all the species examined in Fig. 3.3 B and C contained at least one gene encoding AOX, there is no correlation between the presence of AOX and the NCU06940 gene. Nonetheless, since the promoter of NCU06940 binds large amount of AOD2 and AOD5 (Fig. 3.1) and that its expression is increased in the presence of CM in an AOD2 and AOD5 dependent fashion (Fig. 3.2B), it seemed to warrant at least preliminary investigation for possible function.

3.1.4 NCU06940 is not involved in stress response

Since NCU06940 transcript levels were significantly increased in the presence of CM (Fig. 3.2B), it is conceivable that the protein is involved in a stress response. Therefore, I investigated the growth of a NCU06940 knock-out strain on various carbon sources, inhibitors, and at different temperatures (Fig. 3.4 A-E). Different carbon sources were examined since at least one gene involved in gluconeogenesis in *N. crassa*, phosphoenolpyruvate kinase (PEPCK), is also known to be controlled by AOD2 and AOD5 (Qi et. al. 2017). Furthermore, both PEPCK and fructose bisphosphatase (FBP) are transcriptionally regulated by the homologues of AOD2 and AOD5 in *Aspergillus nidulans* (Suzuki et. al. 2012) and *P. anserina* (Bovier et. al. 2014).

A.

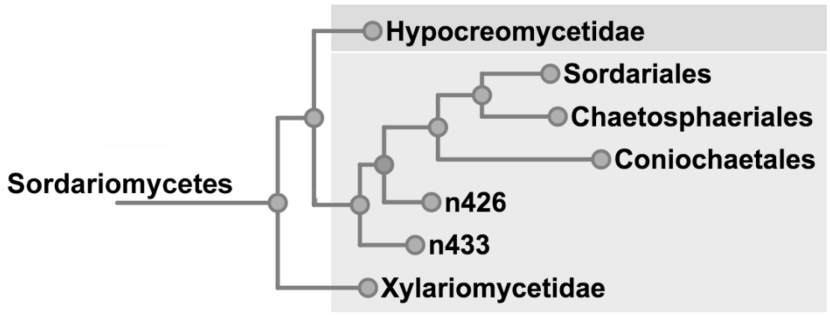
Hypocreomycetidae
Sordariales
Chaetosphaeriales
Coniochaetales
Sordariomycetes
n426
n433
Xylariomycetidae

B.

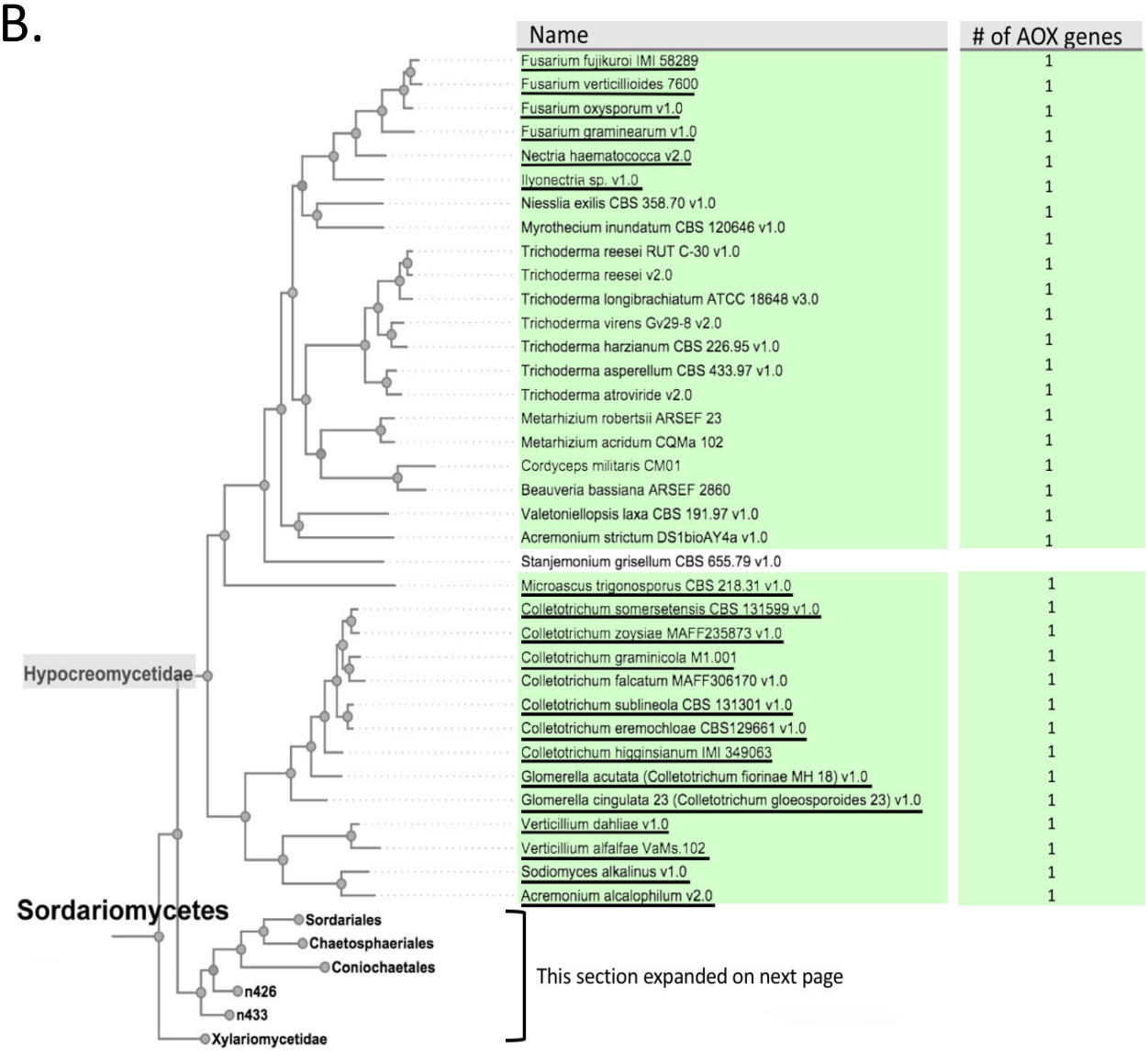
Name
# of AOX genes
Fusarium fujikuroi IMI 58289 1
Fusarium verticillioides 7600 1
Fusarium oxysporum v1.0 1
Fusarium graminearum v1.0 1
Nectria haematococca v2.0 1
Ilyonectria sp. v1.0 1
Niesslia exilis CBS 358.70 v1.0 1
Myrothecium inundatum CBS 120646 v1.0 1
Trichoderma reesei RUT C-30 v1.0 1
Trichoderma reesei v2.0 1
Trichoderma longibrachiatum ATCC 18648 v3.0 1
Trichoderma virens Gv29-8 v2.0 1
Trichoderma harzianum CBS 226.95 v1.0 1
Trichoderma asperellum CBS 433.97 v1.0 1
Trichoderma atroviride v2.0 1
Metarhizium robertsii ARSEF 23 1
Metarhizium acridum CQMa 102 1
Cordyceps militaris CM01 1
Beauveria bassiana ARSEF 2860 1
Valetoniellopsis laxa CBS 191.97 v1.0 1
Acremonium strictum DS1bioAY4a v1.0 1
Stanjemonium grisellum CBS 655.79 v1.0
Microascus trigonosporus CBS 218.31 v1.0 1
Colletotrichum somersetensis CBS 131599 v1.0 1
Colletotrichum zoysiae MAFF235873 v1.0 1
Colletotrichum graminicola M1.001 1
Colletotrichum falcatum MAFF306170 v1.0 1
Colletotrichum sublineola CBS 131301 v1.0 1
Colletotrichum eremochloae CBS129661 v1.0 1
Colletotrichum higginsianum IMI 349063 1
Glomerella acutata (Colletotrichum fiorinae MH 18) v1.0 1
Glomerella cingulata 23 (Colletotrichum gloeosporoides 23) v1.0 1
Verticillium dahliae v1.0 1
Verticillium alfalfae VaMs.102 1
Sodiomyces alkalinus v1.0 1
Acremonium alcalophilum v2.0 1
Hypocreomycetidae
Sordariomycetes
Sordariales
Chaetosphaeriales
Coniochaetales
n426
n433
Xylariomycetidae
This section expanded on next page

C.

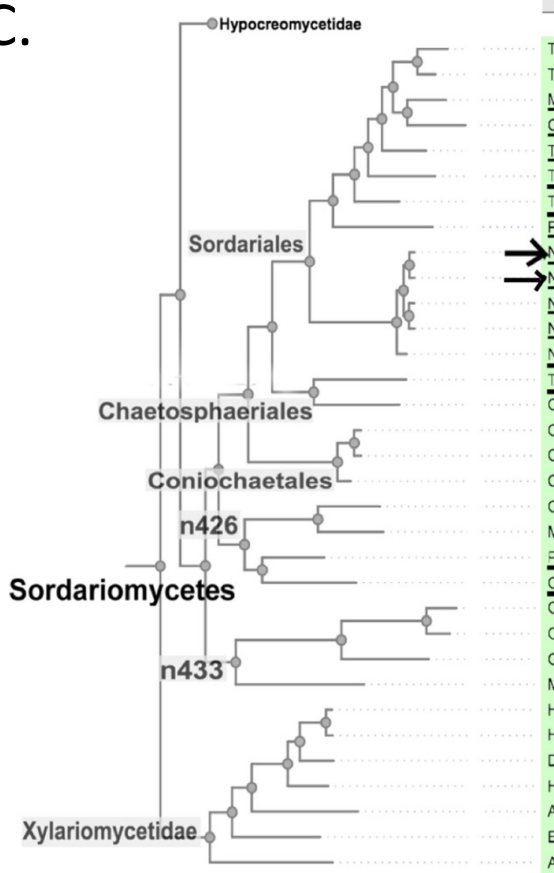

Name	# of AOX genes
Thielavia hyrcaniae CBS 757.83 v1.0	2
Thielavia appendiculata CBS 731.68 v1.0	2
Myceliophthora thermophila (Sporotrichum thermophile) v2.0	1
Chaetomium globosum v1.0	1
Thielavia terrestris v2.0	2
Thielavia antarctica CBS 123565 v1.0	2
Thielavia arenaria CBS 508.74 v1.0	1
Podospora anserina S mat+	1
Neurospora crassa OR74A v2.0	2
Neurospora crassa FGSC 73 trp-3 v1.0	2
Neurospora tetrasperma FGSC 2509 mat a v1.0	1
Neurospora tetrasperma FGSC 2508 mat A v2.0	1
Neurospora discreta FGSC 8579 mat A	1
Thozetella sp. PMI_491 v2.0	1
Chaetosphaeria innumera	1
Coniochaeta ligniaria NRRL 30616 v1.0	1
Coniochaeta ligniaria CBS 111746	1
Coniochaeta sp. PMI_546 v1.0	1
Cryphonectria parasitica EP155 v2.0	1
Melanconium sp. NRRL 54901 v1.0	1
Phaeoacremonium aleophilum UCRPA7	1
Calosphaeria pulchella	1
Ophiostoma piliferum	1
Ophiostoma piceae UAMH 11346	1
Grosmannia clavigera kw1407	1
Magnaporthe grisea v1.0	1
Hypoxylon sp. CO27-5 v1.0	1
Hypoxylon sp. EC38 v1.0	1
Daldinia eschscholzii EC12 v1.0	1
Hypoxylon sp. CI-4A v1.0	1
Anthostoma avocetta NRRL 3190 v1.0	1
Eutypa lata UCREL1	1
Apiospora montagnei NRRL 25634 v1.0	1

Figure 3.3. NCU06940 homologues exist only in some Sordariomycetes species. The protein sequence of NCU06940 was examined by BLASTED against translated nucleotide databases in the Mycocosm platform at the Joint Genome Institute (http://genome.jgi-psf.org/). The only hits obtained were within the clade Sordariomycetes. **A)** An expansion of subclasses and orders under class Sordariomycetes. **B)** Expansion of species under the sub-class Hypocreomycetidae. **C)** Expansion of species of the orders Sordariales, Chaetosphaeriales, Coniochaetales, and sub-class Xylariomycetidae. The species that have homologues of NCU06940 are underlined while species that have AOX and the corresponding number of AOX genes are given on the right. Arrows to the left of the species name indicate *N. crassa* strains. Trees were generated by MycoCosm (Grigoriev et. al. 2014).

A. 15℃

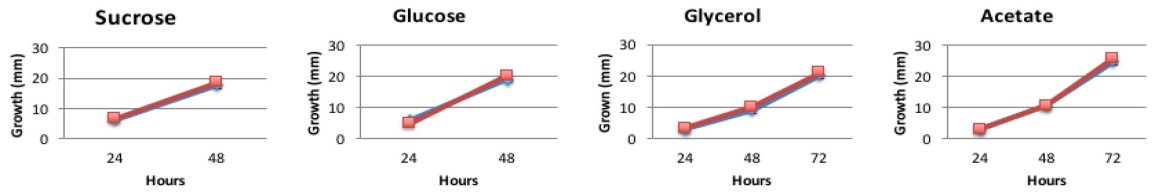

B. 30℃

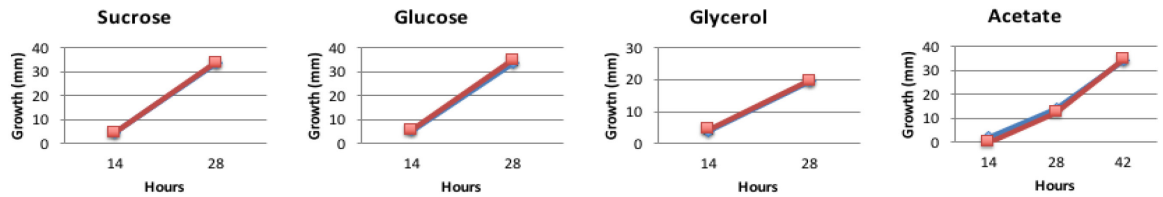

C. 37℃

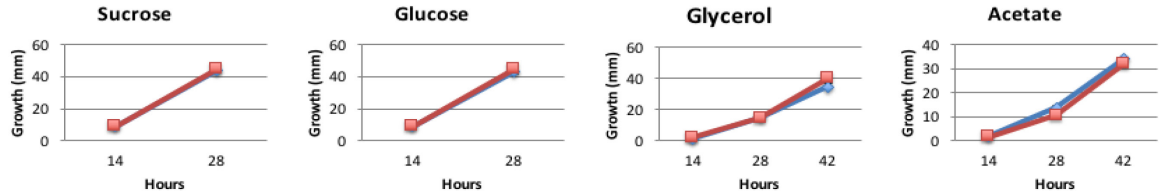

D. 40℃

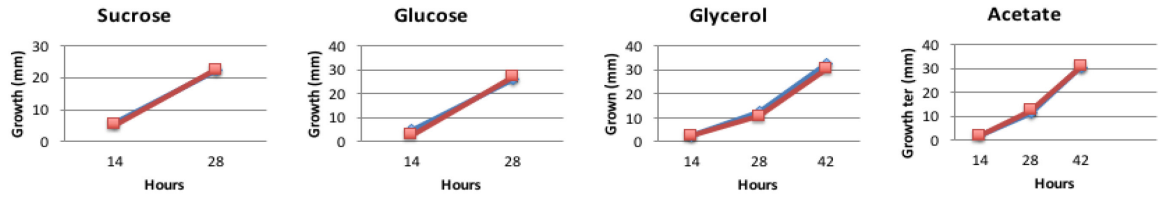

E. Chloramphenicol and Antimycin A (sucrose) (30℃)

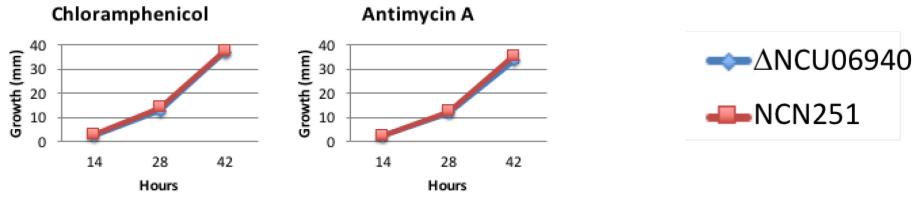

Figure 3.4. Growth of the NCU06940 knock-out strain under various conditions. Conidiaspores from both a wild-type (NCN251) and the ΔNCU06940 strain were counted and adjusted to 10^5/10 μL. 10 μL was inoculated at the center of a petri dish containing Vogel's medium with the indicated carbon source. Three to five replicates were measured for each condition. The strains were grown at 15℃ **(A)**, 30℃ **(B)**, 37℃ **(C)** and 40℃ (**D)** on acetate, glycerol, sucrose and glucose as indicated. In addition, the strains were grown on sucrose medium in the presence of CM or AA at 30℃ **(E).** Blue diamonds represent ΔNCU06940, while red squares are NCN251. Growth rate was determined by measuring hyphal growth from the point of inoculation at the indicated time. Error bars represent the standard error of the mean but are too small to observe.

The typical laboratory carbon source for *N. crassa* is glucose or sucrose. To determine if growth was reduced on poor carbon sources for the NCU06940 knock-out, I compared growth on sucrose, glucose, glycerol and acetate. Strains were also grown at different temperatures, including 30℃, the standard growth temperature used in our lab for *N. crassa*, 15℃, 37℃, and 40℃. Considering that NCU06940 expression is up-regulated in the presence of CM, growth was also measured in the presence of both CM and AA at 30℃.

Both the wild-type (NCN251) and NCU06940 knock-out strains grew best on sucrose and glucose, regardless of the temperature (Fig. 3.4 A, B, C, D). Both strains grew more slowly on glycerol and acetate with the growth rate on acetate being the slowest. However, there was no difference in growth rate between the strains under any of the conditions. Additionally, there was no obvious difference in growth between the wild-type and the mutant in the presence of CM or AA (Fig. 3.4E). These data indicate that there is no impact on linear hyphal growth due to the loss of NCU06940 under the conditions tested.

The recent ChIP-seq study showed that AOD2 and AOD5 control the expression of several genes involved in energy production and metabolism (Qi et. al. 2017). Conceivably, NCU06940 is involved in one of those processes. However, the unusual nature of the protein, with no homologues outside of the Sordariomycetes, and even the loss of the gene from many members of this class, would imply a very specific function.

3.2 Unexpected expression of *aod-1* in strain T11-76

3.2.1 The mutant tyrosinase allele does not affect uninduced *aod-1* expression levels

As mentioned in the Introduction (section 1.10), Descheneau et al. (2005) reported that T11-76, a tyrosinase mutant (T^-) that was developed as a reporter strain for a mutagenesis screen,

had high levels of *aod-1* transcript in uninduced (-CM) conditions compared to standard wild-type lab strains (Fig. 3.5). Despite the presence of this mRNA, no AOD1 protein could be detected. A similar result was seen for the parent (T1P11) of the reporter strain (Descheneau et. al. 2005, unpublished). These observations raised two obvious questions. First, why are relatively high levels of *aod-1* mRNA produced in the absence of inducing conditions in this strain. Second, why is no AOD1 protein detectable even though *aod-1* mRNA is produced. I began by investigating the first question.

Because T1P11 carries the mutant tyrosinase gene (T^- allele), it was of interest to ask if the T^- allele was the cause of *aod-1* expression upregulation in non-inducing conditions. The Nargang lab had earlier reported that the tyrosinase mutation did not segregate with the high uninduced *aod-1* transcript levels (Descheneau et al. 2005). However, the number of progeny analyzed was not reported. Furthermore, the progeny strains were lost. To verify these data and to generate progeny strains for further analysis, our lab repeated the genetic analysis. A cross between an *aod-1* wild-type strain (NCN233) and the T1P11 strain was set up by a Biology 499 student (Adrian Lahola-Chomiak) who also did a preliminary characterization of the cross progeny. I completed a more detailed analysis with a more precise characterization of the state of the tyrosinase gene in the progeny. Because the tyrosinase gene is closely linked to the *al-2* albino gene (10 map units), I set out to verify the presence or absence of the tyrosinase mutations in approximately equal numbers of *al-2*$^-$ and *al-2*$^+$ progeny. The presence of the T^- or T^+ allele was evaluated by PCR amplification and sequencing of the region of the T gene known to contain mutations in the T^- allele. Progeny strains (referred to simply by their isolation numbers) 3, 4, 19, 34, and 36 were all wild-type (T^+) for the tyrosinase gene, while strains 6, 9, 16, 23, 26, and 33 were all mutant (T^-) for the tyrosinase gene (Table 3.1). It should be noted that other

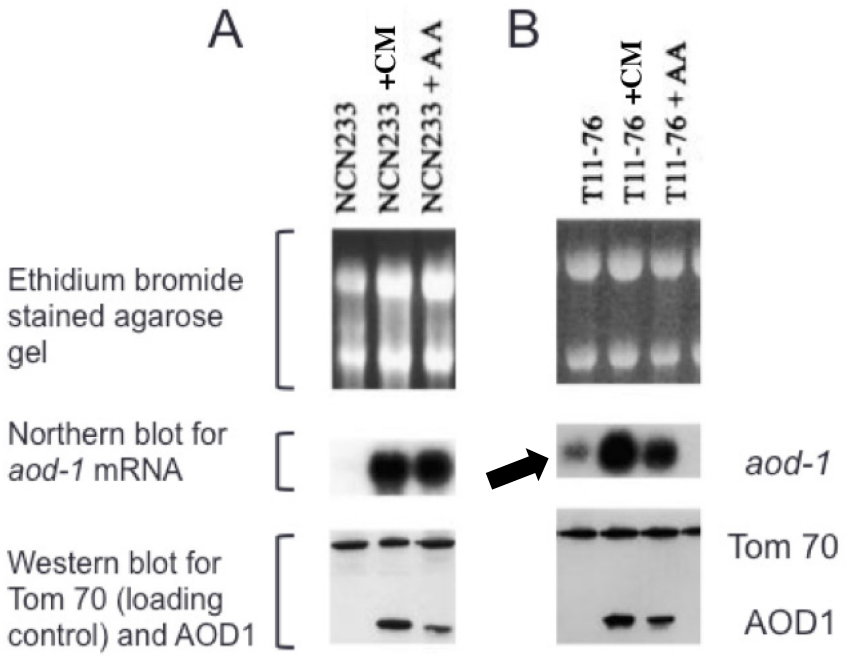

Figure 3.5. *aod-1* transcript and protein in wild-type NCN233 and the tyrosinase mutant T11-76. **A.** *aod-1* transcript is not detectable by Northern Blot in NCN233 (wild-type) grown in standard conditions (absence of CM) but is present when the strain is grown in the presence of CM (+ CM) or antimycin A (+ AA). AOD1 protein is present in cells grown in the presence of CM (+CM) or AA (+AA) as shown on the Western Blot. **B.** *aod-1* transcript is present in T11-76 (T mutant) when the strain is grown in standard conditions (Arrow) or in the presence of CM or AA. No AOD1 protein is observed in T11-76 under standard growth conditions, but is observed in the presence of CM or AA. Figure modified from Descheneau et. al 2005.

Table 3.1. Segregation of the tyrosinase gene (T) alleles and other markers in the NCN233 x T1P11 cross. The tyrosinase gene allele was evaluated by PCR amplification and sequencing of the product. All strains were grown for 14 hours, RNA was isolated, and cDNA was generated. PCR was set up with primers designed to amplify a portion of the tyrosinase gene known to contain mutations in the *T*$^-$ allele (Descheneau, PhD thesis). These PCR products were sequenced. Six of the eleven progeny strains were found to be tyrosinase mutants (*T*$^-$), while five were found to be wild-type (*T*$^+$). Strains mutant for the *al-2* gene are denoted as *al*$^-$ while wild-type strains are *al* $^+$. The albino phenotype was evaluated visually as either white or orange conidia. Strains auxotrophic for pantothenic acid are denoted as pan$^-$ while wild-type strains are pan$^+$. Pantothenic requirement was determined by evaluating growth or no growth on medium lacking pantothenate.

Strain	NCN233	T1P11	3	4	6	9	16	19	23	26	33	34	36
Tyrosinase	T^+	T^-	T^+	T^+	T^-	T^-	T^-	T^+	T^-	T^-	T^-	T^+	T^+
Al	al^+	al^-	al^+	al^+	al^-	al^-	al^-	al^+	al^-	al^-	al^+	al^+	al^+
Pan	pan^-	pan^+	pan^-	pan^-	pan^-	pan^+	pan^+	pan^+	pan^+	pan^-	pan^-	pan^-	pan^+

genetic markers in the cross (*al-2* and *pan-1*) have previously been shown to have no effect on *aod-1* expression (F. E. Nargang personal communication).

Next, I measured the amount of *aod-1* mRNA present in the parental and progeny strain by qPCR following growth in the absence of CM. With respect to defining high and low expression levels in this study, progeny that had greater than 4-fold the level of *aod-1* mRNA present in uninduced wild-type cells were arbitrarily designated as "high" (progeny 9, 16, 19, 23 and 26), while progeny with below 4-fold level of mRNA were designated as "low" (progeny 3, 4, 6, 33, 34, 36). With respect to the traits of tyrosinase (T^+or T^-) and *aod-1* mRNA levels (high or low), the cross yielded three parental, high *aod-1* mRNA, T^- progeny (9, 16 and 23) and three parental, low *aod-1* mRNA T^+ progeny (3, 4, 34). If the tyrosinase allele was determining AOX transcript levels, I would expect all T^- progeny strains to have high *aod-1* expression levels and all T^+ progeny to have low *aod-1* expression levels. However, strain 19, which is T^+, had elevated levels of *aod-1* transcript, while strains 6 and 33, which are T^-, had low levels of *aod-1* transcript (Fig. 3.6). These data provide evidence that the state of the tyrosinase gene is not involved in the uninduced high level of expression of *aod-1* that is observed in some strains. In addition, although the number of progeny analyzed was quite low, the finding that six progeny had low levels of *aod-1* transcripts, while five had high levels, suggests that the phenotype is determined by a single gene.

3.2.2 Sequencing of aod-1, aod-2 and aod-5 in T1P11

The most obvious possible explanations for the production of *aod*-1 mRNA in strain T1P11 in non-inducing conditions would include: 1) A mutation in the *aod-1* promoter that allows it to be transcribed in the absence of an inducing signal or 2) mutations in the *aod-2* or

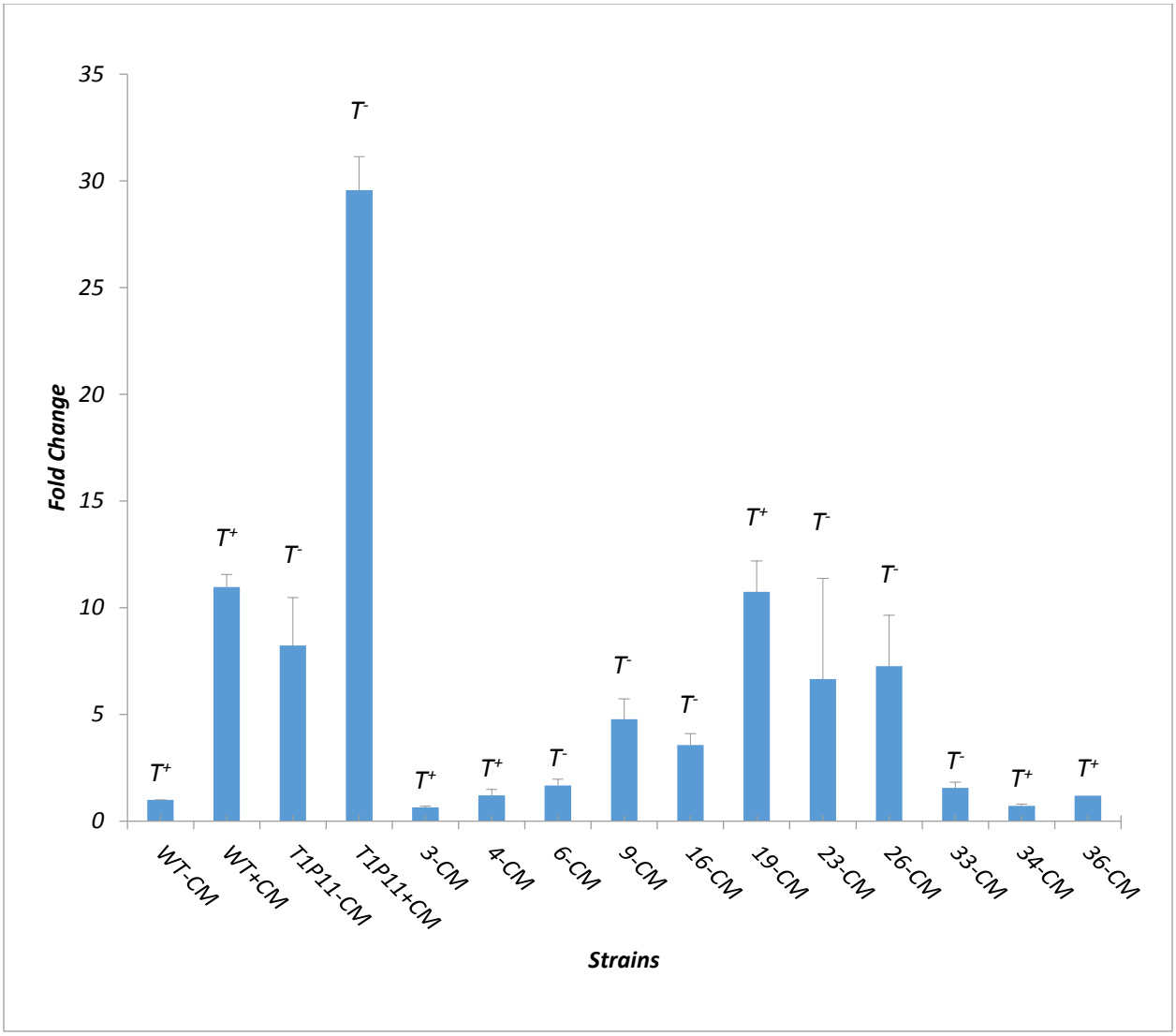

Figure 3.6. *aod-1* transcript levels in tyrosinase cross parental strains WT (wild-type strain NCN233) and T1P11 and progeny strains. Strains were grown in –CM medium for 16 hours and 18 hours in +CM. RNA was extracted and cDNA was generated. The expression levels (blue bars) of *aod-1* mRNA were determined by qPCR with four biological replicates (each with three technical replicates) standardized to *β-tubulin*. Tyrosinase mutant strains are denoted with *T*- and non-mutants with *T*+. Error bars represent the standard error of the mean.

aod-5 genes that would make the known transcription factors constitutively active. In the fungus *Podospora anserina*, RSE2 and RSE3 (the orthologues of *N. crassa*'s AOD2 and AOD5, respectively) are essential for inducing AOX. Single amino acid mutations have been characterized in these transcription factors that result in higher levels of *aod-1* transcripts in non-inducing conditions (Sellem et. al. 2009).

To address these possibilities, Iman Asaria, an undergraduate student, had begun to sequence *aod-1, aod-2,* and *aod-5* in T1P11. The region of interest in *aod-1* was the promoter region, since a mutation could exist in T1P11 that causes the promoter to be constitutively active. The genes for the transcription factors *aod-2* and *aod-5* were also sequenced to look for mutations that could cause them to be active even in non-inducing conditions. Because the transcription factors are considered to be constitutively bound to the promoter of the genes they regulate, (Descheneau et. al. 2005; Qi et. al. 2017) a change in their amino acid sequence could be responsible for the production of *aod-1* mRNA seen in T1P11, as observed for the *P. anserina* mutants mentioned above. I completed the sequencing begun by Iman by PCR amplifying fragments of each gene and sequencing sections using the sequencing primers summarized in Table 2.2 of Materials and Methods.

Although the complete history of the development of strain T1P11 is not obvious in the literature, most common *N. crassa* lab strains are derived from strain OR74A. There are three versions of the sequenced genome for this reference strain. One is available at NCBI (https://www.ncbi.nlm.nih.gov/), the other at the Mycocosm data base (http://genome.jgi.doe.gov/programs/fungi/index.jsf), and the last at the FungiDB database http://fungidb.org/fungidb/). A fourth N. crassa strain (FGSC73) of opposite mating type is also available at Mycocosm (http://genome.jgi.doe.gov/programs/fungi/index.jsf). The sequences

from T1P11 that were obtained by Iman and me for the *aod-1* promoter, the *aod-2* gene, and the *aod-5* gene matched exactly to all the reference sequences in the regions examined (Fig. 3.7 A, B, C) with one exception. There was a single transition (T to C) in the 5′ untranslated region (UTR) of *aod-5*. The change occurs at position -815 relative to the A of the ATG start codon taken as position 1. It seems very unlikely that the 5′UTR of *aod-5* could cause the protein to become constitutively active. Thus, it appears there are no relevant changes in the T1P11 sequence at the *aod-1, aod-2* or *aod-5* loci to account for the observed increase in transcripts. It should be noted that whole genome sequencing data from T1P11 that was obtained after the above analysis (see below) are in agreement with our results.

3.2.3 Whole genome sequencing of high and low *aod-1* transcript expressing strains

In an attempt to identify other candidate genes that might be responsible for the upregulation of *aod-1* transcripts observed in certain strains of *N. crassa*, genomic DNA was extracted from several progeny and the parental strains of our NCN233 x T1P11 cross. Strains 3, 4, and 6, were chosen as low expressing progeny while 19, 23, and 26 were chosen as high expressing (Fig. 3.6). Our collaborators at Oregon State University sequenced the DNAs we supplied and mounted the data in G-browse (http://ascobase.cgrb.oregonstate.edu/cgi-bin/gb2/gbrowse/ncrassa_public/) and supplied a .vcf file with the data for each strain. This file was opened in Excel, and conditional filtering criteria were applied to the strains (see Materials and Methods section 2.11).

Given that the results of NCU233 x T1P11 cross suggested that the presence of high levels of *aod-1* transcripts in the absence of CM might be due to a mutation in a single gene, I examined the Excel sequence files for all differences in the high expressing strains (T1P11, 19,

A.

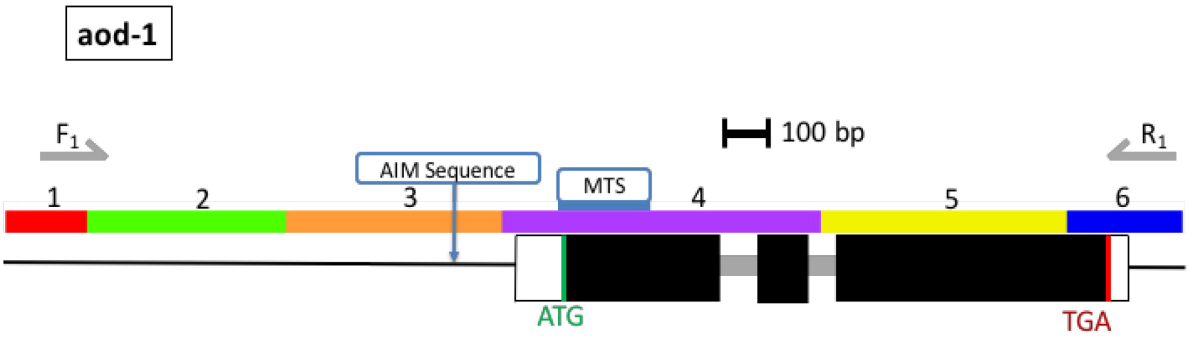
aod-1
F1
100 bp
R1
AIM Sequence
MTS
1
2
3
4
5
6
ATG
TGA

B.

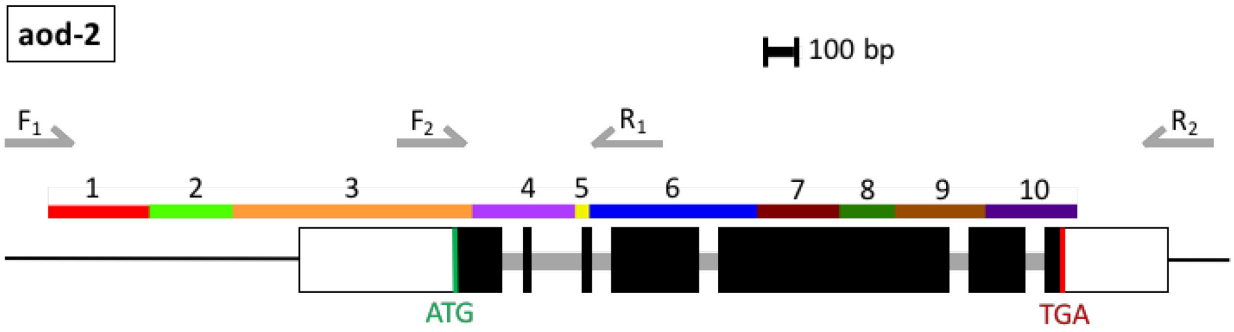
aod-2
100 bp
F1
F2
R1
R2
1
2
3
4
5
6
7
8
9
10
ATG
TGA

C.

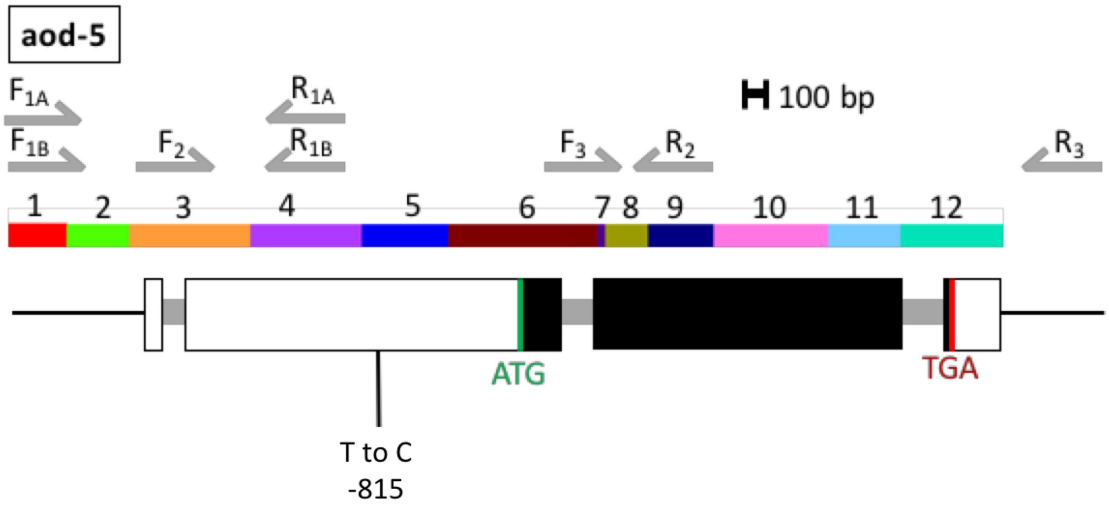

Figure 3.7. Results of sequencing *aod-1, aod-2* and *aod-5* in strain T1P11. T1P11 genomic DNA was isolated by former 399 student (Iman Asaria). PCR primers (F1A, R1A, F1B, R1B, F2, R2, F3, R3; refer to Materials and Methods Table 2.2) were used to amplify fragments of the different genes. PCR products were electrophoresed on an agarose gel for purification. DNA was extracted and purified and segments of the genes indicated by the numbered, colored boxes were sequenced by sequencing primers, (sequences given in Materials and Methods Table 2.2). Each number indicates a segment of the gene sequenced by a sequencing primer. Within the gene representations, white boxes are UTRs, thin grey boxes are introns, and thick black boxes are exons. Green indicates the translational starts (ATG) and red indicates the stop codons (TGA). **A)** *aod-1*: no changes found relative to the standard sequences. **B)** *aod-2*: No changes were found in the *aod-2* gene. **C)** *aod-5:* The *aod-5* gene had one base-pair substitution in the 5′UTR (T to C) prior to the coding sequence. Number shown with the mutation indicates the number of bases upstream from the A of the ATG start codon.

23, and 26) that were not present in any low expressing strains (Table 3.2). This filtering process was accompanied by a program designed in Visual Basics for Applications (VBA) in Excel that took the genomic position of the mutation and matched it to known coding regions of genes in the *N. crassa* genome obtained from transcripts for *Neurospora crassa* OR74A (assembly 10) supplied to us by the Freitag Lab at Oregon State University (see Materials and Methods section 2.10 and 2.11). A total of 123 genes were changed in T1P11, 48 genes in strain 26, 151 genes in strain 23 and 105 genes in strain 19. These genes were then compared among all strains using a Venn diagram (Venny program; see Materials and Methods section 2.11). This process narrowed the search down to mutations in two different candidate genes that were common among all high-expressing *aod-1* strains (Table 3.2 and Fig. 3.8).

One of the candidate genes, NCU05180 (*kinesin-9*), contained 4 mutations relative to the reference sequence. Three mutations were single nucleotide changes (all G to A changes) located in the 3′UTR. The fourth change was also a G to A transition that occurred in the coding region of exon 3 or 4, depending on the splice variant considered. The latter change would result in an amino acid change from aspartic acid to asparagine very near the C-terminus of the protein (Fig. 3.9A). This change affects amino acid residue number 740 of the 743 residue long protein, or 906 of the 909 residue long protein, depending on the splice variant. Since all three wild-type reference strain sequences lack the G to A changes in the 3′UTR, as well as the G to A change in the coding sequence, we consider the changes as mutations. The amino acid sequences of *kin-9* orthologues were aligned in fungal species from the Sordariomycetes, Eurotiomycetes, Saccharomycotina, and Taphrinomycotina phyla. Clustal revealed that the Asp is conserved in some more closely related fungal species such as *Magnaporthe oryzae,* and *Aspergillus nidulans*, but not in more distantly related species like *Yarrowia lipolytica* or

Table 3.2. Number of changes present in the genome of high-expressing *aod-1* strains compared to the reference sequence and absent in the low-expressing strains. Changes include single base pair substitutions, deletions and insertions. These changes were present throughout the genome, including coding regions, UTRs, exons, and introns. The number of changes remaining after excluding changes also found in low-expressing strains is indicated in the second row. The changes were then run through the FindData VBA program in Excel (see Materials and Methods) to identify changes found only in coding regions of genes (last row). The last row gives numbers of genes with changes in coding sequences.

	T1P11	Strain 26	Strain 23	Strain 19
Total number of changes compared to reference sequence	19166	29164	62011	55628
Total number of changes after excluding changes also present in low-expressing aod-1 *strains*	4434	2932	2842	1932
Total number of genes with changes in coding regions	123	48	151	105

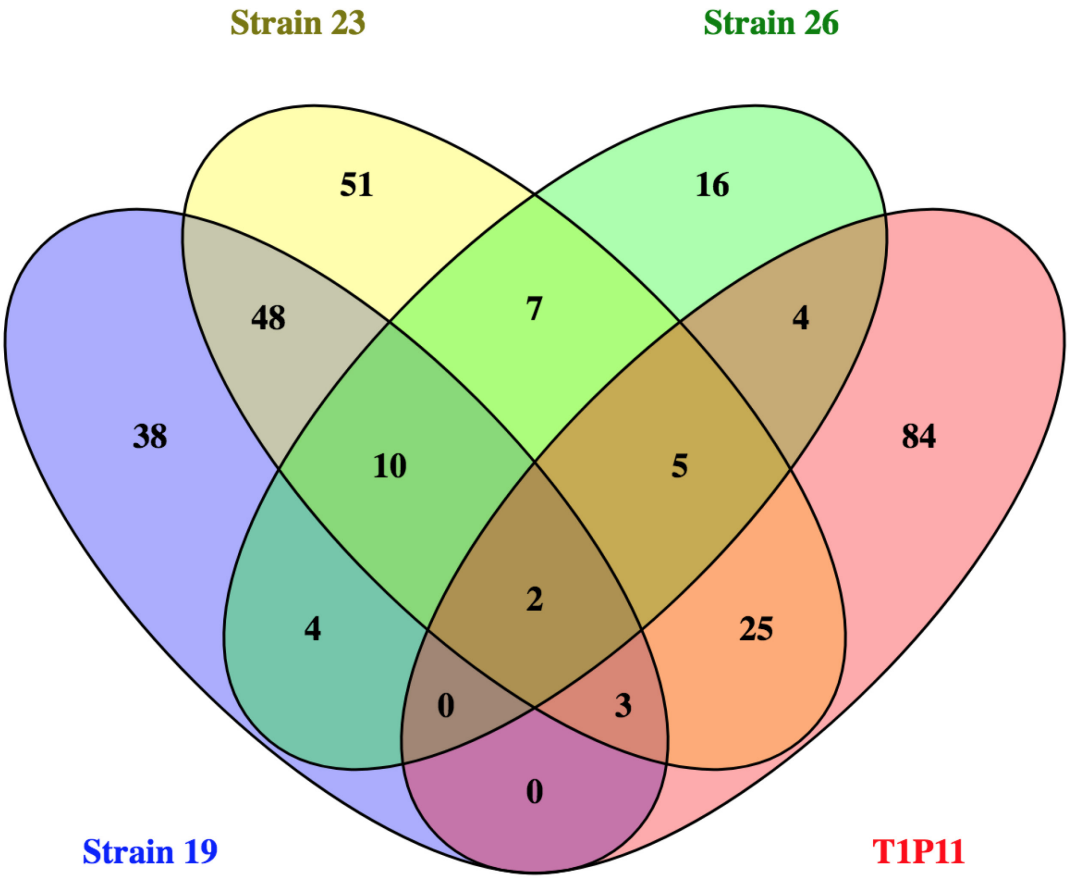

Figure 3.8. Venn diagram of changes in coding regions of genes relative to the reference sequence for high-expressing *aod-1* strains. Positions of changes in coding sequences found only in high-expressing strains were inserted into the FindData VBA program. Individual NCU numbers were listed using the program for each strain (see Materials and Methods section 2.11). Exclusive and common NCU numbers among the strains were determined by the VENNY program (http://bioinformatics.psb.ugent.be/webtools/Venn/) which displays the data in a Venn diagram. The number "2" in the center represents the two genes *flbA* (NCU08319) and *kin-9* (NCU05180) that contained changes common to all four strains.

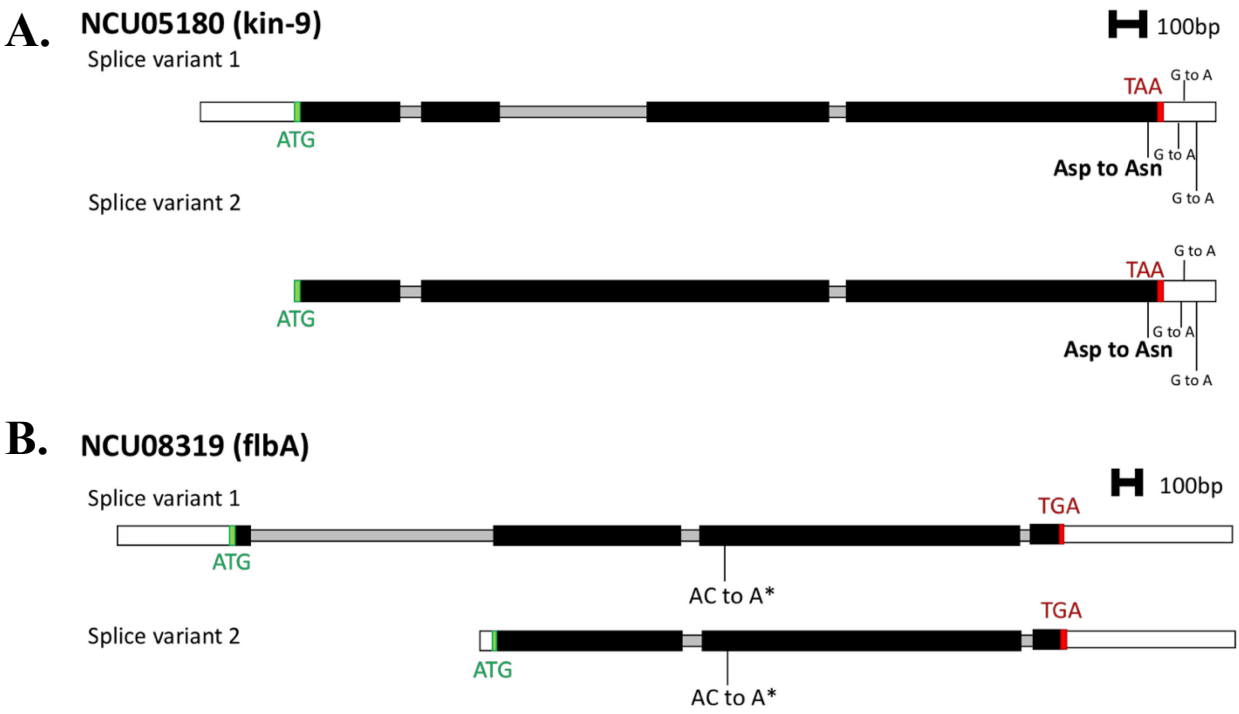
A.
NCU05180 (kin-9)
100bp
Splice variant 1
TAA
G to A
ATG
G to A
Asp to Asn
G to A
Splice variant 2
G to A
TAA
ATG
G to A
Asp to Asn
G to A
B.
NCU08319 (flbA)
100bp
Splice variant 1
TGA
ATG
AC to A*
Splice variant 2
TGA
ATG
AC to A*

Figure 3.9. Location of mutations in *kin-9* (NCU05180) and *flbA* (NCU08319) in strains T1P11, 19, 23 and 26. Genomic DNA was isolated from parental strains NCN233, and T1P11, as well as progeny strains 3, 4, 6, 19, 23, 26. Genomic DNA was sequenced by our collaborators at Oregon State University. Mutations in strains that had high *aod-1* expression levels in the absence of CM (T1P11, 19, 23, 26) were detected using conditional formatting and filtering criteria applied in Excel. A VBA program searched through a list of coding regions in genes based on mutation positions resulting in two candidate genes that carried mutations in all high *aod-1* expressing strains, relative to the reference sequences that were not present in any low expressing strain. White boxes are UTRs, grey boxes are introns, and black boxes are exons. Green indicates translational start (ATG) and red indicates the stop codon (TAA or TGA). **A)** The *kin*-9 gene (NCU05180). A transition mutation (G to A) was located in codon 740 of splice variant 1, or in codon 906 of splice variant 2 on chromosome 4 resulting in an amino acid change from aspartic acid (Asp) to asparagine (Asn) in exon 3, or 4, depending on the splice variant. Three other G to A differences (indicated as short, vertical lines above and below the 3′UTR) were located 3, 176, and 179 bp after the stop (TAA) in the 3′UTR. **B)** The *flbA* gene (NCU08319). A deletion mutation was located at codon 338 of splice variant 1, or codon 322 of splice variant 2 resulting in a frameshift in exon two or three that would truncate the protein from 766 amino acids to 375 amino acids in variant 1 or 750 amino acids to 359 amino acids in variant 2.

Schizosaccharomyces pombe (Fig. 3.10). AmiGO2 gene ontology bioinformatics analysis (Ruepp et. al. 2004) revealed that the gene product of NCU05180 is most likely involved with the cytoskeleton and is predicted to be associated with microtubules and vesicle mediated transport. There are kinesins that are known to act as transcription factors. For example, OsGDD1 is a plant kinesin and directly regulates the transcription of OSKO2 in rice by binding to the promoter of OSKO2 (Li et al., 2012). OsKO2 is an ent-kaurene oxidase involved in the gibberellin biosynthesis pathway (Ko et al., 2008). However, there is no evidence available to suggest any such role for *N. crassa kin-9.* Examining the NCU05180 predicted protein sequence using "search for conserved domains within a protein" at NCBI (https://www.ncbi.nlm.nih.gov/Structure/cdd/wrpsb.cgi) revealed two domains: a myosin/kinesin motor domain and an SMC_N (structural maintenance of chromosome, N-terminal) domain. The motor domain was found in all the proteins in the alignment except for *S. pombe* (Fig. 3.9). A search for conserved domains in the *S. pombe* closest *kin-9* homologue (SPBC15D4.01c (kinesin-like protein *Klp9*)) identified only a "kinesin-like protein domain". The SMC_N domain was only conserved in *N. crassa, M. oryzae,* and *A. nidulans.* The presence of a motor domain is not unexpected for a kinesin related protein. The significance of the single SMC_N motif, without a corresponding motif at the C-terminus, is unknown, since SMC proteins typically have domains at their N- and C-termini that associate to form a structure with ATPase activity (Nasmyth and Haering, 2005; Matityahu and Onn, 2018; Yuen and Gerton, 2018). Given that the change in NCU05180 is relatively conservative and does not occur in either of the functional domains identified in the protein, it seems unlikely that this mutation has any effect on *aod-1* transcript levels.

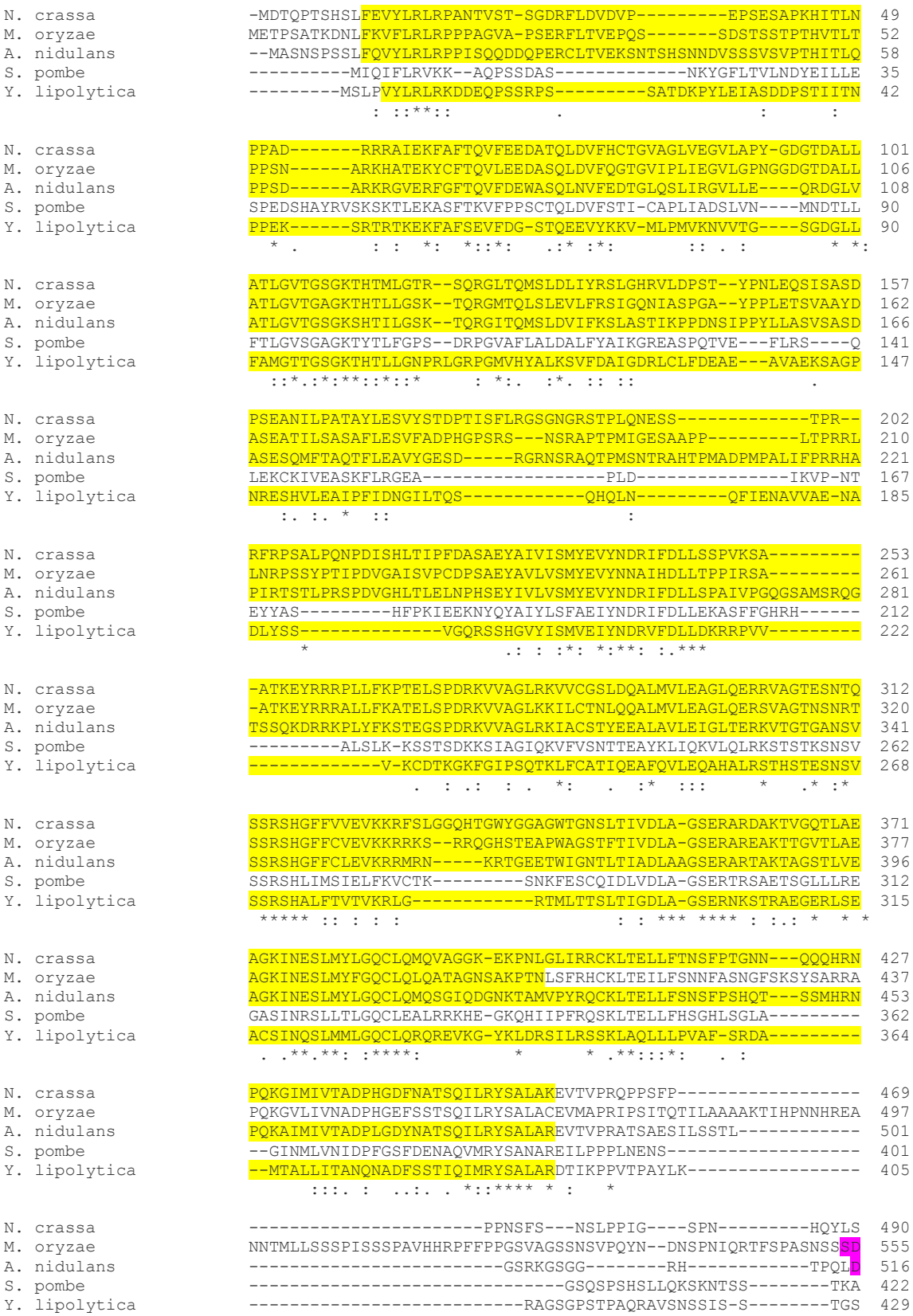
N. crassa -MDTQPTSHSLFEVYLRLRPANTVST-SGDRFLDVDVP---------EPSESAPKHITLN 49
M. oryzae METPSATKDNLFKVFLRLRPPPAGVA-PSERFLTVEPQS-------SDSTSSTPTHVTLT 52
A. nidulans --MASNSPSSLFQVYLRLRPPISQQDDQPERCLTVEKSNTSHSNNDVSSSVSVPTHITLQ 58
S. pombe ----------MIQIFLRVKK--AQPSSDAS------------NKYGFLTVLNDYEILLE 35
Y. lipolytica ---------MSLPVYLRLRKDDEQPSSRPS---------SATDKPYLEIASDDPSTIITN 42
N. crassa PPAD-------RRRAIEKFAFTQVFEEDATQLDVFHCTGVAGLVEGVLAPY-GDGTDALL 101
M. oryzae PPSN------ARKHATEKYCFTQVLEEDASQLDVFQGTGVIPLIEGVLGPNGGDGTDALL 106
A. nidulans PPSD------ARKRGVERFGFTQVFDEWASQLNVFEDTGLQSLIRGVLLE----QRDGLV 108
S. pombe SPEDSHAYRVSKSKTLEKASFTKVFPPSCTQLDVFSTI-CAPLIADSLVN----MNDTLL 90
Y. lipolytica PPEK------SRTRTKEKFAFSEVFDG-STQEEVYKKV-MLPMVKNVVTG----SGDGLL 90
N. crassa ATLGVTGSGKTHTMLGTR--SQRGLTQMSLDLIYRSLGHRVLDPST--YPNLEQSISASD 157
M. oryzae ATLGVTGAGKTHTLLGSK--TQRGMTQLSLEVLFRSIGQNIASPGA--YPPLETSVAAYD 162
A. nidulans ATLGVTGSGKSHTILGSK--TQRGITQMSLDVIFKSLASTIKPPDNSIPPYLLASVSASD 166
S. pombe FTLGVSGAGKTYTLFGPS--DRPGVAFLALDALFYAIKGREASPQTVE---FLRS----Q 141
Y. lipolytica FAMGTTGSGKTHTLLGNPRLGRPGMVHYALKSVFDAIGDRLCLFDEAE---AVAEKSAGP 147
N. crassa PSEANILPATAYLESVYSTDPTISFLRGSGNGRSTPLQNESS-------------TPR-- 202
M. oryzae ASEATILSASAFLESVFADPHGPSRS---NSRAPTPMIGESAAPP---------LTPRRL 210
A. nidulans ASESQMFTAQTFLEAVYGESD-----RGRNSRAQTPMSNTRAHTPMADPMPALIFPRRHA 221
S. pombe LEKCKIVEASKFLRGEA-----------------PLD---------------IKVP-NT 167
Y. lipolytica NRESHVLEAIPFIDNGILTQS------------QHQLN---------QFIENAVVAE-NA 185
N. crassa RFRPSALPQNPDISHLTIPFDASAEYAIVISMYEVYNDRIFDLLSSPVKSA--------- 253
M. oryzae LNRPSSYPTIPDVGAISVPCDPSAEYAVLVSMYEVYNNAIHDLLTPPIRSA--------- 261
A. nidulans PIRTSTLPRSPDVGHLTLELNPHSEYIVLVSMYEVYNDRIFDLLSPAIVPGQGSAMSRQG 281
S. pombe EYYAS---------HFPKIEEKNYQYAIYLSFAEIYNDRIFDLLEKASFFGHRH------ 212
Y. lipolytica DLYSS--------------VGQRSSHGVYISMVEIYNDRVFDLLDKRRPVV--------- 222
N. crassa -ATKEYRRRPLLFKPTELSPDRKVVAGLRKVVCGSLDQALMVLEAGLQERRVAGTESNTQ 312
M. oryzae -ATKEYRRRALLFKATELSPDRKVVAGLKKILCTNLQQALMVLEAGLQERSVAGTNSNRT 320
A. nidulans TSSQKDRRKPLYFKSTEGSPDRKVVAGLRKIACSTYEEALAVLEIGLTERKVTGTGANSV 341
S. pombe ---------ALSLK-KSSTSDKKSIAGIQKVFVSNTTEAYKLIQKVLQLRKSTSTKSNSV 262
Y. lipolytica -------------V-KCDTKGKFGIPSQTKLFCATIQEAFQVLEQAHALRSTHSTESNSV 268
N. crassa SSRSHGFFVVEVKKRFSLGGQHTGWYGGAGWTGNSLTIVDLA-GSERARDAKTVGQTLAE 371
M. oryzae SSRSHGFFCVEVKKRRKS--RRQGHSTEAPWAGSTFTIVDLA-GSERAREAKTTGVTLAE 377
A. nidulans SSRSHGFFCLEVKRRMRN-----KRTGEETWIGNTLTIADLAAGSERARTAKTAGSTLVE 396
S. pombe SSRSHLIMSIELFKVCTK---------SNKFESCQIDLVDLA-GSERTRSAETSGLLLRE 312
Y. lipolytica SSRSHALFTVTVKRLG------------RTMLTTSLTIGDLA-GSERNKSTRAEGERLSE 315
N. crassa AGKINESLMYLGQCLQMQVAGGK-EKPNLGLIRRCKLTELLFTNSFPTGNN---QQQHRN 427
M. oryzae AGKINESLMYFGQCLQLQATAGNSAKPTNLSFRHCKLTEILFSNNFASNGFSKSYSARRA 437
A. nidulans AGKINESLMYLGQCLQMQSGIQDGNKTAMVPYRQCKLTELLFSNSFPSHQT---SSMHRN 453
S. pombe GASINRSLLTLGQCLEALRRKHE-GKQHIIPFRQSKLTELLFHSGHLSGLA--------- 362
Y. lipolytica ACSINQSLMMLGQCLQRQREVKG-YKLDRSILRSSKLAQLLLPVAF-SRDA--------- 364
N. crassa PQKGIMIVTADPHGDFNATSQILRYSALAKEVTVPRQPPSFP------------------ 469
M. oryzae PQKGVLIVNADPHGEFSSTSQILRYSALACEVMAPRIPSITQTILAAAAKTIHPNNHREA 497
A. nidulans PQKAIMIVTADPLGDYNATSQILRYSALAREVTVPRATSAESILSSTL------------ 501
S. pombe --GINMLVNIDPFGSFDENAQVMRYSANAREILPPPLNENS------------------- 401
Y. lipolytica --MTALLITANQNADFSSTIQIMRYSALARDTIKPPVTPAYLK----------------- 405
N. crassa ----------------------PPNSFS---NSLPPIG----SPN---------HQYLS 490
M. oryzae NNTMLLSSSPISSSPAVHHRPFFPPGSVAGSSNSVPQYN--DNSPNIQRTFSPASNSSSD 555
A. nidulans -------------------------GSRKGSGG--------RH------------TPQLD 516
S. pombe ------------------------------GSQSPSHSLLQKSKNTSS--------TKA 422
Y. lipolytica --------------------------RAGSGPSTPAQRAVSNSSIS-S--------TGS 429


N. crassa FQQTLESAALEISRLQEDLTYLRHALDSERSLR--EQAEAHLLSMEDKMVELEQAIREDC 548
M. oryzae DRATMEAAALEIARLSEELEYMRQSCETERARR--VEAEDQLLSVEDRLIDLEQEIREDC 613
A. nidulans LAEDLEKALAEIERLTAENERLSLRLTEEEVLR--AETETALIVSEERCLLIEQEVREEC 574
S. pombe LTSHLEQL----------QQENQQLR------MLLADADSEMMNLEYEIRQQM 459
Y. lipolytica TMSHMSSASH----------TSHDDTKDNLIRTIAALQEQLYQAQQREDALEIQIREEV 478
N. crassa AEEFEKRLELEVNRWKTIVDGERERGEEFWRGKWGVFERMVEADGDVDMDMDVDSPKKPE 608
M. oryzae AAEFEQRLAVELARWKASMELEKERGEEHWDRKIEVYERAANVQVLATDG-DENDGDN-- 670
A. nidulans WAEMDERMEQERKRWQAAWDEQTGHNDDHIDKKIELLSQRFQIHEDPQP---------- 623
S. pombe TREMEERVSEVERTFLTKLLEESAQGIEYTDQKLEKMGGWMKKLQDENSEKTETIA---- 515
Y. lipolytica NQEMETHMEQMRQWYLDQLDQATDAAQNFTDKKISILGRRVNSDN---------- 523
N. crassa NTRLVETRTAEGQEARRQLEILADENERLQRENESLKQALAACIDPAKSTSKNKSPSRRS 668
M. oryzae ----------KENVLIENLEEENTRLRREVQVLKRELLG----------RSPTKRK 706
A. nidulans ----------SSDERVQELEFENDRLRSKITALERELN-CRSPSKKSSSKNA----- 664
S. pombe ----------QLEQIIEELHEELRSLEEE-------SIKESSATQQNENQHKRSSRK 555
Y. lipolytica ----------VSDELVKLRKE----------NQLL---KQ 540
N. crassa PSRSRRKKAQLNYAE---DDDGFFQELKRDQGDMAMDGFGEGNGVG----GSHGTGSPTK 721
M. oryzae PLAERDDLATEDMAAPHQTGDSLHS----KMEQLRVSEVGRASSTSNSSRATVQSTAGGS 762
A. nidulans ALETSRNA---NILG----RESDIEVALRKMDQLKLADS-----MF------KSPAVNTP 706
S. pombe LLYE----DKQAIQEAHT-INTKRKLW-PQSTLIQAPNSDDE----------ENVPSPSP 599
Y. lipolytica RLNV----DKENVEIAHG-PDSFRS----------D------- 561
N. crassa KKRIRRLGAKKWGQGLDDDDPF---------- 743
M. oryzae PRKVRKLVAKRWDLSAANDDGF---------- 784
A. nidulans GKKQRKMATRKWDLAPEDDL---------- 726
S. pombe KKK---VVSPIKPLSPSRRPPLTSLYSGTTDIDINEL 633
Y. lipolytica ---------- 561

Figure 3.10. Clustal alignment of *kin-9* homologues in the phylum Ascomycota of the fungi. The amino acid sequences of Sordariomycetes species *Neurospora crassa kin-9* kinesin-like protein (NCU05180) splice variant 1, *Magnaporthe oryzae* MGG_05060 kinesin family protein; Eurotiomycete species *A. nidulans nidulans* AN3124 kinesin family protein; Saccharomycotina species *Yarrowia lipolytica* YALIOE10879p protein; and Taphrinomycotina species *Schizosaccharomyces pombe* SPBC15D4.01c were aligned using the Clustal Omega program (https://www.ebi.ac.uk/Tools/msa/clustalo/). The closest homologue to the *N. crassa kin-9* in the other organisms was selected for comparison. The position of the motor and SMC_N domains are shown by yellow and pink highlighting, respectively. The location of the D to N change present in the four high-expressing *aod-1 N. crassa* strains is highlighted in green. The D residue highlighted in green is not conserved in the *S. pombe* or *Y. lipolytica* proteins. "*****" (asterisk) indicates positions that have a single, fully conserved residue; "**:**" (colon) indicates conservation between residues of strongly similar properties - scoring > 0.5 in the Gonnet PAM 250 matrix. "**.**" (period) indicates conservation between residues of weakly similar properties scoring ≤ 0.5 in the Gonnet PAM 250 matrix.

The second gene change was a single base pair deletion of a cytosine in the *flbA* gene (NCU08319) (Fig. 3.9B). Loss of *flbA* results in loss of the GTPase activity of the GPCR. This change occurs in exon 2 (codon 322) or exon 3 (codon 338), depending on the splice variant of the gene. This deletion would result in a truncation of the protein from 766 amino acids to 375 amino acids for variant 1, or 750 amino acids to 359 amino acids for variant 2. Either of these changes would be predicted to have a severe effect on the protein as important functional domains for G-protein signalling and its regulation would be lost (Fig. 3.11).

Although there are no studies of the gene in *N. crassa,* in *Aspergillus nidulans, flbA* is a negative regulator of the Gα subunit of the GPCR. Studies conducted on a *ΔflbA* mutant in *Aspergillus niger* have shown that loss of the gene affects conidiation (Lee and Adams, 1994; Krijgsheld et al., 2013). Additionally, a microarray analysis conducted in 2013 in *A. niger* examined the effect of *flbA* inactivation on the transcriptome. The study reported genes that had greater than or equal to 2-fold changes in expression. One of the top 50 upregulated genes in the *ΔflbA* background was the *A. niger* AOX-encoding gene, *aox1* (Krijgsheld and Wösten, 2013). Therefore, *flbA* is a strong candidate gene for the observed upregulation of *N. crassa aod-1* in certain strains.

3.2.4 Confirmation of candidate gene *flbA*

To confirm that the mutation in *flbA* (NCU08319) was implicated in the upregulation of *aod-1* transcripts, qPCR was conducted on two strains of opposite mating type with a deletion of NCU08319 (ΔNCU08319) obtained from the *N. crassa* knock out library. These strains were first examined by PCR analysis of extracted genomic DNA to ensure that NCU08319 was knocked out in both mating types. This was shown to be the case (Supplemental Fig. 1). Both

```
N.crassa_NCU08319      MSHEGVVHQFGGIGGKMAAGSSSSRSTNSDSSSPVVALQAGHRSTGSTVNSSKSRSASSS
A.nidulans_5893        ----------------MPTSIST---------A---PLSQ-----GSP--------PSSL
                                      * :. *:         :    *.      **          **

N.crassa_NCU08319      ISTISSSANTGSAPATGTSG-----TASNTPSSHSSSSSSSSSTTVSALAGNTIAKAKSN
A.nidulans_5893        IDYQPQSVPSSSSPPPSTAAAAAAAVVVAVPSSSSPVD-----LGLPSF-----TSTSSL
                       *.   .*. :.*:*  .*:.     ..  .*** *  .       : ::     :.:.*

N.crassa_NCU08319      SVRDPVAKPPYPAVSGSQTRQQAHSHLSSLSVSSQRTGGIF-ALAAAALDKTLA---GLG
A.nidulans_5893        ITSDVPATTTTPSFTGSVI--------GSIS---RRNRRSFAALAREKTSSALANLSSIG
                        . *  *.   *:.:**          .*:*   :*.   * ***    ..:**   .:*

N.crassa_NCU08319      E---PRIRSRQSNG----------RLSAGP---ESPVGGPLLPGPDKSSRSRSASRSSPE
A.nidulans_5893        STTNSSLRQSASSGSLQKHSRKASQLSVGEISGFVPLSPPLSDGSGSSEQSS--------
                       .     :*.  *.*          :**.*      *:. **  * ..*.:*

N.crassa_NCU08319      DERYLASSLVPRDPNPPSQPYSE-TDPNRPLPVRVSRVDNKMHQTSSRLLRMTDDDRPFT
A.nidulans_5893        SAPFEPLSAVTEQPNPAAERRRQTIQLVPPISENIPVSPAKMHQTSSRLLRMTEDDRPFT
                       .  :   * * .:*** ::   :  :   *:  .:     *************:******

N.crassa_NCU08319      KDFKDLFSTLIVSLLPLSAHRVRLTKVEHTFLSEDAINNLGSLKFSQSNRMPDPKDPSRI
A.nidulans_5893        KDFMDLFSTLMVSL-KLDSHRVRFTKYDHTFTSEEAINNLGSLKFSQSNRMPDPKDPSRI
                       *** ******:***  *.:****:** :*** **:*************************

N.crassa_NCU08319      VTTTTTTTTFSMAKDMARSICQRFLEARFIESADGRYQQVYSMKGSVWQLTPKGISILDRF
A.nidulans_5893        VTTTTTTTTFSMAKEMARSVCQRFVDARFIESVDGKYSHTFPLKGALYQLTPKGINILQRF
                       *************:****:****::******.**:*.:.: :**:::*******.**:**

N.crassa_NCU08319      CSRNGIQQKQVAELIGNS--LPQIVILERNPQTDKVLTDRALIEVIFRRFIGPNGFNIKQ
A.nidulans_5893        CQRNGITARHVIDVLESPRNTMQLVNLERDTETDKLSHDRATIEVIFRRFAGQDGPNVKS
                       *.****  ::* ::: .     *:* ***: :***:  *** ******** * :* *:*.

N.crassa_NCU08319      SVSSADSDSLSDYRDGLTGVKMAAERKVNGRTYRDTFTGKAATDWLMDCSTAVDRRETIE
A.nidulans_5893        SVSSSDSDSLSDYSNGLVGVKMARERKVGDKICANTFTGKAAVDWLMDCSTTIEPRETVL
                       ****:******** :**.***** ****..:   :*******.********::: ***:

N.crassa_NCU08319      IASLFVEYELMEAVQQDKAHMQQNPGHHLFQPTKHAIYQVTPKGKDLVNGALVRGRPSES
A.nidulans_5893        IAELFVKYGLITVLQEDRSMPQVENSLVAFQPSKNAIYAITERGQRVC-GWLARDKPRDT
                       **.***:* *: .:*:*::  * : .   ***:*:*** :* :*: :  * *.*.:* ::

N.crassa_NCU08319      DGHSASRSVGIARDSNTQRLDKILNENSLRLLFRENLRETHCEENLAFYLDTDEFVRQCR
A.nidulans_5893        ---TTYDSRGIPRDSNNARLNHILQDPALRLLFREFLRFSLCEENLSFYIDVSEFTTQYH
                          ::  * ** ****. **::**:: :******* ** : *****:**:*..**. * :

N.crassa_NCU08319      AAIDLAQRSPNSAASLDGIKEIMAQAYGIYNAFLAPGSPCELNIDHQLRNNLATRMTKAV
A.nidulans_5893        KFDKVG-----HFKKPDAVRETLAAAYGLYNAFLAPGSPCELNIDHALRNSLASRMTKAV
                          .:.        . *.::* :* ***:***************** ***.**:******

N.crassa_NCU08319      GQDVTMIDTLREVMALFEDAQNAVFKLMASDSVPKFLRNPKYEQTLRNYDFDSITPVH--
A.nidulans_5893        GDDDSMLKSLQEVVQLFEMAQTSVFKLMSSDSVPKFLRDPKYSAILQEHDVDDLIGGGRS
                       *:* :*:.:*:**: *** **.:*****:*********:***.  *:::*.*.:

N.crassa_NCU08319      ---GQGRMVERSQSRSNRT
A.nidulans_5893        YSPTPGNVPERSMSRSQRS
                            *.: *** ***:*:
```

Figure 3.11. Sequence alignment of *flbA* proteins. The amino acid sequence of *Neurospora crassa flbA* (NCU08319) and *Aspergillus nidulans flbA* (AN5893) and were aligned in Clustal. Highlighted in red is the position prior to the insertion of an "A" nucleotide in the *flbA* gene of *N. crassa* high expressing *aod-1* strains. This insertion would lead to the formation of a premature stop codon and the truncation of the protein. Highlighted in yellow is the DEP (Dishevelled, Egl-10 and Pleckstrin) domain which is involved in G-protein signaling. Highlighted in gray is the RGS (Regulator of G-protein signaling) domain which is critical for activity. Both domains are necessary for normal protein function and both are well conserved in *N. crassa* and *A. nidulans*. The truncation event is predicted to render the mutated NCU08319 non-functional in high-expressing *aod-1* strains due to the loss of these domains. "*****" (asterisk) indicates positions which have a single, fully conserved amino acid residue; "**:**" (colon) indicates conservation between residues with strongly similar properties - scoring > 0.5 in the Gonnet PAM 250 matrix. "**.**" (period) indicates conservation between residues with weakly similar properties scoring ≤ 0.5 in the Gonnet PAM 250 matrix.

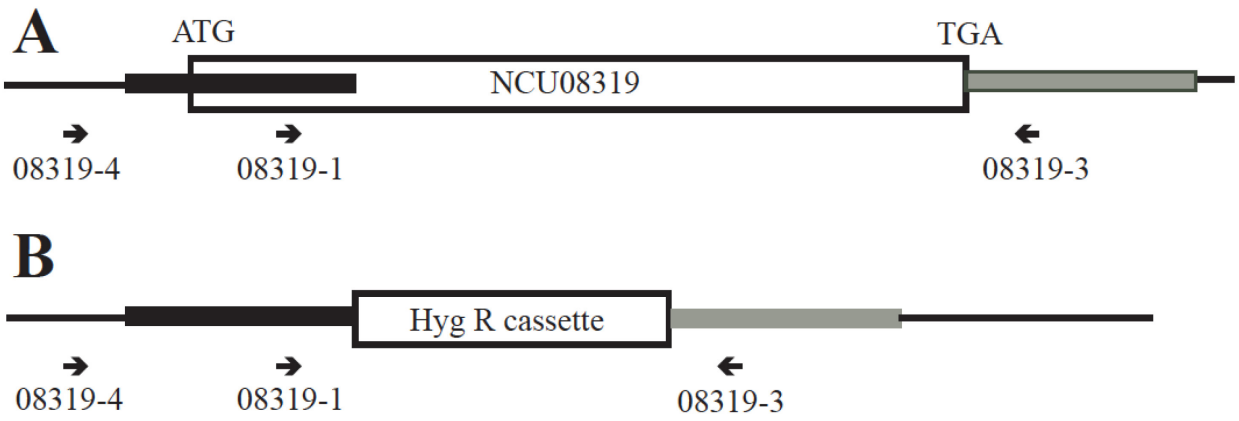

C PCR with primers 08319-4 to 08319-3

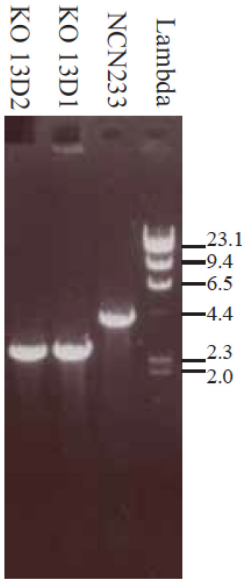

Prediction for NCN233: 4.1 kb
Prediction for KOs: 2.7 kb

D PCR with primers 08319-1 to 08319-3

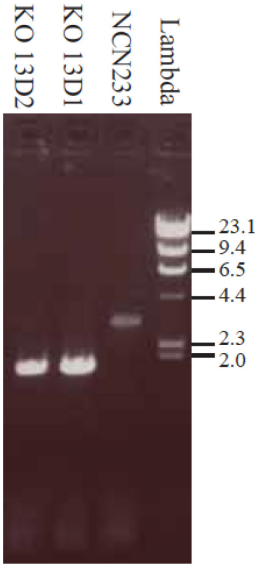

Prediction for NCN233: 3.3 kb
Prediction for KOs: 1.9 kb

Supplemental Figure 1. Wild-type (strain NCN233) and knockout (KO) versions of the NCU08319 locus. **A)** Wild-type locus for the NCU08319 gene encoding *flbA*. The white box represents the coding region of the gene. The positions of the start (ATG) and stop (TGA) codons are shown. The black bar to the left represents the 5′ flanking region used to promote integration of the knockout construct at the correct locus by the *N. crassa* knock out project. The grey bar to the right represents the flanking sequence for the 3′ region integration. The position and orientation of primers used in PCR of genomic DNA isolates from wild-type and knockout strains are shown as small arrows with the primer name. **B)** The structure of the locus following replacement of the NCU08319 gene by the HygR (Hygromycin resistance) cassette. PCR primers are shown as in panel A. **C)** Results of PCR using primers 08319-4 and 08319-3 and with template genomic DNA isolated from the indicated strains. NCN233 contains a wild-type locus (panel A) while the KO strains contain the HygR replacement (panel B). *HindIII* fragments of lambda phage DNA were used as standards and their size in kilobase pairs is indicated on the right. The predicted sizes of PCR products are given at the bottom of the panel. **D)** As in C except the PCR primers were 08319-1 and 08319-3. PCR analysis was conducted by Frank Nargang.

mating types of the knock out were analyzed: ΔNCU08319 (position 13D1 in the knock out library) mating type *a* and ΔNCU08319 mating type *A* (position 13D2 in the knock out library plate array). The knock out strains were grown in medium lacking CM, RNA was isolated and cDNA was synthesized. Following qPCR, ΔΔCT values for both mating types of ΔNCU08319 were compared to strains T1P11 and NCN233, both grown in the absence of CM. The analysis revealed that ΔNCU08319 (13D1) had elevated *aod-1* transcript levels as observed in T1P11. However, ΔNCU08319 (13D2) had a wide range of results between biological replicates, resulting in the large error bars seen in Fig. 3.12. It should be noted that three out of four of the biological replicates for mating type A (13D2) had very low CT values (i.e.; high *aod-1* mRNA levels). Therefore, one biological replicate gave rise to the large error bar. Thus, mating type A most likely also has elevated transcript levels. CT values for *β-tubulin* were consistent for all strains analyzed. Taken together, all these data suggest that the deletion mutation in *flbA* identified by genomic sequencing analysis results in the high uninduced levels of *aod-1* mRNA in strain T1P11.

3.3 Evidence for regulation of *aod-1* mRNA Translation

3.3.1 *aod-1* mRNA amount and AOX protein amount are not strongly correlated

As discussed in section 3.2, the original strains observed with high uninduced levels of *aod-1* mRNA appeared to be devoid of AOD1 protein (Descheneau et al., 2005). I wished to investigate this observation further and began by determining if any strains with high uninduced levels of *aod-1* mRNA contained AOD1 protein. The strains were examined by Western blot of mitochondria isolated from cells grown in both –CM and +CM conditions. All strains produced AOD1 in the presence of CM. Interestingly, faint bands of AOD1 protein were observed

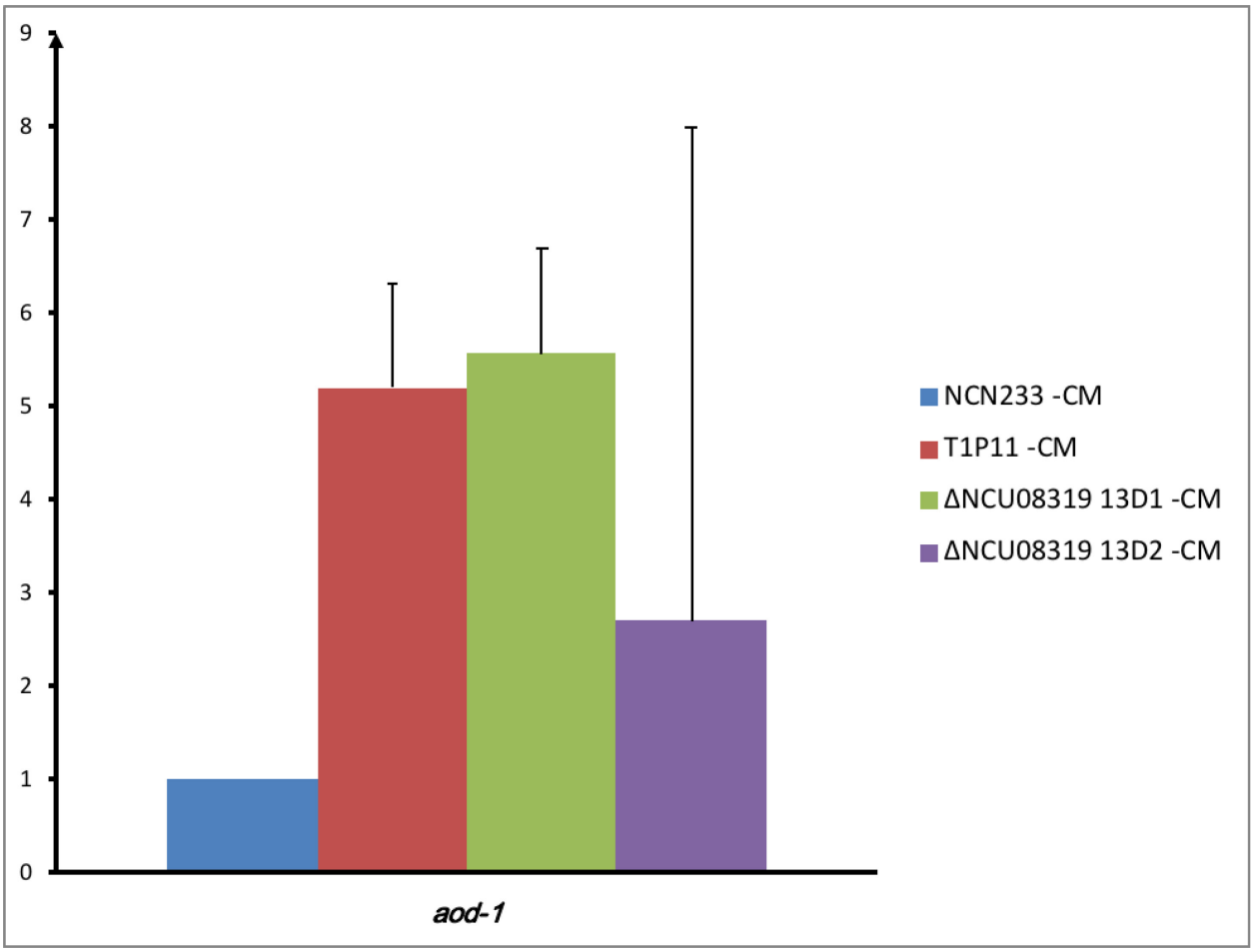

Figure 3.12. *aod-1* transcript levels in NCN233 (wild-type control), T1P11, and ΔNCU08319 mating type *a* (13D1) and *A* (13D2). Strains were grown in –CM medium for 14 hours, RNA was extracted and cDNA was generated. The expression levels of *aod-1* mRNA were determined by qPCR with four biological replicates (three technical replicates each) and standardized to *β-tubulin*. ΔΔCT values were obtained by standardizing to wild-type, NCN233. Error bars represent the standard error of the mean.

following growth in –CM conditions for strains 26 (high uninduced transcript levels) and 17 (unknown levels of transcript), while a stronger band was observed for strain 23 (high uninduced transcript levels) (Fig. 3.13). Strains 6 (low uninduced transcript levels), 9 (high uninduced transcript levels), 11 (unknown levels of transcript), 16 (high uninduced transcript levels) and 19 (high uninduced transcript levels) had no observable AOD1 protein present in uninduced conditions (Fig. 3.13).

One simple explanation might be that there is a direct relationship between the amount of *aod-1* mRNA observed in a certain strain and the amount of AOD1 protein produced. However, this did not appear to be true. Comparison of the qPCR data (Fig. 3.6) with the Western blot results (Fig. 3.13) revealed no clear relationship between the amount of transcript detected and the amount of protein present. For example, the amount of *aod-1* mRNA present in uninduced T1P11 and uninduced progeny strain 19 was similar to the amount in the CM-induced (+CM) wild-type strain NCN233 (Fig. 3.6). However, mitochondria from uninduced T1P11 and strain 19 contained no detectable AOD1 protein, while the CM induced NCN233 contained large amounts of the protein (Fig. 3.13). If there was a simple relationship between amount of mRNA and amount of protein, I would have expected to see AOD1 protein levels for the uninduced T1P11 and strain 19 to be similar to what was seen in the wild-type in the presence of CM. Similarly, strains 16 and 9 had elevated transcript levels that resulted no detectable protein. These data strongly suggest that some pos*t*-transcriptional mechanism controls AOX protein level in addition to the previously described transcriptional control of the *aod-1* gene (Chae et al., 2007a, 2007b; Tanton et al., 2003; Qi et al., 2016).

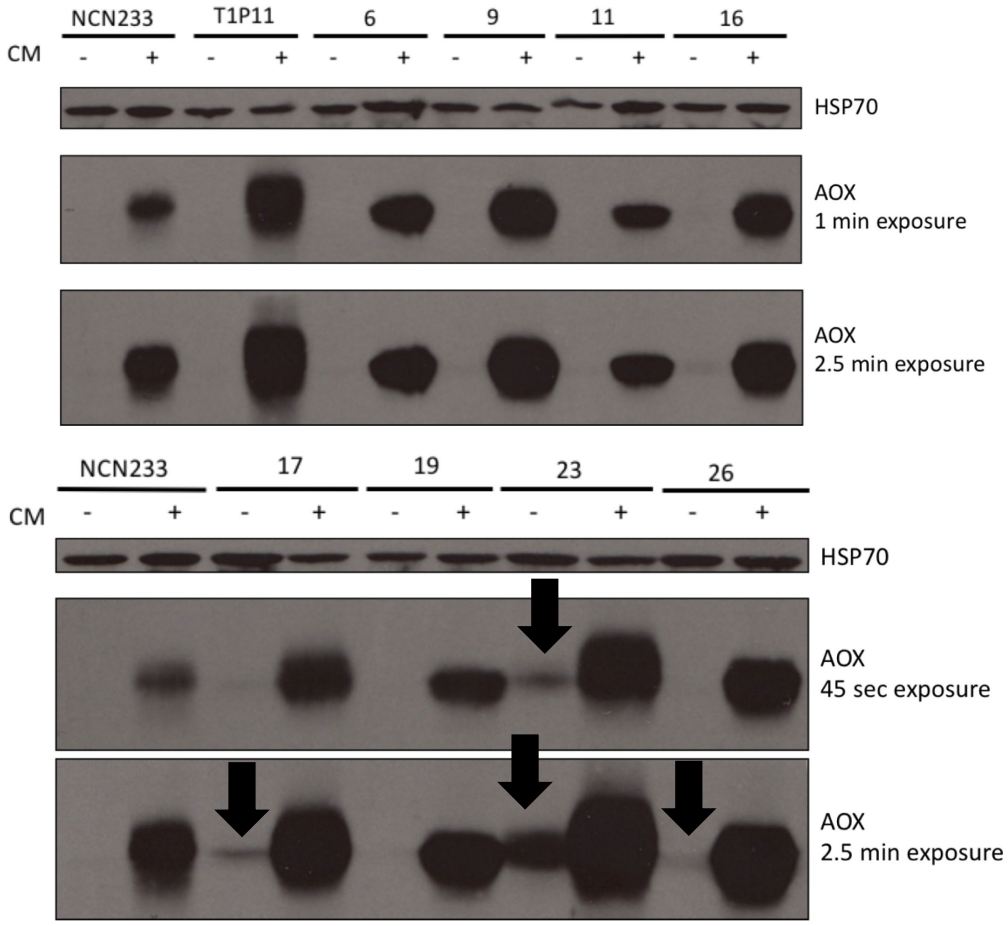

Figure 3.13. AOD1 protein in parental and selected progeny strains. Cultures of the parental wild-type NCN233 and T1P11 strains, and the indicated progeny strains, were grown in the absence of CM (-CM) for 14 hr, and for 16 hr in the presence of CM (+CM). Mitochondria were isolated, subjected to SDS-PAGE and Western blotting with a short and long exposure. Fractions were analyzed for the presence of AOD1 protein using an AOD1 antibody. Hsp70 served as a loading control. Strains 17, 23, and 26 all had detectable AOD1 protein in cultures grown in non-inducing conditions (arrows). (Note that strains 11 and 17 were not among the strains examined by qPCR for *aod-1* mRNA levels (Fig. 3.6)).

3.3.2 AOD1 is not sequestered in the cytosol under non-inducing conditions

Since *aod-1* mRNA was successfully translated in T1P11 and strain 19 when they are grown in inducing conditions (Fig. 3.13), it is possible that growth in CM results in the production of a signal to initiate protein synthesis from the *aod-1* mRNA. One obvious possibility for achieving such control would be by either recruiting RNA-binding proteins essential for translation or by removing proteins that are inhibiting translation under non-inducing conditions. However, since the Western analysis in Fig. 3.13, and previous work on AOX expression was done using purified mitochondria, it is also possible that the protein is made, but not imported into mitochondria in the absence of CM. It is also conceivable that the protein is made but is rapidly degraded in strains with high uninduced levels of *aod-1* mRNA.

If the protein is being synthesized in the cytosol but not being imported into the mitochondria in the absence of CM, I would expect to find the protein in the cytosol. To determine if the protein is present in the cytosol in –CM conditions, I grew T1P11, NCN233, and three biological replicates of progeny strain 23, which had the greatest abundance of protein in mitochondria following growth in non-inducing conditions (Fig. 3.13). Cytosolic fractions were isolated and Western blotted for the presence of AOD1 protein. All strains grown in the presence of CM contained small amounts of AOD1 protein in the cytosol, which was more apparent in the longer exposure (Fig. 3.14). Because this band was present for all of the strains including the wild-type in inducing conditions, it is most likely just trace amounts of protein that had not yet been imported into the mitochondria. However, no strain grown under non-inducing conditions contained detectable AOD1 in the cytosol. Thus, it appears that AOX is not sequestered in the cytosol under non-inducing conditions for any strain.

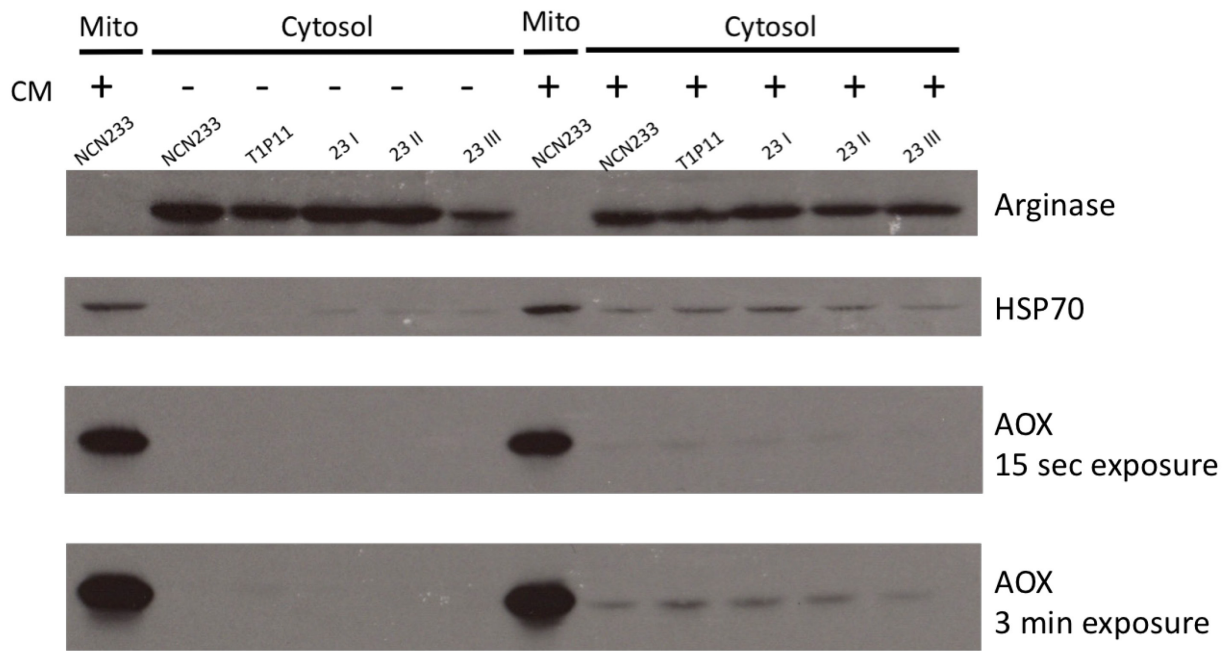

Figure 3.14. Western Blot analysis for AOD1 protein in cytosolic fractions. NCN233, T1P11, and three biological replicates (I, II, III) of strain 23, were grown in both the absence (–CM) and presence of chloramphenicol (+CM). Cytosolic fractions (cytosol) were isolated, proteins were separated by SDS-PAGE, blotted to PVDF membrane and probed with the antibodies indicated on the right. Wild-type NCN233 mitochondria (Mito) isolated from cells grown in the presence of CM served as a control for AOD1. Arginase served as a cytosolic protein loading control, and HSP70 as a mitochondrial loading control. Two exposures were taken for AOD1.

3.3.3 AOD1 is not made and rapidly degraded in the absence of an inducing signal

As mentioned in the previous section, another possibility for the lack of AOD1 protein in strains expressing high uninduced levels of *aod-1* transcript, was that the AOD1 protein is made in –CM growth conditions but has a short half-life due to rapid degradation. Thus, there may be signals produced in the presence of CM that serve to prevent the degradation. If so, it is possible that the lack of a substantial AOD1 band observed in strains such as T1P11, 9, 23 and 26 in non-inducing conditions is due to protein degradation. Therefore, I wished to determine if previously synthesized AOD1 protein would be rapidly degraded once the inducing signal was removed. Strains NCN233 and T1P11 were grown in +CM medium. A small sample of the culture was taken following 18 hr growth and mitochondria were isolated. The remaining culture was then filtered and washed to remove medium containing CM. The mycelium pads were then transferred to medium without CM and growth was continued. Samples were taken after 2, 4, and 6 hr of growth in –CM. Mitochondria were isolated and subjected to Western blotting for AOD1. If rapid degradation occurred in the absence of inducing signal, I would expect disappearance of the AOD1 band. This was not the case. Protein amounts gradually decreased at similar rates in both T1P11 and NCN233 (Fig. 3.15). Thus, rapid degradation of AOD1 in the absence of inducing signal can be excluded as a general mechanism because there was detectable protein for at least 6 hr after the signal was removed. The small decrease of AOD1 protein seen over the course of the experiment is likely due to the dilution of the protein with continued growth in the absence of an inducing signal. The data described above remove two possible explanations for the absence of AOD1 protein and suggest that *aod-1* mRNA present under non-inducing conditions may be subject to translational control as the most obvious explanation.

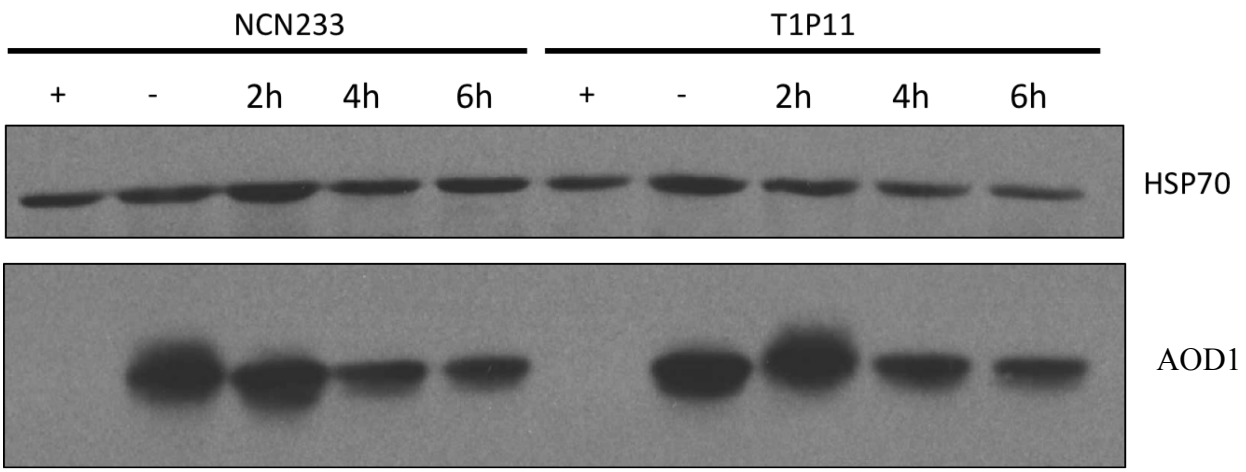

Figure 3.15. The AOD1 protein is not rapidly degraded in the absence of an inducing signal. The wild-type strain NCN233 and strain T1P11 were grown in –CM (-) for 16 hr and +CM (+) conditions for 18 hr. After growth in +CM medium for 18 hr, mycelia were harvested under sterile conditions and suspended in medium without CM. These cultures were grown for 2 hr (2h), 4 hr (4h), and 6 hr (6h). After each time point, cultures were harvested and mitochondria were isolated. Proteins were subjected to SDS-PAGE followed by Western blotting for the AOD1 protein. HSP70 served as a loading control.

3.4 5′ and 3′UTR replacements of *aod-1*

If translational control was the reason for observing little to no AOD1 protein, despite the presence of *aod-1* mRNA in certain strains grown under non-inducing conditions, this could be achieved in one of two ways. First, it is possible that a regulatory protein(s) is bound to the mRNA and prevents its translation in the absence of the appropriate inducing signal. Alternatively, a protein(s) required for translation may not bind to the mRNA unless an inducing signal is present. There are precedents for both these negative and positive types of translational control in the literature (Abdelmohsen, 2012; Oliveira et al., 2017). Furthermore, such effects are most often mediated by proteins binding to the 5′ and/or 3′ UTR regions of the target mRNAs (Oliva et al., 2015; Szostak and Gebauer, 2013). Preliminary work on constructs with modified 5′ and 3′ UTRs is described in the Appendix.

3.5 High variability in levels of aod-1 mRNA in certain strains

An interesting observation from the qPCR data was the variable results seen for certain progeny strains as shown by the large range of ΔCT values and large error bars. Originally, four biological replicates that appeared to be consistent were graphed (Fig. 3.6). However, further analysis revealed that there was high variance among replicates in some strains. To gain a better understanding of the range in data, additional qPCR experiments were performed and all ΔCT values obtained from all qPCR runs were collected and graphed for all the strains. Strains 19, 23 and 26 had the widest range of ΔCT values obtained from the biological replicates, with strain 23 having the greatest range in values (Fig. 3.16)

Due to the wide range in the values for *aod-1* mRNA in certain strains, it was conceivable that, by chance, in the studies described above (Fig. 3.13, section 3.3.1), the –CM

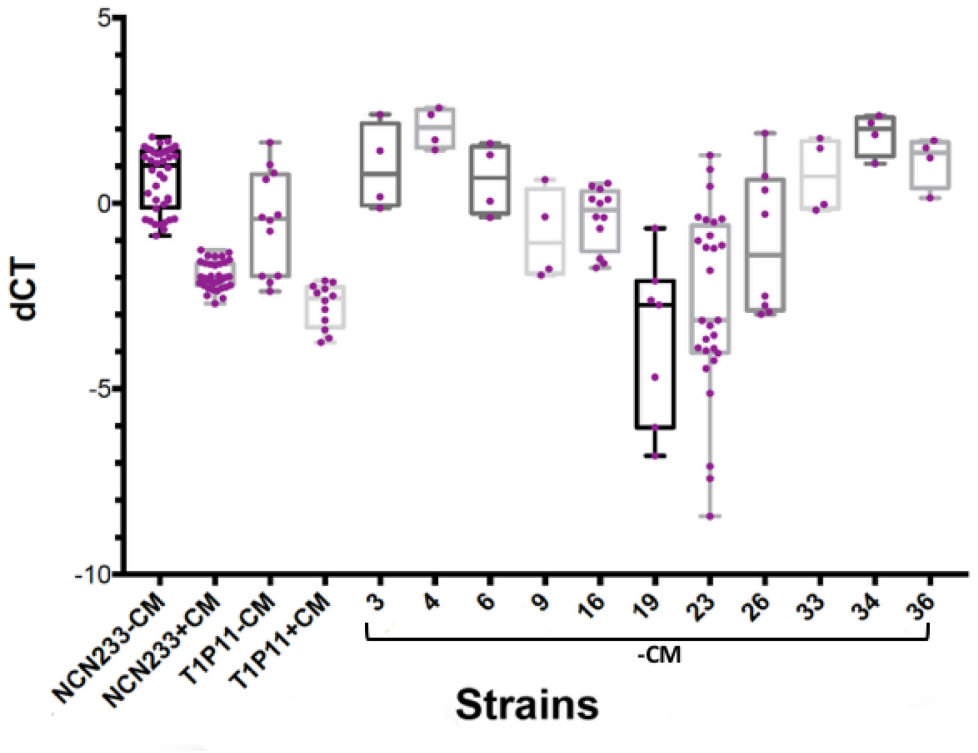

Figure 3.16. Variation in expression levels of *aod-1* transcript. *Aod-1* ∆CT values for parental and progeny strains are shown as box and whisker plots. Parental (T1P11 and wild-type NCN233) and progeny (3, 4, 6, 9, 16, 19, 23, 26, 33, 34 and 36) cultures were grown in the presence (+CM), or absence (-CM) of CM. RNA was isolated, converted to cDNA and analyzed by qPCR. ∆CT values for *aod-1* were calculated by standardizing to *B-tubulin.* Each dCT value is denoted by a purple dot (•). Whiskers were generated to span the maximum and minimum points while box plots show the median with 50% of values (indicated by the line inside the box).

cultures examined by Western blot happened to correspond to cultures with low *aod-1* mRNA (since qPCR samples and mitochondrial isolation samples were from different cultures). Thus, it could be that uninduced cultures with high *aod-1* mRNA levels actually do contain large amounts of AOD1 protein, but were simply missed in my previous analysis. To explore this concept further, a greater number of biological replicates for strains 19 and 23, which had the largest ΔCT ranges (Fig. 3.16) and had observable AOD1 protein in the first Western analysis (Fig. 3.13), were examined for the presence of AOD1 protein. The replicates were grown in – CM conditions, mitochondria were isolated, and blotted for AOD1 protein. Strain 19 had no observable AOD1 protein at the shortest exposure time, but the longer exposure showed very faint bands in all the biological replicates (Fig. 3.17A). One replicate (A) for strain 23 had an observable AOD1 protein band at the low exposure time. A longer exposure revealed the presence of AOD1 protein for biological replicates C and E (Fig. 3.17B). In these experiments, all of the replicates were grown at the same time, under the same conditions, with no known variations in medium, temperature, growth time, or stress conditions. Thus, unknown factors appear to cause variability in AOD1 content between cultures of the same strain.

As mentioned above, up to this point, cultures had been grown and either processed only for RNA extraction or for mitochondrial isolation to be used for Western analysis. There had been no simultaneous comparison of a single culture's transcript and protein levels. Because of the variation in transcript and protein amounts of strain 23 cultures, five biological replicates were grown and each was examined individually via both qPCR and Western Blot analysis in the absence of CM. Samples for qPCR were taken after 14 hrs. The remainder of the culture was harvested after an additional 2 hr of growth for isolation of mitochondria. qPCR results were converted to ΔΔCT values and graphed. Replicate E had the greatest amount of detectable

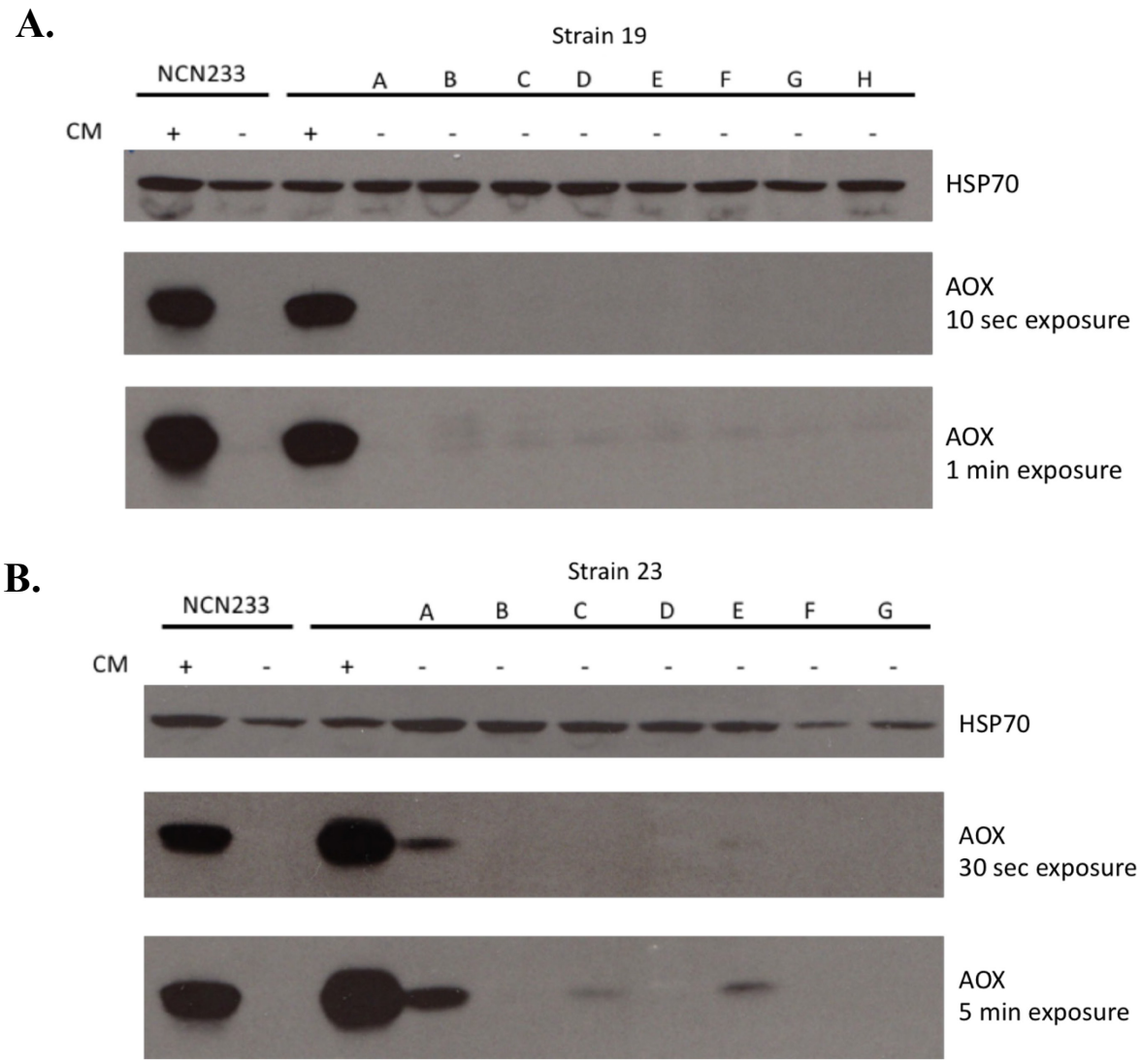

Figure 3.17. AOD1 protein in different cultures of strains 19 and 23. Eight biological replicates (A to H) of strain 19 **(A)** and seven biological replicates (A to G) of strain 23 **(B)** were grown in the absence of CM (-CM) for 16 hr. Mitochondria were isolated and subjected to SDS-PAGE and Western blotting. Fractions were analyzed for the presence of AOD1 protein using an antibody to the protein. Hsp70 served as a loading control. Long and short exposures were taken to detect varying amounts of protein. NCN233 +CM and –CM mitochondrial fractions were included as an AOD1 control.

transcript, followed by biological replicate A (Fig. 3.18A). Therefore, replicate E would be predicted to have the greatest abundance of AOD1 protein, followed by replicate A. However, Western Blot analysis revealed that biological replicate A had more AOD1 protein than replicate E (Fig. 3.18B). Western blot results revealed no detectable protein for replicates B, C and D (Fig. 3.18B). Thus, it appears that the amount of *aod-1* mRNA in uninduced cultures does not directly correlate with the amount of AOD1 protein.

To quantify the level of AOD1 protein in biological replicate A, I prepared two-fold serial dilutions of NCN233 mitochondrial fractions isolated from +CM cultures and electrophoresed these on the same gel as a mitochondrial sample from the strain 23, replicate A, -CM culture. A Western blot was then done to estimate levels of AOD1 protein. The Western analysis revealed that the protein abundance for replicate A grown in the absence of CM is approximately four fold less than the protein amount of NCN233 grown in the presence of CM (Fig. 3.18C). However, the transcript amount for NCN233 +CM cultures are typically about 10-fold more *aod-1* mRNA than NCN233 -CM cultures (Fig. 3.6), while the strain 23 replicate A has over 100-fold as much transcript as NCN233-CM (Fig. 3.18A). Based on these numbers for the transcripts, it would be predicted that replicate A would have approximately 10-fold more AOD1 protein than NCN233 +CM rather than 4-fold less. Again, these data support the hypothesis for a mechanism of post-transcriptional control, most likely at the level of translation.

A.

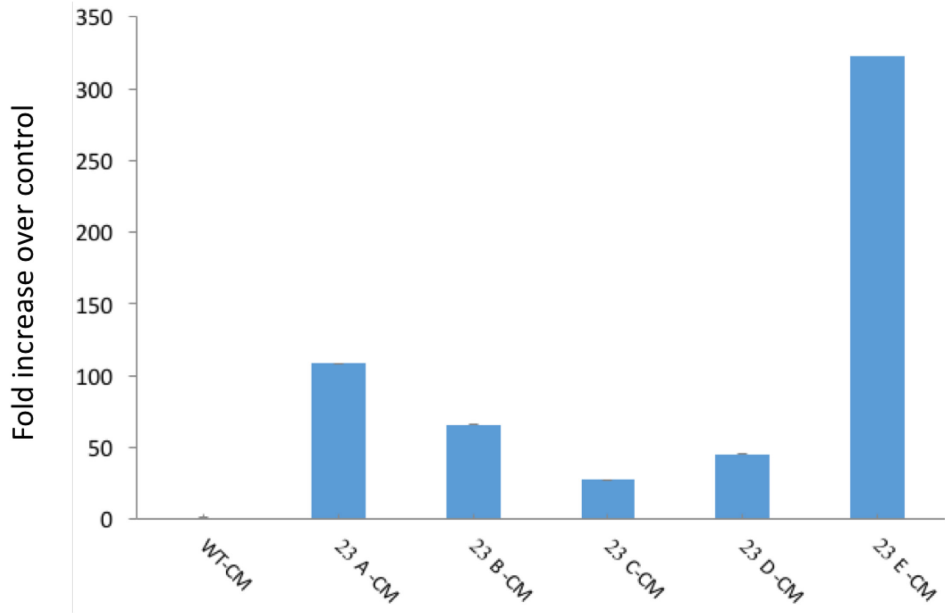
Fold increase over control
350
300
250
200
150
100
50
0
WT-CM
23 A-CM
23 B-CM
23 C-CM
23 D-CM
23 E-CM

B.

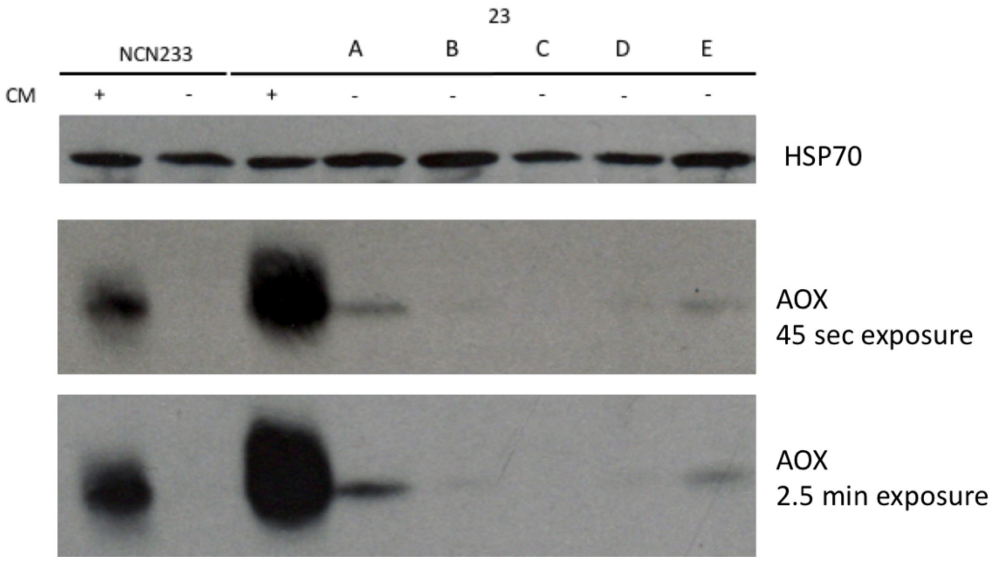
23
NCN233
A
B
C
D
E
CM
+
-
+
-
-
-
-
-
HSP70
AOX
45 sec exposure
AOX
2.5 min exposure

C.

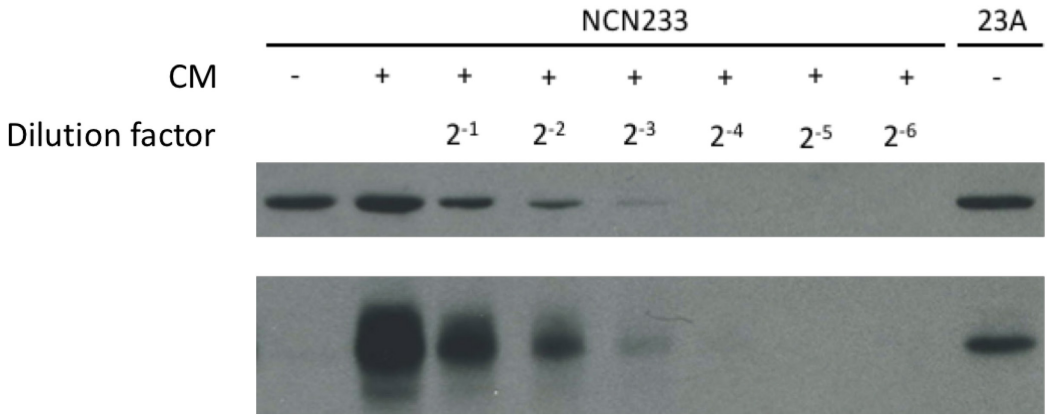

Figure 3.18. qPCR and Western blot results for *aod-1* transcript and protein of five biological replicates of strain 23. NCN233 and five biological replicates (A to E) of strain 23 cultures were grown in the presence (+CM), or absence (-CM) of CM. **A)** Samples from cultures grown in the absence of CM were taken for RNA extraction after 14 hours, while the bulk of the culture was harvested after 16 hours for mitochondrial isolation. RNA extracts were converted to cDNA, analyzed by qPCR, and ΔΔCT values were graphed. Error bars represent the standard error of the mean but they are representative of technical replicates, and are therefore very small and cannot be readily seen. **B**) Isolated mitochondria were subjected to SDS-PAGE and analyzed for AOD1 protein by Western Blot. Wild-type NCN233 grown in both media (+CM and –CM) served as a control. Hsp70 served as a loading control. Two different exposures were taken to detect varying amounts of protein. **C)** Relative AOD1 protein abundance in replicate 23 A was determined relative to to serially-diluted NCN233 +CM mitochondrial fractions. Hsp70 served as a loading control.

4.0 Discussion

4.1 NCU06940

ChIP-seq experiments performed by Zhigang Qi in our lab confirmed the binding of the AOD2 and AOD5 transcription factors to the *aod-1* promoter (Qi et al., 2016). In addition, binding to the upstream region of several other genes was detected. The most robust peaks were found to be upstream of a gene that encodes the hypothetical protein NCU06940. Using qPCR analysis on strains lacking AOD2 or AOD5, I demonstrated that the expression of NCU06940 was dependent on these proteins. Furthermore, qPCR analysis revealed an increase in the expression of the gene when cells were grown in the presence of CM. Therefore, the knockout strain, available from the *N. crassa* knockout project, was grown in the presence of CM and AA to determine if NCU06940 played a role in the response to these two inhibitors, perhaps related to AOX function. However, no effect on growth rate compared to wild-type was detected (Figure 3.4). Similarly, no effect was seen by altering the growth temperature. Studies conducted in *P. anserina* and *A. nidulans*, organisms with AOD2 and AOD5 orthologues, revealed a role for the transcription factors in the expression of gluconeogenic genes (Bovier et al., 2014; Suzuki et al., 2012). Similarly, the ChIP-seq work with *N. crassa* revealed that the AOD2 and AOD5 transcription factors have a role in regulating PEPCK (phosphoenolpyruvate carboxykinase), a gene involved in gluconeogenesis, as well as other genes involved in energy metabolism (Qi et al., 2016). Therefore, the growth of the knock-out strain was also tested on different carbon sources (Figure 3.4). However, there were no differences in growth between the NCU06940 knockout and the wild-type strain.

The stress tests conducted for the NCU06940 knockout were by no means exhaustive. Other tests might include nutrient deprivation, osmotic stress, or acidic and alkaline growth environments. However, given that the predicted protein has no functional domains based on bioinformatics analysis, it does not seem warranted to examine random possible functions. In summary, since NCU06940 has no known functional domains, is not an essential gene, and only exists in some members of the order Sordariomycetes, it is difficult to hypothesize what its function may be.

4.2 High level of *aod-1* transcript in strain T1P11

My second project began with an attempt to determine the cause of high levels of *aod-1* transcripts observed under non-inducing conditions in strain T1P11. Because T1P11 was known to be mutated in the *tyrosinase* gene, I set out to determine if the loss of tyrosinase played a role in *aod-1* transcription. This was done by analyzing the progeny of a cross between a wild-type strain and T1P11 that had been set up by an undergraduate student. Analysis of *aod-1* transcript levels and identifying strains with the *T*$^{-}$ mutation showed no correlation between progeny strains that have the tyrosinase mutations and high *aod-1* expression. This result was not unexpected, as the main function of *tyrosinase* is in the biosynthesis of the pigment melanin (Kupper et. al. 1989).

I then examined the *aod-1, aod-2,* and *aod*-5 genes in T1P11 to determine if any mutations in these genes or flanking regions could explain the effect. No mutations in these genes relative to any sequenced wild-type strain were found except for one change in the upstream region of *aod-5.* Thus, alterations in these genes could be ruled out as a cause of the effect.

The only remaining possibility was that one or more gene mutation(s) elsewhere in the genome was responsible for the overexpression of *aod-1*, therefore implicating a role for such a gene(s) in the regulation of transcription of the *aod-1* gene. Genomic DNA from an equal number of high and low expressing *aod-1* progeny strains, as well as the parental NCN233 and T1P11 strains, was sent to our collaborates at Oregon State University for sequencing. The sequence was determined for all the strains and the data entered into a VCF (variant call format) file. Upon receiving the sequencing data, I analyzed it to find gene mutations that might be responsible for the high uninduced expression of *aod-1* by comparing the sequence from all strains.

Many programs exist for analyzing whole genome sequencing data. For example, the sequenced genomes were initially launched on a Java program called Integrative Genomics Viewer or IGV (Robinson et al 2011; Thorvaldsdóttir et. al. 2013). The individual genomes of the strains were compared to the *Neurospora crassa* OR74A (Assembly 10) genome. IGV allows the user to scroll through a genome. Although the ease of using the application was appealing, it was extremely time consuming and prone to human errors when it came to analyzing mutations. Opening the VCF file sequencing results in Excel provided a list of all changes in each strain in separate columns. Each change was also associated with a precise position of the *N. crassa* genome. There were tens of thousands of mutations to annotate in eight different strains. It was likely that most of the mutations existed in intergenic regions, or, if they were within a gene, they would be in non-coding regions that would likely have no effect on gene function. For example, strain T1P11 had 19166 changes in its genome compared to the reference sequence. Changes also present in low-expressing strains were filtered out, for a total of 4435 changes to analyze.

Out of these 4435 changes, 1297 were in coding regions of known genes. Many genes had multiple changes so that the total number of genes with changes in coding regions was 124.

It should be noted that the data would have been easier to analyze if an annotated SNP library existed for *Neurospora crassa*. SNP libraries are readily available for many human cell lines (https://www.ncbi.nlm.nih.gov/dbvar/content/org_summary/), as well as other organisms including *Arabidopsis thaliana* (Schmid et. al. 2003) and *Saccharomyces cerevisiae* (Otero et. a. 2010). The availability of SNP-related data and software for these organisms makes it possible to analyze, interpret, and manage thousands of mutations. Unfortunately, no SNP-library or SNP-related software for *N. crassa* was available to use. Therefore, I used a combination of filtering tools in Excel, along with a FindData program written in Visual Basics for Application (VBA) (see Materials and Methods section 2.11 for details) to identify changes in coding regions of genes exclusive to high-expressing *aod-1* strains (detailed below).

4.3 A mutation in *FlbA* (NCU08319) results in the upregulation of *aod-1* transcripts

The FindData code in VBA identified two candidate genes that are mutated relative to the reference sequence and present in all four high *aod-1* expressing strains (strains 19, 23, 26 and T1P11) but not mutated in any of the low *aod-1* expressing strains (3, 4, 6, and NCN233). One of the genes was NCU05180 and was identified in fungiDB as *kinesin-9* (*kin-9*). NCU05180 had four mutations, one of which was in a coding region. Kinesin proteins are grouped into 14 different families. They are involved in the maintenance and function of the cytoskeleton, and, more specifically, in microtubule plus-end-directed transport. Kinesin proteins are characterized by their conserved motor domain where ATP and microtubule binding occur (Berk et. al. 2000). Although nothing in the literature exists to evaluate the specific role of the *N. crassa kin-9*,

function predictions based on MIPS_funcat available on FungiDB indicate that it may be involved in vesicle-mediated transport. Although there are kinesins known to have transcription regulating activity by acting as transcription factors and binding to promoters of specific genes (such as OSGDD1 discussed in section 3.2.3), the lack of DNA-binding domains in *kin-9* suggests that it would most likely not have this function. The mutation in NCU05180 results in an amino acid change from aspartic acid to asparagine. However, the Asp affected is near the C-terminal end of the protein. It is conserved in the Sordariomycetes and some other fungal phyla, but not all. It does not seem likely that this relatively conservative mutation would grossly affect the function of the protein. Furthermore, it is not immediately obvious how a small alteration in a kinesin would play a role in the regulation of *aod-1* transcription. To confirm that NCU05180 does not play a role in regulating AOX, qPCR for *aod-1* transcripts could be conducted on an ΔNCU05180 knock-out strain.

The second gene identified seems more likely to be involved in the upregulation of *aod-1* transcripts in non-inducing conditions. The mutation in *flbA* (NCU08319) is a deletion of a single base pair within the coding region resulting in a frameshift that severely truncates the protein. A transcriptome microarray study in *A. niger* reported 1152 genes whose expression was altered by two-fold or more in a *ΔflbA* mutant (Krijgsheld et al., 2013). The genes reported were altered by a factor of equal to or greater than 2-fold in expression level. One of the top upregulated genes was *aox1,* which encodes the *A. niger* AOX. Gene expression was measured in three different concentric zones of colony growth on agar plates: zone 1 was the oldest, central-most zone, zone 3 was the intermediate zone, and zone 5 was the youngest, most peripheral zone. These zones were examined because *ΔflbA* strains have altered secretomes. For example, a larger number of proteins can be identified in the *ΔflbA* secretome as compared to

wild-type (Krijgsheld et al., 2013). Interestingly, the level of upregulation of *aox1* varied between zones. In the central zone, the expression of *aox1* was increased 5.5 fold over wild-type. At the intermediate zone, the increase in expression was almost 8-fold. The periphery saw the most upregulation of *aox1* at almost 18-fold more expression than wild-type *A. niger*. It is currently unknown how or why the *flbA* mutation affects *aod-1* (or *aox1* in *A. niger*) transcription. Based on studies done in Aspergillus, *flbA* negatively regulates the G-alpha subunit of the heterotrimeric G-protein complex (Seo et. al. 2005). However, to my knowledge, it is unknown if the G-protein complex is involved in the regulation of *aod*-1.

Interestingly, although the *N. crassa aod-1* transcripts are upregulated in the *flbA* mutants, these transcripts are not translated into AOD1 protein. Presumably, a signal(s) that is present when the sETC is perturbed is not present in the mutated *flbA* strains to allow these upregulated transcripts to be translated. Although Western blot analysis on the knockout *flbA* strain (ΔNCU08319) has not been done, it is presumed that there would be no protein in the absence of an inducing signal, as seen in the strains containing the deletion frameshift mutation. The possibility that the mutation affects the activity of the *aod-1* transcription factors seems unlikely. The *A. niger* transcriptome study did report 20 transcription factors that are upregulated in the Δ*flbA* strain. Although many of those were zinc cluster transcription factors, the orthologues of AOD2 and AOD5 were not among those listed as affected in the mutant strain (Krijgsheld et. al. 2013).

Although my results have shown that the *flbA* knock out strain from the *N. crassa* knock out library has a phenotype similar to the deletion mutant strains analyzed in this study, it would be prudent to perform a gene rescue of the ΔNCU08319 strain or T1P11 with the wild-type *flbA* gene. This should restore wild-type levels of uninduced *aod-1* transcripts and would verify the

involvement of the *flbA* gene in the regulation of *aod-1* transcription. This is being conducted by our collaborators at the Freitag Lab at Oregon State University. This proof is especially desirable because of known problems with strains in the *N. crassa* knock out library (Chinnici et al., 2014; Fu et al., 2011; Nishka Kishore, thesis). Even though we have shown that the strains do contain the correct deletion, it has been observed that many other mutations may exist in a given knock out strain from the library.

4.4 Evidence for post-transcriptional regulation of *aod-1* expression

The high amount of uninduced *aod-1* transcript but very low to undetectable AOD1 protein levels observed in some *N. crassa* strains such as T1P11 was puzzling. It was conceivable that in the absence of an inducing signal, the protein was either not imported into the mitochondria or was rapidly degraded. I showed that the protein did not accumulate in the cytosol and that there was no apparent system for rapid degradation without the presence of an inducing signal. Thus, it was most likely that the protein was not being made, and some form of translational control was in place to prevent synthesis of the AOD1 protein under non-inducing conditions.

I hypothesized that a post-transcriptional regulatory region may exist in the *aod-1* mRNA. Such regions have been identified in other transcripts. For example, in c-myc mRNA, a *cis*-acting sequence element, contains a ~250 bp sequence in the coding region called the coding-region instability determinant (CRD). This region is bound by a protein called the coding-region instability determinant binding protein (CRD-BP). CRD-BP is highly expressed in fetal and neonatal tissues, and is found in most cell lines. When bound to the CRD, the protein protects the c-myc mRNA from endonucleolytic cleavage resulting in enhanced expression (Noubissi et. al. 2010). However, the majority of proteins that control translation of mRNAs bind to either the

5′UTR or 3′UTR of those transcripts (Gebauer et. al. 2012). Several specific protein binding sites on mRNAs have been identified in both the 3′UTR and 5′ UTR of transcripts in mammalian cells, as summarized in Table 4.1. Sequencing of cloned cDNAs in our lab has shown that the 5′ UTR of the *aod-1* mRNA is variable in length and generally quite short (Tanton et. al. 2003). Most transcripts were found to have a 19-56 nucleotide 5′UTR with multiple transcript start sites identified (Fig. 4.1A). The relatively short length of the 5′UTR region in many transcripts makes it seem unlikely that it serves as a site for binding proteins involved in translational control. The 3′UTR is over 150 nucleotides long and may be more likely to be involved as a control region (Fig. 4.1B). As illustrated in Table 4.1, AU-rich sequences in particular have been well characterized as 3′UTR binding motifs for several RNA-binding proteins (RBPs) in mammalian cells. The 3′UTR of the *aod-1* gene does appear to be rich in AU/U regions. Some potential RBP motifs, based on results from the RNA-binding protein database (RBPDB) binding site prediction tool (http://rbpdb.ccbr.utoronto.ca/) are underlined in Fig. 4.1B.

In many eukaryotes, micro-RNAs (miRNAs) play a regulatory role by interacting with the UTR regions. miRNAs are encoded in the genome of most, if not all, eukaryotes. They are transcribed as small (approximately 21-22 nucleotides), non-coding RNA molecules that regulate translation in eukaryotes (He and Hannon, 2004). In plants and animals, the most common role of miRNAs is to post-transcriptionally downregulate genes by blocking translation or by promoting degradation of mRNA (Bartel, 2004; Shabalina and Koonin, 2008). Pre-miRNAs are processed by DICER, an enzyme present in the cytoplasm of the cell that cuts the pre-miRNA into mature miRNA (Macrae et al., 2006). In plants and animals, miRNAs regulate genes involved in a wide range of cellular activities, and have been shown to be players in disease,

Table 4.1. Examples of some RNA-binding proteins and their binding sites as described in the literature. The RNA-binding proteins (RBP), the locations of their binding sites within an untranslated region (UTR) of the transcript, general binding sequence (Sequence), known binding motifs (Known Motifs), and their functions (Function) are summarized from various literature sources given as references. Motifs were obtained from the Attract database (https://attract.cnic.es/). * indicates that that up to 64 known motifs were identified by the database. 29 were selected for the table based on strongest binding affinity measured by a quality score determined by the probability of observing a motif bound by the below indicated RBPs in an experiment from the literature analyzed by the database, such as UV cross-linking or EMSA.

RBP	UTR	Sequence	Known Motifs	Function
AUF1	mostly 3'UTR	AU-rich sequences	UUAGGG, AGAUAU, AGUAGG, AUUUAUUUA, AUUUA, UUAGGA, AAUUUA, AAAAAAA, UUAGGG UUAGAG	Promotes degradation and enhances mRNA stability in mRNAs involved in cell cycle, apoptosis, stress response (Liao et. al. 2007; Raineri et. al. 2004; Vázquez-Chantada et. al. 2010; Zucconi et. al. 2011)
TIA1 and TIAR	3' and 5'UTR	3' - AU/U rich sequences 5' - Terminal oligopyrimidine tracts (5'TOP)	UUUUUUG, AUUUA, CUUUUC, CUUUUUU, CUUUUG, GUUUUG, GUUUUA, UUUUUUAUUUU, AUUUUUG, AUUUUUU, UUUUUU, UUUUUUU, CUUC, GUUUUUUUUC, AUUUUG, GUUUA, UUUUUCG, AUUC, CUUUG, GUUUUC, AUUUUUU, UUUUUUC, AUUUC, AUUUUUC, GUUUC, GUUUUUC, UUUUUUG, CUUUC, CUUUUUC, UUUUUCU, CUUUUA, UUUUUUUUU, GUUUUUG, GUUUG, CUUUUUA, AUUUUC, UUUUUGG, UUCUCCUUUC, CUUUA, UUUUUGU	Halt mRNA translation under stress conditions (Kim et. al. 2011; Gilks et. al. 2004)
HUR	3' and 5' UTR	AU-rich sequences	UUUU, UUAGUUU, UUUAUUU, CCCCCCC, UUUAGUU, AUUU, UUUUU, AUUUA, UUUAUUUAUUU, UUUGGUU, UUUAUUU, AUUUU, AUUUAUUUAUUU, UUUUUUU, UUUAUUU, UUUGUUU, UUGUUUU, UUUUUUG, UUAUUUU, UUUAUUUAUUUA, UUGAUUU, UUAUUUU, UUAUUUAUU, UUGGUUU	Stabilizes mRNAs of proteins involved in cell cycle, proliferation, and cell survival (López de Silanes et. al. 2004; Abdelmohsen et. al. 2010; Abdelmohsen et. al. 2008; Hinman and Lou, 2008; López de Silanes et. al. 2005; Kuwano et. al. 2008; Abdelmohsen et. al. 2007; Yi et. al. 2010)
TTP	3' UTR	AU-rich sequences	AUUUA, UUAUUUAUU, CUUGU, AAUAA, UUGUGC, UUGUGG, UUAUUUAUU, AAAAAAUAAAG, AAUAAAGAAAG, AAUAAAUAAAG, AAAAAAGAAAG, UCCUCU, UCUUGU, ACCUCU, CCUUCU, CCUUGC, CCCUCU, ACUUCC, ACUUUC, UCUUCC, CCCUGC, CCCUUU, ACCUGU, UCUUUC, ACUUCU, UCCUGU, UCCUUC, ACCUUU, ACCUCC*	Promotes decay of mRNAs involved in cancer and inflammation (Sanduja et. al. 2012)
Nucleolin	3' UTR	AU-rich and/or G-rich sequences	AUUCGACCCGGG, AUUCGAGCCGGG, AUUCGAGCCGCG, AUUCGACCCGCG, AAUCCCGAAG, AUUCGACCCGAG, AUUCGAACCGCG, AUUCGAUCCGUG, AUUCGAACCGAG, AUUCGAUCCGCG, AUUCGAACCGGG, AUUCGACCCGUG, AUUCGAGCCGAG, UCCCGAG, AUUCGAUCCGGG, UGCACAGAAGG, AUUCGAACCGUG, AUUCGAUCCGAG, AUUCGAGCCGUG	Promotes mRNA stability in some genes, degradation in others (Abdelmohsen et. al. 2011)
IRP1	5' UTR	30nt stem-loop structure (iron responsive element)	CAGUN	Blocks translation of mRNA connected to iron storage and metabolism (Goss et. al. 2011)
YB-1	TGF-β1 5'UTR	G/C-rich sequence with stem-loop	AACAUC, AACAUCA, AACAUCG, AACAUCU, AGAAC, CAACCACAA, CAACCACACCAC, CACC, CACCACCACC, CAUC, CAUCAUC, CAUCGC, CAUCUG, CCCUGCG, CCUGCGG, CUGCGGU, GAUC, GAUCUG, GCCUGCG, GGUCUGC, UCCAGCAA	Translational inhibition of TGF-β1 mRNA (Jenkins et. al. 2010)

Figure 4.1. Defining UTRs for the *aod-1* gene. **A)** Promoter and 5′-UTR sequence of *aod-1*. Transcription start sites were identified by sequencing of cloned cDNAs and PCR products (Chae et al., 2007). The putative TATA box is bolded and the ATG translation start site is bolded in green. Single digit numbers beneath the underlined bases indicate the number of times a position was identified as a transcription start site. **B)** 3′UTR and transcription end sites preceding the position of the poly-A tail were also identified by sequencing of cloned cDNAs and PCR products (Chae et al., 2007). The TGA translation stop codon is indicated in bold red. The numbers beneath the underlined bases indicate the number of times a position was identified as immediately preceding the poly-A tail. The closest such site occurred over 150 base-pairs away from the stop codon. Potential RBP motifs obtained from the RNA-Binding Protein DataBase (http://rbpdb.ccbr.utoronto.ca/) are underlined in panel B.

development, and metabolism (Frost and Olson, 2011; Lu et al., 2007; Vidigal and Ventura, 2015; Wang et al., 2008). Studies conducted on the fungus *Cryptococcus neoformans* using reporter genes showed that miRNAs miR1 and miR2 were able to suppress the expression of URA5 (involved in the biosynthesis of uracil) and CLC1 (encodes a chloride channel necessary for pigmentation in *C. neoformans*) (Jiang et al., 2012). While this study was able to show that miR1 and miR2 are capable of silencing gene targets *in vitro*, the span of their gene targets is unknown.

milRNAS (MicroRNA-like microRNAs) have been found in some plants, some fungi, and some bacteria, and are produced much like miRNAs, which are derived from stem-loop structures processed by DICER. However, they differ in that they do not require certain proteins, such as QDE-1 (an RNA-dependent RNA polymerase) and QDE-3 (a DNA helicase) for processing that would categorize them as true miRNAs (Chen et al., 2014). A qPCR study conducted on the fungus *Fusarium oxysporum* f. sp. *niveum* (*Fon*) revealed the down-regulation of toxin-related gene expression by milRNAs (Jiang et al., 2017). The role of milRNAs in *N. crassa* is not as clear. As with *C. neoformans*, studies done on Neurospora milRNAs demonstrated their ability to silence reporter-gene constructs with complimentary milRNA sequences, demonstrating that they have the potential to silence endogenous gene targets (Lee et al., 2010). However, further studies are needed.

If proteins or other molecules that post-transcriptionally regulate *aod-1* recognize specific sequences in the 3′UTR, then altering the sequence of the UTR would be expected to have an effect on *aod-1* expression. To determine if this was the case, I replaced the 3′UTR region of the *aod-1* transcript with the UTR of *β-tubulin*. Although studies in mammalian cells have found that *β-tubulin* has an auto-regulation mechanism that controls the degradation of *β-tubulin*

mRNA, the region involved in the control consists of 13 bp that includes the first 4 translated codons (Saussede-Aim et. al. 2009; Gay et. al. 1989). Because of this, I decided to replace the 5′UTR of *aod-1* with the 5′UTR of the MOM protein porin. In the literature, I was unable to find any evidence for a control mechanism in the 3′ UTR region of *β-tubulin* transcripts, nor any evidence for a control mechanism in the 5′UTR region of *porin*. Furthermore, UTR replacements for the purpose of promoter or UTR function studies have been undertaken in other organisms, such as C. *elegans,* with *β-tubulin* as the replacement gene (Merritt et. al. 2008). As discussed in the Appendix, my experiments (outlined in Fig. 4.2) using the modified 5′ and 3′UTR constructs did not yield clear data on the function of these regions.

4.5 *Neurospora crassa aod-1* exhibits biological noise in some strains

An interesting observation from the qPCR data was the variable results seen for certain progeny strains, as shown by the large range of ΔCT values and large error bars (Figure 3.14). Originally, four biological replicates were graphed that appeared to be quite consistent (Figure 3.6). However, further analysis revealed that there was high variance among replicates in some strains. To gain a better understanding of the range in data, all ΔCT values obtained from all qPCR runs were collected and graphed for all the strains. Strains 19, 23 and 26 had the widest range of ΔCT values obtained from the biological replicates, with 23 having the greatest variance (Fig. 3.14).

One possible explanation for this variation may be related to the differing effect of the *flbA* mutation on AOX expression in regions of the *A. niger* hyphal system depending on age, as mentioned previously (Section 4.3). That is, the cultures from which RNA was extracted for my

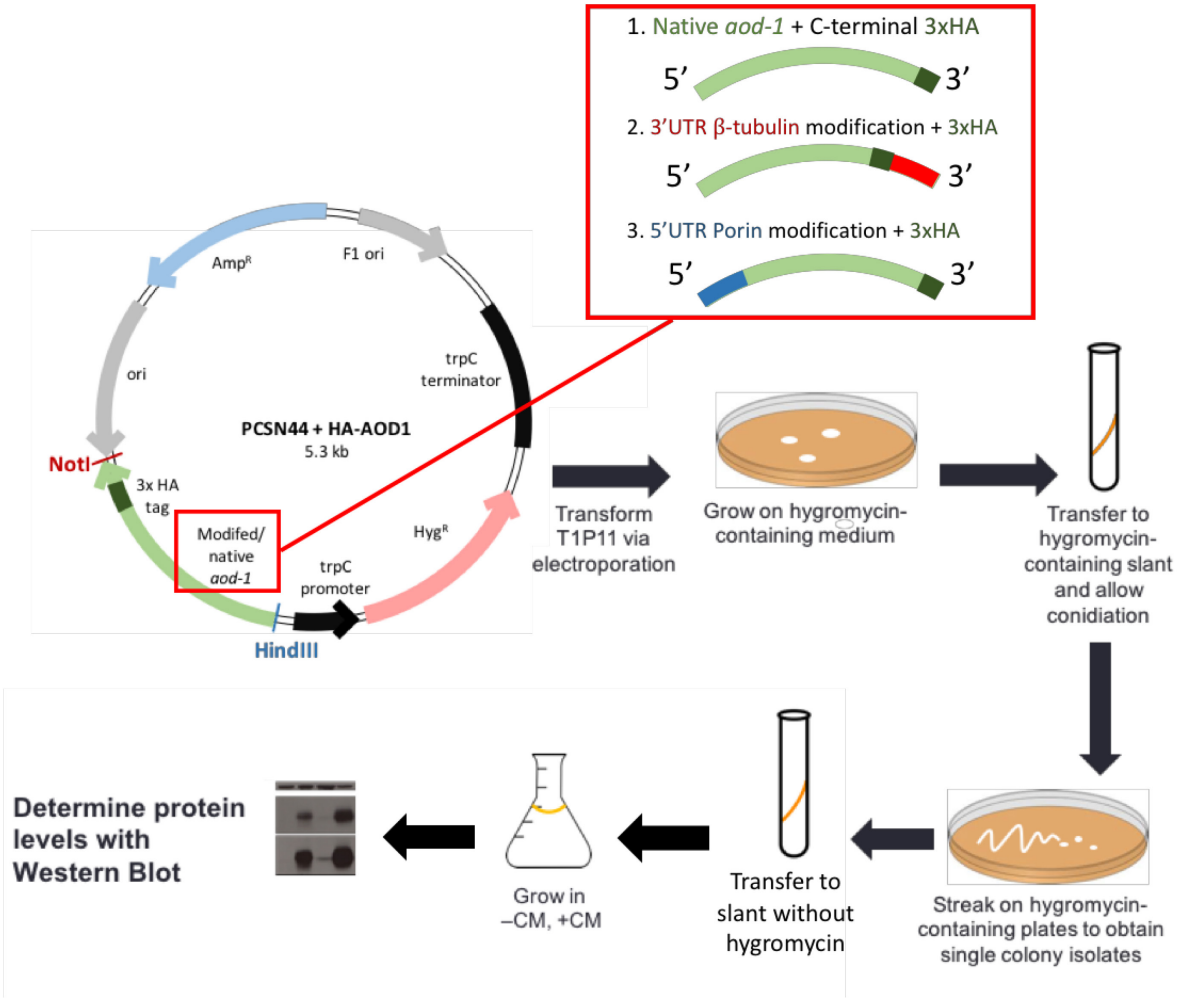
1. Native aod-1 + C-terminal 3xHA
5′
3′
2. 3′UTR β-tubulin modification + 3xHA
5′
3′
3. 5′UTR Porin modification + 3xHA
5′
3′
Amp^R
F1 ori
ori
trpC terminator
PCSN44 + HA-AOD1
5.3 kb
NotI
3x HA tag
Modifed/ native aod-1
Hyg^R
trpC promoter
HindIII
Transform T1P11 via electroporation
Grow on hygromycin-containing medium
Transfer to hygromycin-containing slant and allow conidiation
Streak on hygromycin-containing plates to obtain single colony isolates
Transfer to slant without hygromycin
Grow in –CM, +CM
Determine protein levels with Western Blot

Figure 4.2. Replacement of 5′ and 3′UTR regions in *aod-1*. The transforming base plasmid is shown as a circle at the top left. The red line connecting to the box at the top right shows the three different variants constructed. For all three variants, the light green, curved bar indicates native *aod-1* sequence, while the dark green box is the triple (3x) HA tag. The 3′UTR of *β-tubulin* is indicated in red (construct 2), while the 5′UTR of *porin* is indicated in blue (construct 3). Strain T1P11 was transformed with each of the three constructs in separate experiments. The first transforming plasmid contained hygromycin resistance (HygR) with the coding region of the *aod-1* gene (tagged with HA at the C-terminus) and the native *aod-1* 3′ and 5′UTRs. The second construct was identical except that the *aod-1* 3′UTR was replaced with that of *β-tubulin.* The third construct was identical to the first except that the 5′UTR of *aod-1* was replaced with that of *porin.* All vectors were linearized with *Kpn*I prior to transformation to maximize integration. Transformants were plated and grown on hygromycin-containing medium. Colonies were picked into slants with medium containing hygromycin, and then streaked on hygromycin-containing plates to obtain single colony isolates. Individual colonies were picked to fresh slants without hygromycin. The chosen transformed strains were grown in media with and without CM. Mitochondria were isolated to determine protein levels in both +CM and –CM conditions via Western blot using antibodies against both the HA tag and the AOD1 protein.

qPCR analysis of *aod-1* transcript levels, were liquid cultures. Typically, the total culture amounted to about 8 g wet weight when harvested. I took only 100 mg from these culture for RNA extraction. The larger culture would consist of both young hyphal regions at growing tips as well as older regions where growth had initiated. I would not have been able to tell the difference between such regions, but my random sampling may have helped generate the large variation observed due to different ages of the cultures that were taken.

Another possibility is that the variation in *aod-1* mRNA in different cultures of the same strain may be similar to that observed for other genes in other systems. Plants and fungi, due to their sessile nature, may be more susceptible to the effects of minor environmental perturbation. Similar to the variation observed in strain 23 among replicates for transcription amount and protein levels, variations in replicates have also been observed in the plant *Arabidopsis thaliana*. For example, replicate plants grown in the same macroenvironment within one genotype of an *Arabidopsis thaliana* line harbored differences in measurable plant traits such as height and total flower number (Hall et. al. 2007). Stochastic variation in gene expression among isogenic cells grown in the same environment is referred to as "noise", and is not uncommon (Blainey et. al. 2014).

While qPCR is generally regarded as the "gold standard" for mRNA quantification, noise in qPCR analysis is inevitable and well documented. Human line (HEK293) cell clones have been shown to have 20% to 40% variability in transcript levels (Kempe et al., 2015a). The reasons for this heterogeneity are not entirely clear. One possibility that has been considered is the effect of certain molecules, such as transcription factors, occurring in low numbers in the cell. Such molecules tend to display large stochastic deviations on an individual cell-by-cell basis compared to their mean number in a cell population. Such fluctuations can be caused by cell

division or “transcriptional bursting”, whereby mRNAs are transcribed in sporadic bursts, followed by a variable period of inactivity (Kempe et al., 2015). Noise attributed to gene expression is typically categorized as either intrinsic noise or extrinsic noise (Elowitz et. al. 2002). Intrinsic noise is defined as the stochasticity of biochemical interactions between particles in the cell, such as interactions between RNA polymerase and DNA, which rely on collisions between the interactants. Extrinsic noise is generated by external factors, ranging from other cellular processes to external environmental factors.

One method to correct or account for such issues is to conduct qPCR analysis on individual cells. The field of mRNA analysis appears to be progressing towards this method for certain applications (Taniguchi et al., 2009). However, this process can be laborious as it involves obstacles such as isolating single cells and amplifying tiny amounts of mRNA from a cell. A qPCR design parameter to minimize technical noise may be to limit the reverse-transcriptase reaction, which converts the mRNA into cDNA, to a single cycle, as efficiency of the reverse transcriptase reaction varies and introduces additional noise (Bengtsson et al., 2008). At present, the most common way to bypass qPCR is to use next-generation sequencing (NGS) technology through RNA-seq. Single-cell-RNA-seq has been utilized in various recent studies of gene expression, ranging from deciphering embryonic development (Hashimshony et. al. 2015) to identifying transcriptional regulatory networks involved in blood development (Moignard et. al. 2015). However, single-cell RNA-seq also has its challenges (Arzalluz-Luque et al., 2017). The low amount of RNA from a single cell introduces technical variability, especially in low expressed transcripts. To alleviate this issue, 30 or more single-cell transcriptomes are pooled together. However, this once again introduces inter-cell variability. Therefore, cell filtering

criteria must be applied to account for differences in cell cycle, as well as size, and is another factor to take into consideration (Buettner et al., 2015; Stegle et al., 2015).

The variation in *aod-1* transcript levels was the greatest in strain 23. One possible explanation for this might be a mutation in the promoter region of *aod-1* strain 23. A study conducted in *S. cerevisiae* examined promoter-mutation-mediated gene expression noise in response to acute antibiotic stress (Blake et. al. 2006). Certain strains with certain mutations did exhibit higher intrinsic noise compared to other strains. However, our genomic sequence of strain 23 revealed no mutations in the *aod-1* gene or its upstream region. Another possible explanation for the high variation in *aod-1* expression observed comes from consideration of a proteomic analysis examining single-cell biological noise in *S. cerevisiae.* This study observed noise in >2500 proteins in rich and minimal media (Newman et. al. 2006). A trend was discovered wherein proteins involved in stress response were shown to have higher levels of noise compared to their housekeeping counterparts, such as ribosomal proteins involved in protein synthesis, that exhibit low noise. One explanation for this observation is that it benefits cell survival. The plasticity introduced by noise may allow cells to modulate at higher gene expression levels and ultimately, allow for better survival under very high stress levels by sampling variability to maximize survival (Zhuravel et. al. 2010). Since *N. crassa aod-1* is regulated in response to mitochondrial stress, it may fall into a class of genes that exhibits high variation of expression.

4.6 Future Directions

The discovery of the *flbA* mutation and its involvement in the regulation of *aod-1* transcripts was an unexpected but interesting finding. Further work on *flbA* could include

analyzing rescued Δ*flbA* strains by qPCR to determine if *aod-1* transcript levels are comparable to wild-type when the gene function is restored. The *A. niger* Δ*flbA* paper (Krijgsheld et al., 2013) also reported the variable expression of *aod-1* transcripts in different concentric zones. Therefore, testing the sections of *N. crassa* hyphae in T1P11 for changes in expression of *aod-1* with age could also be performed. Because *flbA* regulates the *FadA* Gα subunit in *Aspergillus,* it would be interesting to see if the *N. crassa flbA* regulates *gna-1,* the *N. crassa FadA* homologue. *N. crassa* interestingly has another two Gα subunits (*gna-2* and *gna-3*) (Won et al., 2012) that may also be regulated by *flbA.* In *Aspergillus,* a dominant loss of function of FadA resulted in similar phenotypes to *flbA* loss of function mutations (Yu et al., 1996). Using the *N. crassa* knock out library, it would be interesting to see if *aod-1* transcript levels are elevated in *gna-1, -2, or -3* loss of function strains.

REFERENCES

A. Haskins, F., Tissieres, A., K. Mitchell, H., and B. Mitchell, M. (1953). Cytochromes and the Succinic Acid Oxidase System of Poky Strains of Neurospora. J. Biol. Chem. 200, 819–826.

Abdelmohsen, K., and Gorospe, M. (2010). Posttranscriptional regulation of cancer traits by HuR. Wiley Interdiscip Rev RNA 1, 214–229.

Abdelmohsen, K., Kuwano, Y., Kim, H.H., and Gorospe, M. (2008). Posttranscriptional gene regulation by RNA-binding proteins during oxidative stress: implications for cellular senescence. Biol. Chem. 389, 243–255.

Abdelmohsen, K. (2012). Modulation of Gene Expression by RNA Binding Proteins: mRNA Stability and Translation. Bind. Protein.

Abderrazak, A., Syrovets, T., Couchie, D., El Hadri, K., Friguet, B., Simmet, T., and Rouis, M. (2015). NLRP3 inflammasome: From a danger signal sensor to a regulatory node of oxidative stress and inflammatory diseases. Redox Biol. 4, 296–307.

Abe, Y., Shodai, T., Muto, T., Mihara, K., Torii, H., Nishikawa, S., Endo, T., and Kohda, D. (2000). Structural Basis of Presequence Recognition by the Mitochondrial Protein Import Receptor Tom20. Cell 100, 551–560.

Ahmed, N., Ronchi, D., and Comi, G.P. (2015). Genes and Pathways Involved in Adult Onset Disorders Featuring Muscle Mitochondrial DNA Instability. Int. J. Mol. Sci. 16, 18054–18076.

Ahmed, N., Ronchi, D., and Comi, G.P. (2015). Genes and Pathways Involved in Adult Onset Disorders Featuring Muscle Mitochondrial DNA Instability. International Journal of Molecular Sciences 16, 18054–18076.

Ajioka, R.S., Phillips, J.D., and Kushner, J.P. (2006). Biosynthesis of heme in mammals. Biochim. Biophys. Acta 1763, 723–736.

Akhter, S., McDade, H.C., Gorlach, J.M., Heinrich, G., Cox, G.M., and Perfect, J.R. (2003). Role of alternative oxidase gene in pathogenesis of Cryptococcus neoformans. Infect. Immun. 71, 5794–5802.

Alexeyev, M.F., LeDOUX, S.P., and Wilson, G.L. (2004). Mitochondrial DNA and aging. Clinical Science 107, 355–364.

Allen, S., Balabanidou, V., Sideris, D.P., Lisowsky, T., and Tokatlidis, K. (2005). Erv1 mediates the Mia40-dependent protein import pathway and provides a functional link to the respiratory chain by shuttling electrons to cytochrome c. J. Mol. Biol. 353, 937–944.

Amchenkova, A.A., Bakeeva, L.E., Chentsov, Y.S., Skulachev, V.P., and Zorov, D.B. (1988).

Coupling membranes as energy-transmitting cables. I. Filamentous mitochondria in fibroblasts and mitochondrial clusters in cardiomyocytes. J. Cell Biol. 107, 481–495.

Amirsadeghi, S., Robson, C.A., McDonald, A.E., and Vanlerberghe, G.C. (2006). Changes in plant mitochondrial electron transport alter cellular levels of reactive oxygen species and susceptibility to cell death signaling molecules. Plant Cell Physiol. 47, 1509–1519.

Andersson, M.E., and Nordlund, P. (1999). A revised model of the active site of alternative oxidase. FEBS Lett. 449, 17–22.

Andronis, E.A., and Roubelakis-Angelakis, K.A. (2010). Short-term salinity stress in tobacco plants leads to the onset of animal-like PCD hallmarks in planta in contrast to long-term stress. Planta 231, 437–448.

Angelova, P.R., and Abramov, A.Y. (2016). Functional role of mitochondrial reactive oxygen species in physiology. Free Radic. Biol. Med. 100, 81–85.

Archibald, J.M. (2015). Endosymbiosis and Eukaryotic Cell Evolution. Curr. Biol. 25, R911–R921.

Armstrong, A.F., Badger, M.R., Day, D.A., Barthet, M.M., Smith, P.M.C., Millar, A.H., Whelan, J., and Atkin, O.K. (2008). Dynamic changes in the mitochondrial electron transport chain underpinning cold acclimation of leaf respiration. Plant Cell Environ. 31, 1156–1169.

Arnold, I., Wagner-Ecker, M., Ansorge, W., and Langer, T. (2006). Evidence for a novel mitochondria-to-nucleus signalling pathway in respiring cells lacking i-AAA protease and the ABC-transporter Mdl1. Gene 367, 74–88.

Arzalluz-Luque, Á., Devailly, G., Mantsoki, A., and Joshi, A. (2017). Delineating biological and technical variance in single cell expression data. Int J Biochem Cell Biol 90, 161–166.

Backes, S., and Herrmann, J.M. (2017). Protein Translocation into the Intermembrane Space and Matrix of Mitochondria: Mechanisms and Driving Forces. Front. Mol. Biosci. 4.

Balkwill, D.L., Drake, G.R., Reeves, R.H., Fredrickson, J.K., White, D.C., Ringelberg, D.B., Chandler, D.P., Romine, M.F., Kennedy, D.W., and Spadoni, C.M. (1997). Taxonomic study of aromatic-degrading bacteria from deep-terrestrial-subsurface sediments and description of Sphingomonas aromaticivorans sp. nov., Sphingomonas subterranea sp. nov., and Sphingomonas stygia sp. nov. Int. J. Syst. Bacteriol. 47, 191–201.

Banci, L., Bertini, I., Calderone, V., Cefaro, C., Ciofi-Baffoni, S., Gallo, A., Kallergi, E., Lionaki, E., Pozidis, C., and Tokatlidis, K. (2011). Molecular recognition and substrate mimicry drive the electron-transfer process between MIA40 and ALR. Proc. Natl. Acad. Sci. U.S.A. 108, 4811–4816.

Barroso, G.V., Puzovic, N., and Dutheil, J.Y. (2017). The Evolution of Gene-Specific Transcriptional Noise Is Driven by Selection at the Pathway Level. Genetics genetics.300467.2017.

Bartel, D.P. (2004). MicroRNAs: genomics, biogenesis, mechanism, and function. Cell 116, 281–297.

Bartoli, C.G., Yu, J., Gómez, F., Fernández, L., McIntosh, L., and Foyer, C.H. (2006). Inter-relationships between light and respiration in the control of ascorbic acid synthesis and accumulation in Arabidopsis thaliana leaves. J. Exp. Bot. 57, 1621–1631.

Bausewein, T., Mills, D.J., Langer, J.D., Nitschke, B., Nussberger, S., and Kühlbrandt, W. (2017). Cryo-EM Structure of the TOM Core Complex from Neurospora crassa. Cell 170, 693–700.e7.

Bender, T., and Martinou, J.-C. (2016). The mitochondrial pyruvate carrier in health and disease: To carry or not to carry? Biochim. Biophys. Acta 1863, 2436–2442.

Bengtsson, M., Hemberg, M., Rorsman, P., and Ståhlberg, A. (2008). Quantification of mRNA in single cells and modelling of RT-qPCR induced noise. BMC Mol. Biol. 9, 63.

Berthold, D.A., Andersson, M.E., and Nordlund, P. (2000). New insight into the structure and function of the alternative oxidase. Biochimica et Biophysica Acta (BBA) - Bioenergetics 1460, 241–254.

Bertrand, H., C. A. Argan and N. A. Szakacs, 1983 Genetic control of the biogenesis of cyanide insensitive respiration in Neurospora crassa. Walter de Gruyter, Berlin, 495-507.

Bhangoo, M.K., Tzankov, S., Fan, A.C.Y., Dejgaard, K., Thomas, D.Y., and Young, J.C. (2007). Multiple 40-kDa Heat-Shock Protein Chaperones Function in Tom70-dependent Mitochondrial Import. Mol. Biol. Cell 18, 3414–3428.

Bhola, P.D., and Letai, A. (2016). Mitochondria-Judges and Executioners of Cell Death Sentences. Mol. Cell 61, 695–704.

Bihlmaier, K., Mesecke, N., Terziyska, N., Bien, M., Hell, K., and Herrmann, J.M. (2007). The disulfide relay system of mitochondria is connected to the respiratory chain. J. Cell Biol. 179, 389–395.

Blainey, P., Krzywinski, M., and Altman, N. (2014). Points of significance: replication. Nat. Methods 11, 879–880.

Blake, W.J., Balázsi, G., Kohanski, M.A., Isaacs, F.J., Murphy, K.F., Kuang, Y., Cantor, C.R., Walt, D.R., and Collins, J.J. (2006). Phenotypic consequences of promoter-mediated transcriptional noise. Mol. Cell 24, 853–865.

Bohnert, M., Rehling, P., Guiard, B., Herrmann, J.M., Pfanner, N., and van der Laan, M. (2010). Cooperation of stop-transfer and conservative sorting mechanisms in mitochondrial protein transport. Curr. Biol. 20, 1227–1232.

Bömer, U., Meijer, M., Guiard, B., Dietmeier, K., Pfanner, N., and Rassow, J. (1997). The sorting route of cytochrome b2 branches from the general mitochondrial import pathway at the preprotein translocase of the inner membrane. J. Biol. Chem. 272, 30439–30446.

Bonner, W.D., and Voss, D.O. (1961). Some Characteristics of Mitochondria Extracted from Higher Plants. Nature 191, 682–684.

Borecký, J., Nogueira, F.T.S., Oliveira, D., P, K.A., Maia, I.G., Vercesi, A.E., and Arruda, P. (2006). The plant energy-dissipating mitochondrial systems: depicting the genomic structure and the expression profiles of the gene families of uncoupling protein and alternative oxidase in monocots and dicots. J. Exp. Bot. 57, 849–864.

Borst, P., and Kroon, A.M. (1969). Mitochondrial DNA: Physicochemical Properties, Replication, and Genetic Function. In International Review of Cytology, J.F.D. and K.W.J. G.H. Bourne, ed. (Academic Press), pp. 107–190.

Bovier, E., Sellem, C.H., Humbert, A., and Sainsard-Chanet, A. (2014). Genetic and functional investigation of Zn(2)Cys(6) transcription factors RSE2 and RSE3 in Podospora anserina. Eukaryotic Cell 13, 53–65.

Braymer, J.J., and Lill, R. (2017). Iron-Sulfur Cluster Biogenesis and Trafficking in Mitochondria. J. Biol. Chem. jbc.R117.787101.

Brix, J., Dietmeier, K., and Pfanner, N. (1997). Differential recognition of preproteins by the purified cytosolic domains of the mitochondrial import receptors Tom20, Tom22, and Tom70. J. Biol. Chem. 272, 20730–20735.

Buettner, F., Natarajan, K.N., Casale, F.P., Proserpio, V., Scialdone, A., Theis, F.J., Teichmann, S.A., Marioni, J.C., and Stegle, O. (2015). Computational analysis of cell-to-cell heterogeneity in single-cell RNA-sequencing data reveals hidden subpopulations of cells. Nat. Biotechnol. 33, 155–160.

Burger, G., Gray, M.W., Forget, L., and Lang, B.F. (2013). Strikingly bacteria-like and gene-rich mitochondrial genomes throughout jakobid protists. Genome Biol Evol 5, 418–438.

Burger, G., Zhu, Y., Littlejohn, T.G., Greenwood, S.J., Schnare, M.N., Lang, B.F., and Gray, M.W. (2000). Complete sequence of the mitochondrial genome of Tetrahymena pyriformis and comparison with Paramecium aurelia mitochondrial DNA. Journal of Molecular Biology 297, 365–380.

Büschges, R., Bahrenberg, G., Zimmermann, M., and Wolf, K. (1994). Nadh: Ubiquinone

oxidoreductase in obligate aerobic yeasts. Yeast 10, 475–479.

Butow, R.A., and Avadhani, N.G. (2004). Mitochondrial Signaling: The Retrograde Response. Mol. Cell 14, 1–15.

Carneiro, P., Duarte, M., and Videira, A. (2004). The main external alternative NAD(P)H dehydrogenase of Neurospora crassa mitochondria. Biochimica et Biophysica Acta (BBA) - Bioenergetics 1608, 45–52.

Castro-Guerrero, N.A., Rodríguez-Zavala, J.S., Marín-Hernández, A., Rodríguez-Enríquez, S., and Moreno-Sánchez, R. (2008). Enhanced alternative oxidase and antioxidant enzymes under Cd(2+) stress in Euglena. J. Bioenerg. Biomembr. 40, 227–235.

Cavalcanti, J.H., Oliveira, G.M., Saraiva, K.D., Torquato, J.P., Maia, I.G., De, D.M., and Costa, J.H. (2013). Identification of duplicated and stress-inducible Aox2b gene co-expressed with Aox1 in species of the Medicago genus reveals a regulation linked to gene rearrangement in leguminous genomes. J. Plant Physiol. 170, 1609–1619.

Chacinska, A., Koehler, C.M., Milenkovic, D., Lithgow, T., and Pfanner, N. (2009). Importing mitochondrial proteins: machineries and mechanisms. Cell 138, 628–644.

Chacinska, A., Pfannschmidt, S., Wiedemann, N., Kozjak, V., Sanjuán Szklarz, L.K., Schulze-Specking, A., Truscott, K.N., Guiard, B., Meisinger, C., and Pfanner, N. (2004). Essential role of Mia40 in import and assembly of mitochondrial intermembrane space proteins. EMBO J. 23, 3735–3746.

Chae, M.S., and Nargang, F.E. (2009). Investigation of regulatory factors required for alternative oxidase production in Neurospora crassa. Physiol. Plant. 137, 407–418.

Chae, M.S., Nargang, C.E., Cleary, I.A., Lin, C.C., Todd, A.T., and Nargang, F.E. (2007a). Two zinc-cluster transcription factors control induction of alternative oxidase in Neurospora crassa. Genetics 177, 1997–2006.

Chae, M.S., Lin, C.C., Kessler, K.E., Nargang, C.E., Tanton, L.L., Hahn, L.B., and Nargang, F.E. (2007b). Identification of an alternative oxidase induction motif in the promoter region of the aod-1 gene in Neurospora crassa. Genetics 175, 1597–1606.

Chaudhuri, M., Ott, R.D., and Hill, G.C. (2006). Trypanosome alternative oxidase: from molecule to function. Trends Parasitol. 22, 484–491.

Chen, E.J., and Kaiser, C.A. (2003). LST8 negatively regulates amino acid biosynthesis as a component of the TOR pathway. J. Cell Biol. 161, 333–347.

Chen, X., Liang, H., Remmen, H.V., Vijg, J., and Richardson, A. (2004). Catalase transgenic mice: Characterization and sensitivity to oxidative stress. Arch. Biochem. Biophys. 422, 197–210.

Chen, X., Liang, H., Remmen, H.V., Vijg, J., and Richardson, A. (2004). Catalase transgenic mice: Characterization and sensitivity to oxidative stress. Archives of Biochemistry and Biophysics, Archives of Biochemistry and Biophysics. 422, 197–210.

Chen, X., Wang, Y., Li, J., Jiang, A., Cheng, Y., and Zhang, W. (2009). Mitochondrial proteome during salt stress-induced programmed cell death in rice. Plant Physiol. Biochem. 47, 407–415.

Chen, Y.-C., Taylor, E.B., Dephoure, N., Heo, J.-M., Tonhato, A., Papandreou, I., Nath, N., Denko, N.C., Gygi, S.P., and Rutter, J. (2012). Identification of a Protein Mediating Respiratory Supercomplex Stability. Cell Metabolism 15, 348–360.

Chen, R., Jiang, N., Jiang, Q., Sun, X., Wang, Y., Zhang, H., and Hu, Z. (2014). Exploring MicroRNA-Like Small RNAs in the Filamentous Fungus Fusarium oxysporum. PLOS ONE 9, e104956.

Chinnici, J.L., Fu, C., Caccamise, L.M., Arnold, J.W., and Free, S.J. (2014). Neurospora crassa Female Development Requires the PACC and Other Signal Transduction Pathways, Transcription Factors, Chromatin Remodeling, Cell-To-Cell Fusion, and Autophagy. PLOS ONE *9*, e110603.

Clifton, R., Lister, R., Parker, K.L., Sappl, P.G., Elhafez, D., Millar, A.H., Day, D.A., and Whelan, J. (2005). Stress-induced co-expression of alternative respiratory chain components in Arabidopsis thaliana. Plant Mol. Biol. 58, 193–212.

Cogliati, S., Enriquez, J.A., and Scorrano, L. (2016). Mitochondrial Cristae: Where Beauty Meets Functionality. Trends in Biochemical Sciences 41, 261–273.

Colot, H.V., Park, G., Turner, G.E., Ringelberg, C., Crew, C.M., Litvinkova, L., Weiss, R.L., Borkovich, K.A., and Dunlap, J.C. (2006). A high-throughput gene knockout procedure for Neurospora reveals functions for multiple transcription factors. Proc. Natl. Acad. Sci. 103, 10352–10357.

Considine, M.J., Holtzapffel, R.C., Day, D.A., Whelan, J., and Millar, A.H. (2002). Molecular distinction between alternative oxidase from monocots and dicots. Plant Physiol. 129, 949–953.

Contreras, L., Drago, I., Zampese, E., and Pozzan, T. (2010). Mitochondria: The calcium connection. Biochimica et Biophysica Acta (BBA) - Bioenergetics 1797, 607–618.

Copeland, W.C. (2008). Inherited Mitochondrial Diseases of DNA Replication. Annu Rev Med 59, 131–146.

Costa-de-Oliveira, S., Sampaio-Marques, B., Barbosa, M., Ricardo, E., Pina-Vaz, C., Ludovico, P., and Rodrigues, A.G. (2012). An alternative respiratory pathway on Candida krusei: implications on susceptibility profile and oxidative stress. FEMS Yeast Res. 12, 423–429.

Costa, J.H., Hasenfratz-Sauder, M.-P., Pham-Thi, A.T., Silva Lima, M. da G., Dizengremel, P., Jolivet, Y., and Fernandes de Melo, D. (2004). Identification in Vigna unguiculata (L.) Walp. of two cDNAs encoding mitochondrial alternative oxidase orthologous to soybean alternative oxidase genes 2a and 2b. Plant Sci. 167, 233–239.

Costa, J.H., Jolivet, Y., Hasenfratz-Sauder, M.-P., Orellano, E.G., da Guia Silva Lima, M., Dizengremel, P., and Fernandes de Melo, D. (2007). Alternative oxidase regulation in roots of Vigna unguiculata cultivars differing in drought/salt tolerance. J. Plant Physiol. 164, 718–727.

Costa, J.H., Mota, E.F., Cambursano, M.V., Lauxmann, M.A., de Oliveira, L.M.N., Silva Lima, M. da G., Orellano, E.G., and Fernandes de Melo, D. (2010). Stress-induced co-expression of two alternative oxidase (VuAox1 and 2b) genes in Vigna unguiculata. J. Plant Physiol. 167, 561–570.

Cox, C.J., Foster, P.G., Hirt, R.P., Harris, S.R., and Embley, T.M. (2008). The archaebacterial origin of eukaryotes. Proc. Natl. Acad. Sci. 105, 20356–20361.

Cox, G.M., Harrison, T.S., McDade, H.C., Taborda, C.P., Heinrich, G., Casadevall, A., and Perfect, J.R. (2003). Superoxide Dismutase Influences the Virulence of Cryptococcus neoformans by Affecting Growth within Macrophages. Infect. Immun. 71, 173–180.

Cvetkovska, M., and Vanlerberghe, G.C. (2012). Coordination of a mitochondrial superoxide burst during the hypersensitive response to bacterial pathogen in Nicotiana tabacum. Plant Cell Environ. 35, 1121–1136.

Dabir, D.V., Leverich, E.P., Kim, S.-K., Tsai, F.D., Hirasawa, M., Knaff, D.B., and Koehler, C.M. (2007). A role for cytochrome c and cytochrome c peroxidase in electron shuttling from Erv1. EMBO J. 26, 4801–4811.

Daems, W.T., and Wisse, E. (1966). Shape and attachment of the cristae mitochondriales in mouse hepatic cell mitochondria. Journal of Ultrastructure Research 16, 123–140.

Das, S., Hajnóczky, N., Antony, A.N., Csordás, G., Gaspers, L.D., Clemens, D.L., Hoek, J.B., and Hajnóczky, G. (2012). Mitochondrial morphology and dynamics in hepatocytes from normal and ethanol-fed rats. Pflugers Arch. 464, 101–109.

De Clercq, I., Vermeirssen, V., Van Aken, O., Vandepoele, K., Murcha, M.W., Law, S.R., Inzé, A., Ng, S., Ivanova, A., Rombaut, D., et al. (2013). The membrane-bound NAC transcription factor ANAC013 functions in mitochondrial retrograde regulation of the oxidative stress response in Arabidopsis. Plant Cell 25, 3472–3490.

Descheneau, A.T. (1974) Isolation and characterization of mutations affecting alternative oxidase regulation in Neurospora crassa. Doctor of Philosophy degree. https://library.ualberta.ca/catalog/3070335. Call number O4D DES.

Descheneau, A.T., Cleary, I.A., and Nargang, F.E. (2005). Genetic evidence for a regulatory

pathway controlling alternative oxidase production in Neurospora crassa. Genetics 169, 123–135.

DiMauro, S. (2013). Mitochondrial DNA Mutation Load. JAMA Neurol 70, 1484–1485.

Ding, W.-X., Li, M., Biazik, J.M., Morgan, D.G., Guo, F., Ni, H.-M., Goheen, M., Eskelinen, E.-L., and Yin, X.-M. (2012). Electron Microscopic Analysis of a Spherical Mitochondrial Structure. J. Biol. Chem. 287, 42373–42378.

Diogo, C.V., Yambire, K.F., Fernández Mosquera, L., Branco F, T., and Raimundo, N. (2017). Mitochondrial adventures at the organelle society. Biochem. Biophys. Res. Commun.

Dohlman, H.G., Song, J., Ma, D., Courchesne, W.E., and Thorner, J. (1996). Sst2, a negative regulator of pheromone signaling in the yeast Saccharomyces cerevisiae: expression, localization, and genetic interaction and physical association with Gpa1 (the G-protein alpha subunit). Mol. Cell. Biol. 16, 5194–5209.

Dojcinovic, D., Krosting, J., Harris, A.J., Wagner, D.J., and Rhoads, D.M. (2005). Identification of a region of the Arabidopsis AtAOX1a promoter necessary for mitochondrial retrograde regulation of expression. Plant Mol Biol 58, 159–175.

Dolezal, P., Likic, V., Tachezy, J., and Lithgow, T. (2006). Evolution of the Molecular Machines for Protein Import into Mitochondria. Science 313, 314–318.

Dong, D.W., Pereira, F., Barrett, S.P., Kolesar, J.E., Cao, K., Damas, J., Yatsunyk, L.A., Johnson, F.B., and Kaufman, B.A. (2014). Association of G-quadruplex forming sequences with human mtDNA deletion breakpoints. BMC Genomics 15, 677.

Donlin, M.J. (2007). Using the Generic Genome Browser (GBrowse). Curr Protoc Bioinformatics *Chapter 9*, Unit 9.9.

Dudek, J., Rehling, P., and van der Laan, M. (2013). Mitochondrial protein import: Common principles and physiological networks. Biochim. Biophys. Acta BBA - Mol. Cell Res. 1833, 274–285.

Dunn, A.K., Karr, E.A., Wang, Y., Batton, A.R., Ruby, E.G., and Stabb, E.V. (2010). The alternative oxidase (AOX) gene in Vibrio fischeri is controlled by NsrR and upregulated in response to nitric oxide. Mol Microbiol 77, 44–55.

Ederli, L., Morettini, R., Borgogni, A., Wasternack, C., Miersch, O., Reale, L., Ferranti, F., Tosti, N., and Pasqualini, S. (2006). Interaction between Nitric Oxide and Ethylene in the Induction of Alternative Oxidase in Ozone-Treated Tobacco Plants. Plant Physiol. 142, 595–608.

El-Khoury, R., and Sainsard-Chanet, A. (2010). Deletion of the mitochondrial NADH kinase increases mitochondrial DNA stability and life span in the filamentous fungus Podospora anserina. Exp. Gerontol. 45, 543–549.

El-Khoury, R., Dufour, E., Rak, M., Ramanantsoa, N., Grandchamp, N., Csaba, Z., Duvillié, B., Bénit, P., Gallego, J., Gressens, P., et al. (2013). Alternative Oxidase Expression in the Mouse Enables Bypassing Cytochrome c Oxidase Blockade and Limits Mitochondrial ROS Overproduction. PLOS Genet. 9, e1003182.

Elowitz, M.B., Levine, A.J., Siggia, E.D., and Swain, P.S. (2002). Stochastic gene expression in a single cell. Science 297, 1183–1186.

Eme, L., Spang, A., Lombard, J., Stairs, C.W., and Ettema, T.J.G. (2018). Archaea and the origin of eukaryotes. Nature Reviews Microbiology 16, 120.

Endo, T., and Yamano, K. (2010). Transport of proteins across or into the mitochondrial outer membrane. Biochim. Biophys. Acta 1803, 706–714.

Endres, M., Neupert, W., and Brunner, M. (1999). Transport of the ADP/ATP carrier of mitochondria from the TOM complex to the TIM22.54 complex. EMBO J. 18, 3214–3221.

Fauron C, Allen JO, Clifton SW, Newton KJ. In: Molecular Biology and Biotechnology of Plant Organelles. Daniell H, Dordrecht CC, editor. Netherlands: Kluwer Academic Publishers; 2004. Plant Mitochondrial Genomes; pp. 151–177.

Feldbrügge, M., Kämper, J., Steinberg, G., and Kahmann, R. (2004). Regulation of mating and pathogenic development in Ustilago maydis. Curr. Opin. Microbiol. 7, 666–672.

Fiorese, C.J., and Haynes, C.M. (2017). Integrating the UPRmt into the mitochondrial maintenance network. Crit. Rev. Biochem. Mol. Biol. 52, 304–313.

Forget, L., Ustinova, J., Wang, Z., Huss, V.A.R., and Franz Lang, B. (2002). Hyaloraphidium curvatum: A Linear Mitochondrial Genome, tRNA Editing, and an Evolutionary Link to Lower Fungi. Molecular Biology and Evolution 19, 310–319.

Fox, T.D. (2012). Mitochondrial protein synthesis, import, and assembly. Genetics 192, 1203–1234.

Frey, T.G., and Mannella, C.A. (2000). The internal structure of mitochondria. Trends Biochem. Sci. 25, 319–324.

Frost, R.J.A., and Olson, E.N. (2011). Control of glucose homeostasis and insulin sensitivity by the Let-7 family of microRNAs. Proc. Natl. Acad. Sci. 108, 21075–21080.

Fu, C., Iyer, P., Herkal, A., Abdullah, J., Stout, A., and Free, S.J. (2011). Identification and Characterization of Genes Required for Cell-to-Cell Fusion in Neurospora crassa. Eukaryotic Cell *10*, 1100–1109

Fukuhara, H., Sor, F., Drissi, R., Dinouël, N., Miyakawa, I., Rousset, S., and Viola, A.M. (1993). Linear mitochondrial DNAs of yeasts: frequency of occurrence and general features. Molecular and Cellular Biology 13, 2309–2314.

Fuss, J.O., Tsai, C.-L., Ishida, J.P., and Tainer, J.A. (2015). Emerging critical roles of Fe–S clusters in DNA replication and repair. Biochim. Biophys. Acta BBA - Mol. Cell Res. 1853, 1253–1271.

Galtier, N. (2011). The intriguing evolutionary dynamics of plant mitochondrial DNA. BMC Biol. 9, 61.

Gay, D.A., Sisodia, S.S., and Cleveland, D.W. (1989). Autoregulatory control of beta-tubulin mRNA stability is linked to translation elongation. Proc Natl Acad Sci U S A 86, 5763–5767.

Gebauer, F., Preiss, T., and Hentze, M.W. (2012). From Cis-Regulatory Elements to Complex RNPs and Back. Cold Spring Harb Perspect Biol 4.

Gentle, I., Gabriel, K., Beech, P., Waller, R., and Lithgow, T. (2004). The Omp85 family of proteins is essential for outer membrane biogenesis in mitochondria and bacteria. The Journal of Cell Biology 164, 19–24.

Gerbeth, C., Schmidt, O., Rao, S., Harbauer, A.B., Mikropoulou, D., Opalińska, M., Guiard, B., Pfanner, N., and Meisinger, C. (2013). Glucose-Induced Regulation of Protein Import Receptor Tom22 by Cytosolic and Mitochondria-Bound Kinases. Cell Metab. 18, 578–587.

Gilks, N., Kedersha, N., Ayodele, M., Shen, L., Stoecklin, G., Dember, L.M., and Anderson, P. (2004). Stress granule assembly is mediated by prion-like aggregation of TIA-1. Mol. Biol. Cell 15, 5383–5398.

Giraud, E., Aken, O.V., Ho, L.H.M., and Whelan, J. (2009). The Transcription Factor ABI4 Is a Regulator of Mitochondrial Retrograde Expression of ALTERNATIVE OXIDASE1a. Plant Physiology 150, 1286–1296.

Giraud, E., Ho, L.H.M., Clifton, R., Carroll, A., Estavillo, G., Tan, Y.-F., Howell, K.A., Ivanova, A., Pogson, B.J., Millar, A.H., et al. (2008). The absence of ALTERNATIVE OXIDASE1a in Arabidopsis results in acute sensitivity to combined light and drought stress. Plant Physiol. 147, 595–610.

Glick, B.S., Brandt, A., Cunningham, K., Müller, S., Hallberg, R.L., and Schatz, G. (1992). Cytochromes c1 and b2 are sorted to the intermembrane space of yeast mitochondria by a stop-transfer mechanism. Cell 69, 809–822.

Gold, V.A.M., Ieva, R., Walter, A., Pfanner, N., van der Laan, M., and Kühlbrandt, W. (2014). Visualizing active membrane protein complexes by electron cryotomography. Nat Commun 5, 4129.

Granatiero, V., De Stefani, D., and Rizzuto, R. (2017). Mitochondrial Calcium Handling in Physiology and Disease. Adv. Exp. Med. Biol. 982, 25–47.

Grant, N., Onda, Y., Kakizaki, Y., Ito, K., Watling, J., and Robinson, S. (2009). Two Cys or Not Two Cys? That Is the Question; Alternative Oxidase in the Thermogenic Plant Sacred Lotus. Plant Physiol. 150, 987–995.

Gray, G.R., Maxwell, D.P., Villarimo, A.R., and McIntosh, L. (2004b). Mitochondria/nuclear signaling of alternative oxidase gene expression occurs through distinct pathways involving organic acids and reactive oxygen species. Plant Cell Rep. 23, 497–503.

Gray, L.R., Rouault, A.A.J., Oonthonpan, L., Rauckhorst, A.J., Sebag, J.A., and Taylor, E.B. (2017). Measuring Mitochondrial Pyruvate Oxidation. In Techniques to Investigate Mitochondrial Function in Neurons, (Humana Press, New York, NY), pp. 321–338.

Gray, M. (1998). Genome structure and gene content in protist mitochondrial DNAs. Nucleic Acids Research 26, 865–878.

Gray, M.W. (1998). Rickettsia, typhus and the mitochondrial connection. Nature 396, 109.

Gray, M.W. (2012). Mitochondrial Evolution. Cold Spring Harb. Perspect. Biol. 4.

Gray, M.W., Lang, B.F., and Burger, G. (2004a). Mitochondria of protists. Annu. Rev. Genet. 38, 477–524.

Grigoriev, I.V., Nikitin, R., Haridas, S., Kuo, A., Ohm, R., Otillar, R., Riley, R., Salamov, A., Zhao, X., Korzeniewski, F., et al. (2014). MycoCosm portal: gearing up for 1000 fungal genomes. Nucleic Acids Res. 42, D699-704.

Gritz, L., and Davies, J. (1983). Plasmid-encoded hygromycin B resistance: the sequence of hygromycin B phosphotransferase gene and its expression in Escherichia coli and Saccharomyces cerevisiae. Gene *25*, 179–188.

Grumbt, B., Stroobant, V., Terziyska, N., Israel, L., and Hell, K. (2007). Functional characterization of Mia40p, the central component of the disulfide relay system of the mitochondrial intermembrane space. J. Biol. Chem. 282, 37461–37470.

Guy, L., and Ettema, T.J.G. (2011). The archaeal 'TACK' superphylum and the origin of eukaryotes. Trends Microbiol. 19, 580–587.

Hakkaart, G.A.J., Dassa, E.P., Jacobs, H.T., and Rustin, P. (2006). Allotopic expression of a mitochondrial alternative oxidase confers cyanide resistance to human cell respiration. EMBO Rep 7, 341–345.

Hall, M.C., Dworkin, I., Ungerer, M.C., and Purugganan, M. (2007). Genetics of microenvironmental canalization in Arabidopsis thaliana. Proc. Natl. Acad. Sci. U.S.A. 104, 13717–13722.

Hämäläinen, R.H., Ahlqvist, K.J., Ellonen, P., Lepistö, M., Logan, A., Otonkoski, T., Murphy, M.P., and Suomalainen, A. (2015). mtDNA Mutagenesis Disrupts Pluripotent Stem Cell Function by Altering Redox Signaling. Cell Rep. 11, 1614–1624.

Han, K.-H., Seo, J.-A., and Yu, J.-H. (2004). Regulators of G-protein signalling in Aspergillus nidulans: RgsA downregulates stress response and stimulates asexual sporulation through attenuation of GanB (Galpha) signalling. Mol. Microbiol. 53, 529–540.

Harbauer, A.B., Zahedi, R.P., Sickmann, A., Pfanner, N., and Meisinger, C. (2014). The protein import machinery of mitochondria-a regulatory hub in metabolism, stress, and disease. Cell Metab. 19, 357–372.

Harman, D. (1956). Aging: a theory based on free radical and radiation chemistry. J. Gerontol. 11, 298–300.

Harman, D. (1969). Prolongation of Life: Role of Free Radical Reactions in Aging. J. Am. Geriatr. Soc. 17, 721–735.

Harman, D. (1972). The biologic clock: the mitochondria? J. Am. Geriatr. Soc. 20, 145–147.

Hawking, Z.L. (2016). Alzheimer's disease: the role of mitochondrial dysfunction and potential new therapies. Bioscience Horizons 9.

Haynes, C.M., Fiorese, C.J., and Lin, Y.-F. (2013). Evaluating and responding to mitochondrial dysfunction: the mitochondrial unfolded-protein response and beyond. Trends Cell Biol. 23, 311–318.

Haynes, C.M., Yang, Y., Blais, S.P., Neubert, T.A., and Ron, D. (2010). The matrix peptide exporter HAF-1 signals a mitochondrial UPR by activating the transcription factor ZC376.7 in C. elegans. Mol. Cell 37, 529–540.

He, L., and Hannon, G.J. (2004). MicroRNAs: small RNAs with a big role in gene regulation. Nat. Rev. Genet. 5, 522–531.

He, C., Hart, P.C., Germain, D., and Bonini, M.G. (2016). SOD2 and the Mitochondrial UPR: Partners Regulating Cellular Phenotypic Transitions. Trends Biochem. Sci. 41, 568–577.

Hill, K., Model, K., Ryan, M.T., Dietmeier, K., Martin, F., Wagner, R., and Pfanner, N. (1998). Tom40 forms the hydrophilic channel of the mitochondrial import pore for preproteins [see comment]. Nature 395, 516–521.

Hoeh, W.R., Stewart, D.T., and Guttman, S.I. (2002). High fidelity of mitochondrial genome transmission under the doubly uniparental mode of inheritance in freshwater mussels (Bivalvia: Unionoidea). Evol. Int. J. Org. Evol. 56, 2252–2261.

Höhr, A.I.C., Lindau, C., Wirth, C., Qiu, J., Stroud, D.A., Kutik, S., Guiard, B., Hunte, C., Becker, T., Pfanner, N., et al. (2018). Membrane protein insertion through a mitochondrial β-barrel gate. Science 359.

Höhr, A.I.C., Straub, S.P., Warscheid, B., Becker, T., and Wiedemann, N. (2015). Assembly of β-barrel proteins in the mitochondrial outer membrane. Biochim. Biophys. Acta BBA - Mol. Cell Res. 1853, 74–88.

Höhr, A.I.C., Straub, S.P., Warscheid, B., Becker, T., and Wiedemann, N. (2015). Assembly of β-barrel proteins in the mitochondrial outer membrane. Biochimica et Biophysica Acta (BBA) - Molecular Cell Research 1853, 74–88.

Honda, Y., Hattori, T., and Kirimura, K. (2012). Visual expression analysis of the responses of the alternative oxidase gene (aox1) to heat shock, oxidative, and osmotic stresses in conidia of citric acid-producing Aspergillus niger. J. Biosci. Bioeng. 113, 338–342.

Horvath, S.E., Rampelt, H., Oeljeklaus, S., Warscheid, B., van der Laan, M., and Pfanner, N. (2015). Role of membrane contact sites in protein import into mitochondria. Protein Science 24, 277–297.

Hu, Q., and Wang, G. (2016). Mitochondrial dysfunction in Parkinson's disease. Transl. Neurodegener. 5.

Huang, T.T., Carlson, E.J., Gillespie, A.M., Shi, Y., and Epstein, C.J. (2000). Ubiquitous overexpression of CuZn superoxide dismutase does not extend life span in mice. J. Gerontol. A. Biol. Sci. Med. Sci. 55, B5-9.

Huh, W.-K., and Kang, S.-O. (2001). Characterization of the gene family encoding alternative oxidase from Candida albicans. Biochem. J. 356, 595–604.

Hulett, J.M., Lueder, F., Chan, N.C., Perry, A.J., Wolynec, P., Likić, V.A., Gooley, P.R., and Lithgow, T. (2008). The Transmembrane Segment of Tom20 Is Recognized by Mim1 for Docking to the Mitochondrial TOM Complex. Journal of Molecular Biology 376, 694–704.

Ivey, F.D., Yang, Q., and Borkovich, K.A. (1999). Positive regulation of adenylyl cyclase activity by a galphai homolog in Neurospora crassa. Fungal Genet. Biol. 26, 48–61.

Jia, Y., Rothermel, B., Thornton, J., and Butow, R.A. (1997). A basic helix-loop-helix-leucine zipper transcription complex in yeast functions in a signaling pathway from mitochondria to the nucleus. Mol. Cell. Biol. 17, 1110–1117.

Jiang, N., Yang, Y., Janbon, G., Pan, J., and Zhu, X. (2012). Identification and Functional Demonstration of miRNAs in the Fungus Cryptococcus neoformans. PLOS ONE 7, e52734.

Jiang, X., Qiao, F., Long, Y., Cong, H., and Sun, H. (2017). MicroRNA-like RNAs in plant pathogenic fungus Fusarium oxysporum f. sp. Niveum are involved in toxin gene expression fine tuning. 3 Biotech 7, 354.

Johnson, D.C., Dean, D.R., Smith, A.D., and Johnson, M.K. (2005). Structure, Function, and Formation of Biological Iron-Sulfur Clusters. Annu. Rev. Biochem. 74, 247–281.

Joseph-Horne, T., Hollomon, D.W., and Wood, P.M. (2001). Fungal respiration: a fusion of standard and alternative components. Biochimica et Biophysica Acta (BBA) - Bioenergetics 1504, 179–195.

Joseph-Horne, T., Wood, P.M., Wood, C.K., Moore, A.L., Headrick, J., and Hollomon, D. (1998). Characterization of a Split Respiratory Pathway in the Wheat "Take-all" Fungus, Gaeumannomyces graminis var.tritici. J. Biol. Chem. 273, 11127–11133.

Kallies, A., Gebauer, G., and Rensing, L. (1998). Heat shock effects on second messenger systems of Neurospora crassa. Arch. Microbiol. 170, 191–200.

Kanneganti, T.-D., Kundu, M., and Green, D.R. (2015). Innate Immune Recognition of mtDNA—An Undercover Signal? Cell Metab. 21, 793–794.

Karnkowska, A., Vacek, V., Zubáčová, Z., Treitli, S.C., Petrželková, R., Eme, L., Novák, L., Žárský, V., Barlow, L.D., Herman, E.K., et al. (2016). A Eukaryote without a Mitochondrial Organelle. Curr. Biol. 26, 1274–1284.

Kauppila, T.E.S., Kauppila, J.H.K., and Larsson, N.-G. (2017). Mammalian Mitochondria and Aging: An Update. Cell Metab. 25, 57–71.

Kempe, H., Schwabe, A., Crémazy, F., Verschure, P.J., and Bruggeman, F.J. (2015). The volumes and transcript counts of single cells reveal concentration homeostasis and capture biological noise. Mol. Biol. Cell 26, 797–804.

Kemper, C., Habib, S.J., Engl, G., Heckmeyer, P., Dimmer, K.S., and Rapaport, D. (2008). Integration of tail-anchored proteins into the mitochondrial outer membrane does not require any known import components. J. Cell. Sci. 121, 1990–1998.

Kennedy, S.R., Salk, J.J., Schmitt, M.W., and Loeb, L.A. (2013). Ultra-Sensitive Sequencing Reveals an Age-Related Increase in Somatic Mitochondrial Mutations That Are Inconsistent with Oxidative Damage. PLOS Genetics 9, e1003794.

Kennell, J. C., Collins, R. A., Griffiths, A. J. F., and Nargang, F. E. (2004) Mitochondrial genetics of Neurospora, in The Mycota II. Genetics and Biotechnology (Kück, U., ed.), 2nd Ed., Springer-Verlag, Berlin, pp. 95–112.

Kim, D.-H., Sarbassov, D.D., Ali, S.M., King, J.E., Latek, R.R., Erdjument-Bromage, H., Tempst, P., and Sabatini, D.M. (2002). mTOR interacts with raptor to form a nutrient-sensitive

complex that signals to the cell growth machinery. Cell 110, 163–175.

Kim, K.S., Rosenkrantz, M.S., and Guarente, L. (1986). Saccharomyces cerevisiae contains two functional citrate synthase genes. Mol. Cell. Biol. 6, 1936–1942.

Kim, H.S., Wilce, M.C.J., Yoga, Y.M.K., Pendini, N.R., Gunzburg, M.J., Cowieson, N.P., Wilson, G.M., Williams, B.R.G., Gorospe, M., and Wilce, J.A. (2011). Different modes of interaction by TIAR and HuR with target RNA and DNA. Nucleic Acids Res. 39, 1117–1130.

Kishore, Nishka. (2015) Expression of alternative oxidase (AOX) in the filamentous fungus Neurospora crassa. Master of Science degree. https://doi.org/10.7939/R3DZ0389D.

Ko, K.-W., Lin, F., Katsumata, T., Sugai, Y., Miyazaki, S., Kawaide, H., Okada, K., Nojiri, H., and Yamane, H. (2008). Functional identification of a rice ent-kaurene oxidase, OsKO2, using the Pichia pastoris expression system. Biosci. Biotechnol. Biochem. *72*, 3285–3288.

Kohn, A.B., Citarella, M.R., Kocot, K.M., Bobkova, Y.V., Halanych, K.M., and Moroz, L.L. (2012). Rapid evolution of the compact and unusual mitochondrial genome in the ctenophore, Pleurobrachia bachei. Mol. Phylogenet. Evol. 63, 203–207.

Komeili, A., Wedaman, K.P., O'Shea, E.K., and Powers, T. (2000). Mechanism of Metabolic Control: Target of Rapamycin Signaling Links Nitrogen Quality to the Activity of the Rtg1 and Rtg3 Transcription Factors. The Journal of Cell Biology 151, 863–878.

Komiya, T., Rospert, S., Koehler, C., Looser, R., Schatz, G., and Mihara, K. (1998). Interaction of mitochondrial targeting signals with acidic receptor domains along the protein import pathway: evidence for the "acid chain" hypothesis. EMBO J 17, 3886–3898.

Koonin, E.V. (2015). Archaeal ancestors of eukaryotes: not so elusive any more. BMC Biol. 13, 84.

Kornmann, B., and Walter, P. (2010). ERMES-mediated ER-mitochondria contacts: molecular hubs for the regulation of mitochondrial biology. J. Cell Sci. 123, 1389–1393.

Kornmann, B., Currie, E., Collins, S.R., Schuldiner, M., Nunnari, J., Weissman, J.S., and Walter, P. (2009). An ER-mitochondria tethering complex revealed by a synthetic biology screen. Science 325, 477–481.

Kováč, L., Lazowska, J., and Slonimski, P.P. (1984). A yeast with linear molecules of mitochondrial DNA. MGG Molecular & General Genetics 197, 420–424.

Kreps, J.A., Wu, Y., Chang, H.-S., Zhu, T., Wang, X., and Harper, J.F. (2002). Transcriptome changes for Arabidopsis in response to salt, osmotic, and cold stress. Plant Physiol. 130, 2129–2141.

Krijgsheld, P., Bleichrodt, R., van Veluw, G.J., Wang, F., Müller, W.H., Dijksterhuis, J., and

Wösten, H. a. B. (2013). Development in Aspergillus. Stud. Mycol. 74, 1–29.

Krijgsheld, P., Nitsche, B.M., Post, H., Levin, A.M., Müller, W.H., Heck, A.J.R., Ram, A.F.J., Altelaar, A.F.M., and Wösten, H.A.B. (2013a). Deletion of flbA results in increased secretome complexity and reduced secretion heterogeneity in colonies of Aspergillus niger. J. Proteome Res. 12, 1808–1819.

Krijgsheld, P., and Wösten, H.A. (2013b). Transcriptome Analysis of Zones of Colonies of the ΔflbA Strain of Aspergillus niger. Fungal Genomics Biol. 3, 1–22.

Ku, C., Nelson-Sathi, S., Roettger, M., Sousa, F.L., Lockhart, P.J., Bryant, D., Hazkani-Covo, E., McInerney, J.O., Landan, G., and Martin, W.F. (2015). Endosymbiotic origin and differential loss of eukaryotic genes. Nature 524, 427–432.

Kujoth, G.C., Hiona, A., Pugh, T.D., Someya, S., Panzer, K., Wohlgemuth, S.E., Hofer, T., Seo, A.Y., Sullivan, R., Jobling, W.A., et al. (2005). Mitochondrial DNA mutations, oxidative stress, and apoptosis in mammalian aging. Science 309, 481–484.

Kupper, U., Niedermann, D.M., Travaglini, G., and Lerch, K. (1989). Isolation and characterization of the tyrosinase gene from Neurospora crassa. J. Biol. Chem. 264, 17250–17258.

Kutik, S., Stojanovski, D., Becker, L., Becker, T., Meinecke, M., Krüger, V., Prinz, C., Meisinger, C., Guiard, B., Wagner, R., et al. (2008). Dissecting membrane insertion of mitochondrial beta-barrel proteins. Cell 132, 1011–1024.

Labbé, K., Murley, A., and Nunnari, J. (2014). Determinants and functions of mitochondrial behavior. Annu. Rev. Cell Dev. Biol. 30, 357–391.

Lafon, A., Han, K.-H., Seo, J.-A., Yu, J.-H., and d'Enfert, C. (2006). G-protein and cAMP-mediated signaling in aspergilli: a genomic perspective. Fungal Genet. Biol. 43, 490–502.

Lambowitz, A.M., and Slayman, C.W. (1971). Cyanide-Resistant Respiration in Neurospora crassa. J. Bacteriol. 108, 1087–1096.

Lambowitz, A.M., Sabourin, J.R., Bertrand, H., Nickels, R., and McIntosh, L. (1989). Immunological identification of the alternative oxidase of Neurospora crassa mitochondria. Mol. Cell. Biol. 9, 1362–1364.

Lapuente-Brun, E., Moreno-Loshuertos, R., Acín-Pérez, R., Latorre-Pellicer, A., Colás, C., Balsa, E., Perales-Clemente, E., Quirós, P.M., Calvo, E., Rodríguez-Hernández, M.A., et al. (2013). Supercomplex assembly determines electron flux in the mitochondrial electron transport chain. Science 340, 1567–1570.

Leal, J., Squina, F.M., Freitas, J.S., Silva, E.M., Ono, C.J., Martinez-Rossi, N.M., and Rossi, A. (2009). A splice variant of the Neurospora crassa hex-1 transcript, which encodes the major

protein of the Woronin body, is modulated by extracellular phosphate and pH changes. FEBS Lett. 583, 180–184.

Lee, B.N., and Adams, T.H. (1994). Overexpression of flbA, an early regulator of Aspergillus asexual sporulation, leads to activation of brlA and premature initiation of development. Mol. Microbiol. 14, 323–334.

Lee, H.-C., Li, L., Gu, W., Xue, Z., Crosthwaite, S.K., Pertsemlidis, A., Lewis, Z.A., Freitag, M., Selker, E.U., Mello, C.C., et al. (2010). Diverse Pathways Generate MicroRNA-like RNAs and Dicer-Independent Small Interfering RNAs in Fungi. Mol. Cell 38, 803–814.

Lenaz, G., and Genova, M.L. (2009). Structural and functional organization of the mitochondrial respiratory chain: a dynamic super-assembly. Int. J. Biochem. Cell Biol. 41, 1750–1772.

Lesnik, C., Golani-Armon, A., and Arava, Y. (2015). Localized translation near the mitochondrial outer membrane: An update. RNA Biol. 12, 801–809.

Li, Q., Ritzel, R.G., McLean, L.L., McIntosh, L., Ko, T., Bertrand, H., and Nargang, F.E. (1996). Cloning and analysis of the alternative oxidase gene of Neurospora crassa. Genetics 142, 129–140.

Li, Z., and Xing, D. (2011). Mechanistic study of mitochondria-dependent programmed cell death induced by aluminium phytotoxicity using fluorescence techniques. J. Exp. Bot. 62, 331–343.

Li, J., Xu, Y., and Chong, K. (2012). The novel functions of kinesin motor proteins in plants. Protoplasma *249*, 95–100.

Liao, B., Hu, Y., and Brewer, G. (2007). Competitive binding of AUF1 and TIAR to MYC mRNA controls its translation. Nat. Struct. Mol. Biol. 14, 511–518.

Liu, X., Kim, C.N., Yang, J., Jemmerson, R., and Wang, X. (1996). Induction of Apoptotic Program in Cell-Free Extracts: Requirement for dATP and Cytochrome c. Cell 86, 147–157.

Liu, Z., Sekito, T., Epstein, C.B., and Butow, R.A. (2001). RTG-dependent mitochondria to nucleus signaling is negatively regulated by the seven WD-repeat protein Lst8p. EMBO J. 20, 7209–7219.

Liu, Z., Sekito, T., Spírek, M., Thornton, J., and Butow, R.A. (2003). Retrograde signaling is regulated by the dynamic interaction between Rtg2p and Mks1p. Mol. Cell 12, 401–411.

Lodish, H., Berk, A., Zipursky, S.L., Matsudaira, P., Baltimore, D., and Darnell, J. (2000). Kinesin, Dynein, and Intracellular Transport.

Loewith, R., and Hall, M.N. (2011). Target of Rapamycin (TOR) in Nutrient Signaling and Growth Control. Genetics 189, 1177–1201.

López de Silanes, I., Zhan, M., Lal, A., Yang, X., and Gorospe, M. (2004). Identification of a target RNA motif for RNA-binding protein HuR. Proc. Natl. Acad. Sci. U.S.A. 101, 2987–2992.

Lu, Y., Thomson, J.M., Wong, H.Y.F., Hammond, S.M., and Hogan, B.L.M. (2007). Transgenic over-expression of the microRNA miR-17-92 cluster promotes proliferation and inhibits differentiation of lung epithelial progenitor cells. Dev. Biol. 310, 442–453.

Luciano, P., Vial, S., Vergnolle, M.A., Dyall, S.D., Robinson, D.R., and Tokatlidis, K. (2001). Functional reconstitution of the import of the yeast ADP/ATP carrier mediated by the TIM10 complex. EMBO J. 20, 4099–4106.

MacKenzie, J.A., and Mark Payne, R. (2007). Mitochondrial Protein Import and Human Health and Disease. Biochim. Biophys. Acta 1772, 509–523.

Macrae, I.J., Zhou, K., Li, F., Repic, A., Brooks, A.N., Cande, W.Z., Adams, P.D., and Doudna, J.A. (2006). Structural basis for double-stranded RNA processing by Dicer. Science 311, 195–198.

Maddi, A., Fu, C., and Free, S.J. (2012). The Neurospora crassa dfg5 and dcw1 Genes Encode α-1,6-Mannanases That Function in the Incorporation of Glycoproteins into the Cell Wall. PLOS ONE 7, e38872.

Magnani, T., Soriani, F.M., Martins, V. de P., Policarpo, A.C. de F., Sorgi, C.A., Faccioli, L.H., Curti, C., and Uyemura, S.A. (2008). Silencing of mitochondrial alternative oxidase gene of Aspergillus fumigatus enhances reactive oxygen species production and killing of the fungus by macrophages. J. Bioenerg. Biomembr. 40, 631.

Magnani, T., Soriani, F.M., Martins, V.P., Nascimento, A.M., Tudella, V.G., Curti, C., and Uyemura, S.A. (2007). Cloning and functional expression of the mitochondrial alternative oxidase of Aspergillus fumigatus and its induction by oxidative stress. FEMS Microbiol. Lett. 271, 230–238.

Mah, J.-H., and Yu, J.-H. (2006). Upstream and downstream regulation of asexual development in Aspergillus fumigatus. Eukaryotic Cell 5, 1585–1595.

Mannella, C.A. (1986). Mitochondrial outer membrane channel (VDAC, porin) two-dimensional crystals from Neurospora. Meth. Enzymol. 125, 595–610.

Mannella, C.A., Colombini, M., and Frank, J. (1983). Structural and functional evidence for multiple channel complexes in the outer membrane of Neurospora crassa mitochondria. Proc Natl Acad Sci U S A 80, 2243–2247.

Mannella, C.A., Pfeiffer, D.R., Bradshaw, P.C., Moraru, I.I., Slepchenko, B., Loew, L.M., Hsieh, C.E., Buttle, K., and Marko, M. (2001). Topology of the mitochondrial inner membrane: dynamics and bioenergetic implications. IUBMB Life 52, 93–100.

Margulis, L. (1970). Origin of Eukaryotic Cells: Evidence and Research Implications for a Theory of the Origin and Evolution of Microbial, Plant, and Animal Cells on the Precambrian Earth (Yale University Press).

Marques, I., Dencher, N.A., Videira, A., and Krause, F. (2007). Supramolecular organization of the respiratory chain in Neurospora crassa mitochondria. Eukaryotic Cell 6, 2391–2405.

Martin, F.N. (1995). Linear mitochondrial genome organization in vivo in the genus Pythium. Current Genetics 28, 225–234.

Martin, W., and Koonin, E.V. (2006). Introns and the origin of nucleus-cytosol compartmentalization. Nature 440, 41–45.

Martin, W., and Müller, M. (1998). The hydrogen hypothesis for the first eukaryote. Nature 392, 37–41.

Martin, W.F., Garg, S., and Zimorski, V. (2015). Endosymbiotic theories for eukaryote origin. Philos. Trans. R. Soc. B Biol. Sci. 370.

Martin, W.F., Neukirchen, S., Zimorski, V., Gould, S.B., and Sousa, F.L. (2016). Energy for two: New archaeal lineages and the origin of mitochondria. BioEssays 38, 850–856.

Martínez-Reyes, I., Diebold, L.P., Kong, H., Schieber, M., Huang, H., Hensley, C.T., Mehta, M.M., Wang, T., Santos, J.H., Woychik, R., et al. (2016). TCA Cycle and Mitochondrial Membrane Potential Are Necessary for Diverse Biological Functions. Mol. Cell 61, 199–209.

Martinus, R.D., Garth, G.P., Webster, T.L., Cartwright, P., Naylor, D.J., Høj, P.B., and Hoogenraad, N.J. (1996). Selective induction of mitochondrial chaperones in response to loss of the mitochondrial genome. Eur. J. Biochem. 240, 98–103.

Matityahu, A., and Onn, I. (2018). A new twist in the coil: functions of the coiled-coil domain of structural maintenance of chromosome (SMC) proteins. Curr Genet *64*, 109–116.

Matsuura, A., and Anraku, Y. (1993). Characterization of the MKS1 gene, a new negative regulator of the Ras-cyclic AMP pathway in Saccharomyces cerevislae. Mol. Gen. Genet. MGG 238, 6–16.

Matus-Ortega, M.G., Cárdenas-Monroy, C.A., Flores-Herrera, O., Mendoza-Hernández, G., Miranda, M., González-Pedrajo, B., Vázquez-Meza, H., and Pardo, J.P. (2015). New complexes containing the internal alternative NADH dehydrogenase (Ndi1) in mitochondria of Saccharomyces cerevisiae. Yeast 32, 629–641.

McCudden, C.R., Hains, M.D., Kimple, R.J., Siderovski, D.P., and Willard, F.S. (2005). G-protein signaling: back to the future. Cell. Mol. Life Sci. 62, 551–577.

McDonald, A., and Vanlerberghe, G. (2004). Branched mitochondrial electron transport in the Animalia: presence of alternative oxidase in several animal phyla. IUBMB Life 56, 333–341.

McDonald, A.E., Amirsadeghi, S., and Vanlerberghe, G.C. (2003). Prokaryotic orthologues of mitochondrial alternative oxidase and plastid terminal oxidase. Plant Mol Biol 53, 865–876.

McDonald, A.E., and Vanlerberghe, G.C. (2006). Origins, evolutionary history, and taxonomic distribution of alternative oxidase and plastoquinol terminal oxidase. Comp. Biochem. Physiol. Part D Genomics Proteomics 1, 357–364.

McDonald, A.E., Vanlerberghe, G.C., and Staples, J.F. (2009). Alternative oxidase in animals: unique characteristics and taxonomic distribution. J. Exp. Biol. 212, 2627–2634.

Medeiros, I.D., Siebert, M.N., de Toledo e Silva, G., Moraes, M.O., Marques, M.R.F., and Bainy, A.C.D. (2008). Differential gene expression in oyster exposed to sewage. Mar. Environ. Res. 66, 156–157.

Meng, T.-C., Fukada, T., and Tonks, N.K. (2002). Reversible Oxidation and Inactivation of Protein Tyrosine Phosphatases In Vivo. Mol. Cell 9, 387–399.

Mereschkowski C. (1905). Über Natur und Ursprung der Chromatophoren im Pflanzenreiche. Biol.Centralbl. 25, 593–604

Merritt, C., Rasoloson, D., Ko, D., and Seydoux, G. (2008). 3′ UTRs are the primary regulators of gene expression in the C. elegans germline. Curr. Biol. 18, 1476–1482.

Mesecke, N., Terziyska, N., Kozany, C., Baumann, F., Neupert, W., Hell, K., and Herrmann, J.M. (2005). A disulfide relay system in the intermembrane space of mitochondria that mediates protein import. Cell 121, 1059–1069.

Milenkovic, D., Gabriel, K., Guiard, B., Schulze-Specking, A., Pfanner, N., and Chacinska, A. (2007). Biogenesis of the essential Tim9-Tim10 chaperone complex of mitochondria: site-specific recognition of cysteine residues by the intermembrane space receptor Mia40. J. Biol. Chem. 282, 22472–22480.

Milenkovic, D., Ramming, T., Müller, J.M., Wenz, L.-S., Gebert, N., Schulze-Specking, A., Stojanovski, D., Rospert, S., and Chacinska, A. (2009). Identification of the Signal Directing Tim9 and Tim10 into the Intermembrane Space of Mitochondria. Mol Biol Cell 20, 2530–2539.

Mishra, P., and Chan, D.C. (2016). Metabolic regulation of mitochondrial dynamics. J Cell Biol 212, 379–387.

Mitchell, M.B., and Mitchell, H.K. (1952). A Case of "Maternal" Inheritance in Neurospora Crassa. Proc. Natl. Acad. Sci. U. S. A. 38, 442–449.

Mittler, R., Vanderauwera, S., Gollery, M., and Van Breusegem, F. (2004). Reactive oxygen

gene network of plants. Trends Plant Sci. 9, 490–498.

Mittova, V., Guy, M., Tal, M., and Volokita, M. (2004). Salinity up-regulates the antioxidative system in root mitochondria and peroxisomes of the wild salt-tolerant tomato species Lycopersicon pennellii. J. Exp. Bot. 55, 1105–1113.

Mittova, V., Tal, M., Volokita, M., and Guy, M. (2003). Up-regulation of the leaf mitochondrial and peroxisomal antioxidative systems in response to salt-induced oxidative stress in the wild salt-tolerant tomato species Lycopersicon pennellii. Plant Cell Environ. 26, 845–856.

Mizutani, A., Yukioka, H., Tamura, H., Miki, N., Masuko, M., and Takeda, R. (1995). Respiratory characteristics in Pyricularia oryzae exposed to a novel alkoxyiminoacetamide fungicide. Phytopathology 85, 306–311.

Moczko, M., Bömer, U., Kübrich, M., Zufall, N., Hönlinger, A., and Pfanner, N. (1997). The intermembrane space domain of mitochondrial Tom22 functions as a trans binding site for preproteins with N-terminal targeting sequences. Mol. Cell. Biol. 17, 6574–6584.

Möglich, A., Ayers, R.A., and Moffat, K. (2009). Structure and Signaling Mechanism of Per-ARNT-Sim Domains. Struct. Lond. Engl. 1993 17, 1282–1294.

Moignard, V., Woodhouse, S., Haghverdi, L., Lilly, A.J., Tanaka, Y., Wilkinson, A.C., Buettner, F., Macaulay, I.C., Jawaid, W., Diamanti, E., et al. (2015). Decoding the regulatory network of early blood development from single-cell gene expression measurements. Nature Biotechnology 33, 269.

Mokranjac, D., and Neupert, W. (2010). The many faces of the mitochondrial TIM23 complex. Biochim. Biophys. Acta BBA - Bioenerg. 1797, 1045–1054.

Moore, A.L., Shiba, T., Young, L., Harada, S., Kita, K., and Ito, K. (2013). Unraveling the heater: new insights into the structure of the alternative oxidase. Annu. Rev. Plant Biol. 64, 637–663.

Morris, A.J., and Malbon, C.C. (1999). Physiological regulation of G protein-linked signaling. Physiol. Rev. 79, 1373–1430.

Mossmann, D., Meisinger, C., and Vögtle, F.-N. (2012). Processing of mitochondrial presequences. Biochimica et Biophysica Acta (BBA) - Gene Regulatory Mechanisms 1819, 1098–1106.

Müller, J.M., Milenkovic, D., Guiard, B., Pfanner, N., and Chacinska, A. (2008). Precursor Oxidation by Mia40 and Erv1 Promotes Vectorial Transport of Proteins into the Mitochondrial Intermembrane Space. Mol. Biol. Cell 19, 226–236.

Murcha, M.W., Kmiec, B., Kubiszewski-Jakubiak, S., Teixeira, P.F., Glaser, E., and Whelan, J. (2014). Protein import into plant mitochondria: signals, machinery, processing, and regulation. J.

Exp. Bot. 65, 6301–6335.

Nakamura, S., Takamura, T., Matsuzawa-Nagata, N., Takayama, H., Misu, H., Noda, H., Nabemoto, S., Kurita, S., Ota, T., Ando, H., et al. (2009). Palmitate induces insulin resistance in H4IIEC3 hepatocytes through reactive oxygen species produced by mitochondria. J. Biol. Chem. 284, 14809–14818.

Nargang, F.E., and Rapaport, D. (2007). Neurospora crassa as a model organism for mitochondrial biogenesis. Methods Mol. Biol. *372*, 107–123.

Nargund, A.M., Fiorese, C.J., Pellegrino, M.W., Deng, P., and Haynes, C.M. (2015). Mitochondrial and nuclear accumulation of the transcription factor ATFS-1 promotes OXPHOS recovery during the UPR(mt). Mol. Cell 58, 123–133.

Nargund, A.M., Pellegrino, M.W., Fiorese, C.J., Baker, B.M., and Haynes, C.M. (2012). Mitochondrial import efficiency of ATFS-1 regulates mitochondrial UPR activation. Science 337, 587–590.

Nasmyth, K., and Haering, C.H. (2005). The structure and function of SMC and kleisin complexes. Annu. Rev. Biochem. *74*, 595–648.

Neimanis, K., Staples, J.F., Hüner, N.P.A., and McDonald, A.E. (2013). Identification, expression, and taxonomic distribution of alternative oxidases in non-angiosperm plants. Gene 526, 275–286.

Neupert, W. (2015). A perspective on transport of proteins into mitochondria: a myriad of open questions. J. Mol. Biol. 427, 1135–1158.

Neves, S.R., Ram, P.T., and Iyengar, R. (2002). G protein pathways. Science 296, 1636–1639.

Newman, J.R.S., Ghaemmaghami, S., Ihmels, J., Breslow, D.K., Noble, M., DeRisi, J.L., and Weissman, J.S. (2006). Single-cell proteomic analysis of S. cerevisiae reveals the architecture of biological noise. Nature 441, 840–846.

Ng, S., Clercq, I.D., Aken, O.V., Law, S.R., Ivanova, A., Willems, P., Giraud, E., Breusegem, F.V., and Whelan, J. (2014). Anterograde and Retrograde Regulation of Nuclear Genes Encoding Mitochondrial Proteins During Growth, Development and Stress. Mol. Plant ssu037.

Ng, S., Giraud, E., Duncan, O., Law, S.R., Wang, Y., Xu, L., Narsai, R., Carrie, C., Walker, H., Day, D.A., et al. (2013a). Cyclin-dependent Kinase E1 (CDKE1) Provides a Cellular Switch in Plants between Growth and Stress Responses. J. Biol. Chem. 288, 3449–3459.

Ng, S., Ivanova, A., Duncan, O., Law, S.R., Aken, O.V., Clercq, I.D., Wang, Y., Carrie, C., Xu, L., Kmiec, B., et al. (2013b). A Membrane-Bound NAC Transcription Factor, ANAC017, Mediates Mitochondrial Retrograde Signaling in Arabidopsis. The Plant Cell 25, 3450–3471.

Niyazov, D.M., Kahler, S.G., and Frye, R.E. (2016). Primary Mitochondrial Disease and Secondary Mitochondrial Dysfunction: Importance of Distinction for Diagnosis and Treatment. Mol. Syndromol. 7, 122–137.

Noctor, G., De Paepe, R., and Foyer, C.H. (2007). Mitochondrial redox biology and homeostasis in plants. Trends in Plant Science 12, 125–134.

Nosek, J., Dinoul, N., Kovac, L., and Fukuhara, H. (1995). Linear mitochondrial DNAs from yeasts: telomeres with large tandem repetitions. MGG Molecular & General Genetics 247, 61–72.

Noubissi, F.K., Nikiforov, M.A., Colburn, N., and Spiegelman, V.S. (2010). Transcriptional Regulation of CRD-BP by c-myc. Genes Cancer 1, 1074–1082.

Nuruzzaman, M., Sharoni, A.M., Satoh, K., Karim, M.R., Harikrishna, J.A., Shimizu, T., Sasaya, T., Oomura, T., Haque, M.A., and Kikuchi, S. (2015). NAC transcription factor family genes are differentially expressed in rice during infections with Rice dwarf virus, Rice black-streaked dwarf virus, Rice grassy stunt virus, Rice ragged stunt virus, and Rice transitory yellowing virus. Front. Plant Sci. 6.

Oliva, G., Sahr, T., and Buchrieser, C. (2015). Small RNAs, 5′ UTR elements and RNA-binding proteins in intracellular bacteria: impact on metabolism and virulence. FEMS Microbiol. Rev. 39, 331–349.

Oliveira, C., Faoro, H., Alves, L.R., and Goldenberg, S. (2017). RNA-binding proteins and their role in the regulation of gene expression in Trypanosoma cruzi and Saccharomyces cerevisiae. Genet. Mol. Biol. 40, 22–30.

Opalińska, M., and Meisinger, C. (2015). Metabolic control via the mitochondrial protein import machinery. Curr. Opin. Cell Biol. 33, 42–48.

Otero, J.M., Vongsangnak, W., Asadollahi, M.A., Olivares-Hernandes, R., Maury, J., Farinelli, L., Barlocher, L., Østerås, M., Schalk, M., Clark, A., et al. (2010). Whole genome sequencing of Saccharomyces cerevisiae: from genotype to phenotype for improved metabolic engineering applications. BMC Genomics 11, 723.

Palade, G.E. (1952). The fine structure of mitochondria. Anat. Rec. 114, 427–451.

Palade, G.E. (1953). An electron microscope study of the mitochondrial structure. J. Histochem. Cytochem. 1, 188–211.

Parikh, V.S., Morgan, M.M., Scott, R., Clements, L.S., and Butow, R.A. (1987). The mitochondrial genotype can influence nuclear gene expression in yeast. Science 235, 576–580.

Parsons, H.L., Yip, J.Y.H., and Vanlerberghe, G.C. (1999). Increased Respiratory Restriction during Phosphate-Limited Growth in Transgenic Tobacco Cells Lacking Alternative Oxidase.

Plant Physiol. 121, 1309–1320.

Paschen, S.A., Waizenegger, T., Stan, T., Preuss, M., Cyrklaff, M., Hell, K., Rapaport, D., and Neupert, W. (2003). Evolutionary conservation of biogenesis of β-barrel membrane proteins. Nature 426, 862–866.

Payne, B.A.I., and Chinnery, P.F. (2015). Mitochondrial dysfunction in aging: Much progress but many unresolved questions. Biochim. Biophys. Acta 1847, 1347–1353.

Pett, W., Ryan, J.F., Pang, K., Mullikin, J.C., Martindale, M.Q., Baxevanis, A.D., and Lavrov, D.V. (2011). Extreme mitochondrial evolution in the ctenophore Mnemiopsis leidyi : Insight from mtDNA and the nuclear genome. Mitochondrial DNA 22, 130–142.

Pfanner, N., van der Laan, M., Amati, P., Capaldi, R.A., Caudy, A.A., Chacinska, A., Darshi, M., Deckers, M., Hoppins, S., Icho, T., et al. (2014). Uniform nomenclature for the mitochondrial contact site and cristae organizing system. J. Cell Biol. 204, 1083–1086.

Planchet, E., Jagadis Gupta, K., Sonoda, M., and Kaiser, W.M. (2005). Nitric oxide emission from tobacco leaves and cell suspensions: rate limiting factors and evidence for the involvement of mitochondrial electron transport. Plant J. 41, 732–743.

Plesofsky, N., and Brambl, R. (1999). Glucose metabolism in Neurospora is altered by heat shock and by disruption of HSP30. Biochim. Biophys. Acta 1449, 73–82.

Pon, L., Moll, T., Vestweber, D., Marshallsay, B., and Schatz, G. (1989). Protein import into mitochondria: ATP-dependent protein translocation activity in a submitochondrial fraction enriched in membrane contact sites and specific proteins. J. Cell Biol. 109, 2603–2616.

Popov-Čeleketić, J., Waizenegger, T., and Rapaport, D. (2008). Mim1 Functions in an Oligomeric Form to Facilitate the Integration of Tom20 into the Mitochondrial Outer Membrane. Journal of Molecular Biology 376, 671–680.

Pritchard, A.E., Seilhamer, J.J., Mahalingam, R., Sable, C.L., Venuti, S.E., and Cummings, D.J. (1990). Nucleotide sequence of the mitochondrial genome of Paramecium. Nucleic Acids Research 18, 173–180.

Qi, Z., Smith, K.M., Bredeweg, E.L., Bosnjak, N., Freitag, M., and Nargang, F.E. (2016). Alternative Oxidase Transcription Factors AOD2 and AOD5 of Neurospora crassa Control the Expression of Genes Involved in Energy Production and Metabolism. G3 g3.116.035402.

Qureshi, M.A.M.H., Haynes, C.M., and Pellegrino, M.W. (2017). The mitochondrial unfolded protein response: signaling from the powerhouse. J. Biol. Chem. jbc.R117.791061.

Raineri, I., Wegmueller, D., Gross, B., Certa, U., and Moroni, C. (2004). Roles of AUF1 isoforms, HuR and BRF1 in ARE-dependent mRNA turnover studied by RNA interference. Nucleic Acids Res. 32, 1279–1288.

Rao, S., Schmidt, O., Harbauer, A.B., Schönfisch, B., Guiard, B., Pfanner, N., and Meisinger, C. (2012). Biogenesis of the preprotein translocase of the outer mitochondrial membrane: protein kinase A phosphorylates the precursor of Tom40 and impairs its import. Mol. Biol. Cell 23, 1618–1627.

Rassow, J., Guiard, B., Wienhues, U., Herzog, V., Hartl, F.U., and Neupert, W. (1989). Translocation arrest by reversible folding of a precursor protein imported into mitochondria. A means to quantitate translocation contact sites. J. Cell Biol. 109, 1421–1428.

Ray, P.D., Huang, B.-W., and Tsuji, Y. (2012). Reactive oxygen species (ROS) homeostasis and redox regulation in cellular signaling. Cell. Signal. 24, 981–990.

Rhoads, D.M., and McIntosh, L. (1992). Salicylic Acid Regulation of Respiration in Higher Plants: Alternative Oxidase Expression. Plant Cell 4, 1131–1139.

Rhoads, D.M., Umbach, A.L., Sweet, C.R., Lennon, A.M., Rauch, G.S., and Siedow, J.N. (1998). Regulation of the cyanide-resistant alternative oxidase of plant mitochondria. Identification of the cysteine residue involved in alpha-keto acid stimulation and intersubunit disulfide bond formation. J. Biol. Chem. 273, 30750–30756.

Ribas-Carbo, M., Aroca, R., Gonzàlez-Meler, M.A., Irigoyen, J.J., and Sánchez-Díaz, M. (2000). The Electron Partitioning between the Cytochrome and Alternative Respiratory Pathways during Chilling Recovery in Two Cultivars of Maize Differing in Chilling Sensitivity. Plant Physiology 122, 199–204.

Roberts, C.W., Roberts, F., Henriquez, F.L., Akiyoshi, D., Samuel, B.U., Richards, T.A., Milhous, W., Kyle, D., McIntosh, L., Hill, G.C., et al. (2004). Evidence for mitochondrial-derived alternative oxidase in the apicomplexan parasite Cryptosporidium parvum: a potential anti-microbial agent target. Int. J. Parasitol. 34, 297–308.

Roberts, S., Goetz, G., White, S., and Goetz, F. (2009). Analysis of Genes Isolated from Plated Hemocytes of the Pacific Oyster, Crassostreas gigas. Mar. Biotechnol. 11, 24–44.

Robinson, J.T., Thorvaldsdóttir, H., Winckler, W., Guttman, M., Lander, E.S., Getz, G., and Mesirov, J.P. (2011). Integrative genomics viewer. Nat. Biotechnol. *29*, 24–26.

Roger, A.J., Muñoz-Gómez, S.A., and Kamikawa, R. (2017). The Origin and Diversification of Mitochondria. Curr. Biol. 27, R1177–R1192.

Rogov, A.G., Sukhanova, E.I., Uralskaya, L.A., Aliverdieva, D.A., and Zvyagilskaya, R.A. (2014). Alternative oxidase: distribution, induction, properties, structure, regulation, and functions. Biochem. Biokhimiia 79, 1615–1634.

Ruepp, A., Zollner, A., Maier, D., Albermann, K., Hani, J., Mokrejs, M., Tetko, I., Güldener, U., Mannhaupt, G., Münsterkötter, M., et al. (2004). The FunCat, a functional annotation scheme for systematic classification of proteins from whole genomes. Nucleic Acids Res. 32, 5539–5545.

Ruiz-Roig, C., Noriega, N., Duch, A., Posas, F., and de Nadal, E. (2012). The Hog1 SAPK controls the Rtg1/Rtg3 transcriptional complex activity by multiple regulatory mechanisms. Mol Biol Cell 23, 4286–4296.

Ruiz, O.H., Gonzalez, A., Almeida, A.J., Tamayo, D., Garcia, A.M., Restrepo, A., and McEwen, J.G. (2011). Alternative Oxidase Mediates Pathogen Resistance in Paracoccidioides brasiliensis Infection. PLoS Negl. Trop. Dis. 5, e1353.

Rychter, A.M., and Mikulska, M. (1990). The relationship between phosphate status and cyanide-resistant respiration in bean roots. Physiol. Plant. 79, 663–667.

Saari, S., Andjelković, A., Garcia, G.S., Jacobs, H.T., and Oliveira, M.T. (2017). Expression of Ciona intestinalis AOX causes male reproductive defects in Drosophila melanogaster. BMC Dev Biol 17.

Saitoh, T., Igura, M., Obita, T., Ose, T., Kojima, R., Maenaka, K., Endo, T., and Kohda, D. (2007). Tom20 recognizes mitochondrial presequences through dynamic equilibrium among multiple bound states. EMBO J 26, 4777–4787.

Saitoh, T., Igura, M., Obita, T., Ose, T., Kojima, R., Maenaka, K., Endo, T., and Kohda, D. (2007). Tom20 recognizes mitochondrial presequences through dynamic equilibrium among multiple bound states. EMBO J. 26, 4777–4787.

Sambrook, J., and D. W. Russell, 2001 *Molecular Cloning: A laboratory manual*. Cold Spring Harbor Laboratory Press, Cold Spring Harbor, N.Y.

Schägger, H., and Pfeiffer, K. (2000). Supercomplexes in the respiratory chains of yeast and mammalian mitochondria. EMBO J. 19, 1777–1783.

Scheckhuber, C.Q., Houthoofd, K., Weil, A.C., Werner, A., De Vreese, A., Vanfleteren, J.R., and Osiewacz, H.D. (2011). Alternative oxidase dependent respiration leads to an increased mitochondrial content in two long-lived mutants of the aging model Podospora anserina. PLoS ONE 6, e16620.

Schertl, P., and Braun, H.-P. (2014). Respiratory electron transfer pathways in plant mitochondria. Front. Plant Sci. 5.

Schleyer, M., and Neupert, W. (1985). Transport of proteins into mitochondria: translocational intermediates spanning contact sites between outer and inner membranes. Cell 43, 339–350.

Schmid, K.J., Sorensen, T.R., Stracke, R., Torjek, O., Altmann, T., Mitchell-Olds, T., and Weisshaar, B. (2003). Large-scale identification and analysis of genome-wide single-nucleotide polymorphisms for mapping in Arabidopsis thaliana. Genome Res. 13, 1250–1257.

Schneider, W.M., Chevillotte, M.D., and Rice, C.M. (2014). Interferon-Stimulated Genes: A Complex Web of Host Defenses. Annu Rev Immunol 32, 513–545.

Schon, E.A., and Area-Gomez, E. (2013). Mitochondria-associated ER membranes in Alzheimer disease. Mol. Cell. Neurosci. 55, 26–36.

Schülke, N., Sepuri, N.B.V., and Pain, D. (1997). In vivo zippering of inner and outer mitochondrial membranes by a stable translocation intermediate. Proc Natl Acad Sci U S A 94, 7314–7319.

Schulz, A.M., and Haynes, C.M. (2015). UPR(mt)-mediated cytoprotection and organismal aging. Biochim. Biophys. Acta 1847, 1448–1456.

Schulz, C., Schendzielorz, A., and Rehling, P. (2015). Unlocking the presequence import pathway. Trends Cell Biol. 25, 265–275.

Schwaiger, M., Herzog, V., and Neupert, W. (1987). Characterization of translocation contact sites involved in the import of mitochondrial proteins. J. Cell Biol. 105, 235–246.

Sekito, T., Liu, Z., Thornton, J., and Butow, R.A. (2002). RTG-dependent mitochondria-to-nucleus signaling is regulated by MKS1 and is linked to formation of yeast prion [URE3]. Mol. Biol. Cell 13, 795–804.

Sekito, T., Thornton, J., and Butow, R.A. (2000). Mitochondria-to-nuclear signaling is regulated by the subcellular localization of the transcription factors Rtg1p and Rtg3p. Mol. Biol. Cell 11, 2103–2115.

Sellem, C.H., Bovier, E., Lorin, S., and Sainsard-Chanet, A. (2009). Mutations in Two Zinc-Cluster Proteins Activate Alternative Respiratory and Gluconeogenic Pathways and Restore Senescence in Long-Lived Respiratory Mutants of Podospora anserina. Genetics 182, 69–78.

Sena, L.A., and Chandel, N.S. (2012). Physiological roles of mitochondrial reactive oxygen species. Mol. Cell 48, 158–167.

Seo, J.-A., Han, K.-H., and Yu, J.-H. (2005). Multiple Roles of a Heterotrimeric G-Protein γ-Subunit in Governing Growth and Development of Aspergillus nidulans. Genetics 171, 81–89.

Setoguchi, K., Otera, H., and Mihara, K. (2006). Cytosolic factor- and TOM-independent import of C-tail-anchored mitochondrial outer membrane proteins. EMBO J 25, 5635–5647.

Shabalina, S.A., and Koonin, E.V. (2008). Origins and evolution of eukaryotic RNA interference. Trends Ecol. Evol. 23, 578–587.

Shiba, T., Kido, Y., Sakamoto, K., Inaoka, D.K., Tsuge, C., Tatsumi, R., Takahashi, G., Balogun, E.O., Nara, T., Aoki, T., et al. (2013). Structure of the trypanosome cyanide-insensitive alternative oxidase. Proc. Natl. Acad. Sci. U.S.A. 110, 4580–4585.

Sideris, D.P., Petrakis, N., Katrakili, N., Mikropoulou, D., Gallo, A., Ciofi-Baffoni, S., Banci, L., Bertini, I., and Tokatlidis, K. (2009). A novel intermembrane space-targeting signal docks cysteines onto Mia40 during mitochondrial oxidative folding. J. Cell Biol. 187, 1007–1022.

Sieger, S.M., Kristensen, B.K., Robson, C.A., Amirsadeghi, S., Eng, E.W.Y., Abdel-Mesih, A., Møller, I.M., and Vanlerberghe, G.C. (2005). The role of alternative oxidase in modulating carbon use efficiency and growth during macronutrient stress in tobacco cells. J. Exp. Bot. 56, 1499–1515.

Simpson, L. (1986). Kinetoplast DNA in trypanosomid flagellates. Int. Rev. Cytol. 99, 119–179.

Singh, G., Pachouri, U.C., Khaidem, D.C., Kundu, A., Chopra, C., and Singh, P. (2015). Mitochondrial DNA Damage and Diseases. F1000Research 4.

Sirrenberg, C., Endres, M., Fölsch, H., Stuart, R.A., Neupert, W., and Brunner, M. (1998). Carrier protein import into mitochondria mediated by the intermembrane proteins Tim10/Mrs11 and Tim12/Mrs5. Nature 391, 36136.

Smaili, S., Hirata, H., Ureshino, R., Monteforte, P.T., Morales, A.P., Muler, M.L., Terashima, J., Oseki, K., Rosenstock, T.R., Lopes, G.S., et al. (2009). Calcium and cell death signaling in neurodegeneration and aging. An. Acad. Bras. Cienc. 81, 467–475.

Smith, E.F., Shaw, P.J., and De Vos, K.J. (2017). The role of mitochondria in amyotrophic lateral sclerosis. Neurosci. Lett.

Spang, A., Saw, J.H., Jørgensen, S.L., Zaremba-Niedzwiedzka, K., Martijn, J., Lind, A.E., Eijk, R. van, Schleper, C., Guy, L., and Ettema, T.J.G. (2015). Complex archaea that bridge the gap between prokaryotes and eukaryotes. Nature 521, 173.

Squina, F.M., Leal, J., Cipriano, V.T.F., Martinez-Rossi, N.M., and Rossi, A. (2010). Transcription of the Neurospora crassa 70-kDa Class Heat Shock Protein Genes Is Modulated in Response to Extracellular pH Changes. Cell Stress & Chaperones 15, 225–231.

Stegle, O., Teichmann, S.A., and Marioni, J.C. (2015). Computational and analytical challenges in single-cell transcriptomics. Nat. Rev. Genet. 16, 133.

Stein, L.D., Mungall, C., Shu, S., Caudy, M., Mangone, M., Day, A., Nickerson, E., Stajich, J.E., Harris, T.W., Arva, A., et al. (2002). The Generic Genome Browser: A Building Block for a Model Organism System Database. Genome Res *12*, 1599–1610.

Stenmark, P., and Nordlund, P. (2003). A prokaryotic alternative oxidase present in the

bacterium Novosphingobium aromaticivorans. FEBS Lett. 552, 189–192.

Stojanovski, D., Bohnert, M., Pfanner, N., and van der Laan, M. (2012). Mechanisms of Protein Sorting in Mitochondria. Cold Spring Harb. Perspect. Biol. 4.

Stojanovski, D., Milenkovic, D., Müller, J.M., Gabriel, K., Schulze-Specking, A., Baker, M.J., Ryan, M.T., Guiard, B., Pfanner, N., and Chacinska, A. (2008). Mitochondrial protein import: precursor oxidation in a ternary complex with disulfide carrier and sulfhydryl oxidase. J. Cell Biol. 183, 195–202.

Stojanovski, D., Rissler, M., Pfanner, N., and Meisinger, C. (2006). Mitochondrial morphology and protein import—A tight connection? Biochimica et Biophysica Acta (BBA) - Molecular Cell Research 1763, 414–421.

Suyama, Y., Fukuhara, H., and Sor, F. (1985). A fine restriction map of the linear mitochondrial DNA of Tetrahyemena pyriformis: genome size, map locations of rRNA and tRNA genes, terminal inversion repeat, and restriction site polymorphism. Current Genetics 9, 479–493.

Suzuki, T., Nihei, C., Yabu, Y., Hashimoto, T., Suzuki, M., Yoshida, A., Nagai, K., Hosokawa, T., Minagawa, N., Suzuki, S., et al. (2004). Molecular cloning and characterization of Trypanosoma vivax alternative oxidase (AOX) gene, a target of the trypanocide ascofuranone. Parasitology International 53, 235–245.

Suzuki, Y., Murray, S.L., Wong, K.H., Davis, M.A., and Hynes, M.J. (2012). Reprogramming of carbon metabolism by the transcriptional activators AcuK and AcuM in Aspergillus nidulans. Mol. Microbiol. 84, 942–964.

Szibor, M., Dhandapani, P.K., Dufour, E., Holmström, K.M., Zhuang, Y., Salwig, I., Wittig, I., Heidler, J., Gizatullina, Z., Gainutdinov, T., et al. (2017). Broad AOX expression in a genetically tractable mouse model does not disturb normal physiology. Dis. Model. Mech. 10, 163–171.

Szostak, E., and Gebauer, F. (2013). Translational control by 3′-UTR-binding proteins. Brief. Funct. Genomics 12, 58–65.

Taanman, J.-W. (1999). The mitochondrial genome: structure, transcription, translation and replication. Biochim. Biophys. Acta BBA - Bioenerg. 1410, 103–123.

Taniguchi, K., Kajiyama, T., and Kambara, H. (2009). Quantitative analysis of gene expression in a single cell by qPCR. Nat. Methods 6, 503–506.

Tanton, L.L., Nargang, C.E., Kessler, K.E., Li, Q., and Nargang, F.E. (2003). Alternative oxidase expression in Neurospora crassa. Fungal Genetics and Biology 39, 176–190.

Taylor, A.B., Smith, B.S., Kitada, S., Kojima, K., Miyaura, H., Otwinowski, Z., Ito, A., and Deisenhofer, J. (2001). Crystal structures of mitochondrial processing peptidase reveal the mode for specific cleavage of import signal sequences. Structure 9, 615–625.

Thomazella, D.P.T., Teixeira, P.J.P.L., Oliveira, H.C., Saviani, E.E., Rincones, J., Toni, I.M., Reis, O., Garcia, O., Meinhardt, L.W., Salgado, I., et al. (2012). The hemibiotrophic cacao pathogen Moniliophthora perniciosa depends on a mitochondrial alternative oxidase for biotrophic development. New Phytol. 194, 1025–1034.

Thorvaldsdóttir, H., Robinson, J.T., and Mesirov, J.P. (2013). Integrative Genomics Viewer (IGV): high-performance genomics data visualization and exploration. Brief. Bioinformatics *14*, 178–192.

Tissieres, A., Mitchell, H.K., and Haskins, F.A. (1953). Studies on the respiratory system of the poky strain of Neurospora. J. Biol. Chem. 205, 423–433.

Towbin, H., Staehelin, T., and Gordon, J. (1979). Electrophoretic transfer of proteins from polyacrylamide gels to nitrocellulose sheets: procedure and some applications. Proc. Natl. Acad. Sci. U.S.A. *76*, 4350–4354.

Trifunovic, A., Wredenberg, A., Falkenberg, M., Spelbrink, J.N., Rovio, A.T., Bruder, C.E., Bohlooly-Y, M., Gidlöf, S., Oldfors, A., Wibom, R., et al. (2004). Premature ageing in mice expressing defective mitochondrial DNA polymerase. Nature 429, 417–423.

Truscott, K.N., Brandner, K., and Pfanner, N. (2003). Mechanisms of Protein Import into Mitochondria. Curr. Biol. 13, R326–R337.

Truscott, K.N., Wiedemann, N., Rehling, P., Müller, H., Meisinger, C., Pfanner, N., and Guiard, B. (2002). Mitochondrial import of the ADP/ATP carrier: the essential TIM complex of the intermembrane space is required for precursor release from the TOM complex. Mol. Cell. Biol. 22, 7780–7789.

Umbach, A.L., and Siedow, J.N. (1993). Covalent and Noncovalent Dimers of the Cyanide-Resistant Alternative Oxidase Protein in Higher Plant Mitochondria and Their Relationship to Enzyme Activity. Plant Physiol. 103, 845–854.

Umbach, A.L., Gonzàlez-Meler, M.A., Sweet, C.R., and Siedow, J.N. (2002). Activation of the plant mitochondrial alternative oxidase: insights from site-directed mutagenesis. Biochim. Biophys. Acta 1554, 118–128.

Umbach, A.L., Ng, V.S., and Siedow, J.N. (2006). Regulation of plant alternative oxidase activity: A tale of two cysteines. Biochim. Biophys. Acta BBA - Bioenerg. 1757, 135–142.

Valero, R.A., Senovilla, L., Núñez, L., and Villalobos, C. (2008). The role of mitochondrial potential in control of calcium signals involved in cell proliferation. Cell Calcium 44, 259–269.

Van Aken, O., Zhang, B., Law, S., Narsai, R., and Whelan, J. (2013). AtWRKY40 and AtWRKY63 modulate the expression of stress-responsive nuclear genes encoding mitochondrial and chloroplast proteins. Plant Physiol. 162, 254–271.

van der Laan, M., Meinecke, M., Dudek, J., Hutu, D.P., Lind, M., Perschil, I., Guiard, B., Wagner, R., Pfanner, N., and Rehling, P. (2007). Motor-free mitochondrial presequence translocase drives membrane integration of preproteins. Nat. Cell Biol. 9, 1152–1159.

Vance, J.E. (2014). MAM (mitochondria-associated membranes) in mammalian cells: Lipids and beyond. Biochimica et Biophysica Acta (BBA) - Molecular and Cell Biology of Lipids 1841, 595–609.

Vanlerberghe, G.C. (2013). Alternative Oxidase: A Mitochondrial Respiratory Pathway to Maintain Metabolic and Signaling Homeostasis during Abiotic and Biotic Stress in Plants. Int. J. Mol. Sci. 14, 6805–6847.

Vanlerberghe, G.C., and McIntosh, L. (1994). Mitochondrial electron transport regulation of nuclear gene expression. Studies with the alternative oxidase gene of tobacco. Plant Physiol 105, 867–874.

Vanlerberghe, G.C., McIntosh, L, and Yip (1998). Molecular localization of a redox-modulated process regulating plant mitochondrial electron transport. Plant Cell 10, 1551–1560.

Vázquez-Chantada, M., Fernández-Ramos, D., Embade, N., Martínez-Lopez, N., Varela-Rey, M., Woodhoo, A., Luka, Z., Wagner, C., Anglim, P.P., Finnell, R.H., et al. (2010). HuR/methyl-HuR and AUF1 regulate the MAT expressed during liver proliferation, differentiation, and carcinogenesis. Gastroenterology 138, 1943–1953.

Vidigal, J.A., and Ventura, A. (2015). The biological functions of miRNAs: lessons from in vivo studies. Trends Cell Biol. 25, 137–147.

Vogel, F., Bornhövd, C., Neupert, W., and Reichert, A.S. (2006). Dynamic subcompartmentalization of the mitochondrial inner membrane. J. Cell Biol. 175, 237–247.

Vögtle, F.-N., Wortelkamp, S., Zahedi, R.P., Becker, D., Leidhold, C., Gevaert, K., Kellermann, J., Voos, W., Sickmann, A., Pfanner, N., et al. (2009). Global Analysis of the Mitochondrial N-Proteome Identifies a Processing Peptidase Critical for Protein Stability. Cell 139, 428–439.

von der Malsburg, K., Müller, J.M., Bohnert, M., Oeljeklaus, S., Kwiatkowska, P., Becker, T., Loniewska-Lwowska, A., Wiese, S., Rao, S., Milenkovic, D., et al. (2011). Dual role of mitofilin in mitochondrial membrane organization and protein biogenesis. Dev. Cell 21, 694–707.

Vukotic, M., Oeljeklaus, S., Wiese, S., Vögtle, F.N., Meisinger, C., Meyer, H.E., Zieseniss, A., Katschinski, D.M., Jans, D.C., Jakobs, S., et al. (2012). Rcf1 Mediates Cytochrome Oxidase Assembly and Respirasome Formation, Revealing Heterogeneity of the Enzyme Complex. Cell Metabolism 15, 336–347.

Wai, T., and Langer, T. (2016). Mitochondrial Dynamics and Metabolic Regulation. Trends Endocrinol. Metab. 27, 105–117.

Wang, Y., Baskerville, S., Shenoy, A., Babiarz, J.E., Baehner, L., and Blelloch, R. (2008). Embryonic stem cell-specific microRNAs regulate the G1-S transition and promote rapid proliferation. Nat. Genet. 40, 1478–1483.

Wang, J., Rajakulendran, N., Amirsadeghi, S., and Vanlerberghe, G.C. (2011). Impact of mitochondrial alternative oxidase expression on the response of Nicotiana tabacum to cold temperature. Physiol Plant 142, 339–351.

Watling, J.R., Grant, N.M., Miller, R.E., and Robinson, S.A. (2008). Mechanisms of thermoregulation in plants. Plant Signal Behav 3, 595–597.

Weidner, U., Geier, S., Ptock, A., Friedrich, T., Leif, H., and Weiss, H. (1993). The gene locus of the proton-translocating NADH: ubiquinone oxidoreductase in Escherichia coli. Organization of the 14 genes and relationship between the derived proteins and subunits of mitochondrial complex I. J. Mol. Biol. 233, 109–122.

Weiss, H., von Jagow, G., Klingenberg, M., and Bücher, T. (1970). Characterization of Neurospora crassa Mitochondria Prepared with a Grind-Mill. European Journal of Biochemistry 14, 75–82.

Wendland, J., K.B. Lengeler, and E. Kothe (1996) "An instant preparation method for nucleic acids of filamentous fungi," *Fungal Genetics Reports*: Vol. 43, Article 23.

West, A.P., Khoury-Hanold, W., Staron, M., Tal, M.C., Pineda, C.M., Lang, S.M., Bestwick, M., Duguay, B.A., Raimundo, N., MacDuff, D.A., et al. (2015). Mitochondrial DNA stress primes the antiviral innate immune response. Nature 520, nature14156.

Wiedemann, N., and Pfanner, N. (2017). Mitochondrial Machineries for Protein Import and Assembly. Annu. Rev. Biochem. 86, 685–714.

Wiedemann, N., Frazier, A.E., and Pfanner, N. (2004). The Protein Import Machinery of Mitochondria. J. Biol. Chem. 279, 14473–14476.

Wiedemann, N., Kozjak, V., Chacinska, A., Schönfisch, B., Rospert, S., Ryan, M.T., Pfanner, N., and Meisinger, C. (2003). Machinery for protein sorting and assembly in the mitochondrial outer membrane. Nature 424, 565–571.

Williams, K.P., Sobral, B.W., and Dickerman, A.W. (2007). A Robust Species Tree for the Alphaproteobacteria. J. Bacteriol. 189, 4578–4586.

Williams, T.A., Foster, P.G., Nye, T.M.W., Cox, C.J., and Embley, T.M. (2012). A congruent phylogenomic signal places eukaryotes within the Archaea. Proc R Soc B 279, 4870–4879.

Wilson, R.J., and Williamson, D.H. (1997). Extrachromosomal DNA in the Apicomplexa.

Microbiol. Mol. Biol. Rev. 61, 1–16.

Wimley, W.C. (2003). The versatile β-barrel membrane protein. Current Opinion in Structural Biology 13, 404–411.

Wollweber, F., von der Malsburg, K., and van der Laan, M. (2017). Mitochondrial contact site and cristae organizing system: A central player in membrane shaping and crosstalk. Biochim. Biophys. Acta 1864, 1481–1489.

Won, S., Michkov, A.V., Krystofova, S., Garud, A.V., and Borkovich, K.A. (2012). Genetic and physical interactions between Gα subunits and components of the Gβγ dimer of heterotrimeric G proteins in Neurospora crassa. Eukaryotic Cell *11*, 1239–1248.

Wright, G., Terada, K., Yano, M., Sergeev, I., and Mori, M. (2001). Oxidative stress inhibits the mitochondrial import of preproteins and leads to their degradation. Exp. Cell Res. 263, 107–117.

Wrobel, L., Sokol, A.M., Chojnacka, M., and Chacinska, A. (2016). The presence of disulfide bonds reveals an evolutionarily conserved mechanism involved in mitochondrial protein translocase assembly. Scientific Reports 6, 27484.

Wrobel, L., Topf, U., Bragoszewski, P., Wiese, S., Sztolsztener, M.E., Oeljeklaus, S., Varabyova, A., Lirski, M., Chroscicki, P., Mroczek, S., et al. (2015). Mistargeted mitochondrial proteins activate a proteostatic response in the cytosol. Nature 524, 485–488.

Xue, C., Hsueh, Y.-P., and Heitman, J. (2008). Magnificent seven: roles of G protein-coupled receptors in extracellular sensing in fungi. FEMS Microbiol. Rev. 32, 1010–1032.

Yaffe, M.P. (1999). The Machinery of Mitochondrial Inheritance and Behavior. Science 283, 1493–1497.

Yamamoto, Y., Kobayashi, Y., Devi, S.R., Rikiishi, S., and Matsumoto, H. (2002). Aluminum Toxicity Is Associated with Mitochondrial Dysfunction and the Production of Reactive Oxygen Species in Plant Cells. Plant Physiology 128, 63–72.

Yang, Q., Li, L., Xue, Z., Ye, Q., Zhang, L., Li, S., and Liu, Y. (2013). Transcription of the major neurospora crassa microRNA-like small RNAs relies on RNA polymerase III. PLoS Genet. 9, e1003227.

Young, J.C., Hoogenraad, N.J., and Hartl, F.U. (2003). Molecular Chaperones Hsp90 and Hsp70 Deliver Preproteins to the Mitochondrial Import Receptor Tom70. Cell 112, 41–50.

Yu, J.-H., Mah, J.-H., and Seo, J.-A. (2006). Growth and Developmental Control in the Model and Pathogenic Aspergilli. Eukaryot Cell 5, 1577–1584.

Yu, J.H., Wieser, J., and Adams, T.H. (1996). The Aspergillus FlbA RGS domain protein antagonizes G protein signaling to block proliferation and allow development. EMBO J. 15,

5184–5190.

Yuen, K.C., and Gerton, J.L. (2018). Taking cohesin and condensin in context. PLOS Genetics *14*, e1007118.

Yukioka, H. (Shionogi and C.L., Inagaki, S., Tanaka, R., Katoh, K., Miki, N., Mizutani, A., and Masuko, M. (1998). Analysis of alternative oxidase gene in mutants of Magnaporthe grisea deficient in alternative, cyanide-resistant, respiration. Ann. Phytopathol. Soc. Jpn. Jpn.

Yukioka, H., Inagaki, S., Tanaka, R., Katoh, K., Miki, N., Mizutani, A., and Masuko, M. (1998). Transcriptional activation of the alternative oxidase gene of the fungus Magnaporthe grisea by a respiratory-inhibiting fungicide and hydrogen peroxide. Biochim. Biophys. Acta 1442, 161–169.

Zara, V., Ferramosca, A., Robitaille-Foucher, P., Palmieri, F., and Young, J.C. (2009). Mitochondrial carrier protein biogenesis: role of the chaperones Hsc70 and Hsp90. Biochemical Journal 419, 369–375.

Zaremba-Niedzwiedzka, K., Caceres, E.F., Saw, J.H., Bäckström, D., Juzokaite, L., Vancaester, E., Seitz, K.W., Anantharaman, K., Starnawski, P., Kjeldsen, K.U., et al. (2017). Asgard archaea illuminate the origin of eukaryotic cellular complexity. Nature 541, 353–358.

Zhao, Q., Wang, J., Levichkin, I.V., Stasinopoulos, S., Ryan, M.T., and Hoogenraad, N.J. (2002). A mitochondrial specific stress response in mammalian cells. EMBO J. 21, 4411–4419.

Zheng, W., Khrapko, K., Coller, H.A., Thilly, W.G., and Copeland, W.C. (2006). Origins of human mitochondrial point mutations as DNA polymerase gamma-mediated errors. Mutat. Res. 599, 11–20.

Zhuravel, D., Fraser, D., St-Pierre, S., Tepliakova, L., Pang, W.L., Hasty, J., and Kærn, M. (2010). Phenotypic impact of regulatory noise in cellular stress-response pathways. Syst Synth Biol 4, 105–116.

Zick, M., Rabl, R., and Reichert, A.S. (2009). Cristae formation-linking ultrastructure and function of mitochondria. Biochim. Biophys. Acta 1793, 5–19.

Zucconi, B.E., and Wilson, G.M. (2011). Modulation of neoplastic gene regulatory pathways by the RNA-binding factor AUF1. Front Biosci (Landmark Ed) 16, 2307–2325.

Appendix

5′ and 3′ UTR modification of *aod-1*

To examine the possibility that the 5′ and/or 3′ UTR of *aod-1* transcripts were involved in translational control, I replaced 100 bp of the *aod-1* 5′UTR sequence with 60 bp of the *N. crassa porin* 5′UTR and 150 bp of the *aod-1* 3′UTR with 200 bp of the *N. crassa β-tubulin* 3′UTR sequence. *β-tubulin* UTRs have been used to replace other UTRs in similar studies (Merritt et al., 2008). The replacements should eliminate any binding sites either for a positive or negative regulatory factor that may be present in the native *aod-1* UTRs. Thus, I would expect that there would be detectable AOD1 protein in -CM conditions in those strains that produce *aod-1* mRNA in non-inducing conditions. The constructs would be inserted randomly into the genome of strain T1P11 and the resident *aod-1* gene would remain.

To differentiate between AOD1 protein produced from the native or modified *aod-1* gene, I designed the UTR-modified constructs to encode an AOD1 protein with a triple HA tag. As a control, I also designed an *aod-1* gene with its native UTRs and a triple HA tag. The constructs were synthesized by BioBasic Inc (Markham, Ontario) and are shown in Appendix Fig. 1. The modified and native *aod-1* constructs were subcloned by BioBasic into a kanamycin resistant plasmid, pUC57, and then sent to the Nargang lab for further manipulation and analysis. The *aod-1* constructs were amplified by PCR primers containing *Hin*dIII and *Not*I sites. The pCSN44 hygromycin and ampicillin resistant plasmid (Staben et al., 1989) was digested with *Hin*dIII and *Not*I, the 5′ ends were dephosphorylated, ligated to the digested amplified PCR product, and transformed into *E. coli* XL Gold Competent cells (Appendix Fig. 2). Transformants were plated on ampicillin-containing LB agar plates. Plasmids were isolated, digested with *Hin*dIII, and checked for the desired size on an agarose gel. The plasmids were

A.

CGTCACAGCAAAGTTAGAAGTTTAACATGAAGCCATTCGCAACTTATGGC
CCAAGACATTTGTTTGTATATTTGCAGGTTCGGAAGCAACCAAGCCATTGCTCAGTCATG
CTGTGTGTCCTATGAGAACAAGTGCGACTGGTGTTCCGTTTCCCTCCGCTCGCTATTACT
GTCAGCAAAATCTCCAACACATAACTCGCCCAAGTGCCCTGTCAACCAACCAACCAACTA
TCAATGATCTCGAAATCTCCTGTGGCTGTCTTTGTGTTGAGTCACAATCCCCCAGTCTTA
GTGTACTTGCTCAGGGGCTCGCTGTTCTTCTGGATATGTACAAGGCTAATCCCGAGAATG
TTGCGGAAGTGGAACTGCGCCCTATGGCTTGTCACCCGGGAGGTCCCGACACCGCCAAAC
AACGACATCCAGCTGACCACCACAATCGATGCCCGGTTGCCACTTTGAGGATTCAAAATG
AAATTTTGTCCTGGTTGAAGATCTGGAGCTTTCCGGGTTCCTTTCGCTAGCGCCCGCTAT
TTGCTTGTTCCTGGATTGTCTTGATGTTAAAAAATGGAGATTGCTTGGGCAGTGTCGGAA
CTCTATTGCTCCTTTGAGACCAGGGACGGACAAACTCGGTGTTTTCAGTCAGCTCTCGTA
TTCCAAATTTTTCCCTGAAAGGAGTTGCAACTGGGGGCAGGAAAGGACGATATAAACGTC
CCGTGTCTAGTGCTGTCCGACACATATGGACCATCATCACAAACCTCAAGCGAGTTCCAT
TACAACTTCACATCACTCCCTAAACTCTCGATGAACACCCC ... ...
GGATTTGAAAGGGCGGAGGTCATCGGTTACCCCTACGACGTCCCCGACTACGCCTACCCC
TACGACGTCCCCGACTACGCCTACCCCTACGACGTCCCCGACTACGCCTGAtcttgggcg
gaaggtcttgacagatggttgtggtttgggttcatgaagccaggcgtttttggaccaagt
tgttgtattatgcgtgttacactagatacccccccactctctttgctgtttctggcgtttt
ggtaaaaaagatactgggttc

B.

CGTCACAGCAAAGTTAGAAGTTTAACATGAAGCCATTCGCAACTTATGGC
CCAAGACATTTGTTTGTATATTTGCAGGTTCGGAAGCAACCAAGCCATTGCTCAGTCATG
CTGTGTGTCCTATGAGAACAAGTGCGACTGGTGTTCCGTTTCCCTCCGCTCGCTATTACT
GTCAGCAAAATCTCCAACACATAACTCGCCCAAGTGCCCTGTCAACCAACCAACCAACTA
TCAATGATCTCGAAATCTCCTGTGGCTGTCTTTGTGTTGAGTCACAATCCCCCAGTCTTA
GTGTACTTGCTCAGGGGCTCGCTGTTCTTCTGGATATGTACAAGGCTAATCCCGAGAATG
TTGCGGAAGTGGAACTGCGCCCTATGGCTTGTCACCCGGGAGGTCCCGACACCGCCAAAC
AACGACATCCAGCTGACCACCACAATCGATGCCCGGTTGCCACTTTGAGGATTCAAAATG
AAATTTTGTCCTGGTTGAAGATCTGGAGCTTTCCGGGTTCCTTTCGCTAGCGCCCGCTAT
TTGCTTGTTCCTGGATTGTCTTGATGTTAAAAAATGGAGATTGCTTGGGCAGTGTCGGAA
CTCTATTGCTCCTTTGAGACCAGGGACGGACAAACTCGGTGTTTTCAGTCAGCTCTCGTA
TTCCAAATTTTTCCCTGAAAGGAGTTGCAACTGGGGGCAGGAAAGGACGATATAAACGTC
CCGTGTCTAGTGCTGTCCGACACATATGGAcaacctcactttctccattca
ccatcatacccgtgtcgccctcacacaacatctttcacaATGAACACCCC ... ...
GGATTTGAAAGGGCGGAGGTCATCGGTTACCCCTACGACGTCCCCGACTACGCCTACCCC
TACGACGTCCCCGACTACGCCTACCCCTACGACGTCCCCGACTACGCCTGAtcttgggcg
gaaggtcttgacagatggttgtggtttgggttcatgaagccaggcgtttttggaccaagt
tgttgtattatgcgtgttacactagatacccccccactctctttgctgtttctggcgtttt
ggtaaaaaagatactgggttc

C.

CGTCACAGCAAAGTTAGAAGTTTAACATGAAGCCATTCGCAACTTATGGC
CCAAGACATTTGTTTGTATATTTGCAGGTTCGGAAGCAACCAAGCCATTGCTCAGTCATG
CTGTGTGTCCTATGAGAACAAGTGCGACTGGTGTTCCGTTTCCCTCCGCTCGCTATTACT
GTCAGCAAAATCTCCAACACATAACTCGCCCAAGTGCCCTGTCAACCAACCAACCAACTA
TCAATGATCTCGAAATCTCCTGTGGCTGTCTTTGTGTTGAGTCACAATCCCCCAGTCTTA
GTGTACTTGCTCAGGGGCTCGCTGTTCTTCTGGATATGTACAAGGCTAATCCCGAGAATG
TTGCGGAAGTGGAACTGCGCCCTATGGCTTGTCACCCGGGAGGTCCCGACACCGCCAAAC
AACGACATCCAGCTGACCACCACAATCGATGCCCGGTTGCCACTTTGAGGATTCAAAATG
AAATTTTGTCCTGGTTGAAGATCTGGAGCTTTCCGGGTTCCTTTCGCTAGCGCCCGCTAT
TTGCTTGTTCCTGGATTGTCTTGATGTTAAAAAATGGAGATTGCTTGGGCAGTGTCGGAA
CTCTATTGCTCCTTTGAGACCAGGGACGGACAAACTCGGTGTTTTCAGTCAGCTCTCGTA
TTCCAAATTTTTCCCTGAAAGGAGTTGCAACTGGGGGCAGGAAAGGACGATATAAACGTC
CCGTGTCTAGTGCTGTCCGACACATATGGACCATCATCACAAACCTCAAGCGAGTTCCAT
TACAACTTCACATCACTCCCTAAACTCTCGATGAACACCCC ... ...
GGATTTGAAAGGGCGGAGGTCATCGGTTACCCCTACGACGTCCCCGACTACGCCTACCCC
TACGACGTCCCCGACTACGCCTACCCCTACGACGTCCCCGACTACGCCTGA
atcattccactcaacattcaggctcctctgcgcacgtaaagtgccaaaggcaataccctgc
tcggtggaatgccgccgggcttgtcgattttacgcacatatgcgcattcttgacttgaagc
ggaggagttcttcgttgcgggttacagtgttttaataaaagaatggtcaaatcaaactgct
agatatacctgtcagac

Appendix Figure 1. Synthetic genes synthesized by BioBasic (Markham, Ontario) for subcloning. For all panels, the triple HA tag is highlighted in gray, the start codon is highlighted in green, and the stop codon is highlighted in red. The coding sequence is not fully shown and is represented with periods (…) shortly after the start codon. The native 5′UTR region is highlighted in turquoise, while the native 3′UTR region is highlighted in yellow. **A.** Unmodified native 3′ and 5′UTR of *aod-1* with triple HA tag. **B.** Triple HA-tagged *aod-1* modified with 5′UTR of porin. The native 5′UTR region is replaced with 60 bp of the 5′UTR of the *N. crassa* porin gene (lower case blue). **C.** Triple HA-tagged *aod-1* modified with *β-tubulin*. The native 3′UTR region is replaced with 200 bp of the 3′UTR of the *N. crassa β-tubulin* gene shown in lower case blue font.

A.

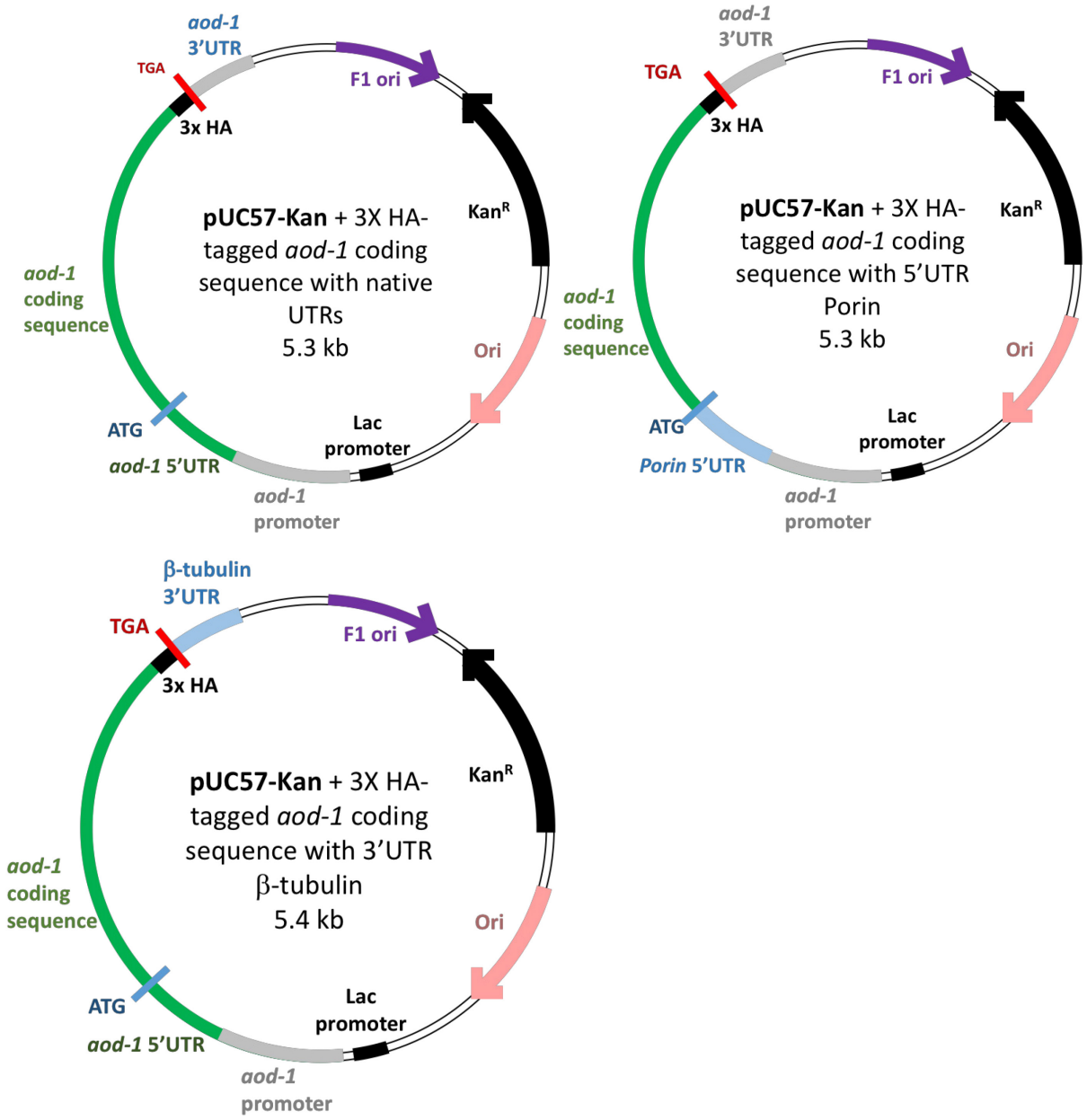
aod-1 3'UTR
TGA
3x HA
F1 ori
Kan^R
pUC57-Kan + 3X HA-tagged aod-1 coding sequence with native UTRs 5.3 kb
aod-1 coding sequence
Ori
ATG
Lac promoter
aod-1 5'UTR
aod-1 promoter
aod-1 3'UTR
TGA
3x HA
F1 ori
Kan^R
pUC57-Kan + 3X HA-tagged aod-1 coding sequence with 5'UTR Porin 5.3 kb
aod-1 coding sequence
Ori
ATG
Lac promoter
Porin 5'UTR
aod-1 promoter
β-tubulin 3'UTR
TGA
3x HA
F1 ori
Kan^R
pUC57-Kan + 3X HA-tagged aod-1 coding sequence with 3'UTR β-tubulin 5.4 kb
aod-1 coding sequence
Ori
ATG
Lac promoter
aod-1 5'UTR
aod-1 promoter

B.

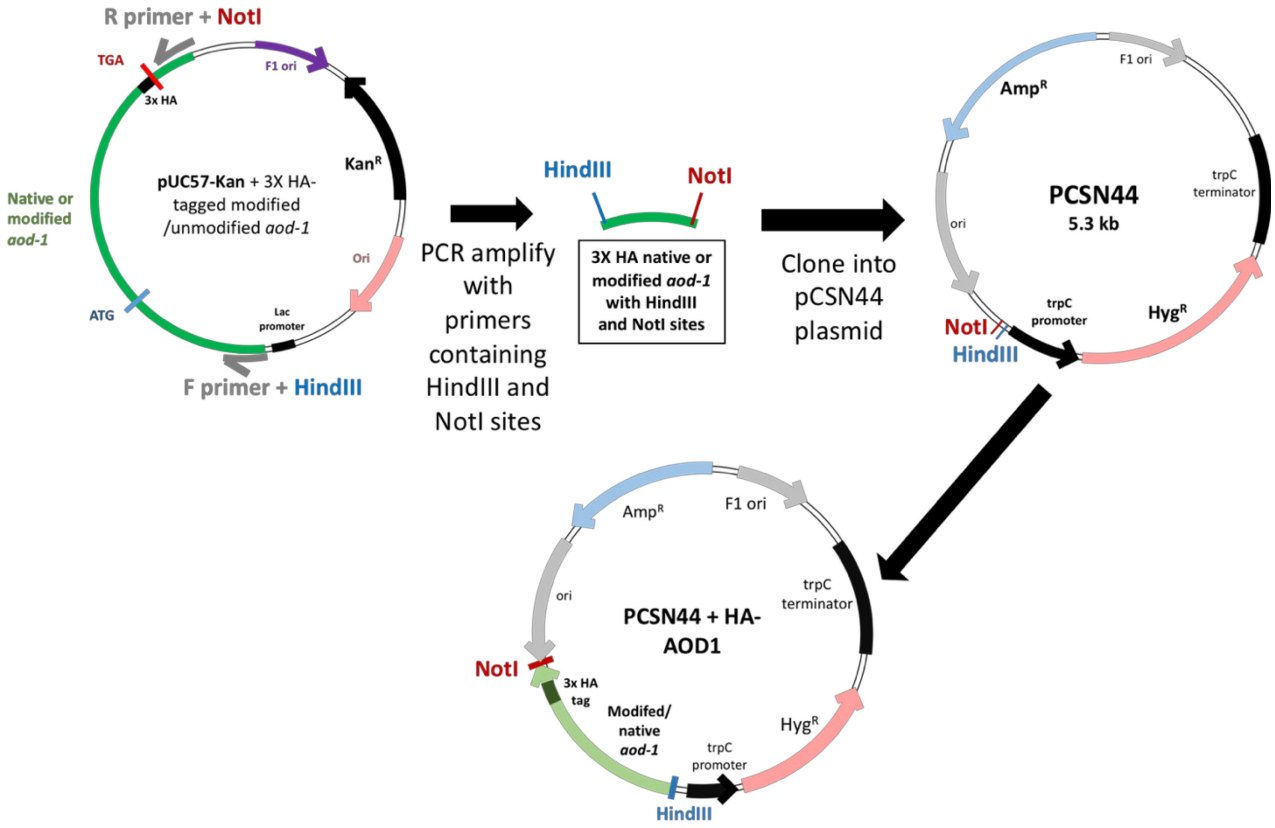
R primer + NotI
TGA
F1 ori
3x HA
Kan^R
pUC57-Kan + 3X HA-tagged modified /unmodified aod-1
Native or modified aod-1
Ori
ATG
Lac promoter
F primer + HindIII
PCR amplify with primers containing HindIII and NotI sites
HindIII
NotI
3X HA native or modified aod-1 with HindIII and NotI sites
Clone into pCSN44 plasmid
Amp^R
F1 ori
PCSN44
5.3 kb
trpC terminator
ori
trpC promoter
Hyg^R
NotI
HindIII
Amp^R
F1 ori
ori
trpC terminator
PCSN44 + HA-AOD1
NotI
3x HA tag
Modifed/ native aod-1
Hyg^R
trpC promoter
HindIII

Appendix Figure 2. Strategy of transforming plasmid construction. **A)** Synthetic gene sequences (refer to Appendix Fig. 1) were synthesized by BioBasic Inc. (Markham, Ontario) and were cloned into the pUC57 plasmid with kanamycin resistance. The native *aod-1* sequence with the triple HA-tag was cloned into a *Stu*I and *Eco*RV site. The triple HA-tagged *aod-1* with the 5′UTR replaced by the 5′UTR sequence of porin was cloned into an *Eco*RV and *Sal*I site. The triple HA-tagged *aod-1* with the 3′UTR replaced by the 3′UTR sequence of the β-tubulin was cloned into a *Sma*I site. **B)** The triple HA-tagged synthetic genes were PCR amplified from the pUC57-Kanamycin resistant plasmid with PCR primers (shown as arrows outside the top left plasmid circle) containing *Not*I and *Hind*III sites (only the *aod-1* sequence with native UTRs is shown as an example, but all three constructs from the plasmids shown in panel A were amplified and cloned as described below). The fragments were ligated into a *Not*I and *Hind*III digested pCSN44 plasmid that encodes ampicillin (Amp^R) and hygromycin (Hyg^R) resistance (Staben et al., 1989). XL10-Gold Ultracompetent *E. coli* cells were transformed with the ligation mixture and plated on LB + ampicillin plates. Colonies were isolated and grown in liquid LB + ampicillin. The plasmids were isolated, linearized, size checked via gel electrophoresis, and used to transform *N. crassa* conidia.

also sequenced as an additional measure to ensure that the final constructs were as designed. Prior to transforming *N. crassa* conidia, the plasmids were linearized to increase *N. crassa* transformation efficiency. T1P11 conidia were then electroporated with the linearized pCSN44 plasmid containing either the HA-tagged modified UTR constructs, or the native HA-tagged *aod-1* gene (summarized in Appendix Fig. 2). Electroporation was as described previously (Margolin et al., 1997, 2000; Tanton et al., 2003).

Ten isolates containing the 3′UTR modified construct (isolates 6, 8, 11, 12, 21, 34, 36, 38, 39 and 40), ten isolates containing the native HA-tagged AOD1 (isolates 10, 19, 24, 25, 26, 29, 30, 36, 40, 50) and 5 isolates containing the 5′UTR modification (1, 2, 8, 19, 31) were obtained based on their ability to grow on medium containing hygromycin. Since the transformation protocol results in random, and possibly incomplete integration of the entire construct into the genome, it was possible that some transformants took up only the hygromycin-resistant portion of the constructs. Therefore, the isolates were examined for expression of the HA tagged AOD1 protein. Strains were grown in liquid media containing CM and mitochondria were isolated. To confirm the presence or absence of the different *aod-1* constructs, Western blots were conducted on mitochondria from the isolates using an HA antibody. Six isolates of the 3′UTR modification (isolates 6, 8, 11, 12, 21, and 38), 2 isolates of the 5′UTR modification (isolates 1 and 2) and 5 isolates of the native HA-tagged AOD1 isolates (isolates 19, 24, 30, 40 and 50) were confirmed to contain the modified or native HA-tagged AOD1 (summarized in Appendix Table 1).

To determine if there was a difference in expression of AOD1 protein in the isolates containing the modified constructs as compared to strain T1P11, the six 3′UTR modified isolates (6, 8, 11, 12, 21 and 38) as well as two 5′UTR modified isolates (1 and 2) were grown in the absence of CM and examined by Western blot for AOD1 protein. If either the 5′ or 3′ *aod-1*

HA-tagged 3'UTR modified isolates	HA Construct	HA-tagged 5'UTR modified isolates	HA Construct	Native AOD1-HA isolates	HA Construct
6	Y	1	Y	10	N
8	Y	2	Y	19	Y
11	Y	8	N	24	Y
12	Y	19	N	25	N
21	Y	31	N	26	N
34	N			29	N
36	N			30	Y
38	Y			36	N
39	N			40	Y
40	N			50	Y

Appendix Table 1. List of isolates tested for presence or absence of HA-containing construct. T1P11 was transformed with constructs containing a hygromycin resistance marker and either a modified 3′UTR *aod-1* construct, a modified 5′UTR *aod-1* construct, or the native *aod-1* 5′ and 3′-UTR sequences. All constructs encoded a C-terminal 3X HA-tagged AOD1 protein. Isolates were grown in +CM containing media, and mitochondria were isolated. Western blots were performed for each isolate using an HA antibody to determine the presence or absence of the construct in each isolate. Y (yes) and N (no) indicate if an isolate expressed the HA-tagged AOD1 protein.

UTR sequence was bound by sequence-specific regulatory proteins that played a role in translational regulation of transcripts, I expected to see HA-tagged AOD1 protein in the –CM UTR-modified mitochondrial fractions. Western blot analysis was conducted on samples using both an HA antibody to detect the modified protein, as well as an AOX antibody to detect the native, untagged protein. The AOX antibody was expected to detect HA-tagged AOD1 protein as well, resulting in two bands migrating at slightly different molecular weights due to the extra 4.3 kb added by the triple HA tag.

As expected, since the endogenous *aod-1* gene was still present in all strains examined, the AOD1 antibody detected AOD1 protein in all isolates grown in the presence of CM (Appendix Fig. 3). Interestingly, all strains containing the 5′ and 3′UTR modified constructs (except the 3′-modified isolates 12 and 21) gave rise to detectable HA-tagged protein in the absence of CM (Appendix Fig. A, B). It is unclear why the AOD1 antibody did not detect the HA-tagged protein. Conceivably, the C-terminal HA-tag disrupts an epitope(s) for the antibody which was made to a C-terminal fragment of AOD1 (Tanton et al., 2003). The band seen in the transformants was not detected in NCN233 or T1P11 in either the presence or absence of CM. This observation makes it highly unlikely that the band seen in the constructs is a non-specific protein that reacts with the HA antibody.

At first glance, the above results seemed to support the involvement of both the 5′ and 3′UTRs in controlling translation of the *aod-1* mRNA. However, examination of the isolates expressing the HA-tagged AOD1 protein in the context of the native *aod-1* 5′ and 3′UTR sequences (Appendix Fig. 3 C) revealed a band of similar size in the mitochondria of these strains. Thus, the results for the modified constructs cannot be attributed to the altered 5′ and/or 3′UTRs.

A.

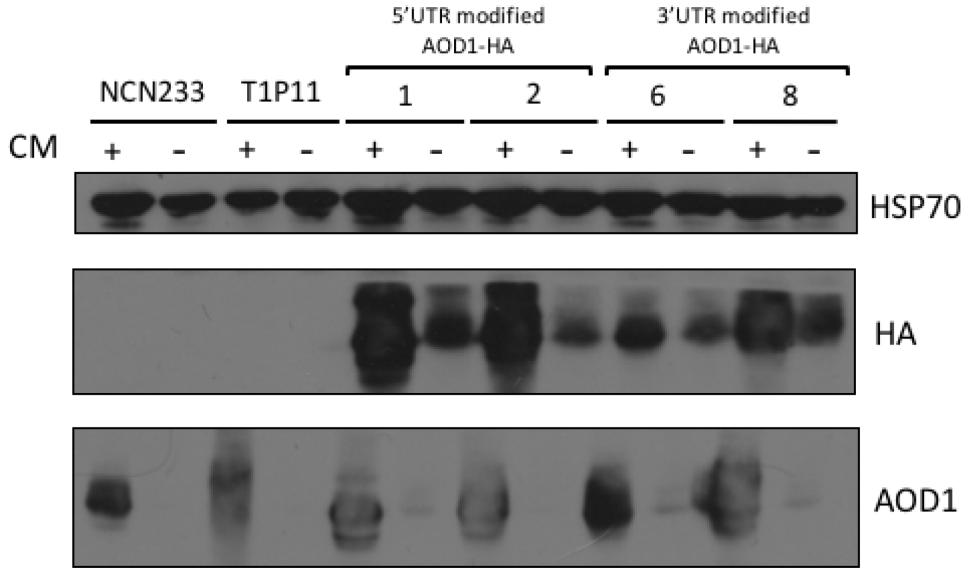
5'UTR modified AOD1-HA
3'UTR modified AOD1-HA
NCN233
T1P11
1
2
6
8
CM
+ - + - + - + - + - + -
HSP70
HA
AOD1

B.

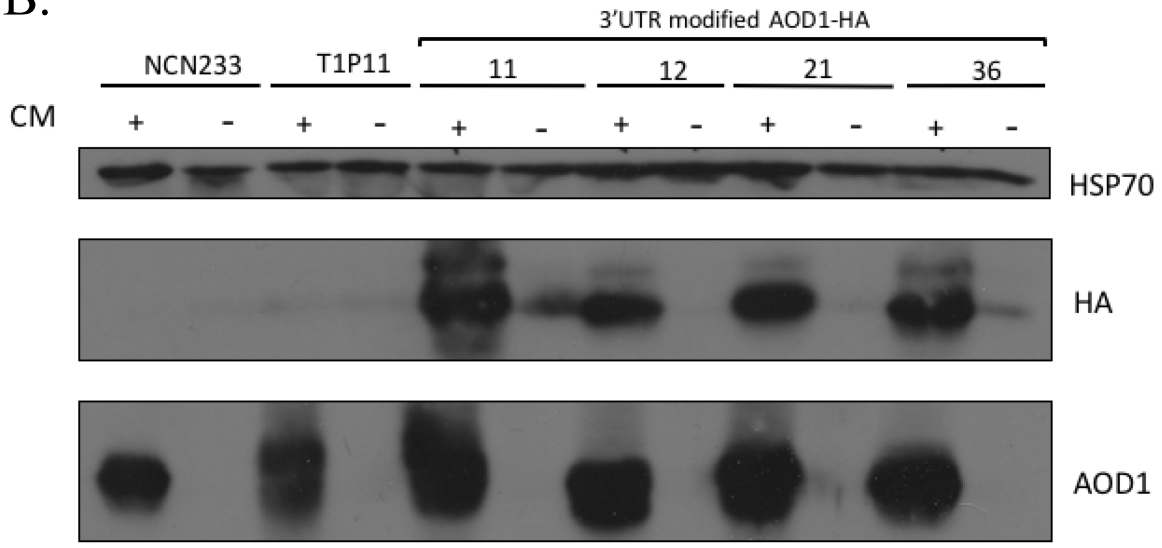
3'UTR modified AOD1-HA
NCN233
T1P11
11
12
21
36
CM
+ - + - + - + - + - + -
HSP70
HA
AOD1

C.

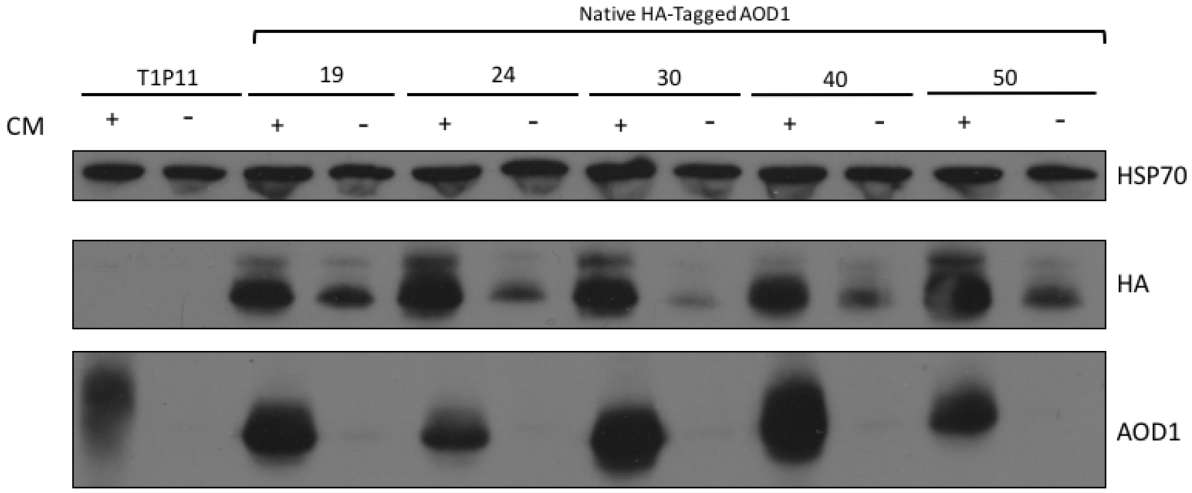

Appendix Figure 3. Western blot analysis of AOD1 proteins in UTR modified and native constructs expressed in strain T1P11. Cultures of wild-type NCN233, untransformed T1P11, and isolates of T1P11 transformed with the 5′UTR modified construct and the 3′UTR modified construct, and the native HA-tagged AOD1 protein constructs were grown in –CM conditions (-) for 16 hours, and +CM conditions (+) for 18 hours. Mitochondria were isolated and subjected to SDS-PAGE. Proteins were transferred to PVDF membrane and examined with antibodies shown on the right. The presence of the native, untagged and unmodified AOD1 protein was detected using an AOD1 antibody while the tagged version was detected with an HA antibody. Hsp70 served as a loading control. **A)** 5′UTR modified and 3′UTR modified isolates with HA-tagged AOD1 construct. **B)** 3′UTR modified isolates with HA-tagged AOD1 construct. **C)** Isolates with native 5′ and 3′UTR sequences with HA-tagged AOD1 construct.

In conclusion, the experiments described above did not allow conclusions about the role of the UTRs to be reached. Explanations for the data seen in the transformants containing the native UTRs with the HA-tagged AOD1 are not obvious. One possibility is that the sequence encoding the HA-tag at the 3′ end of the *aod-1* coding sequence interferes with a bonafide role of the 3′UTR in translational control. However, investigation into this possibility is beyond the scope of this thesis.

REFERENCES

Margolin, B., Freitag, M., and Selker, E. (1997). Improved plasmids for gene targeting at the his-3 locus of Neurospora crassa by electroporation. Fungal Genet. Rep. *44*, 34–36.

Margolin, B., Freitag, M., and Selker, E. (2000). Improved plasmids for gene targeting at the his-3 locus of Neurospora crassa by electroporation: Correction. Fungal Genet. Rep. *47*, 112.

Merritt, C., Rasoloson, D., Ko, D., and Seydoux, G. (2008). 3′ UTRs are the primary regulators of gene expression in the C. elegans germline. Curr. Biol. *18*, 1476–1482.

Staben, C., B. Jensen, M. Singer, J. Pollock, M. Schechtman, J. Kinsey, and E. Selker. 1989. Use of a bacterial Hygromycin B resistance gene as a dominant selectable marker in Neurospora crassa transformation. Fungal Genet Newslet. 36:79-81.

Tanton, L.L., Nargang, C.E., Kessler, K.E., Li, Q., and Nargang, F.E. (2003). Alternative oxidase expression in Neurospora crassa. Fungal Genet. Biol. *39*, 176–190.